UNIVERSITY
OF MICHIGAN
MAY 28 1953
PHYSICS
LIBRARY

REGISTERED No. M. 3121

PROCEEDINGS

OF THE

INDIAN ACADEMY OF SCIENCES

VOL. XXXVII] *SECTION A* [No. 3

COMMEMORATION

OF THE

JUBILEE OF THE DISCOVERY

OF THE

RAMAN EFFECT

MARCH 1953

PRINTED AT THE BANGALORE PRESS, BANGALORE CITY, BY G. SRINIVASA RAO, SUPERINTENDENT, AND PUBLISHED BY THE INDIAN ACADEMY OF SCIENCES, BANGALORE.

Yours truly
C. V. Raman
28.2.1953

A NEW RADIATION*

By Prof. C. V. Raman

1. Introduction

I propose this evening to speak to you on a new kind of radiation or light-emission from atoms and molecules. To make the significance of the discovery clear, I propose to place before you the history of the investigations made at Calcutta which led up to it. Before doing so, however, a few preliminary remarks regarding radiation from atoms and molecules will not be out of place.

Various ways are known to the physicist by which atoms or molecules may be caused to emit light, as for instance, heating a substance or bombarding it with a stream of electrons. The light thus emitted is usually characteristic of the atoms or molecules and is referred to as *primary* radiation. It is also possible to induce radiation from atoms and molecules by illuminating them strongly. Such light-emission is referred to as *secondary* radiation. The familiar diffusion of light by rough surfaces may be cited as an example of secondary radiation, but strictly speaking, it hardly deserves the name, being an effect occurring at the boundaries between media of different refractive indices and not a true volume-effect in which all the atoms and molecules of the substance take part. The first case discovered of secondary radiation really worthy of the name was the phenomenon of fluorescence whose laws were elucidated by the investigations of Sir George Stokes. This is a familiar effect which is exhibited in a very conspicuous manner in the visible region of the spectrum by various organic dye-stuffs. I have here a bottle of water in which an extremely small quantity of fluorescein is dissolved. You notice that when placed in the beam of light from the lantern, it shines with a vivid green light, and that the colour of the emission is not altered, though its brightness is changed, by placing filters of various colours between the bottle and the lantern. A violet filter excites the green fluorescence strongly, while a red filter has but little effect.

Another kind of secondary radiation whose existence has been experimentally recognized more recently is the scattering of light by atoms and molecules. It is this scattering that gives us the light of the sky, the blue colour of the deep sea and the delicate opalescence of large masses of clear

*Inaugural Address delivered to the South Indian Science Association, on Friday, the 16th March 1928, at Bangalore.

ice. I have here a large bottle of a very clear and transparent liquid, toluene, which as you notice contains hardly any dust-particles, but the track of the beam from the lantern passing through it is visible as a brilliant blue cone of light. This internal opalescence continues to be visible even after the most careful purification of the liquid by repeated distillation *in vacuo*. A similar opalescence is shown, though much less brightly, by dust-free gases and vapours, and also by solids. A large clear block of ice shows a blue colour in the track of the beam when sunlight passes through it. The blue opalescence of blocks of clear optical glass is also readily demonstrable. The molecular scattering of light is thus a phenomenon common to all states of matter.

During the past seven years, the scattering of light in transparent media has been the subject of intensive experimental and theoretical investigation at Calcutta, and it is the researches made on this subject that have led to the discovery which I shall lay before you this evening. One important outcome of our researches has been to show that while light-scattering is in one sense a molecular phenomenon, in another sense it is a bulk-effect having a thermal origin. It is the thermal agitation of the molecules which causes them to be distributed and orientated in space with incomplete regularity, and it is the local fluctuations in the properties of the medium thus arising which give rise to optical heterogeneity and consequent diffusion of light. The subject of light-scattering is thus a meeting ground for thermodynamics, molecular physics and the wave-theory of radiation. That the combination of theories in such diverse fields of physics gives us predictions which have been experimentally verified, is one of the triumphs of modern physics.

2. A NEW PHENOMENON

While the quantitative investigations made at Calcutta have in the main substantiated the thermodynamic-wave-optical theory of light-scattering, indications appeared even in our earliest studies of a new phenomenon which refused to fit in with our preconceived notions. Thus, in some observations made by me[1] with the assistance of Mr. Seshagiri Rao in December 1921, it was found that the depolarisation of the light transversely scattered by distilled water measured with a double-image prism and Nicol increased very markedly when a violet filter was placed in the path of the incident light. More careful investigations made with dust-free liquids[2] in 1922, confirmed this effect and showed it to exist also in methyl and ethyl alcohols, and to a lesser degree in ether. It was also noticed that the colours of the scattered

[1] *Molecular Diffraction of Light*, Calcutta University Press, February 1922.
[2] C. V. Raman and K. S. Rao, *Phil. Mag.*, Vol. 45, p. 633, 1923.

light from the different liquids studied did not match perfectly. An important advance was made when Dr. Ramanathan[3] working at Calcutta in the summer of 1923, investigated the phenomenon more closely and discovered that it was not a true dependence of the depolarisation on the wavelength of the scattering radiation but was due to the presence in the scattered light of what he described as " a trace of fluorescence". This was shown by the fact that the measured depolarisation depended on whether the blue filter used was placed in the path of the incident beam or of the scattered light, being smaller in the latter case. Accepting the explanation of the effect as " weak fluorescence ", it naturally became important to discover whether it was due to some impurity present in the substance. Dr. Ramanathan tested this by careful chemical purification followed by repeated slow distillation of the liquid at the temperature of melting ice. He found that the effect persisted undiminished.

The investigation of this species of " weak fluorescence " has ever since 1923 been on our programme of research at Calcutta. Krishnan,[4] who investigated 60 liquids for light-scattering in the spring and summer of 1924, made systematic studies of the phenomenon, and found that it was shown markedly by water, ether, all the monohydric alcohols and a few other compounds. He pointed out that the liquids which exhibit the effect have certain family relationships amongst themselves, and that they are also substances whose molecules are known to be polar. The chemical importance of the subject led to Mr. S. Venkateswaran attempting to make a fuller study of it in the summer of 1925, but without any special success. The research was discontinued at the time but was resumed by him later in the current year (January, 1928). The remarkable observation was made that the visible radiation which is excited in pure dry glycerine by ultra-violet radiation (sunlight filtered through Corning glass G. 586) is *strongly polarised.*

The possibility of a similar effect in gases and vapours was also borne in mind and repeatedly looked for by the workers at Calcutta. The feebleness of the scattering in gases and vapours, and the infructuousness of the earlier efforts in this direction, however discouraged progress.

3. Its Universality

Though the phenomenon was described in the paper of Dr. Ramanathan and Mr. Krishnan as a " feeble fluorescence ", the impression left on my mind at the time was that we had here an entirely new type of secondary

[3] K. R. Ramanathan, *Proc. Ind. Assoc. Cultn. Science*, Vol. 8, p. 190, 1923.
[4] K. S. Krishnan, *Phil. Mag.*, Vol. 50, p. 697, 1925.

radiation distinct from what is usually described as fluorescence. The publication of the idea was however discouraged by the belief then entertained that only a few liquids exhibited the effect and by the supposition that it was unpolarised in the same way as ordinary fluorescence in liquids. Indeed, a chemical critic might even have asserted that the effect was in each case due to a trace of dissolved fluorescent impurity present in the substance which our efforts at purification had failed to remove. Early this year, however, a powerful impetus to further research was provided when I conceived the idea that the effect was some kind of optical analogue to the type of X-ray scattering discovered by Prof. Compton, for which he recently received the Nobel Prize in Physics. I immediately undertook an experimental re-examination of the subject in collaboration with Mr. K. S. Krishnan and this has proved very fruitful in results. The first step taken in the research was to find whether the effect is shown by all liquids. The method of investigation was to use a powerful beam of sunlight from a heliostat concentrated by a 7″ telescope objective combined with a short focus lens. This was passed through a blue-violet filter and then through the liquid under examination contained in an evacuated bulb and purified by repeated distillation *in vacuo*. A second filter of green glass was used which was complementary in colour to the blue-violet filter. If it were placed in the track of the incident light, all illumination disappears, while, if it be placed between the bulb and the observer's eye, the opalescent track within the liquid continued to be visible, though less brightly. All the liquids examined (and they were some 80 in number) showed the effect in a striking manner. There was therefore no longer any doubt that the phenomenon was universal in character; with the bulb of toluene on the lantern, you see that the effect is readily demonstrable. The cone of light vanishes when I place the violet and green filters together, but it appears when I transfer the latter to a place between my audience and the observation bulb.

Now the test with the complementary filters is precisely that ordinarily used for detecting fluorescence and indeed was first suggested by Stokes in his investigations on the subject. You may therefore rightly ask me the question how does this phenomenon differ from fluorescence? The answer to the question is, firstly, that it is of an entirely different order of intensity. A more satisfactory proof was however forthcoming when Mr. Krishnan and myself examined the polarisation of this new type of radiation and found that it was nearly as strong as that of the ordinary light-scattering in many cases, and is thus quite distinct from ordinary fluorescence which is usually unpolarised.

This is shown for the case of toluene in Figs. 1 and 2 in Plate XVI. Fig. 1 is a photograph of the scattering by toluene of sunlight filtered through a blue-violet glass. It was taken through a double-image prism of iceland spar with an exposure of 3 seconds. Fig. 2 is a picture with an additional complementary filter of green glass interposed in front of the camera lens. The exposure necessary is now increased greatly by the insensitiveness of the plate to green light, and had to be as much as 25 minutes. It will be noticed that the polarisation of the track as shown by the difference in brightness of the two polarised images is quite as prominent in Fig. 2 as in Fig. 1.

I may also mention that Mr. Krishnan and myself have succeeded in detecting the new radiation and observing its partial polarisation in a number of organic vapours and also in the gases CO_2 and N_2O. The problem in these cases is one of securing sufficient intensity of scattering for the effect to be detectable through the complementary filter. This can be secured by heating up the substance in a sealed bulb or by using steel observation-vessels for containing the compressed gases, so as to obtain sufficient density of the scattering molecules. The question of the background against which the track is observed is also of great importance.

The new type of secondary radiation is also observable in crystals such as ice, and in amorphous solids. It is thus a phenomenon whose universal nature has to be recognised.

4. Line-Spectrum of New Radiation

That the secondary radiation passes the complementary filter and yet is strongly polarised to an extent comparable with the ordinary molecular scattering, is clear evidence that we have in it an entirely new type of secondary radiation which is distinct from either the ordinary scattering or the usual type of fluorescence. A striking and even startling confirmation of this view is furnished by an examination of its spectrum. Preliminary observations with sunlight filtered through a combination which passes a narrow range of wave-lengths, showed the spectrum of the new radiation to consist mainly of a narrow range of wave-lengths clearly separated from the incident spectrum by a dark space. This encouraged me to take up observations with a monochromatic source of light. A quartz mercury lamp with a filter which completely cuts out all the visible lines of longer wave-length than the indigo line 4,358 A.U. was found to be very effective. When the light from such a lamp was passed through the bulb containing a dust-free liquid, and the spectrum of the scattered light was observed through a direct-vision spectroscope, it was found to exhibit two or more sharp bright lines in the blue and green regions of the spectrum. These

lines are not present in the spectrum of the incident light or in the unfiltered light of the mercury arc and are thus manufactured by the molecules of the liquid.

Figs. 3 (1) and 3 (2), and Figs. 4 (1) and 4 (2) show the phenomenon. They are spectrograms taken with a small Hilger quartz instrument of the scattering by liquid benzene. Fig. 3 was taken with the light from the quartz mercury arc filtered through a blue glass which allows the wave-lengths from about 3,500 A.U. to 4,400 A.U. to pass through. Fig. 3 (1) represents the incident spectrum and Fig. 3 (2) the scattered spectrum, and the latter shows a number of sharp lines not present in Fig. 3 (1). These are indicated in the figure. Figs. 4 (1) and (2) similarly represent the incident and scattered spectra with benzene liquid, the filter used being a potassium permanganate solution. Here again the new lines which appear are indicated in the figure. Visual observations were also made using a quinine sulphate solution together with the blue glass as a filter and thus cutting off all the radiations except 4,358 A.U. from the incident spectrum. Some of the modified lines then disappear, leaving only those of longer wave-length. It is thus clear that each line in the incident spectrum gives rise to at least two lines in the scattered spectrum, one in the original or unmodified position, and a second in a shifted position of longer wave-length. There is thus a striking analogy with the Compton effect in the X-ray region.

There has, as yet, not been sufficient time for photographing the spectra from a large number of liquids, or even for measuring the photographs already obtained. Visual observations have however been made with a large number of liquids. There is an astonishing similarity between the spectra obtained with different liquids. When only the 4,358 line was used, most liquids showed in the spectrum of the scattered light, a bright line in the blue-green region of the spectrum (about 5,000 A.U.), whose position was practically the same for chemically similar liquids such as pentane, hexane and octane for instance. There was, however, recognizable difference in the position of the modified line when other liquids such as benzene or water were used. When the 4,047 line of the mercury arc was let in by removing the quinine sulphate solution, a second modified line in the blue region of the spectrum was seen with most liquids.

Photographs obtained so far with benzene and toluene suggest that there may be several modified lines, and that each modified line may be a doublet in some cases. In many liquids, the scattered spectrum shows in addition to sharp lines also an unmistakable continuous spectrum accompanying it. Carbon disulphide behaves in an exceptional manner, showing a diffuse band,

Observations already made show that the new lines in the scattered spectrum are usually markedly polarised; they also suggest that a continuous spectrum, when present, is less markedly polarised.

5. Nature of the New Radiation

The discovery set out above naturally opens up an array of problems for investigation. The most pressing question is, how is the modified scattered radiation, as we may call it, generated by the molecules of the liquid? As a tentative explanation, we may adopt the language of the quantum theory, and say that the incident quantum of radiation is partially absorbed by the molecule, and that the unabsorbed part is scattered. The suggestion does not seem to be altogether absurd and indeed such a possibility is already contemplated in the Kramers-Heisenberg theory of dispersion. If we accept the idea indicated above, then the difference between the incident and scattered quanta would correspond to a quantum of absorption by the molecule. The measurement of the frequencies of the spectral lines thus opens a new pathway of research into molecular spectra, particularly those in the infra-red region.

If a molecule can take up part of the incident quantum of radiation and scatter the remaining part, then it might also be capable of adding a quantum of its own characteristic frequency to the incident radiation when scattering it. In such a case we should expect a modified line of *increased* frequency. Such a result appears to be shown in Fig. 3 (2) of Plate XVI, as a solitary line in the extreme left of the photograph. This result, however, requires to be confirmed by more photographs and with other liquids. So far it would appear that a degradation of frequency is more probable than an enhancement. It is too early to speculate at present on the origin of the continuous radiation observed in some cases, whether it is due to changes in the molecule itself, or whether it arises from inelastic collisions of the second kind within the liquid resulting in *partial* transformation of the incident quantum of radiation into translatory kinetic energy of the molecules. When further data are obtained, it should be possible to express a definite opinion on this point, and also on the role played by the solvent in the explanation of ordinary fluorescence.

6. Relation to Thermodynamics

As explained in the Introduction, the ordinary scattering of light can be regarded equally well as a molecular effect, and as a bulk effect arising from the thermodynamic fluctuations of the whole medium. The question arises whether the new type of secondary radiation is exclusively molecular

effect or not, and whether it is related in any way to thermodynamics. The question is obviously one to be answered by experiment and theory conjointly. The comparative study of the effect at different temperatures and in different states of aggregation of matter is obviously of great importance in this connection. It has already been remarked that the effect is observable in gases and vapours and indeed it is found possible to determine its intensity and polarisation in the gaseous state. It is also of great interest to remark that the solid crystal ice also shows the sharp modified lines in the scattered spectrum in approximately the same positions as pure water. The only observations made with amorphous solids are with optical glass. Here the modified scattered spectrum consists of diffuse bands and not sharp lines. Whether this is generally true for all amorphous solids, and whether any changes occur at low and high temperatures remains to be determined by experiment.

7. COHERENT OR NON-COHERENT RADIATION ?

An important question to be decided in the first instance by experiment is whether the modified scattered radiations from the different molecules are incoherent with each other. One is tempted to assume that this must be the case, but a somewhat astonishing observation made with liquid carbon dioxide contained in steel observation vessels gives us pause here. It was found on blowing off the CO_2 by opening a stop-cock, a cloud formed within the vessels which scattered light strongly in the ordinary way. On viewing the cloud through the complementary filter, the scattered radiation of modified frequency also brightened up greatly. This would suggest that the assumption of non-coherence is unjustifiable. Further, some qualitative observations suggest that the modified scattering by a mixture of carbon disulphide and methyl alcohol also brightens up notably at the critical solution temperature. Quantitative observations are necessary to decide the very fundamental question here raised.

8. POSSIBLE X-RAY ANALOGIES

If a quantum of radiation can be absorbed in part and scattered in part in the optical region of the spectrum, should not similar phenomena also occur in X-ray scattering ? The type of scattering discovered by Prof. Compton may possibly be only one of numerous other types of scattering with modified frequencies, some with a line spectrum and some in the nature of continuous radiation. The extreme ultra-violet region of the spectrum may also furnish us with numerous examples of the new type of radiation, which clearly occupies a position intermediate between scattering and fluorescence,

Proc. Ind. Acad. Sci., A, vol. XXXVII, Pl. XVI

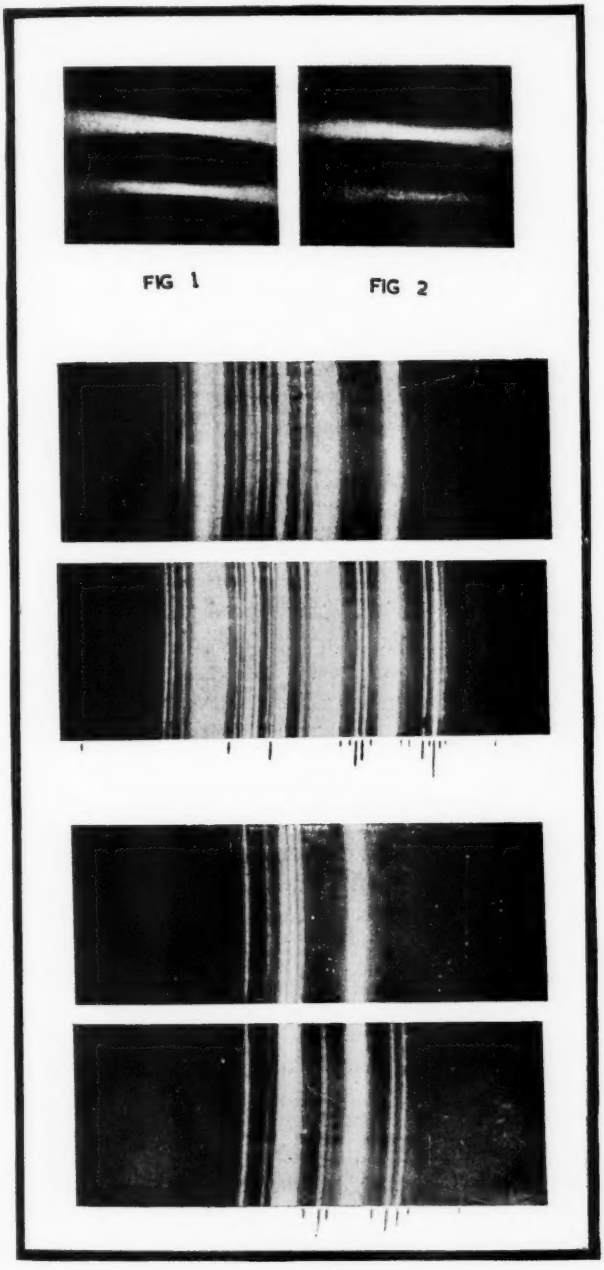

Polarisation of Scattering

FIG. 1. Unmodified

FIG. 2. Modified

FIG. 3. (1) Incident Spectrum

(2) Scattered Spectrum

FIG. 4. (1) Incident Spectrum

(2) Scattered Spectrum

9. Conclusion

We are obviously only at the fringe of a fascinating new region of experimental research which promises to throw light on diverse problems relating to radiation and wave-theory, X-ray optics, atomic and molecular spectra, fluorescence and scattering, thermodynamics and chemistry. It all remains to be worked out.

I have to add in conclusion that I owe much to the valuable co-operation in this research of Mr. K. S. Krishnan, and the assistance of Mr. S. Venkateswaran and other workers in my laboratory.

The line spectrum of the new radiation was first seen on the 28th February 1928. The observation was given publicity the following day.

(Issued separately, 31st March 1928.)

THE MOLECULAR SCATTERING OF LIGHT

Nobel Lecture Delivered at Stockholm, 11th December 1930

By Sir C. V. Raman

1. The Colour of the Sea

In the history of science, we often find that the study of some natural phenomenon has been the starting point in the development of a new branch of knowledge. We have an instance of this in the colour of skylight, which has inspired numerous optical investigations, and the explanation of which, proposed by the late Lord Rayleigh, and subsequently verified by observation, forms the beginning of our knowledge of the subject of this lecture. Even more striking, though not so familiar to all, is the colour exhibited by oceanic waters. A voyage to Europe in the summer of 1921 gave me the first opportunity of observing the wonderful blue opalescence of the Mediterranean Sea. It seemed not unlikely that the phenomenon owed its origin to the scattering of sunlight by the molecules of the water. To test this explanation, it appeared desirable to ascertain the laws governing the diffusion of light in liquids, and experiments with this object were started immediately on my return to Calcutta in September 1921. It soon became evident, however, that the subject possessed a significance extending far beyond the special purpose for which the work was undertaken, and that it offered unlimited scope for research. It seemed indeed that the study of light-scattering might carry one into the deepest problems of physics and chemistry, and it was this belief which led to the subject becoming the main theme of our activities at Calcutta from that time onwards.

2. The Theory of Fluctuations

From the work of the first few months, it became clear that the molecular scattering of light was a very general phenomenon which could be studied not only in gases and vapours but also in liquids and in crystalline and amorphous solids, and that it was primarily an effect arising from molecular dis-array in the medium and consequent local fluctuations in its optical density. Except in amorphous solids, such molecular dis-array could presumably be ascribed to thermal agitation, and the experimental results appeared to support this view. The fact that molecules are optically anisotropic and can orientate freely in liquids was found to give rise to an additional type of scattering. This could be distinguished from the scattering

due to fluctuations in density by reason of its being practically unpolarised, whereas the latter was completely polarised in the transverse direction. The whole subject was critically reviewed and the results till then obtained were set out in an essay published by the Calcutta University Press in February 1922.

The various problems requiring solution indicated in this essay were investigated with the aid of a succession of able collaborators. It is possible to mention briefly only a few of the numerous investigations which were carried out at Calcutta during the six years 1922 to 1927. The scattering of light in fluids was studied by Ramanathan over a wide range of pressures and temperatures with results which appeared to support the " fluctuation " theory of its origin. His work also disclosed the remarkable changes in the state of polarisation which accompany the variations of intensity with temperature in vapours and in liquids. Liquid mixtures were investigated by Kameswara Rao, and furnished optical proof of the existence in such systems, of simultaneous fluctuations of density, composition and molecular orientation. Srivastava studied the scattering of light in crystals in relation to the thermal fluctuations of density and their increase with temperature. Ramdas investigated the scattering of light by liquid surfaces due to thermal agitation, and established a relation between surface-tension and surface-opalescence. He also traced the transition from surface-opalescence to volume-opalescence which occurs at the critical temperature. Sogani investigated X-ray diffraction in liquids, in order to connect it with their optical behaviour and test the application of fluctuation theory to X-ray scattering.

3. The Anisotropy of Molecules

As stated above, the state of polarisation of the light scattered in fluids is connected with the optical anisotropy of the molecules. Much of the work done at Calcutta during the years 1922 to 1927 was intended to obtain data concerning this property and to establish its relations with various optical phenomena. Krishnan examined a great many liquids, and by his work showed very clearly the dependence of the optical anisotropy of the molecule on its chemical constitution. Ramakrishna Rao studied the depolarisation of scattered light in a very large number of gases and vapours and obtained information of high importance for the progress of the subject. Venkateswaran studied the scattering of light in aqueous solutions to find the influence on it of electrolytic dissociation. Ramachandra Rao investigated liquids having highly elongated molecules and also highly polar substances over a wide range of temperature, and discovered the influence of molecular shape and molecular association on the depolarisation of scattered light in liquids,

The interpretation of the observations with liquids involved the development of a molecular theory of light-scattering in dense media which was undertaken by Ramanathan, myself and Krishnan. A revised opalescence formula was derived which differed from that of Einstein and yielded results in better agreement with observation. Krishnan and myself also published a series of investigations showing how the optical anisotropy of the molecules deduced from light-scattering could be utilized to interpret the optical and dielectric behaviour of fluids and also the electric, magnetic and mechanical birefringence exhibited by them. The conclusions derived from these studies enabled a connection to be established between the molecular anisotropy observed in fluids and the optical, electric and magnetic aelotropy exhibited by solids in the crystalline state.

4. A NEW PHENOMENON

The investigations referred to above were in the main guided by the classical electromagnetic theory of light, the application of which to the problems of light-scattering is chiefly associated with the names of Rayleigh and of Einstein. Nevertheless, the possibility that the corpuscular nature of light might come into evidence in scattering was not overlooked and was in fact elaborately discussed in the essay of February 1922 which was published at least a year before the well-known discoveries of Compton on X-ray scattering. While our experiments in the main appeared to support the electromagnetic theory of light, evidence came to hand at a very early stage of the investigations of the existence of a phenomenon which seemed to stand outside the classical scheme of thought. The scattering of light in transparent fluids is extremely feeble, much weaker in fact than the Tyndall effect usually observed in turbid media. It was experimentally discovered that associated with the Rayleigh-Einstein type of molecular scattering, was another and still feebler type of secondary radiation, the intensity of which was of the order of magnitude of a few hundredths of the classical scattering and differed from it in not having the same wave-length as the primary or incident radiation. The first observation of this phenomenon was made at Calcutta in April 1923 by Ramanathan who was led to it in attempting to explain why in certain liquids (water, ether, methyl and ethyl alcohols), the depolarisation of scattered light varied with the wave-length of the incident radiation. Ramanathan found that after exhaustive chemical purification and repeated slow distillation of the liquid in vacuum, the new radiation persisted undiminished in intensity, showing that it was a characteristic property of the substance studied and not due to any fluorescent impurity. Krishnan observed a similar effect in many other liquids in 1924,

and a somewhat more conspicuous phenomenon was observed by me in ice and in optical glasses.

5. The Optical Analogue of the Compton Effect

The origin of this puzzling phenomenon naturally interested us, and in the summer of 1925, Venkateswaran attempted to investigate it by photographing the spectrum of the scattered light from liquids, using sunlight filtered through colour screens, but was unable to report any decisive results. Ramakrishna Rao in his studies on the depolarisation of scattering during 1926 and 1927 looked carefully for a similar phenomenon in gases and vapours, but without success. This problem was taken up again by Krishnan towards the end of 1927. While his work was in progress, the first indication of the true nature of the phenomenon came to hand from a different quarter. One of the problems interesting us at this time was the behaviour in light-scattering of highly viscous organic liquids which were capable of passing over into the glassy state. Venkateswaran undertook to study this question, and reported the highly-interesting result that the colour of sunlight scattered in a highly-purified sample of glycerine was a brilliant green instead of the usual blue. The phenomenon appeared to be similar to that discovered by Ramanathan in water and the alcohols, but of much greater intensity, and, therefore, more easily studied. No time was lost in following up the matter. Tests were made with a series of filters transmitting narrow regions of the solar spectrum and placed in the path of the incident beam, which showed that in every case the colour of the scattered light was different from that of the incident light, and was displaced from it towards the red. The radiations were also strongly polarised. These facts indicated a clear analogy between the empirical characters of the phenomenon and the Compton effect. The work of Compton had made familiar the idea that the wave-length of radiation could be degraded in the process of scattering, and the observations with glycerine suggested to me that the phenomenon which had puzzled us ever since 1923 was in fact the optical analogue of the Compton effect. This idea naturally stimulated further investigation with other substances.

The chief difficulty which had hitherto oppressed us in the study of the new phenomenon was its extreme feebleness in general. This was overcome by using a 7-inch refracting telescope in combination with a short-focus lens to condense sunlight into a pencil of very great intensity. With these arrangements and using complementary light-filters in the path of the incident and scattered beams, as was done by Ramanathan in 1923, to isolate the modified radiations, it was found that they could be readily observed in a great

many liquids, and that in many cases they were strongly polarised. Krishnan, who very materially assisted me in these investigations, found at the same time that the phenomenon could be observed in several organic vapours, and even succeeded in visually determining the state of polarisation of the modified radiations from them. Compressed gases such as CO_2 and N_2O, crystalline ice and optical glasses also were found to exhibit the modified radiations. These observations left little doubt that the phenomenon was really a species of light-scattering analogous to the Compton effect.

6. ITS SPECTROSCOPIC CHARACTERS

Thanks to the vastly more powerful illumination made available by the 7-inch refractor, the spectroscopic examination of the effect, which had been abandoned in 1925 as indecisive, now came within the reach of direct visual study. With a Zeiss cobalt-glass filter placed in the path of the incident beam, and one or other of a series of organic liquids as the scattering substance, a band in the blue-green region was observed by me in the spectrum of the scattered light, separated by a dark interval from the indigo-violet region transmitted by the filter. Both of these regions in the spectrum became sharper when the region of transmission was narrowed by the insertion of an additional filter in the incident beam. This suggested the employment, instead of sunlight, of the highly monochromatic radiations given by a mercury arc in combination with a condenser of large aperture and a cobalt-glass filter. With these arrangements, the spectrum of the scattered light from a variety of liquids and solids was visually examined, and the startling observation was made that the spectrum generally included a number of sharp lines or bands on a diffuse background which were not present in the light of the mercury arc.

The quartz mercury lamp was so powerful and convenient a source of monochromatic illumination that, at least in the case of liquids and solids, photographing the spectrum of scattered light was found to present no extraordinary difficulties. The earliest pictures of the phenomenon were in fact taken with a portable quartz spectrograph of the smallest size made by the firm of Hilger. With a somewhat larger instrument of the same type, Krishnan obtained very satisfactory spectrograms with liquids and with crystals on which measurements of the desired precision could be made, and on which the presence of lines displaced towards the violet was first definitely established. The experimental difficulties were naturally greater in the case of gases or vapours, though they could be lessened by working with the substance under pressure. With an improvised instrument of large aperture

(F/1·8), Ramdas obtained the first spectrograms with a gaseous substance (ether vapour) at atmospheric pressure.

In interpreting the observed phenomena, the analogy with the Compton effect was adopted as the guiding principle. The work of Compton had gained general acceptance for the idea that the scattering of radiation is a unitary process in which the conservation-principles hold good. Accepting this idea it follows at once that, if the scattering particle gains any energy during the encounter with the quantum, the latter is deprived of energy to the same extent, and accordingly appears after scattering as a radiation of diminished frequency. From thermodynamic principles, it follows that the reverse process should also be possible. Adopting these ideas, the actual observations could be interpreted, and the agreement of the observed displacements with the infra-red frequencies of the molecules made it clear that the new method opened up an illimitable field of experimental research in the study of the structure of matter.

7. Interpretation of the Effect

It appears desirable to emphasise that though the conservation principle of Compton is useful in interpreting the effects disclosed by experiment, it is by itself insufficient to explain the observed phenomena. As is well known from studies on molecular spectra, a gaseous molecule has four different species of energy of increasing orders of magnitude, namely, those corresponding to translatory motion, rotation, vibration and electronic excitation. Each of these, except the first, is quantized and may be represented by an integer in an extended sequence of quantum numbers. The aggregate energy of a molecule may, therefore, assume any one out of a very large number of possible values. If we assume that an exchange of energy occurs in the collision between the molecule and the quantum, and limit ourself to the cases in which the final energy of the molecule is less than that of the incident quantum, we arrive at the result that the spectrum of the scattered light should contain an immense number of new lines and should in fact rival in its complexity the band spectrum of the molecule observed in the emission or absorption of light. Nothing more different from what is actually observed can be imagined than the foregoing picture. The most conspicuous feature revealed by experiment is the beautiful simplicity of the spectra of even complicated polyatomic molecules obtained in light-scattering, a simplicity that is in striking contrast to the extreme complexity of their emission or absorption spectra. It is this simplicity that gives to the study of light-scattering its special significance and value. It is clear that the

effect actually observed was not and could not have been foreseen from an application of the conservation principles.

The general principle of correspondence between the quantum and classical theories enunciated by Niels Bohr enables us, on the other hand, to obtain a real insight into the actual phenomena. The classical theory of light-scattering tells us that if a molecule scattering light is moving, rotating or vibrating, the scattered radiations may include certain frequencies, different from those of the incident waves. This classical picture, in many respects, is surprisingly like what we actually observe in the experiments. It explains why the frequency shifts observed fall into three classes, translational, rotational and vibrational, of different orders of magnitude. It explains the observed selection rules, as for instance, why the frequencies of vibration deduced from scattered light include only the fundamentals and not the overtones and combinations which are so conspicuous in emission and absorption spectra. The classical theory can even go further and give us a rough indication of the intensity and polarisation of the radiations of altered frequency. Nevertheless, the classical picture has to be modified in essential respects to give even a qualitative description of the phenomena, and we have, therefore, to invoke the aid of quantum principles. The work of Kramers and Heisenberg, and the newer developments in quantum mechanics which have their root in Bohr's correspondence principle seem to offer a promising way of approach towards an understanding of the experimental results. But until we know much more than we do at present regarding the structure of molecules, and have sufficient quantitative experimental knowledge of the effect, it would be rash to suggest that they afford a complete explanation of it.

8. THE SIGNIFICANCE OF THE EFFECT

The universality of the phenomenon, the convenience of the experimental technique and the simplicity of the spectra obtained enable the effect to be used as an experimental aid to the solution of a wide range of problems in physics and chemistry. Indeed, it may be said that it is this fact which constitutes the principal significance of the effect. The frequency-differences determined from the spectra, the width and character of the lines appearing in them, and the intensity and state of polarisation of the scattered radiations enable us to obtain an insight into the ultimate structure of the scattering substance. As experimental research has shown, these features in the spectra are very definitely influenced by physical conditions, such as temperature and state of aggregation, by physico-chemical conditions, such as mixture, solution, molecular association and polymerisation, and most essentially by

chemical constitution. It follows that the new field of spectroscopy has practically unrestricted scope in the study of problems relating to the structure of matter. We may also hope that it will lead us to a fuller understanding of the nature of light, and of the interactions between matter and light.

9. Some Concluding Remarks

From a physical point of view, the quantitative study of the effect with the simplest molecules holds out the largest hope of fundamental advances. The beautiful work of McLennan with liquefied gases, and of R. W. Wood and Rasetti are pioneer investigations in this field which command the highest admiration. The quantitative study of the effect with crystals of the simplest possible chemical constitution is naturally of great importance. The case of the diamond, which has been investigated by Ramaswamy, Robertson and Fox, and with especial completeness by Bhagavantam, is of special interest. Very surprising results have been obtained with this substance, which may be the pathway to a fuller understanding of the nature of the crystalline state. I should also like to draw attention to the work of Krishnamurti, who has traced a remarkable dependence of the intensity of the spectral lines observed in scattering on the nature of the chemical bond and followed the transition from the homopolar to the heteropolar type of chemical combination. Krishnamurti's observation that the paramagnetism of crystals apparently influences the observed intensity of the displaced lines is one of the most remarkable ever made in this new field of research.

TWENTY-FIVE YEARS OF RESEARCH ON THE RAMAN EFFECT

By S. Bhagavantam

(From the Physical Laboratories, Osmania University, Hyderabad, India)

Received February 26, 1953

1. Over-all Picture

Intensive experimental work on the scattering of light carried on continuously at Calcutta since the year 1921 culminated in the discovery by Professor Raman in 1928 of the new radiation phenomenon, now known as the Raman Effect. The first announcement of the discovery with a description of its principal features was made in a lecture by Professor Raman under the title "A New Radiation" on March 16, 1928, and the text of that epoch-making paper is being reproduced in these *Proceedings*. This year marks its twenty-fifth anniversary and it appears appropriate to present a review of the large amount of scientific literature that has grown around this branch of knowledge.

A statistical analysis of the trends in this subject was made by Hibben[1] in 1938 with some interesting results. He observed that even by that time, there appeared nearly seventeen hundred publications on different aspects; India being the most prolific producer of research in this subject as an individual geographical unit. The subject was being investigated in the laboratories of practically every country in the world, but Germany, United States, France, Italy, Belgium and Japan had made notable contributions. Though the early interest was exhibited essentially by physicists, its gradual passage into the hands of chemists and physical chemists became quickly evident. The present position is that we have over 3,000 published papers on the subject, the United States and India together accounting for nearly half of them. Even now there is a wide and sustained interest and the indications are that workers desire to explore new fields of investigation to which this powerful tool may be applied, and it is likely that such an interest will continue for a long time in specific schools of research that have come to be established but perhaps not in the general laboratories.

In the field of spectroscopy, the study of Raman effect has furnished numerous data which are complementary in nature in several important

[1] *Proc. Ind. Acad. Sci.*, 1938, **8**, 294.

cases to those obtained from a study of the infra-red region and this aspect has in a large measure been the motive force which attracted experimental spectroscopists and resulted in a simultaneous development of the technique both in the infra-red and the visible regions. The rapidly accumulating results from these two fields gave a fresh impetus to the study of molecular constitution and the normal oscillations of postulated molecular structures with special reference to the inter-atomic forces that exist in such structures. Quite an appreciable number of simple molecules have been dealt with in an exhaustive manner by rigorous theoretical methods and fundamental results have been obtained in regard to their structures. Empirical methods of great ingenuity have also been devised from time to time for dealing with the more complicated structures and much progress made.

In the field of chemistry, an amazing variety of problems such as polymerisation, hydrogen bonding, free rotation, identification of isomers and the nature of valency have been viewed and tackled from such new angles with this new tool that a distinctive branch of chemical physics may be said to have been born in the past decade or two.

The study of isotopes, verification of polarization and intensity rules and an analysis of the rotational and vibrational branches in the Raman spectra of simpler molecules were some of the earliest directions in which the physicists interested themselves. The results of such studies are now fairly widely accepted and they constitute considerable portions of treatises dealing with modern molecular physics. An interesting consequence of the experimental work having gone ahead of the theory, as soon as Raman effect began to be applied to a study of molecular structure, is the pressing into service of more powerful mathematical methods for such purposes. The theory of groups has been one such and its application to problems of molecular physics has been greatly enriched in the years that followed the discovery of Raman effect.

A study of the solid and liquid states, covering purely physical as well as physico-chemical aspects, has also been stimulated. Contributions of a fundamental nature have been made and the subject of crystal physics in particular, may be said to have been given a new orientation altogether. In the following pages, these and other advances will be described by way of summarising the achievements of the last two and a half decades that followed the discovery of the Raman effect.

2. Introduction

The equipment, originally used by Raman, consisting of the scattering substance, *viz.*, a glass bulb of distilled liquid or a block of ice or of optical

glass, a quartz mercury lamp with a condensing lens and a pocket spectroscope is the simplest experimental set-up which one can think of in connection with a major effect of this kind in Physics. Such an assembly, which is generally available in almost any laboratory, may still be used very successfully for demonstrating the effect. For purposes of detailed studies with liquids, the glass bulb has been replaced by more complicated containers; the mercury lamp by a variety of more powerful sources and the pocket spectroscope by high dispersion and large aperture spectrographs. In fact, some very spectacular developments in these directions have taken place in recent years that to-day we are able to photograph weak Raman lines with exposures of a few seconds only. Some of these will be briefly described in the following pages.

As actually observed, the effect is now well known to consist in the appearance of new lines (or in some cases bands) and generally also some unresolved continuous radiation in the spectrum of the scattered light, besides the lines originally present in the incident radiation. Each line in the incident spectrum, if of sufficient intensity, gives rise to its own set of lines or bands and associated continuous spectrum; the frequency shifts of each of these new lines as measured from the parent one being independent of the incident radiation and therefore characteristic of the material studied and to some extent the nature of its aggregation. The effect may be observed in a great variety of substances and in diverse physical states and conditions. The lines themselves generally show easily recognisable differences in their intensity and in their width, some being sharp and others diffuse or even broad.

The radiations (Raman lines) when observed in transversely scattered light are often strongly polarized. The degree of polarization varies much from one line to another; sharp lines which are completely polarized on the one hand and broad bands and unresolved continuum depolarized nearly completely (86%) on the other being extreme examples between which all other cases lie.

The continuous spectrum also shows great variations in intensity with different materials. It generally appears as wings extending unsymmetrically on either side of the parent line and showing limiting depolarization. In this case, it is most probably an unresolved and unquantised rotational effect. A continuous spectrum, having possibly a different origin, appears with very viscous liquids and sometimes may be so strong as to overpower all the other lines. A similar effect develops progressively in liquids which undergo chemical change on exposure to light.

In the case of free molecules scattering light, we encounter three different kinds of effect, an electronic effect, a rotational effect and a vibrational effect, the classification indicating the particular type of energy in the molecule which is added to or given up. The most common type of Raman scattering, encountered in matter of all states, is the vibrational effect and consists of lines or bands with moderate or large frequency shifts. In liquids generally, the rotation of molecules ceases to be quantised and owing to closeness of packing and large moments of inertia, unresolved wings in the neighbourhood of the parent line are frequently observed. Matters become even more complicated in the case of solids and these wings are replaced by broad bands, sometimes even sharp lines, indicating that we are there dealing with exchange of energy between the solid and the incident radiation involving specific quanta which we now know to correspond to oscillations of the crystal lattice. Lines which arise from a parent radiation on its lower frequency side as a result of the light quantum giving up some of its energy to the molecule ($h\nu$ + molecule $\rightarrow$molecule* + $h\nu^-$) are called Stokes Raman lines. Some of them, if strong enough, have their counterparts, called Anti-Stokes Raman lines, arising from the same parent radiation but appearing on its higher frequency side as a result of the light quantum getting more energy from the molecule which is already in an excited condition ($h\nu$ + molecule*$\rightarrow$molecule + $h\nu^+$).

The above features are so marked and so general that in the first few days or months of the discovery, they were all noticed and recorded. They are now regarded as the highlights of Raman effect which, every one who starts experimental work in the subject, seeks to reproduce and verify.

3. Developments in Experimental Technique

During the early years, since it was necessary to study the Raman spectra of as many substances as possible, much attention was not paid to the development of powerful experimental technique. With comparatively less intense sources and moderately good spectrographs, satisfactory results were obtained. Liquids were the easiest to study. Certain special types of containers and arcs of special shapes (spirals and tubes) were developed in connection with the study of crystals and crystal powders but the real major advance was in connection with the study of the phenomenon in gases. The use of high pressure containers for gases and of the resonance λ 2537 of mercury from a cooled arc with a magnet to pull the discharge in the desired direction for illumination are noteworthy developments.

Very quickly, the need arose for more powerful methods by which to tackle substances available in very small quantities and also by which to

study with comparative ease, routine problems such as testing samples for the presence of specific constituents and so on. This resulted in a phenomenol development of both the source and the spectrograph. Arcs as well as lamps of the most varied designs have been employed and the trend was in the direction of using many high intensity (sometimes up to sixteen) mercury arcs arranged cylindrically round the container tube. In all such cases, since a large amount of energy is dissipated in the lamp, effective cooling is essential and now-a-days we have standardised sources of this type, specially intended for the study of Raman effect, manufactured by quite a few firms. With such sources and using reasonably powerful spectrographs, strong Raman lines in liquids can be readily seen with rested eyes and photographed with an exposure of a few seconds.

In many cases, investigators built their own spectrographs effecting an optimum compromise between the light gathering power and large dispersion, the two principal features required of such an instrument. The French school of physicists have pressed into service instruments with an aperture ratio as high as F/0·7 and some of the American workers used instruments which have a dispersion and resolving power sufficient to separate lines which are only 1 $cm.^{-1}$ apart.

Special methods had also to be developed for obtaining the depolarization factors of Raman lines. Early investigations on this aspect have brought to light several interesting experimental points, which were hitherto overlooked. These relate to convergence errors, apparent polarization caused by the spectrograph and corrections that arise from the use of glass windows, photographic plates and the failure of reciprocity laws in photography, polarizers and so on. Some authors made the incident light perpendicular to the scattered beam, as nearly as feasible, by using narrow blackened grooves for collimating the light and others evaluated and applied corrections for convergence. If the horizontal and vertical components are photographed simultaneously, errors caused by variations in intensity and other related factors are eliminated. Errors introduced by the spectrograph have been eliminated in one investigation by using a nicol prism and a half-wave plate in front of its slit. For photographing the parallel component for illumination in a vertical plane, the axis of the Nicol is kept horizontal with that of the half-wave plate parallel thereto. In order to obtain the perpendicular component, the axis of the half-wave plate is rotated through 45°, thus rotating the electric vector of the light passing through it by 90°. Thus each component is photographed with the electric vector horizontally placed in both cases, thereby eliminating the losses due to reflection by the prisms of the spectrograph. Polaroids have also been

extensively used for this type of work. In one arrangement, the tube of liquid is wrapped with transparent polarizing material so that only light polarized with its electric vector parallel to the axis of the tube is allowed to illuminate the liquid. Four mercury arcs placed alongside the tube and round it furnished the illumination. Two exposures are made, one with all lamps lighted and the polaroid in place and the other with only some lamps lighted but the polaroid removed. This provides a rapid methed of picking out the completely polarized lines as they will be greatly weakened in comparison with those that are depolarized. Polaroids have also come into fairly extensive use by investigators to suit their special requirements. Circularly polarized light has been employed by some authors for tackling special problems.

4. Theory of the Raman Effect: General

A general theory of the Raman effect, based on quantum principles and the already known results of molecular physics, is now fairly well established. As has already been stated, the discovery of Raman effect, in its original form, consists in the appearance in the scattered light of new lines or bands and sometimes even continuous spectrum with changed frequencies, arising from one or other of the incident radiations when light falls on matter consisting of molecules. The state of aggregation of these molecules need not be confined to any particular type for the phenomenon to be exhibited, for the discoverer himself realised that solids—crystalline or amorphous; liquids and gases can all be made to scatter light and that the scattered light will contain new radiations characteristic of each case. It is, however, necessary that the interacting medium should consist of groups of atoms mutually linked by some sort of electronic forces as valencies in molecules and in other ways in solids but atoms alone in an isolated condition have not been known to exhibit the phenomenon. This is a feature which does not seem to have been clearly recognised and emphasised in the past by all the workers on Raman effect. There have been attempts to obtain and record an event which may ultimately be attributed to the exchange of energy between an atom and incident radiation in the way of Raman scattering but without success.[2] Raman effect thus may be regarded as elastic scattering of light by matter composed of groups of atoms joined together by molecular or other forces in any state of aggregation with attendant exchange of energy and a consequent frequency shift of the scattered light in relation to that of the incident light. It is a type of interaction between the nuclear-electronic

[2] The author of this article gave long exposures with Argon gas using mercury light in the ultra-violet for illumination, in the hope of recording some kind of Raman transitions in the visible region, but did not succeed.

system which we call the molecule in some cases and the lattice (crystalline, amorphous or quasi-crystalline) in others and incident radiation. All evidence is in favour of presuming that the grip for the radiation on the nuclear system is provided through the electron atmosphere when the incident radiation induces optical polarization in it. The differences between the wave number of the incident radiation and that of the scattered light are intimately connected with the energy states of the molecule or of the scattering system which may be a group of molecules if it is an extended solid. These energy differences, in the case of molecules, are mostly due to the different energy states (vibrational and rotational) and when studied, along with the results of infra-red absorption wherever necessary, furnish complete and most useful information about the molecules and their structures. In this picture, the scheme of exchange of energy is very simply depicted as

$$\text{Molecule} + h\nu_1 \rightleftarrows \text{Molecule}^* + h\nu_2.$$

The exchange can take place in either direction. From left to right, the molecule is receiving energy and ν_2 the frequency of the Raman line will be less than ν_1 the frequency of the incident line. From right to left, the molecule is giving up surplus energy and ν_1 the frequency of the Raman line will be more than ν_2 the frequency of the incident line. In the former case, we get Stokes Raman lines and in the latter, we get anti-Stokes Raman lines.

In the fuller picture, the appearance or otherwise of a spectral line in Raman scattering resulting from a transition of the molecule from a vibrational state with the quantum number v_1 to that with the quantum number v_2 pertaining to the normal co-ordinate Q will depend upon the survival or the vanishing of the integral

$$\int \alpha\,(\mathrm{Q})\,\psi_{v_1}{}^{*}\,(\mathrm{Q})\,\psi_{v_2}\,(\mathrm{Q})\,d\mathrm{Q},$$

where $\alpha\,(\mathrm{Q})$ is the symmetric tensor relating to the polarizability of the molecule in the normal configuration Q. $\alpha\,(\mathrm{Q})$ may be expanded as follows:

$$\alpha\,(\mathrm{Q}) = \alpha_0 + \left(\frac{\partial\alpha}{\partial\mathrm{Q}}\right)_0 \mathrm{Q} + \tfrac{1}{2}\left(\frac{\partial^2\alpha}{\partial\mathrm{Q}^2}\right)_0 \mathrm{Q}^2 + \ldots.$$

and substituted in the integral. If the oscillations are simple harmonic, ψ_{v_1} and ψ_{v_2} are Hermite polynomials of degree v_1 and v_2 respectively and if we confine ourselves to $\Delta v = \pm 1$ and neglect higher powers, the portion of the integral involving α_0 vanishes on account of the orthogonality of the eigenfunctions, the intensity finally depending upon

$$\int \left(\frac{\partial\alpha}{\partial\mathrm{Q}}\right)_0 \mathrm{Q}\,\psi_v\,(\mathrm{Q})\,\psi_{v+1}{}^{*}\,(\mathrm{Q})\,d\mathrm{Q}.$$

If we substitute the actual values of the normalized eigenfunctions appropriate to a harmonic oscillator and simplify the above integral, we obtain the intensity as proportional to[3]

$$\frac{a^2}{2}\left(\frac{\partial a}{\partial Q}\right)_0^2 (v+1).$$

Thus, a normal oscillation will give rise to a Raman line of finite intensity, only when there is a first order variation of the polarizability of the molecule with respect to the corresponding normal co-ordinate. In some cases, without going into the physical magnitude of such a variation, we may, by the application of certain tests, say whether the symmetry of the normal oscillation in question at all permits the existence of such a first order variation and if it does not, we conclude that the line is forbidden to appear as a fundamental in Raman scattering.

a, as has been mentioned above, is in fact a symmetric tensor and consists therefore of six components. The arguments outlined apply individually to each of these components and strictly speaking, a Raman transition between two vibrational levels v_1 and v_2 can have a finite intensity if the integral involving even one of these six quantities is different from zero.

Similarly, if a Raman line due to transition between two rotational levels is to have a finite intensity, we can see in a general way that $\left(\frac{\partial a}{\partial Q}\right)_0$ should exist where Q is a normal co-ordinate corresponding to pure rotation. This term is obviously zero, if the molecule is optically spherically symmetrical, for rotations about all axes and such molecules cannot give rise to rotational Raman lines. In order that a molecule may give rise to rotational Raman lines, it should be optically anisotropic at least with reference to some one axis, the rotation about which will then cause a variation of the polarizability and the incident radiation can induce a Raman transition of the rotational type.

The above arguments are of a general nature and have to be carefully examined in greater detail, if we are to understand more fully the selection rules and the polarization phenomena. Further complications arise if a molecule is capable of going into more than one normal configuration in executing the dynamically permissible small oscillations about its equilibrium position. These aspects will be studied in the next section.

---

[3] See S. Bhagavantam and T. Venkatarayudu, *Theory of Groups and Its Application to Physical Problems* (1951), for further details.

5. THEORY OF THE RAMAN EFFECT: VIBRATIONS OF POLYATOMIC MOLECULES

A molecule consisting of nuclei and electrons may be regarded as a system of particles, kept in equilibrium by certain forces. If we are dealing with nuclear oscillations, the presence of electrons, because of their relatively low mass, may be ignored to a first approximation, and the problem of studying its dynamics becomes simpler. A configuration in which this system of particles can remain permanently at rest is defined as an equilibrium configuration of the system. Suppose the system is initially displaced from such a stable equilibrium configuration but is still near it. The tendency is then to return to that position, which is one of lesser potential energy. Often, the particles in the system remain always in the neighbourhood of their respective equilibrium positions and never acquire large velocities or large amplitudes. Motions of this type are called vibrations about the equilibrium configuration with small amplitudes. If $q_1, q_2, \ldots q_n$ are the co-ordinates necessary to specify a configuration, the kinetic energy of the system at any instant will be a homogeneous quadratic function of the time derivatives $\dot{q}_1, \dot{q}_2, \ldots \dot{q}_n$. Since T is always positive, it follows that it is a positive definite quadratic form in these time derivatives. If the equilibrium configuration is taken as the standard one and if the system is displaced from such a configuration to another described by $q_1, q_2, \ldots q_n$ as above by a set of forces constituting a conservative force field, then work is done on the system and the potential energy acquired will be denoted by V, where V is a function of $q_1, q_2, \ldots q_n$. If we expand V in ascending powers of $q_1, q_2, \ldots q_n$, the term independent of the co-ordinates can be omitted as it does not enter the equations of motion which contain only the derivatives of V. There cannot be terms which are linear in the quantities $q_1, q_2, \ldots q_n$ as $\frac{\partial V}{\partial q_r}$ should be equal to zero. Thus, only the second and higher degree terms in the potential energy function enter into the equations of motion.

If we choose $q_1, q_2, \ldots q_n$ in such a way that they represent displacements or deviations from the equilibrium values of chosen parameters in respect of the molecular system, they are always necessarily small. In other words $q_1, q_2, \ldots q_n$ may all be so chosen that they are individually zero in the standard or the equilibrium configuration. Since we are dealing with small oscillations about the equilibrium configuration, it follows that we need retain only the terms of the lowest order in the kinetic energy function T and replace the coefficients of the squares and products of $q_1, q_2, \ldots q_n$ by the constant values which they assume when $q_1, q_2, \ldots q_n$ are each put equal to zero. The kinetic energy is therefore a homogeneous quadratic

function of $\dot{q}_1, \dot{q}_2, \ldots \dot{q}_n$ with constant coefficients. Neglecting the higher terms in the potential energy expression also, V can be expressed as a homogeneous quadratic form in the co-ordinates q. The kinetic and potential energies of the system may thus be written generally as

$$T = \tfrac{1}{2} \Sigma a_{ij} \dot{q}_i \dot{q}_j; \quad i, j = 1, 2, \ldots n$$

$$V = \tfrac{1}{2} \Sigma b_{ij} q_i q_j; \quad i, j = 1, 2, \ldots n$$

n is the number of co-ordinates necessary and it will be so, if in this case the system has $\frac{n}{3}$ particles. These two expressions can be simultaneously reduced to canonical forms by a suitable choice of co-ordinates $Q_1, Q_2, \ldots Q_n$ which are linear combinations of q's giving

$$2T = \Sigma \dot{Q}_k^2; \quad 2V = \Sigma \lambda_k Q_k^2;$$

The Q's are called the normal co-ordinates and each Q corresponds to a normal mode of oscillation. The λ's in the latter expression can be shown to be the roots of the equation

$$\begin{vmatrix} b_{11} - \lambda a_{11} & b_{12} - \lambda a_{12} & \ldots\ldots\ldots & b_{1n} - \lambda a_{1n} \\ \ldots\ldots & \ldots\ldots & \ldots\ldots & \ldots\ldots \\ \ldots\ldots & \ldots\ldots & \ldots\ldots & \ldots\ldots \\ b_{n1} - \lambda a_{n1} & b_{n2} - \lambda a_{n2} & \ldots\ldots\ldots & b_{nn} - \lambda a_{nn} \end{vmatrix} = 0$$

The choice of q's may be made in many ways. For instance if x_i, y_i, z_i are the Cartesian rectangular co-ordinates of the ith particle in the system chosen with reference to a set of co-ordinates whose origin is at the equilibrium position of the ith atom, then the set $x_1, y_1, z_1 \ldots x_{n/3}, y_{n/3}, z_{n/3}$ which will be n in number for $\frac{n}{3}$ particles may just as well be the q's. In the equilibrium configuration, they will all be obviously zero. In the alternative, q's may be suitable linear combinations of x, y, z's and so on. The solution of the problem of normal oscillations in any one case is very much facilitated, if this determinantal equation can be factorized and it can be factorized in many cases.

Q's thus obtained have special properties. When the kinetic and potential energies are put in terms of them, they assume the canonical form as already mentioned and we have

$$2T = \Sigma \dot{Q}_k^2; \quad 2V = \Sigma \lambda_k Q_k^2;$$

the Lagrangian equation of motion corresponding to any normal co-ordinate Q_r being written as

$$\frac{d}{dt}\left(\frac{\partial T}{\partial \dot{Q}_r}\right) - \frac{\partial T}{\partial Q_r} = -\frac{\partial V}{\partial Q_r}$$

which reduces to $\ddot{Q}_r = -\lambda_r Q_r$.

The important result follows that each normal co-ordinate corresponds to an independent mode of vibration of the system and this is called a normal mode. If the quantities $\lambda_1, \lambda_2, \ldots \lambda_n$ are positive, as is the case with a stable equilibrium configuration, they all represent the frequencies of various possible normal modes of oscillation about the equilibrium configuration. From the elementary laws of simple harmonic motion, we have

$$\lambda_r = 4\pi^2 \nu_r^2,$$

where ν_r is the frequency of Q_r. If the coefficient λ of any normal co-ordinate Q is distinct from other λ's, the corresponding normal mode is said to be non-degenerate. On the other hand, if two or more Q's have the same coefficient, the corresponding modes are said to be degenerate and the degree of degeneracy is equal to the number of Q's which have the same frequency. In such a case, the choice of the particular Q's is not unique.

In order to obtain the normal modes and frequencies in an actual case, we have to first set up the general quadratic forms of the potential and kinetic energies and find out suitable combinations of the variables so that the potential and kinetic energies expressed in terms of the altered variables may not contain cross terms. When the number of particles in a system is small, the above procedure may conveniently be followed. The method, however, becomes increasingly complicated with increasing number of particles in a dynamical system. One of the major developments in this branch, stimulated by the discovery of the Raman effect and its application to the study of normal vibrations of a large variety of moleculer systems, has been the pressing into service of a new and powerful mathematic tool, namely, the Theory of Groups. Group theoretical methods, developed during the past decade or two, have greatly simplified the work and have yielded remarkable results. We shall now deal with them in some detail.

The symmetry properties of molecules permit the factorization of the determinantal equation relating to the normal oscillations and the methods of group theory have been very successfully applied for a study of these symmetry properties. Wigner,[4] Placzek and Teller[5] and Tisza[6] had done

[4] *Göttingen Nachricten*, 1930, 133.
[5] *Zeit. f. Phys.*, 1930, **81**, 209.
[6] *Ibid.*, 1933, **82**, 48.

pioneering work in this field. Several other authors applied these methods in great detail. Molecules, if regarded as composed of nuclei alone, are systems of points and as such exhibit elements of symmetry. Rotational axes, reflection planes and their combinations are such elements of symmetry and these are called covering operations. They constitute, when enumerated fully, a point group which will be characteristic of the symmetry of the molecule. Each such element can be made to correspond to an analytical expression or a transformation matrix and the group of matrices arising from the group of covering operations is called a matrix representation thereof.

Let $Q_1, Q_2, \ldots Q_p$ be a set of normal co-ordinates of a dynamical system. We consider a configuration in which all the normal co-ordinates, except one say Q_r with frequency ν_r, vanish. If we now perform a symmetry operation R of the point group appropriate to the molecule, we obtain a new configuration which we represent by the symbol RQ_r. Since a symmetry operation is such that the distance between any two points of the system remains unaltered, the configuration RQ_r has the same potential energy as Q_r, provided the potential energy remains invariant whenever the mutual distances between all points of the body remain unaltered. This is, of course, true if we make our original assumptions regarding the function V suitably. But RQ_r is not a normal co-ordinate of the original system as the individual particles are no longer in the neighbourhood of their respective equilibrium positions. In fact, the motion described in RQ_r is such that a particle leaves the neighbourhood of its equilibrium position and goes over into the neighbourhood of the equilibrium position of one of its equivalents. We can, however, derive from the configuration RQ_r, a geometrically identical configuration $\overline{R}Q_r$ in the following way. If by means of the operation R, the *l*th particle goes over to the *k*th particle, we shall suppose that the *k*th particle remains in its own neighbourhood but gets the motion of the *l*th particle. By applying this process to all particles, we keep them in their original neighbourhoods and this ensures the invariance of the kinetic energy. The new configuration thus obtained, namely, $\overline{R}Q_r$, has the same potential and kinetic energies as Q_r and therefore represents a normal co-ordinate having the same frequency ν_r as that of Q_r. It is either identical with Q_r or is distinct from Q_r but degenerate with Q_r. Adopting this procedure for all the symmetry operations of the point group appropriate to the system, we obtain the several normal co-ordinates $\overline{R}Q_r$ which have the same frequency ν_r. If $Q_1, Q_2, \ldots Q_r$ is a complete set of linearly independent normal co-ordinates chosen from the whole lot $\overline{R}Q_r$, then the oscillation in question, with a frequency ν_r is said to be *f*-fold degenerate. Similarly, we

take another normal co-ordinate of frequency ν_s and as before obtain a set of linearly independent normal co-ordinates. Proceeding thus, we divide all the normal co-ordinates of the system into linearly independent sets, each set containing one or more normal co-ordinates but of the same frequency only.

In the language of group theory, the above process is to be described as one of separating the manifold of normal oscillations into irreducible sub-manifolds. Each irreducible sub-manifold may be associated with an irreducible representation of the group of symmetry operations. In the reducible representation Γ defined by all the normal co-ordinates, every symmetry operation R corresponds to an $\overline{\mathrm{R}}$ as defined above and every $\overline{\mathrm{R}}$ corresponds to an appropriate matrix made up of transformation matrices corresponding to the irreducible sub-manifolds f, s and so on arranged diagonally. This constitutes a representation defined by the normal co-ordinates. In this representation, the sum of all the diagonal elements in the matrix corresponding to a given R will be called the character of the operation R.

On the other hand, if we take any set of three mutually perpendicular axes X, Y, Z and through the equilibrium position of each particle in the given system, choose three axes parallel to the X, Y, Z system and if x_r, y_r, z_r are the co-ordinates of the rth particle in its displaced position with reference to the axes through its equilibrium position, we can describe any configuration Q_r in terms of x's as well. In fact all the Q's can be expressed as linear functions of x's and the relation between the two sets of co-ordinates may be given by a transformation matrix in the form

$$\begin{Bmatrix} Q_1 \\ Q_2 \\ \vdots \\ Q_n \end{Bmatrix} = [\mathrm{T}] \begin{Bmatrix} x_1 \\ y_1 \\ \vdots \\ z_{n/3} \end{Bmatrix}$$

where T is a matrix of n rows and n columns. While Q's define a representation Γ of the point group, the x's define an equivalent representation Γ' of the point group because every matrix in the representation Γ will only have to be transformed by T to give rise to the corresponding matrix in the representation Γ'. For this reason, the character of any operation R in the two representations Γ and Γ' is the same.[7] It is easy to calculate the

[7] For a prpof of this statement and for a fuller amplification of these ideas, see S. Bhagavantam and T. Venkatarayudu, *Theory of Groups and Its Application to Physical Problems* (1951).

character of an operation R in the reducible representation defined by the co-ordinates $x_1, y_1, \ldots$ etc. If the symmetry operation R takes over the particle 1 into the position of particle k, we have in general a relation of the type

$$Rx_k = ax_l + by_l + cz_l$$

and the character arising from x_k is zero. Similarly the characters arising from y_k and from z_k are zero. If, on the other hand, the kth particle is invariant under the operation R, we have

$$Rx_k = x_k \cos\phi - y_k \sin\phi$$
$$Ry_k = x_k \sin\phi + y_k \cos\phi$$
$$Rz_k = \pm z_k,$$

the + or − sign in the last relation being used according as R is a pure rotation or a rotation-reflection through ϕ. In the above equations, the axis of rotation is taken as the Z axis itself and the X and Y axes lie in a plane perpendicular to it. This choice of axes may not coincide with that taken in the beginning but it will not affect the character arising from a given R. It, therefore, follows that $1 + 2\cos\phi$ and $-1 + 2\cos\phi$ are the characters for a pure rotation and a rotation-reflection respectively. We thus arrive at the result that an invariant point under the operation R gives rise to the character $\pm 1 + 2\cos\phi$ whereas points which are not invariant do not contribute anything to the character. Hence in the reducible representation Γ' defined by the Cartesian co-ordinates, the character of any operation R is $U_R(\pm 1 + 2\cos\phi)$, where U_R is the number of particles that remain in their original position when R is performed.

It has already been pointed out that the representations defined by the normal co-ordinates and the Cartesian co-ordinates are equivalent. The character of an operation R is therefore the same in the two representations. In the previous paragraph we obtained the character of an operation R in the representation defined by the Cartesian co-ordinates. The same expression, namely, $U_R(\pm 1 + 2\cos\phi)$, should therefore be equal to the character of the operation R in the representation Γ defined by the normal co-ordinates $Q_1, Q_2, \ldots Q_n$. We have seen that the normal co-ordinates can be divided into sets of irreducible manifolds and each set corresponds to an irreducible representation Γ_i. If there are n_i such sets that belong to a particular irreducible representation Γ_i, it follows that n_i is the number of times the representation Γ_i is contained in the representation Γ. To obtain the number n_i we use the formula

$$n_i = \frac{1}{N} \Sigma h_\rho \chi_\rho'(R) \chi_i(R),$$

where N is the order of the point group G. $\chi_\rho'(R)$ is the compound character and stands for the expression $U_R(\pm 1 + 2\cos\phi)$ and $\chi_i(R)$ is the character of the operation R in the ith irreducible representation of the group G.

The number derived in this manner includes the normal co-ordinates relating to translations and rotations of the point system as a whole. We can, however, exclude them by removing from $\chi_\rho'(R)$ the character arising from translations and rotations. Considering first translations, we note that the n vectors giving the displacements of the particles in a translation are equivalent to a single vector. The unit vectors X, Y, Z relating to the three translations transform under R as

$$RX = X\cos\phi - Y\sin\phi$$
$$RY = X\sin\phi + Y\cos\phi$$
$$RZ = \pm Z,$$

the + or − sign in the last relation being used according as R is a pure rotation or a rotation-reflection. Hence the character arising from the normal co-ordinates corresponding to translations is $\pm 1 + 2\cos\phi$.

Next, let the displacements of the n particles be such that they represent a rotation of the system as a whole. This state may be expressed by means of the displacement l of a point with the co-ordinates x, y, z. The three components of l are

$$l_x = y\delta z - z\delta y;\quad l_y = z\delta x - x\delta z;\quad l_z = x\delta y - y\delta x;$$

if $\delta x, \delta y, \delta z$ are the components of the rotation vector. l transforms under a rotation through ϕ around the Z axis to l' where

$$l_x' = l_x\cos\phi + l_y\sin\phi$$
$$l_y' = -l_x\sin\phi + l_y\cos\phi$$
$$l_z' = l_z.$$

If the operation is a rotation-reflection through ϕ, the transformation will be

$$l_x' = -l_x\cos\phi - l_y\sin\phi$$
$$l_y' = l_x\sin\phi - l_y\cos\phi$$
$$l_z' = l_z.$$

Thus the character arising from a pure rotation is $1 + 2\cos\phi$ and from a rotation-reflection is $1 - 2\cos\phi$. Finally from the formula

$$n_i = \frac{1}{N}\Sigma\, h_\rho\, \chi_\rho'(R)\, \chi_i(R),$$

we obtain (1) the number of normal modes coming under Γ_i including translations and rotations, (2) the number of translations only, (3) the number of rotations only, (4) the number of normal modes excluding the translations and rotations if we use respectively for $\chi_\rho'(R)$ the four expressions

(1) $\chi_\rho'(R) = U_R(\pm 1 + 2\cos\phi)$

(2) $\chi_\rho'(R) = \pm 1 + 2\cos\phi$

(3) $\chi_\rho'(R) = 1 \pm 2\cos\phi$

(4) $\chi_\rho'(R) = (U_R - 2)(1 + 2\cos\phi)$ or $U_R(-1 + 2\cos\phi)$.

In the last case, the first alternative corresponds to a pure rotation and the second to a rotation-reflection.

These are most useful formulæ and have enabled the subject of vibrational Raman effect to be studied with great ease in many moleculer systems. As has been shown by several authors, by the application of these methods, a considerable amount of useful information can be obtained, not only about how the determinantal equation relating to normal oscillations will factorize on account of the symmetry of the molecule but also about the selection rules and polarization characters of these oscillations as and when they are observed in either Raman effect or infra-red absorption.

6. Raman Effect and Chemical Problems

Apart from very extensive application to a study of molecular structure and chemical constitution, Raman effect has touched numerous other problems of chemistry and in fact to-day its pursuit has very much shifted from the hands of physicists to chemists and physical chemists. Hindered rotation, hydrogen bonding, study of chemical reactions, isotopic substitution, chemical analysis and identification of certain types of compounds are only a few of the recent developments.

In the study of molecular structure, the formulation of interatomic forces has been an important line of speculation and different types of forces have been tried from time to time. One of the principal assumptions has been that only central forces act between the atoms in a molecule, that is the force acting on a given atom in a molecule is the resultant of the attractions and repulsions by all the other atoms. These forces depend only on the distances between various atoms and lie along the lines connecting them. Consequently, the potential energy will be purely a quadratic function of the changes of the distances between the nuclei without any cross products. As an example, we may consider the pyramidal structures of the type XY_3 represented by the tetratomic molecules like ammonia and the trichlorides

of P, As, Sb, Bi, etc. This structure possesses the symmetry elements appropriate to the point group C_{3v} and the Character Table and other necessary data for such molecules are given, as follows, in the usual notation.

Normal Modes of PCl_3, etc.

C_{3v}	E	$2C_3$	3σ	n_i	n_i'	Raman	Infra-red
A_1 ..	1	1	1	3	2	P	A
A_2 ..	1	1	−1	1	0	*f*	*f*
E ..	2	−1	0	4	2	D	A
U_R ..	4	1	2				
$h_\rho \chi_\rho'$ ..	12	0	6				
$h_\rho \phi_\rho'$ ..	6	0	6				
$2\cos\phi$ $(\pm 1 + 2\cos\phi)$ ..	6	0	2				
$\pm 1 + 2\cos\phi$ ..	3	0	1				

There are two non-degenerate vibrations (ν_1 and ν_2) under the class A_1, both active in Raman effect as well as infra-red absorption and two doubly degenerate vibrations (ν_3 and ν_4) under the class E, again both of which are active in Raman effect as well as infra-red absorption. The six degrees of freedom, excluding rotations and translations, are thus accounted for and if we designate the mass of the atom at the apex by M and that of each of the atoms at the base by m, we can obtain

$$\lambda_1 + \lambda_2 = \left(\frac{1}{m} + \frac{3}{M}\cos^2\beta\right) K_1 + \frac{3K_2}{m} \tag{1}$$

$$\lambda_1\lambda_2 = \frac{3}{m}\left(\frac{3m + M}{mM}\right)\cos^2\beta K_1 K_2 \tag{2}$$

$$\lambda_3 + \lambda_4 = \left(\frac{1}{m} + \frac{3}{2M}\sin^2\beta\right) K_1 + \frac{3K_2}{2m} \tag{3}$$

$$\lambda_3\lambda_4 = \frac{3}{4m}\left(\frac{2 - \sin^2\beta}{m} + \frac{3}{M}\sin^2\beta\right) K_1 K_2 \tag{4}$$

The connection between λ and ν has already been explained. In the above expressions, K_1 and K_2 are force constants arising from the variation of distances between the apex and each of the base atoms and between the base atoms themselves respectively. β is the angle between one of the edges of

the pyramid and the axis of symmetry. These expressions were first obtained by Dennison and have since been derived by slightly varying methods by several authors.[8] Validity of the assumption of central forces can be checked as, in many such molecules, all the four frequencies have been measured. The angle β may be obtained from the observed frequencies, for by dividing (4) by (2), we have

$$\cos^2\beta = \frac{1}{4\dfrac{\nu_3^2\nu_4^2}{\nu_1^2\nu_2^2} + \dfrac{3m - M}{3m + M}}. \qquad (5)$$

The following table, taken from Herzberg's book, is very instructive.

Fundamental Frequencies, Force Constants and Angles for the Pyramidal Molecules XY_3, Assuming Central Forces

Molecule	Observed frequencies (cm.$^{-1}$)				β observed	β calculated	Force constants from ν_3, ν_4, β observed, and equations (3) and (4)		Frequencies ν_1 and ν_2 from k_1, k_2, β observed, and equations (1) and (2)	
	ν_1	ν_2	ν_3	ν_4			k_1	k_2	ν_1	ν_2
NH_3 ..	3337	950	3414	1628	69°	73°	3·89	2·83	4473	859
ND_3 ..	2419	749	2555	1191	69°	72°	5·05	2·29	3133	679
PH_3 ..	2327	991	2421	1121	62°	63°	2·57	1·04	2991	784
PD_3 ..	1694	730	..	806	62°	..	..	..	..	..
PF_3 ..	890	531	840	486	62°	56°	3·58	2·93	1045	380
PCl_3 ..	510	257	480	190	64°	51°	1·94	0·63	459	184
PBr_3 ..	380	162	400	116	65°	55°	1·79	0·47	203	203
AsF_3 ..	707	341	644	274	60°	45°	3·23	0·88	723	240
$AsCl_3$ ..	410	193	370	159	59°	50°	·73	0·51	404	154
$SbCl_3$ ..	360	165	320	134	57°	45°	1·49	0·38	357	130
$BiCl_3$ ..	288	130	242	96	57°	25°	0·94	0·20	270	90
							× 10^5 dynes/ cm.	× 10^5 dynes/ cm.		

The agreement between β observed and β calculated and ν_1 and ν_2 observed and ν_1 and ν_2 calculated is "fair in most cases although a few big

[8] See G. Herzberg, *Infra-Red and Raman Spectra of Polyatomic Molecules* (1945). This form and the subsequent data have been taken from this book.

discrepancies occur". This is an illustration of the extent to which central forces generally agree with the facts of observation.

It is interesting to specialise the equations (1) to (4) by putting $\beta = \sin^{-1} 1/\sqrt{3}$; $m = M$ and $K_1 = K_2$ when they will become applicable to tetrahedral molecules like P_4, studied by the author of the present article soon after the discovery of the Raman effect.[9] The results are given below:

$$\lambda_1 = \frac{4K_1}{m}; \quad \lambda_2 = \lambda_3 = \frac{2K_1}{m}; \quad \lambda_4 = \frac{K_1}{m}.$$

They show that there should be three frequencies in the ratio of $2 : \sqrt{2} : 1$. Actually three frequencies at about 606, 465 and 363 cm.$^{-1}$ have been observed with P_4. There is a slight but significant departure between the expected ratio and the ratio of the observed frequencies, again indicating the inadequacy in detail but the adequacy in approximation of the picture furnished by the so-called central forces.

The next assumption widely employed in the literature is closer to the chemist's view of interatomic binding and is called the valence force system. In this system, a strong restoring force in the line of every valence bond is assumed whenever the distance between any two atoms bound by such a bond is changed. In addition, a restoring force opposing a change of the angle between two valence bonds connecting any one atom with two others is assumed. Non-linear symmetric triatomic molecules like H_2O are excellent examples of such studies. The expressions appropriate to the three normal frequencies, all of which are active in infra-red and Raman effect, are[10]

$$\lambda_1 + \lambda_2 = \frac{K_1}{m}\left(1 + \frac{2m}{M}\cos^2\alpha\right) + \frac{2K_3}{m}\left(1 + \frac{2m}{M}\sin^2\alpha\right)$$

$$\lambda_1\lambda_2 = \frac{4K_1K_3}{m}\left(\frac{1}{M} + \frac{1}{2m}\right)$$

$$\lambda_3 = \left(\frac{1}{m} + \frac{2\sin^2\alpha}{M}\right)K_1$$

K_1 is the force in respect of the stretching of the valency bond and K_3 is the resistance to the change of angle between the two valency bonds meeting at the central atom. M is the mass of the central atom, in this case O and m that of each of the outer ones, in this case H and α is the semi-angle between the valency bonds. Investigations of the above expressions by Penney and

---

[9] *Ind. J. Phys.*, 1930, **5**, 35.

[10] See S. Bhagavantam and T. Venkatarayudu, *Theory of Groups and Its Application to Physical Problems* (1951).

Sutherland and a few others with reference to actual data have shown that in this type of molecules, the valence force field is much superior to the central field.

In the case of phosphorus, the present writer has obtained fuller expressions involving valence forces and in the notation of this article, the frequencies work out as

$$\lambda_1 = \frac{4K_1}{m}; \quad \lambda_2 = \lambda_3 = \frac{1}{m}\left[2K_1 + \frac{8K_2}{R^2}\right];$$

$$\lambda_4 = \frac{1}{m}\left[K_1 + \frac{6K_2}{R^2}\right].$$

R is the length of each valence bond and m is the mass of the phosphorus atom. Since two constants are involved in these three measurable frequencies, this set gives again a much better representation of facts.

It has often been found that neither the central force system nor the valence force system nor even a combination of both is able to account fully for the observed frequencies. More general force fields, in some cases approaching the most general one possible, have been tried and we shall not go into them now. One of the more interesting results, from the point of view of a chemist, is that the stretching and bending force constants for various bonds and bond angles are nearly invariant in different molecules. On the other hand, the fact that the stretching force constants for the C ≡ C, C = C and C — C links are approximately 15, 10 and 5×10^5 dynes/cm. is noteworthy. The appearance of frequencies characteristic of specific groups or linkages has been of great help to the chemist in the analysis of the observed vibrational spectra particularly of organic molecules and complex structures.

Formation of molecular aggregates, either as regular polymers or by loose association such as hydrogen bonding and so on, has been extensively studied. Individual examples are many and all of them cannot be referred to here. The polymeric form of SO_3 at lower temperatures and its breaking up at higher temperatures is one of the earliest cases to be studied under this category. Water molecules and their associated forms in the liquid and solid states were the subject of investigation and discussion by a number of investigators. Cleveland[11] and co-workers have worked out a method, with the help of Raman spectra, of following the transition of the aldol-aldehyde mixture to the trimer of isobutyraldehyde. The breaking up of dimers and polymers by the addition of water in several acids, alcohols and so on has also been studied, mostly in a qualitative manner.

[11] *Jour. Amer. Chem. Soc.*, 1943, **65**, 1714.

The C = O frequency has played a great part in enabling the Raman spectroscopists to study the phenomenon of hydrogen bonding. In carboxylic acids, there is a considerable shift of this frequency towards the lower side indicating the formation of dimers through this link. This frequency in a substance like acetone is considerably reduced when studied in the presence of water molecules, presumably as a result of hydrogen bonding between the donor group C = O and the acceptor group O — H. The C = O bond is pictured as delivering the necessary charge to maintain the hydrogen bond O....H resulting in a redistribution of the electron binding around the double bond and a consequent weakening of this bond. The corresponding C = O frequency is lowered appreciably. Such a phenomenon does not take place in neutral solvents like CCl_4.

Chemists have recognized for many years, the existence of stereo-isomers arising out of some kind of restricted rotation around a carbon-carbon double bond but always believed that free rotation existed about a carbon-carbon single bond. This means that compounds like CH_3—CH_3 and CH_2Cl—CH_2Cl can only occur in one form. In the past few years, considerable evidence based on Raman spectroscopy and thermal and electric measurements has been accumulated to indicate that the principle of free rotation is not correct and that in general there are distinct potential minima in one complete rotation about a single bond. Contribution of Raman effect studies to this branch of chemistry has been considerable and the most noteworthy results have been obtained by Langseth and Bernstein, Glockler and Sage and Mizushima and co-workers.[12] By studying the Raman spectra of some 1, 2-dihalogenoethanes in the liquid and solid states, they have shown that for many of them, there is only one potential minimum in one complete rotation about a carbon-carbon single bond as axis and the molecules generally assume what may be called the transform. Further, by comparing the Raman effect data with infra-red measurements, it has been shown that most of the lines observed only in the liquid state should be taken as arising from the vibrations of a second configuration becoming stable in the liquid besides the trans form. The energy difference between these isomers is small but definite.

Similarly in ethane, recent investigations have established the existence of hindered rotation about the carbon-carbon bond, the potential restricting the internal rotation being about 2750 calories. This corresponds to a torsional frequency of one methyl group against the other of 275 $cm.^{-1}$ for

[12] An excellent summary is given by Mizushima in his Peter C. Reilly Lectures in Chemistry at the University of Notre Dame.

C_2H_6 and 200 cm.$^{-1}$ for C_2D_6. Using the Raman and infra-red data, calculations have been made[13] of the entropy of methyl mercaptan (CH_3SH) and the results are shown to lead to the formulation of a potential of 1,460 calories per mole hindering the free rotation of the methyl group relative to the SH bond.

Structures of several interesting compounds like cyclohexane, cyclopropane, sulphur and so on have been fully discussed and in many cases established beyond all doubt.

Deuterium substitution has furnished a whole branch of organic chemistry for the study of isotope effects in relation to Raman scattering. A detailed study of the results obtained with H_2, HD and D_2 in the gaseous state and of the results obtained with H_2O, HDO and D_2O in the liquid state has been of great utility in the realm of simpler molecules. Similarly, a study of benzene and deuterated benzenes has been of help in solving the problem of the structure of benzene in a most satisfactory manner. Many other fully deuterated or partly deuterated organic compounds have been studied with much success. Isotopes of carbon and chlorine are amongst the other elements which have played a part in the Raman spectra investigations.

Amongst the studies directed towards analysis and identification, particular mention should be made of the detection of specific hydrocarbons in samples of petroleum. Several authors have developed rapid and easy methods for such purposes. The octane number of aviation fuel and its relation to anti-knock properties has attracted the attention of Raman spectroscopists and the statement, first given by Bonino, namely, "The square root of the sum of the squares of the intensities of all Raman lines between 600 and 1,000 cm.$^{-1}$ increases with the octane number of the fuel" is of considerable interest and shows the potentialities of this tool of research.

7. Raman Effect and Solid State

There are certain outstanding features regarding the Raman spectra of solids. They are (*a*) there is a general correspondence between the vibrational lines observed in the Raman spectrum of a solid and in that of the corresponding liquid, (*b*) in no case has quantised rotation been detected in solids but many of them show low frequency lines which may be explained as arising from oscillations of the lattice about the equilibrium configuration, (*c*) such lines are often replaced by continuous and unresolved wings in the Raman spectra of the corresponding melts, (*d*) the Raman lines

[13] G. Glockler, *Rev. Mod. Phys.*, 1943, **15**, 111.

observed in most solids, with probably the exception of the amorphous ones, are quite sharp and small in number, and (*e*) in ionic substances like NaCl, the effect is recorded only with great difficulty and that too in the second order.

The author of the present article has shown that much useful information may be gathered by studying the Bravais cell of the smallest size in a crystal as if it were a point group and treating it like a molecule with the appropriate symmetry. It is assumed that what is true of one Bravais cell is true of all cells both statically and dynamically. If the non-equivalent points in the Bravais cell can be divided into groups such that the forces between one group and the other are comparatively feeble, whereas the forces that exist between the members of any one group are quite strong, then it can be shown that the oscillation spectrum will consist of lines divided in a clear-cut manner into low frequency ones and high frequency ones. The low frequency ones are called external oscillations and they involve the movement of whole groups as such against each other. The high frequency ones are called internal oscillations and they involve the movement of individual points within a group against each other. Such studies have been extremely useful in throwing light on interatomic forces in different types of crystals and in quite a few cases, have helped the elucidation and extension of the existing knowledge.

A number of Indian and French workers studied the behaviour of Raman lines observed in different directions with incident polarized light and crystals oriented differently. The intensities of many of the Raman lines change considerably with changing orientations of the crystal axes with reference to the directions of incidence and observation. Such investigations are intimately connected with the interior structure of crystals and yield valuable information. For instance, Aynard[14] studied the orientation of water molecules in gypsum. The Indian workers[15] have studied calcite, sodium nitrate, gypsum, naphthalene and a few other substances by this method in great detail.

Diamond has been very extensively studied, in fact more fully than perhaps any other solid. It shows a sharp and intense line with a frequency shift of $1333 \cdot 8\ \text{cm.}^{-1}$ at -180° C., $1332 \cdot 1\ \text{cm.}^{-1}$ at the room temperature and $1316 \cdot 4\ \text{cm.}^{-1}$ at 860° C. This line stands out most prominently in relation to the other feebler lines that have been recorded. Owing to the importance of this case, amongst others, R. S. Krishnan by using specially

[14] *Compter Rendus*, 1940, **211**, 647.

[15] See papers by J. M. K. Nedungadi and by S. Bhagavantam in *Proc. Ind. Acad. Sci.*, 1939–42.

developed technique, has recorded its second order Raman spectrum and some very faint lines show up in his work. The frequency shifts observed by him are specific in number and are all explained as overtones or combinations of the eight fundamental frequencies, attributed to the diamond structure, a result which comes out of the ideas developed by Professor Raman in respect of crystal dynamics. The numerical values of these fundamental frequencies have been calculated by K. G. Ramanathan as 1332, 1250, 1232, 1149, 1088, 1008, 752 and 620 by making certain assumptions regarding the interatomic forces. The highest frequency 1332 is triply degenerate and is the only mode which is active in Raman effect. All other frequencies, which are also degenerate to different degrees, are inactive as fundamentals in Raman effect but may appear as overtones or combinations with varying intensities. In a series of papers in the *Proceedings of the Indian Academy of Sciences*, workers from the Bangalore school have tried to reconcile the experimental observations in all their details with the calculations of K. G. Ramanathan based on new ideas put forward by Professor Raman.

Such experiments have been extended to many other crystals as well and the fact that they furnish a spectroscopic method of directly obtaining information about the normal frequencies of a crystal lattice has in a way given a fresh impetus to the whole subject of crystal dynamics. Born was the first to develop a theory of crystal oscillations. He showed that the normal oscillations of an infinitely extending chain of atoms with harmonic binding between adjacent ones, fall into two distinct classes, which have been named the acoustical and the optical, the distinction arising from the fact that the sign of the displacement is the same for the neighbouring atoms in the acoustic case whereas it is different in the optical one. The frequencies are spread continuously over wide ranges, the actual distribution depending upon the masses and the forces. Born extended these arguments to infinitely extending three-dimensional crystal lattices and showed that similar results may be obtained for such cases as well. In contradiction to this result, Raman concludes that " in the normal modes of vibration of the structure of a crystal, equivalent atoms in adjacent cells have the same amplitude of vibration, while their phases are either the same or else opposite in successive cells of the lattice along each of its three axes". This gives $2\times2\times2$ or 8 distinct situations regarding the relative phases of the vibrations in a unit cell and in those surrounding it. If there are p atoms in the unit cell, there will be $3p$ variables and $24p$ solutions representing normal modes. Three of these are simple translations. $24p - 3$ solutions remain out of which $3p - 3$ will be such that in them, what is true of the phase in the chosen unit cell

will be true of the phase in all the other unit cells, whereas the remaining $21p$ are such that in them, the phases of vibration are opposite in adjacent cells along one, two or all three of the axes of the lattice. Symmetry of the crystal may result in some of these normal modes having identical frequencies owing to degeneracy.

The fact that the frequency shifts exhibited by crystals are in general sharply defined lines and are relatively few in number is explained by associating them with one or more of the $3p - 3$ primary oscillations. The remaining $21p$ modes are inactive in Raman effect but may appear as overtones and combinations in the second order as feeble lines, which is actually the case with many crystals.

Apart from stimulating the above new ideas regarding solid state, the discovery itself has proved a powerful experimental tool for collecting data regarding the spectra of many crystalline substances under varying physical conditions of temperature, orientation, polymorphic modification and so on.

8. RAMAN EFFECT AS A BRANCH OF SPECTROSCOPY

It was realised, almost immediately after the discovery, that practically all the data that were till then obtained by studying the near and far infra-red absorption spectra of molecules could be collected, in many cases with greater facility, by studying the Raman spectra. This becomes possible because the frequency shifts arise, as has already been explained, by transfer of rotational and vibrational energies between radiation and molecules and in that form they may be studied in the visible region of the spectrum. In quite a few cases, it was later realised that the selection rules operate in such a way, where the molecule possesses a centre of symmetry for instance, that the Raman frequencies and the infra-red frequencies are mutually exclusive so that studies in Raman effect serve as complementary to studies in infra-red. All this has meant the opening up of a new branch altogether of molecular spectroscopy and several laboratories have been devoting themselves to the collection of data regarding complicated organic molecules.

Besides this, a few aspects of interest to the physical spectroscopist have also lent themselves for study. For instance, the phenomenon of alternating intensities in the rotational Raman spectra, has been of great help in supplementing the conclusions reached regarding nuclear statistics, specific heats and molecular constants in simple molecules like hydrogen, deuterium, nitrogen, oxygen and so on. It may be shown[16] that the ratio of the statis-

[16] See Bhagavantam and Venkatarayudu, *Theory of Groups and Its Application to Physical Problems* (1951).

tical weights of the symmetric and anti-symmetric rotational levels is $\frac{I+1}{I}$ or $\frac{I}{I+1}$, depending on whether the nuclei follow Bose-Einstein or Fermi-Dirac statistics. I is the nuclear spin moment in Bohr units. Some of the important results obtained are that hydrogen nuclei obey Fermi-Dirac statistics with nuclear spins $\frac{1}{2}$; deuterium, nitrogen and oxygen nuclei obey Bose-Einstein statistics with nuclear spins one, one and zero respectively.

All diatomic molecules and all linear symmetrical polyatomic molecules exhibit a rotational Raman spectrum because of their optical anisotropy and the selection rule in such cases is $\Delta J = 0, \pm 2$.

Amongst the polyatomic molecules of the symmetrical type, CO_2 and C_2H_2 have been studied. In the case of CO_2, all lines with odd J are missing just as in O_2 and in the case of C_2H_2, all lines with even J are weak as in H_2. These results are to be expected.

The absence of a rotational Raman spectrum for CH_4 has been used to conclude that CH_4 has tetrahedral symmetry with a point group T_d.

A line corresponding to a frequency shift of 121 cm.$^{-1}$ has been recorded by Rasetti in the Raman spectrum of nitric oxide gas and this has been assigned to an electronic transition $^2P_{\frac{1}{2}} \rightarrow {}^2P_{3/2}$. Besides this, some electronic transitions have been reported in the Raman spectra of a few solutions of rare earth salts but they remain unconfirmed.

Amongst the other spectroscopically interesting phenomena observed and studied, mention may be made of (*a*) the Fermi resonance effect which consists in the splitting of a line, if its frequency is close to an overtone or combination of the appropriate type as in carbon dioxide, carbon tetrachloride and so on, (*b*) the Tunnel effect resulting in two lines in the place of one as in the case of ammonia where owing to two possible equilibrium positions of the nitrogen atom in relation to the plane of the three hydrogens, there can be two potential minima in the energy curve relating to the fundamental vibration, (*c*) appearance of overtone lines or second order Raman scattering in some cases, (*d*) splitting of degenerate frequencies when symmetrical groups of atoms go into building up of crystals with lower symmetry as with SO_4 group in gypsum and in anhydrite and (*e*) the verification of Teller-Redlich product rules in the spectra of isotopic molecules.

Thus, Raman spectroscopy to-day is a specialised branch and every spectroscopic laboratory makes provision for its study as an important tool of research.

9. CONCLUSION

In the foregoing pages, a very brief summary is given of the main trends in Raman effect studies since their inception by Professor Raman in 1928 to date. No attempt has been made to either give exhaustive references or treat any particular aspect in a complete manner because such an attempt would have immediately resulted in each section growing into a large volume by itself. There have appeared several monographs and a few good books dealing with the subject and this article is not intended to replace any of them in part or in whole. On the other hand, the author has tried to indicate in appropriate places the extent of the influence which the workers in Raman effect have been able to exert on different branches of modern physics and chemistry and also draw attention to the lines along which new work has been stimulated by this discovery. Solution of many chemical problems is an example of the former and the application of group theoretical methods to molecular oscillations is an example of the latter. There is still very sustained interest and twenty-five years of research on the subject has created for it a prominent place in the field of modern physics and of modern chemistry as an investigational tool of great power.

THE SCATTERING OF LIGHT IN FUSED QUARTZ AND ITS RAMAN SPECTRUM

By Dr. R. S. Krishnan, F.A.Sc.

(From the Department of Physics, Indian Institute of Science, Bangalore 2)

Received March 4, 1953

1. Introduction

Although quartz in the crystalline form has been the subject of numerous investigations, very little work appears to have been done on the scattering of light in fused quartz. This is mainly due to the fact that till recently it was not possible to obtain fairly large specimens of fused quartz of good optical quality. Most of the specimens prepared in the early days had inclusions of air bubbles, the presence of which made accurate measurements on the scattering of light very difficult. The Thermal Syndicate Ltd., recently supplied to the Department a rectangular block ($1'' \times 1'' \times 2''$) with polished faces of fused quartz of optical A quality. This specimen was completely free of any inclusions and exhibited a perfectly bluish track when a beam of light was passed through the same. The acquisition of such a specimen has enabled the author to make a detailed study of the scattering of light and the Raman effect in fused quartz.

2. Some Preliminary Observations

Ever since 1935, the Department of Physics at this Institute has been getting fused quartz materials (such as discs, plates, tubes, rods, etc.) from the Thermal Syndicate Ltd., England. It was found that transparent specimens of fused quartz when exposed to the radiation from a water-cooled, magnet-controlled quartz mercury arc developed a pale violet colouration. Similar colouration is also exhibited by the walls of an ordinary quartz mercury arc after it is run for several hours. Usually, when a plate is exposed to the ultraviolet radiation it develops uniform violet colouration. But a rod of fused quartz (AA quality) of dimension (2 cm. in diameter and 6 cm. long) purchased from the Thermal Syndicate Ltd., in 1939, exhibited a very peculiar behaviour. In order to take the Raman spectrum of the specimen using the λ 2536 excitation, it was covered with black paper at the two ends and also on the sides excepting for two long apertures along the side for illumination. The uncovered portion of the rod was exposed to the strong ultraviolet radiation from a water-cooled magnet-controlled quartz mercury arc. After an hours' exposure, a fairly large number of

violet coloured streaks developed inside the specimen. These streaks coiled round the axis of the rod. Further exposure did not increase the number of streaks. A photograph exhibiting the streaks is reproduced in Fig. 2 *a* on Plate XVII. An end-on view of the streaks is reproduced in Fig. 2 *b* on Plate XVII. The direction of illumination is indicated by the arrow. It is surprising to note that the streaks appeared not only in the direction of illumination but were concentrated in the outer regions, the central portion near the axis of the rod being comparatively free from streaks. This will be evident from a careful examination of the photograph reproduced in Fig. 2 *b*.

When specimens of fused quartz acquired a violet colour on exposure to the far ultraviolet radiations, they were found to be less transparent to λ 2536 radiation than the colourless ones. The spectrum of the light scattered by such coloured specimens under λ 2536 excitation exhibited a weak fluorescence extending from λ 2536 to the visible region. No attempt was, however, made to examine the fluorescence of such specimens in the visible region. Because of the colouration and consequent diminution of transparency to λ 2536 radiation, it was not possible till recently to take satisfactory photographs of the Raman spectrum of fused quartz using λ 2536 excitation.

The violet colour as well as the fluorescence exhibited by fused quartz disappeared completely when the specimens were heated above 250° C. The streaks developed in the fused quartz rod and shown in Figs. 2 *a* and 2 *b* also disappeared on heating. When a specimen which had its colour removed by single heating was exposed to the far ultraviolet radiations it again acquired slight violet colour but not to the same extent. It was noticed that after repeated and prolonged heating and cooling, certain specimens did not acquire the violet colour under ultraviolet excitation.

The rectangular block of fused quartz of optical A quality was, however, found to be free from the troubles mentioned above. As such it was possible to study not only the Rayleigh scattering but also the Raman effect in fused quartz using this specimen and the λ 2536 excitation.

3. The Scattering of Light

The rectangular block of optical fused quartz was first tested for any residual strain. Careful examination of the specimen under crossed polaroids and also using a polariser and a Babinet compensator indicated that it was free from any strain. The interior of specimen was then scanned for any inclusions by sending a powerful condensed beam of sunlight through

it and observing the track inside in the forward direction. It was found to be perfectly free from inclusions of any kind. The depolarisation factors ρ_u, ρ_v and ρ_h were then measured visually employing the Cornu method. The source of illumination was a 40 ampere projection lantern (Magnarc). The convergence of the incident beam was reduced to a minimum. The measured values of ρ_u, ρ_v and ρ_h for ordinary light are 11·5%, 5% and 80% respectively. When the incident beam was polarised with vibrations horizontal, the two tracks of the transversely scattered beam as observed through a Wollaston double-image prism were found to be slightly different in colour at the matching position. In view of this fact and in view of the feebleness of the scattering for this case, ρ_h could not be measured with the same accuracy as ρ_u and ρ_v. In any case, it has been definitely established that ρ_h is less than 100% and that the scattering in fused quartz is multipolar in character. In this respect fused quartz behaves in the same way as ordinary glass (Krishnan, 1936).

The intensity of scattering in fused quartz was measured as follows:— A glass cell with flat windows nearly of the same dimensions as the fused quartz specimen was made as the container for dust-free ether. Using two photo-multiplier tubes and a " ratio circuit ", the intensity of the transversely scattered light in pure ether was compared with that in fused quartz. White light with blue filter was used as the source of radiation. It was found that the scattering in fused quartz was only 1/3·5 of that of pure ether. In ordinary silicate glasses, on the other hand, the intensity of scattering is nearly of the same order or greater than that in ether (Krishnan, 1936).

The absolute intensity of thermal scattering per unit volume of fused quartz could be calculated using the well-known relation

$$I = \frac{\pi^2 k T n^8}{2\lambda^4} \left[\frac{p_{12}^2 + p_{44}^2}{C_{11}} + \frac{p_{44}^2}{C_{44}} \right], \qquad (1)$$

where I represents the intensity of light scattered by a unit volume of the isotropic substance, when the incident light is of unit intensity. The values of the elastic constants C_{11} and C_{44} and the photo-elastic constants p_{12} and p_{44} for fused quartz were taken from the measurements of K. Vedam (1950). The value of I comes to about $1{\cdot}63 \times 10^{-7}$ for λ 4358. Taking the absolute intensity of the transversely scattered light for benzene as $49{\cdot}5 \times 10^{-6}$ for λ 4358 (Carr and Zimm, 1950), and the ratio of intensities of scattering in benzene and ether as 3·06, the observed intensity of scattering in the specimen of fused quartz can be expressed in absolute values as equal to $4{\cdot}84 \times 10^{-6}$. The data for light scattering in fused quartz are summarised below:—

TABLE I. *Fused Quartz*

ρ_u	ρ_v	ρ_h	Intensity of Rayleigh scattering, observed I_0	Intensity of thermal scattering, theoretical I_t	$\frac{I_0}{I_t}$
11·5%	5%	80%	$4{\cdot}84\times10^{-6}$	$1{\cdot}63\times10^{-7}$	29·7

It is evident from a perusal of the figures given in Table I that the observed intensity of scattering in fused quartz is about 30 times greater than the value calculated on the basis of equation (1). This fact supports the view that in fused quartz also there is molecular aggregation as in the case of ordinary glass. The value of the ratio I_0/I_t is of the order of 80 and above in the case of the ordinary silicate glasses.

4. THE DOPPLER-SHIFTED COMPONENTS

To a first approximation, one can assume that the intensity of scattering given by equation (1) above represents the total intensity of the Doppler-shifted components arising from the scattering of thermal elastic waves in the medium. The intensity of these components in fused quartz is therefore only one-thirtieth of that of the observed intensity of Rayeligh scattering (see Table I). As such, in order to record the Doppler-shifted components, it is necessary to employ the best experimental conditions. These are provided by the use of the ultraviolet technique of excitation. Using the λ 2536 radiation as exciter and a mercury vapour filter in the path of the scattered light, the author successfully recorded the Doppler-shifted components in the fused quartz rod mentioned in the Introduction at two different temperatures. A preliminary report of the results was published in *Nature* (Krishnan, 1950). The experiment has now been repeated with the rectangular specimen of fused quartz of optical quality. The photographs of the Doppler-shifted components for transverse scattering and backward scattering taken with a Hilger three-metre quartz spectrograph are reproduced in Figs. 3 *a* and 3 *b* on Plate XVII respectively.

It may be remarked that the components appear broader for the transverse scattering (Fig. 3 *a*) than for the backward scattering (Fig. 3 *b*). This is due to the fact that the angle of scattering in the former case was less well defined than that in the latter case. In the case of transverse scattering, although the arc was kept close, the angle of convergence was limited

to about 15° by the use of opaque parallel vanes. In both cases only the Brillouin components due to the longitudinal sound waves are observed.

The unmodified line has been completely cut off by the mercury vapour filter. It will be observed that the component on the longer wavelength side is less intense than the one on the shorter wavelength side. This asymmetry in intensity is more prominent for the transverse scattering than for the backward scattering. This is due to the fact that the absorption of mercury vapour is not confined to λ 2536·5, but extends though feebly but asymmetrically on either side, the absorption being greater on the longer wavelength side (Mitchell and Zemansky, 1934). Due to this effect the Brillouin components are also reduced in intensity, and this reduction in intensity is more for a component which is nearer to the exciting line than for one on the same side but farther away. The measured separation of the Brillouin components for the two cases are given in Table II.

TABLE II

$\Delta\nu$	Transverse scattering cm.$^{-1}$	Backward scattering cm.$^{-1}$
Observed ..	1·83	2·22
Calculated ..	1·68	2·36

The values of the Doppler shifts calculated from the known value of the elastic constant of fused quartz on the basis of the Brillouin formula are given in Table II. The agreement between the theoretical and experimental values of the shifts is fairly satisfactory.

5. THE RAMAN SPECTRUM

The Raman spectrum of fused quartz was recorded by Gross and Romanova (1929), Kujumzelis (1935) and Langenberg (1937). They used the λ 4358 radiation of the mercury arc for excitation. Using the λ 2536 resonance radiation of mercury as exciter and optical A quality of fused quartz specimen, the Raman spectrum has been photographed. The photograph taken with a Hilger medium quartz spectrograph and with an exposure of eight hours is reproduced in Fig. 1 *a* on Plate XVII. The corresponding microphotometer record is reproduced in Fig. 1 *b*.

The recorded spectrum exhibits only one intense fairly sharp line with a frequency shift of 495 cm.$^{-1}$ Besides this, the spectrum consists of five

broad lines and six bands of varying intensities and widths. The frequency shifts of these are entered in Table III. They are also indicated in the figure. The values of the frequency shifts reported by Gross and Romanova and Kujumzelis are also given in the same table. The most important new result is the appearance of a broad and intense band at $30 \rightarrow 120$ cm.$^{-1}$ which has not been recorded before. This band has its maximum intensity at the low frequency end and the intensity falls off continuously as one moves away from the exciting line. There is a weak continuum extending from 30 cm.$^{-1}$ to about 500 cm.$^{-1}$ and showing fairly well-defined limits at the two ends. This continuum masks the discrete nature of the three broad lines at 285, 370 and 430 cm.$^{-1}$ The lines at 635 and 660 cm.$^{-1}$ are very faint. The bands at $775 \rightarrow 805$ cm.$^{-1}$ and at $810 \rightarrow 845$ cm.$^{-1}$ lie close to each other thereby giving the appearance of a single band.

TABLE III

Raman Spectrum of Quartz

Frequency Shifts in Wavenumbers

Crystalline quartz	Fused Quartz		
	Author	Gross and Romanova	Kujumzelis
128	30 → 120 v.s.		
207			
266	285 b, s.	265, 325	230 → 450
356	370 b, v.s.	365	
394, 403	430 b, v.s.	450	
466	495 v.s.	500	500
	635 v.w.	625	607
695	660 v.w.	660	
796	775 → 805 s.	790 → 830	780 → 840
809	810 → 845 f.s.		
	885 → 940 v.w.		
1063, 1082	1022 → 1098 f.s.	1020 → 1070	1030 → 1090
1160, 1227	1140 → 1245 w.	1180 → 1230	1160 → 1230

v.s. = very strong; *s* = strong; *b* = broad; *v.w.* = very weak; *w* = weak; *f.s.* = fairly strong

The band at $885 \rightarrow 940$ cm.$^{-1}$ is extremely faint and can be observed in the photograph only with some difficulty. It can be seen more clearly in the microphotometer record. Both Kujumzelis and Langenberg reported the existence of a line at about 607 cm.$^{-1}$ This line even if present in the

spectrum taken by the author would have fallen on the mercury line λ 2576 which has a separation of 609 cm.$^{-1}$ from λ 2536.

The frequency shifts of the principal Raman lines observed in the spectrum of crystalline quartz are given in column 1 of Table III. The most intense line of crystalline quartz, 466 cm.$^{-1}$, appears shifted to 495 cm.$^{-1}$ in fused quartz. As is to be expected, the Raman bands observed in the case of fused quartz correspond roughly to the lines of crystalline quartz. It will be interesting to study the Raman spectrum of fused quartz at liquid-air temperatures.

I wish to express my appreciation of the valuable assistance rendered by Dr. P. S. Narayanan who took some of the spectrograms illustrating this paper.

6. Summary

A detailed study of the scattering of light in fused quartz and its Raman spectrum has been made. A rectangular specimen of fused quartz of optical A quality has been used. The depolarisation factors ρ_u, ρ_v and ρ_h have been measured. They are respectively 11·5%, 5% and 80%. The intensity of scattering in fused quartz is found to be 1/3·5 of that in pure dust-free ether. The Doppler-shifted components in the light scattered by fused quartz have been recorded using λ 2536 excitation both for the case of transverse scattering and backward scattering. The observed frequency shifts are in general agreement with those calculated from the known elastic constants of fused quartz.

The Raman spectrum of fused quartz has been recorded with λ 2536 excitation. The recorded spectrum exhibits six lines and six bands of varying width and intensity. The frequency shifts are 285, 370, 430, 495, 635, 660, 30 → 120, 775 → 805, 810 → 845, 885 → 940, 1022 → 1098 and 1140 → 1245 cm.$^{-1}$ Besides, there is a weak continuum extending from 30 cm.$^{-1}$ to 500 cm.$^{-1}$ with well-defined edges.

References

Carr and Zimm .. *Jour. Chem. Phys.*, 1950, **18**, 1616.
Gross and Romanova .. *Z. f. Physik.*, 1929, **55**, 749.
Krishnan, R. S. .. *Proc. Ind. Acad. Sci.*, 1936, 3 A, 211.
——— . *Nature*, London, 1950, **165**, 933.
Kujumzelis .. *Z. f. Physik.*, 1935, **100**, 222.
Langenberg .. *Ann. d. Physik.*, 1937, **28**, 104.
Mitchell and Zemansky .. *Resonance Radiation of Excited Atoms*, 1934.
Vedam, K. .. *Phy. Rev.*, 1950, 77, 472.

DESCRIPTION OF PLATE

FIG. 1 *a*. The Raman spectrum of fused quartz taken with a Hilger medium quartz spectrograph using λ 2536 as exciter.

FIG. 1 *b*. Its microphotometer record.

FIG. 2 *a*. The streaks developed in a specimen of fused quartz under far ultraviolet irradiation.

FIG. 2 *b*. End-on view of the same.

FIG. 3 *a*. An enlarged photograph showing the Brillouin components in the light scattered transversely by fused quartz taken with a Hilger three-metre quartz spectrograph and λ 2536 as exciter.

FIG. 3 *b*. Same for backward scattering.

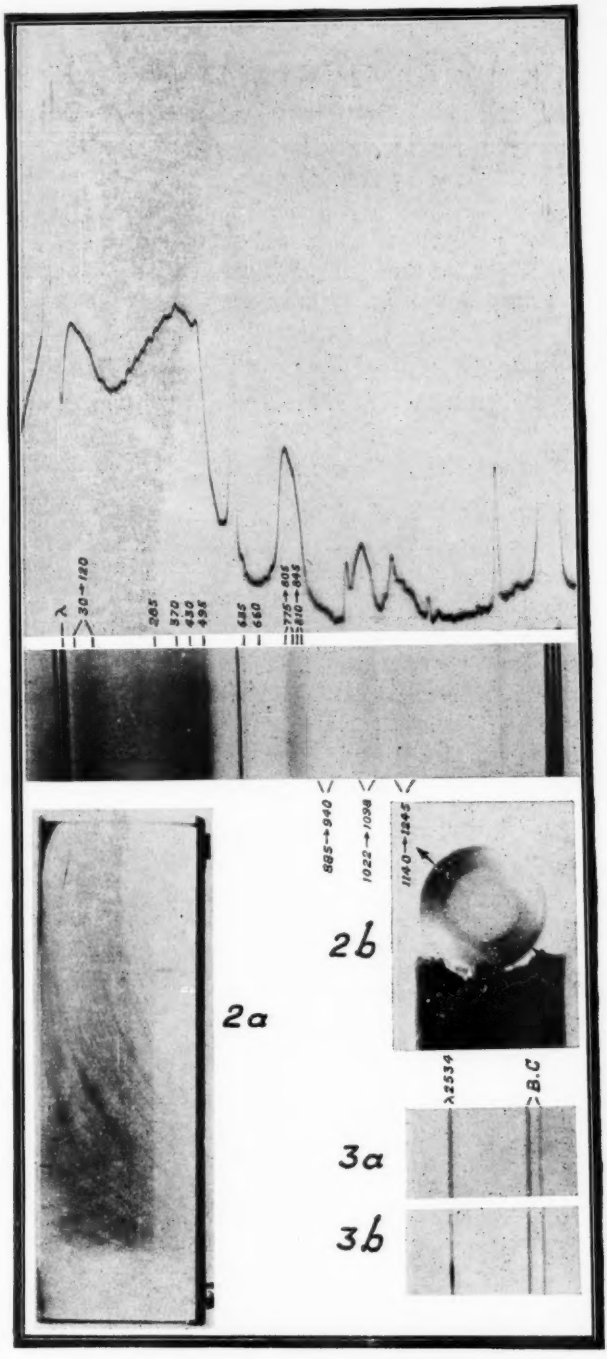
λ
30→120
265
370
430
495
635
660
775→805
810→845
1b
1a
885→940
1022→1038
1140→1245
2b
2a
λ2534
B.C
3a
3b

PHASE RECIPROCITY RELATION IN LIGHT SCATTERING

By N. L. Ramanathan

(From the Department of Physics, Indian Institute of Science, Bangalore-3)

Received January 30, 1953

(Communicated by Prof. R. S. Krishnan, F.A.SC.)

1. Introduction

In a series of papers which appeared in the *Proceedings of the Indian Academy of Sciences*, Krishnan (1934, 1938 and 1939) demonstrated a remarkable phenomenon in the scattering of light by colloids. This phenomenon designated "Krishnan Effect" has important applications in the study of the size, shape and structure of the particles in colloidal systems. Krishnan also derived a reciprocity relation which states that:—The intensity of the horizontal component (H_v) in the light scattered transversely when the incident light is polarised with vibrations vertical is equal to that of the vertical component (V_h) of the scattered light when the incident beam is polarised with vibrations horizontal.

$$H_v = V_h. \tag{1}$$

A direct experimental proof of this result was also given by Krishnan.

Basing himself on these results of Krishnan, Perrin (1942) made a general study of the polarisation of the light scattered by colloidal particles of size comparable to the wavelength of the incident light. Using Stokes' linear representation of the polarisation of light beams, it has been shown that in the case of an asymmetric medium, the scattering through a given angle and for a given wavelength is characterised by sixteen coefficients, which express the four polarisation parameters of the scattered beam in terms of the four corresponding parameters of the incident beam. The law of reciprocity leads to six relations between these sixteen coefficients, and consequently the scattering by an asymmetric medium is characterised by ten independent coefficients only. In the case of a symmetrical medium, however, four of these coefficients become equal to zero leaving only six. Two reciprocity relations are operative in this case. The first of these reciprocity relations is the same as the one established by Krishnan. In this paper, results are reported which verify experimentally the second reciprocity relation in the case of a symmetrical medium.

2. THEORETICAL RESULTS

It is necessary to clarify what is meant by a symmetrical medium. Perrin defines it as follows: "A symmetrical medium has the centre of any large spherical volume as a centre of symmetry and any plane through this centre as a plane of symmetry". For example an isotropic distribution of anisotropic particles may be considered to be statistically isotropic. On the other hand, an optically active medium is asymmetric.

In 1852, Stokes gave a representation of polarised light in terms of four parameters, which are certain functions of the intensity, azimuth, and ellipticity of the beam. The four parameters, usually denoted by I, M, C and S give a complete description of the polarisation characteristics of the light beam. We shall describe the polarisation characteristics of a beam by a set of four symbols (I, M, C, S). The relations between the parameters I_i, M_i, C_i and S_i of the incident beam and I_s, M_s, C_s and S_s of the scattered beam are homogeneous and linear, as is shown by Perrin, who assumes that the linear character of light scattering is maintained in the superposition of non-coherent beams. Since the Stokes' parameters are additive for such superposition, it can be shown that

$$\begin{aligned} I_s &= a_{11} I_i + a_{12} M_i + a_{13} C_i + a_{14} S_i \\ M_s &= a_{21} I_i + a_{22} M_i + a_{23} C_i + a_{24} S_i \\ C_s &= a_{31} I_i + a_{32} M_i + a_{33} C_i + a_{34} S_i \\ S_s &= a_{41} I_i + a_{42} M_i + a_{43} C_i + a_{44} S_i, \end{aligned} \tag{2}$$

where a_{ik} are the sixteen scattering coefficients. For scattering by an isotropic medium, the sixteen scattering coefficients will depend only on the wavelength of light and the angle of scattering for the given medium. Symmetry and reciprocity arguments reduce the number of coefficients in special cases. Symmetry conditions demand that,

$$a_{13} = a_{14} = a_{23} = a_{24} = a_{31} = a_{32} = a_{41} = a_{42} = 0. \tag{3}$$

Consequently, for a symmetrical medium, relations (2) are reduced to

$$\begin{aligned} I_s &= a_{11} I_i + a_{12} M_i \\ M_s &= a_{21} I_i + a_{22} M_i \\ C_s &= a_{33} C_i + a_{34} S_i \\ S_s &= a_{43} C_i + a_{44} S_i. \end{aligned} \tag{4}$$

Further, the law of reciprocity leads to the following relations:—

$$a_{12} = a_{21} \tag{5 a}$$

$$a_{34} = -a_{43} \tag{5 b}$$

Krishnan considered the special cases of incident beams with linear polarisation either horizontal (1, 1, 0, 0) or vertical (1, − 1, 0, 0). These excitation conditions involve only the coefficients a_{11}, a_{12}, a_{21} and a_{22} and the relation $H_v = V_h$ obtained by him is equivalent to the first relation (5 *a*). It is possible to establish the validity of the second relation in a simple way by using appropriately polarised incident beams and also appropriate analysers. Here, we have to use beams for which M = 0 and C and S have values 1 or − 1.

Let us consider a parallel beam of monochromatic light incident on the scattering medium along O_1Z_1 as shown in Fig. 1. The beam is scattered

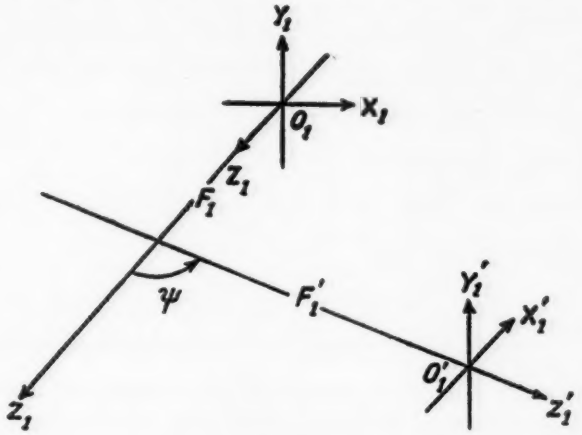

FIG. 1

at the point O along $O_1'Z_1'$ making an angle ψ with O_1Z_1. The co-ordinate axes chosen here are the same as specified by Perrin. In Fig. 1, O_1X_1, O_1Y_1 and O_1Z_1 are the axes for the incident beam $O_1'X_1'$, $O_1'Y_1'$ and $O_1'Z_1'$ for the scattered beam; both of these are right-handed. All positive and negative signs in the following consideration are assigned with reference to this system of axes.

For a beam linearly polarised at angle θ, the Stokes parameters are (1, cos 2θ, sin 2θ, 0). Hence for $\theta = \pm 45°$ we get (1, 0, $\pm$ 1, 0). Similarly for a beam passing through a quarter wave plate with its fast axis along

OY_1 and a nicol at any angle θ, we have the parameters $(1, \cos 2\theta, 0, \sin 2\theta)$. Therefore for circularly polarised light, for which θ must be $\pm 45°$, the parameters become $(1, 0, 0, \pm 1)$ depending on whether the rotation is left-handed or right-handed.

Consider now a beam linearly polarised at angle θ_1 to the horizontal. Its parameters are

$$(1, +\cos 2\theta_1, \sin 2\theta_1, 0). \tag{6}$$

If this beam is scattered by a symmetrical medium, we get from (4) and (6)

$$\begin{aligned} I_1' &= a_{11} + a_{21} \cos 2\theta_1 \\ M_1' &= a_{21} + a_{22} \cos 2\theta_1 \\ C_1' &= a_{33} \sin 2\theta_1 \\ S_1' &= a_{43} \sin 2\theta_1. \end{aligned} \tag{7}$$

If the scattered beam is observed through a birefringent crystal with its axes vertical and horizontal, introducing a phase difference ϕ_2, then the parameters are

$$I_1',\ M_1',\ (C_1' \cos \phi_2 - S_1' \sin \phi_2),\ (C_1' \sin \phi_2 + S_1' \cos \phi_2).$$

The intensity J_1 of this beam is,

$$J_1 = \tfrac{1}{2} (I_1' + M_1' \cos \theta_2 - C_1' \cos \phi_2 \sin 2\theta_2 + S_1' \sin \phi_2 \sin 2\theta_2).$$

Substituting from (7), we get

$$\begin{aligned} J_1 = \tfrac{1}{2} [&a_{11} + a_{21} \cos 2\theta_1 + (a_{21} + a_{22} \cos 2\theta_1) \cos 2\theta_2 \\ &- a_{33} \sin 2\theta_1 \cos \phi_2 \sin 2\theta_2 + a_{43} \sin 2\theta_1 \sin \phi_2 \sin 2\theta_2]. \end{aligned} \tag{8}$$

This is the residual intensity of a beam which is originally linearly polarised at θ_1 and the light scattered from which is observed through an elliptic analyser defined by (ϕ_2, θ_2). If now the incident beam is elliptically polarised and the scattered beam is observed through a linear analyser, it can be shown in the same manner as above that the intensity J_2 is given by

$$\begin{aligned} J_2 &= \tfrac{1}{2} (I_2' + M_2' \cos 2\theta_1 - C_2' \sin 2\theta_1) \\ &= \tfrac{1}{2} [a_{11} + a_{21} \cos 2\theta_1 + (a_{21} + a_{22} \cos 2\theta_1) \cos 2\theta_2 \\ &\quad - a_{33} \sin 2\theta_1 \cos \phi_1 \sin 2\theta_2 - a_{34} \sin 2\theta_1 \sin \phi_1 2\theta_2], \end{aligned} \tag{9}$$

where ϕ_1 is the phase difference introduced by the birefringent crystal[1] in the incident beam, θ_1 is the angle between the plane of the polariser in the incident beam and the horizontal and θ_2 is angle of the analyser to the horizontal.

3. Application of the Above Theory to Particular Cases

Consider two cases (1) $\theta_1 = 45°$, $\phi_1 = 0$ and (2) $\theta_1 = 45°$, $\phi_1 = 90°$ in the incident beam. We then get incident beams polarised at 45° in the former case and left circularly polarised in the latter. Suppose we analyse the first beam by a combination of a birefringent plate (ϕ_2) and a linear polariser at θ_2 and the second beam by a linear analyser alone at θ_2, then the final intensities of the two beams become

$$J_1 = \tfrac{1}{2}[a_{11} + a_{21}\cos 2\theta_2 - a_{33}\cos\phi_2 \sin 2\theta_2 + a_{34}\sin\phi_2 \sin 2\theta_2] \qquad (10\,a)$$

and

$$J_2 = \tfrac{1}{2}[a_{11} + a_{21}\cos 2\theta_2 - a_{34}\sin 2\theta_2] \qquad (10\,b)$$

Case 1.—When $\theta_2 = -45°$, $\phi_2 = 90°$, *i.e.*, when the linear polarisers are parallel and both the quarter wave plates have their fast axes in the same direction (vertical)

$$J_1 = \tfrac{1}{2}(a_{11} + a_{43}); \text{ and } J_2 = \tfrac{1}{2}(a_{11} - a_{34}) \qquad (11)$$

Case 2.—When $\theta_2 = 45°$, $\phi_2 = -90$, *i.e.*, when the polarisers are crossed and the fast axes of the quarter wave plates are parallel

$$J_1 = \tfrac{1}{2}(a_{11} - a_{43}); \text{ and } J_2 = \tfrac{1}{2}(a_{11} + a_{34}) \qquad (12)$$

Case 3.—When $\theta_2 = 45°$, $\phi_2 = -90°$, *i.e.*, when the polarisers are parallel, but the fast axes are at right angles

$$J_1 = \tfrac{1}{2}(a_{11} - a_{43}); \text{ and } J_2 = \tfrac{1}{2}(a_{11} - a_{34}) \qquad (13)$$

Case 4.—When $\theta_2 = -45°$ and $\phi_2 = -90°$, *i.e.*, when the polarisers are crossed and the fast axes are at right angles

$$J_1 = \tfrac{1}{2}(a_{11} + a_{43}); \text{ and } J_2 = \tfrac{1}{2}(a_{11} + a_{34}) \qquad (14)$$

Case 5.—There is no analyser in the path of the scattered light. The scattered intensities in this case can be readily shown to be given by

$$J_1 = a_{11}, \qquad J_2 = a_{11} \qquad (15)$$

and the equality of the observed scattered intensities would be a test of equality of intensity of the incident beams.

If our reciprocity relation $a_{34} = -a_{43}$ is true, then in cases (i) and (ii) the intensities J_1 and J_2 will be equal; but in cases (iii) and (iv) they will be unequal. The essential condition appears to be that the two quarter wave plates should have their fast axes parallel for the two intensities to be equal. It is immaterial whether the two fast axes are both horizontal or both vertical. Also, the equality is maintained whether the polarisers are parallel

or crossed (with θ_1, $\theta_2 = \pm 45°$). On the other hand, if the axes of the quarter wave plates are crossed, this equality does not hold.

In fact, from the general equations (8) and (9) for J_1 and J_2, it is seen that $J_1 = J_2$ if $\phi_1 = \phi_2$ for any pair of values θ_1, θ_2 provided the reciprocity relation $a_{34} = -a_{43}$ holds.

4. EXPERIMENTAL VERIFICATION

In order to verify the results obtained above, the following experimental set-up was used (see Fig. 2). Light from a mercury arc A, collimated

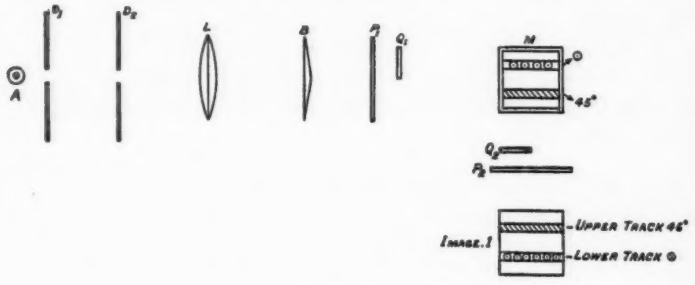

FIG. 2

by diaphragms D_1 and D_2 and monochromatised by a green filter F, was split up into two beams of equal intensities by means of a biprism B. A polaroid P_1 polarised the beam at $+ 45°$ to the horizontal. The upper beam was in addition passed through a quarter wave plate Q_1 with its fast axis vertical before traversing the scattering medium M, which in this case was dilute milk. In effect, the upper beam was left circularly polarised and the lower beam was linearly polarised at $+ 45°$ giving the required exciting conditions. Both the beams were scattered by the colloidal medium. In the transverse horizontal direction the lower scattered track was observed through a quarter wave plate Q_2 (with its axes kept vertical and horizontal) and a polaroid P_2 at 45°, whereas the upper one was viewed through the same polaroid P_2 only. It was possible to keep the quarter wave plate Q_2 with its fast axis either vertical or horizontal. The analyser P_2 was also capable of rotation. The tracks were viewed and later photographed for the five different orientation of the analysers mentioned in Cases (1) to (5) in the previous section. The lower beam corresponds to J_1 and the upper to J_2 of equation (11).

The photographs of the tracks for the five cases are reproduced in Fig. 3 on Plate XVIII.

Case I.—$\theta_2 = 45°$, $\phi_2 = 90°$

The two tracks in the scattered light are of equal intensity.

Case II.—$\theta_2 = -45°$, $\phi_2 = 90°$

Again the intensities are equal; but compared to Case I, the tracks are less bright.

Case III.—$\theta = 45°$, $\phi_2 = -90°$

The two scattered tracks are of unequal intensity.

Case IV.—$\theta = -45°$, $\phi_2 = -90°$

Here again the tracks differ widely in intensity.

Case V.—No analyser.

The intensities are equal, showing that the incident tracks are of the same intensity.

In addition, a visual examination of the scattered tracks indicated that when the quarter wave plates used were similar, the intensities of the tracks remained equal to each other, whatever may be the orientations of the polaroids P_1 and P_2. It therefore follows that the essential condition for equality is the equality of phase change introduced by the birefringent plate.

5. Discussion

The observed equality of intensity of the two scattered tracks for Cases I and II mentioned above establishes the validity of the relation (5 *b*), *i.e.*, $a_{34} = -a_{43}$. The present investigation thus gives for the first time experimental proof for the existence of a second reciprocity relation for symmetrical media. This second relation may be distinguished from Krishnan's relation by naming it as "The Phase Reciprocity Relation".

Table I

Case	Orientations of polariser and analyser				Relation between corresponding type of polarisers and analysers		Intensities of the tracks J_1 and J_2
	Lower beam		Upper beam				
	Polariser	Analyser	Polariser	Analyser	Linear	Circular	
I	+45	Rt. ⊙	Lt. ⊙	+ 45	Parallel	Crossed	Equal
II	+45	Rt. ⊙	Lt. ⊙	− 45	Crossed	Parallel	Equal
III	+45	Rt. ⊙	Lt. ⊙	+ 45	Parallel	Parallel	Unequal
IV	+45	Rt. ⊙	Lt. ⊙	− 45	Crossed	Crossed	Unequal

The significance of the negative sign in the phase reciprocity relation is clearly brought out as follows from an analysis of the polarisation characters in the four cases studied (see Table I). When the linear and circular analysers are both parallel or both crossed, the two scattered tracks are not of the same intensity, whereas when one of them is parallel and other crossed, the intensities are equal. This is a direct consequence of the presence of the negative sign in the relation, 5 (*b*). The sign of the coefficients in the case of dilute milk, the medium used in the present experiment has also been determined. The absolute intensities of the scattered tracks in Case II were found to be less than those in Case (I). It can therefore be inferred from equations (11) and (12) that a_{34} is negative and a_{43} is positive.

My thanks are due to Professor R. S. Krishnan for his guidance and kind interest in the work. I am grateful to Dr. G. N. Ramachandran and Dr. S. Ramaseshan for valuable suggestions.

SUMMARY

The paper describes the experimental verification of a second reciprocity relation in the scattering of light by colloids the existence of which was first pointed out by Perrin. This is in addition to the reciprocity relation established by Krishnan (1935). This second relation has essentially to do with the phase changes which occur in the scattering and has the form $a_{34} = -a_{43}$ for a symmetrical medium having no optical activity, where a_{34} and a_{43} are two of the coefficients in the linear representation relating the Stokes parameters (I, M, C, S) of the incident and scattered beams.

REFERENCES

1. R. S. Krishnan .. *Proc. Ind. Acad. Sci.*, 1934, **1**, 211, 717, 782, 915; 1938, **7**, 21, 91; 1939, **10**, 395.
Kolloid. Zeit., 1938, **2**, 84.
2. Francis Perrin .. *Journ. Chem. Phys.*, 1942, **10**, 410.
3. C. G. Stokes .. *Trans. Camb. Phil. Soc.*, 1852, **9**, 399.

(1)

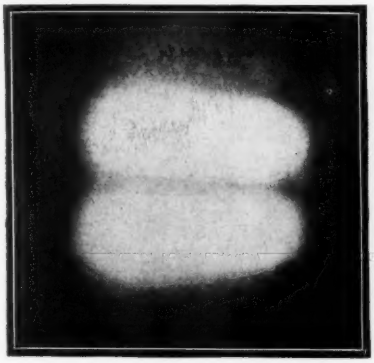

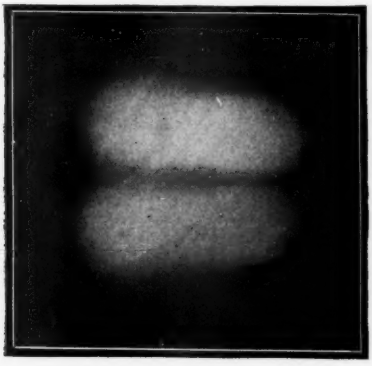

(2)

(3)

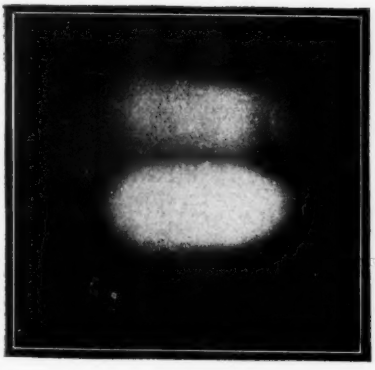

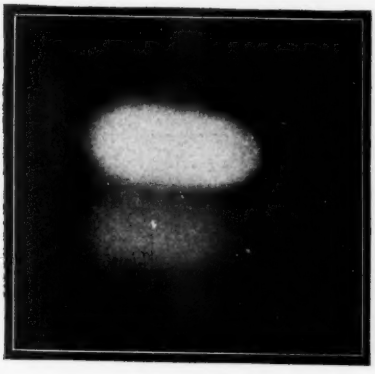

(4)

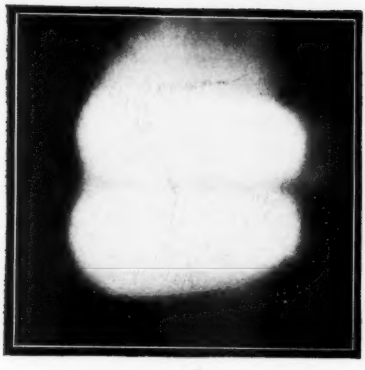

(5)

RAMAN SPECTRA OF CRYSTALLINE SULPHATES OF ZINC, MAGNESIUM AND SODIUM

By C. Shantakumari*

(Department of Physics, Indian Institute of Science, Bangalore-3)

Received January 30, 1953

(Communicated by Prof. R. S. Krishnan, F.A.SC.)

1. Introduction

A study of the Raman spectra of the sulphates in the form of single crystals is of interest in view of the information it will provide regarding their lattice spectra, the symmetry of the SO_4 ion in these crystals, and the influence of the water of crystallisation on their spectra. Further, some of the hydrated sulphates are efflorescent and the difficulties met with in recording their complete spectra, using λ 4048 and λ 4358 of mercury, are considerable (Bouhet and Lafont, 1949). Hence the author carried out an investigation of the Raman spectra of the hydrated sulphates of zinc, magnesium, magnesium-ammonium and sodium and also of Thenardite (anhydrous sodium sulphate), using the λ 2537 radiation of mercury as exciter, and the results are given below.

2. Experimental Details and Results

In all these cases, the Raman spectra excited by λ 2537 were recorded with the help of a Hilger medium quartz spectrograph having a dispersion of about 140 cm.$^{-1}$ in the above region. Using a slit width of 0·035 mm., the time of exposure necessary to get a well exposed spectrogram was of the order of 16 hours.

Zinc and Magnesium Sulphates.—These have been studied in the past by Krishnamurthy (1930), Nisi (1931) and Rao (1941), Krishnamurthy utilized the powder technique, while the other two used single crystals. Among them Rao recorded the maximum number of lines, namely, eight (455, 613, 981, 1046, 1101, 3226, 3285 and 3458 cm.$^{-1}$) in the case of magnesium sulphate and eleven (57, 94, 252, 375, 447, 608, 986, 1120, 1057, 3207 and 3395 cm.$^{-1}$) with zinc sulphate. Recently a detailed investigation has been made of the Raman spectrum of Epsomite ($MgSO_4.7H_2O$) by Bouhet and Lafont (1949). These authors have confined themselves to a thorough analysis of the polarisation and intensities of the Raman frequencies due

* Now Lecturer in Physics, St. Theresa's College, Ernakulam.

to the sulphate ion for different orientations of the crystal. But they have failed to record any of the low frequency lines.

The specimens used in the present investigation were grown from aqueous solutions by the method of slow evaporation. The crystals grown thus were always strongly elongated in the direction of the *c*-axis. The exciting radiation was incident on the *b* (010) face of the crystal and the transversely scattered light was taken along the *c*-axis. The frequency shifts of the 24 Raman lines observed with magnesium sulphate are 56, 75, 97, 118, 150, 252, 303, 445, 461, 609, 620, 986, 1059, 1064, 1076, 1098, 1134, 1148, 3185, 3228, 3338, 3406, 3446, and 3485 cm.$^{-1}$ and those of the 23 lines with zinc sulphate are 56, 70, 104, 128, 151, 212, 252, 373, 396, 445, 461, 609, 620, 990, 1057, 1062, 1094, 1121, 1141, 3154, 3392, 3436 and 3512 cm.$^{-1}$ All the Raman lines in these sulphates both in the high and low frequency regions appear very diffuse. In the case of magnesium sulphate, the group of lines at about $\sim$1105 cm.$^{-1}$ is extremely complex. It is present as a wide band extending from 1040 to 1170 cm.$^{-1}$ However, closer examination reveals that this group consists of three intense doublets, whereas Bouhet and Lafont have reported the existence of fourteen lines in this region. But among these, eight are very feeble in intensity. The frequency shifts of the intense ones recorded by them agree well with those of the three doublets observed by the author. The very faint lines 449 and 615 cm.$^{-1}$ reported by them could not be identified in the spectrum recorded by the author.

The low frequency lines of zinc sulphate are in general more intense than those of magnesium sulphate. All the seven lattice lines of magnesium sulphate and the four lattice lines 70, 128, 151 and 212 cm.$^{-1}$ of zinc sulphate have been recorded for the first time. The line at 258 cm.$^{-1}$ is strong in both sulphates. In the case of zinc sulphate, this line is accompanied on the low frequency side by a band which shows a faint maximum at 212 cm.$^{-1}$

Magnesium-Ammonium Sulphate.—The Raman spectrum of magnesium-ammonium sulphate was studied by Nayar (1938) who recorded two Raman lines of frequency shifts 3284 and 3399 cm.$^{-1}$ and three bands of frequency shifts 2848, 3070 and 3192 cm.$^{-1}$ The first two are due to water molecules, while the last three are to be attributed to the vibrations of the NH_4 ion. The present study reveals as many as 23 Raman lines of which eighteen have been recorded for the first time. The frequency shifts of these are 54 (4), 89 (3), 130 (7), 147 (5), 198 (5), 220 (1), 265 (2), 455 (12), 622 (7), 979 (20), 1061, 1072, 1091, 1102, 1127, 1141, 1433 (8), 1469 (1), 2830 (3), 3060, 3281 (5), 3331 (5) and 3396 (5) cm.$^{-1}$ The figures within brackets give rough estimate of the relative intensities of the lines. Since the intense group of lines at

about 1100 cm.$^{-1}$ consists of close doublets, and appears to be in reality a number of close lines, the relative intensities have been left out.

Thenardite and Glauber's Salt.—Thernardite, the naturally occurring form of anhydrous sodium sulphate, was studied in the form of crystal powder by Krishnamurthy (1930). He recorded a single Raman line with a frequency shift of 996 cm.$^{-1}$ The Raman spectrum of Glauber's salt, which is the hydrated form of the same salt with 10 molecules of water of crystallisation, was photographed by Nisi (1931) and it exhibited three lines with frequency shifts 991, 1125 and 3438 cm.$^{-1}$

The Raman spectrum of thenardite recorded by the author revealed the existence of 13 Raman lines, the frequency shifts of which are 52, 76, 122, 164, 451, 467, 609, 624, 665, 995, 1087, 1117 and 1133 cm.$^{-1}$ In the case of Glauber's salt the light was incident along the X-axis of the crystal and the scattered light was taken in the perpendicular direction. These crystals, themselves strongly efflorescent were almost reduced to powder after fifteen minutes of exposure to the strong ultraviolet source. Moreover, as the salt decomposed at 32·5° C., the heat due to proximity of the arc was found to be sufficient to melt the crystal. To overcome this difficulty the following method was used. A small brass box was provided with two quartz windows on adjacent sides, one for the incident light and the other for the transversely scattered light. The lid of this box was closed air-tight by means of vacuum grease. To one of the sides of the box was attached a short brass rod and this was kept at the centre of a copper vessel containing a mixture of ice and salt. The crystal was kept in the desired orientation inside the box and the above-mentioned arrangement served to maintain the crystal at a temperature far below its melting point and thus prevent the decomposition of the crystal. The frequency shifts of the lines recorded are 53, 134, 158, 231, 292, 441, 463, 571, 590, 609, 627, 992, 1088, 1117, 1136, 3271, 3332, 3378, 3438 and 3516 cm.$^{-1}$

3. Discussion

Zinc and Magnesium Sulphates.—These are isomorphous and form double salts in any proportion. At ordinary temperatures they crystallise in the orthorhombic system with seven molecules of water of crystallisation and belong to the point group D_2 and consequently possess three binary axes of symmetry. The unit cell contains 4 molecules. It is easily seen that in both cases the number of lattice lines observed is very small compared to that which can be theoretically expected. However, it is reasonable to suppose that of the theoretically possible ones, the rotatory type of lattice oscillations has negligible intensity as the polarisability of the free SO_4 ion

is known to be spherically symmetric and is not distorted very much in the crystal. In addition, some of the lattice oscillations may have nearly the same frequency, but to establish this it is necessary to study the intensity and polarisation of the lattice lines for different orientations.

Frequencies of the SO_4 Ion.—The proper symmetry of the SO_4 ion in zinc and magnesium sulphates is no longer T_d but only C_1. However, X-ray studies show that one of its planes of symmetry coincides with the XZ plane of the crystal with its two-fold axis making an angle of about 35° with the Z-axis. Due to the lower symmetry, the degenerate oscillations of the free ion split in the crystal, so that all the nine distinct modes of the free SO_4 ion can appear in Raman effect. Further as there are 4 such groups in the unit cell and each oscillation by coupling can give rise to 4 internal oscillations of the crystal, one totally symmetric and the other three antisymmetric with respect to the binary axes of symmetry, there are 36 Raman active frequencies due to the sulphate ion. Of these 9 belong to the totally symmetric class and the remaining 27 to the antisymmetric class. Following the method adopted by Couture (1947) in the case of barytes and celestite, Bouhet and Lafont (1949) have been able to study the tensor appertaining to the variations of polarisability for the different oscillations and for different orientations of the crystal and assign the observed frequencies to the various possible internal oscillations of the SO_4 ion. The frequencies observed by the author in the case of Epsomite and included in Table 1 are in agreement with those of Bouhet and Lafont. However, the small splitting due to the presence of 4 sulphate groups could not be identified by the author as separate lines as the spectrograph used had a dispersion of about 140 cm.$^{-1}$ only. A comparison of the results obtained in the case of magnesium and zinc

TABLE 1

Type	$MgSO_4.7H_2O$	Type	$ZnSO_4.7H_2O$
B_1, B_3	445	B_1, B_3	445
B_2	461	B_2	461
A_1	609	A_1	609
B_1, B_2	620	B_1, B_2	620
A_1	986	A_1	990
A_1	1059	A_1	1057
B_3	1064	B_3	1062
B_2, B_3	1076	A_1, B_1, B_3	1094
A_1, B_3, B_1	1098	A_1, B_2	1121
A_1	1134	B_1, B_3	1141
B_1, B_3	1148		

sulphates, in the light of the above-mentioned work of Bouhet and Lafont enables one to assign the observed frequencies as in Table I above.

Water Bands.—Hibben reported the existence of five water bands with frequency shifts at 3184, 3227, 3404, 3445, and 3481 cm.$^{-1}$ in the case of magnesium sulphate and three at 3151, 3436 and 3503 cm.$^{-1}$ in the case of zinc sulphate. The spectra recorded by the author exhibits in addition to these, one band at 3328 cm.$^{-1}$ in magnesium sulphate and one at 3342 cm.$^{-1}$ in the case of zinc sulphate. In Table II are given the frequency shifts corresponding to the maxima of water bands in crystalline magnesium and zinc sulphates recorded by the author and those in manganous and ferrous sulphates heptahydrates investigated by Rao (1941).

TABLE II

Substance	Maxima of water bands					
$MgSO_4.7H_2O$	3185	3228	3328	3406 3445	3485	..
$ZnSO_4.7H_2O$	3154	..	3342	3436	..	3512
$FeSO_4.7H_2O$	..	3225	3337	3432	..	3543
$MnSO_4.7H_2O$	..	..	3399	3467	..	..

The bands which exist in common to all the sulphates are the ones in the region of 3350 and 3450 cm.$^{-1}$ Apart from this no direct relation seems to exist in the characteristics of the water bands of these sulphates though all of them have analogous crystal structure and contain the same number of molecules of water of crystallisation.

Magnesium-Ammonium Sulphate.—This double sulphate of magnesium and ammonium crystallises in the monoclinic system with six molecules of water of crystallisation. Tne space group is C_{2h}^5 and the unit cell contains 2 molecules of $MgSO_4(NH_4)_2SO_4.6H_2O$. The character table derived by taking magnesium ion, ammonium ion and sulphate ions as separate groups and neglecting the water of crystallisation shows that there should be 12 rotatory and 12 translatory types of lattice oscillations active in Raman effect. But in the spectrogram only seven are observed and the difference might be due to the same reasons as those given in the case of zinc and magnesium sulphates. However, there is a great similarity between the lattice spectrum of $MgSO_4.7H_2O$ and that of the double sulphate.

Internal Oscillations.—Due to the low symmetry of the SO_4 ion in this crystal there is a removal of the degeneracy as in the cases studied above and the four distinct frequencies of the free tetrahedral SO_4 ion split up into 9 distinct modes and a further splitting also is caused by the coupling of the four SO_4 ions which the unit cell contains. The recorded spectrum exhibits 10 Raman lines which can be attributed to these. However, for a detailed analysis, polarisation data are necessary.

Frequencies due to the NH_4-Ion.—In contrast to the complete removal of degeneracy observed in the case of the SO_4 ion we find that only four lines which can be attributed to the NH_4 ion are present in the crystal though all of them have frequency shifts higher than the known frequencies of the free NH_4 ion.

In fact no line corresponding to ν_2 (3162 cm.$^{-1}$) of the free ion could be identified in this case.

Water Bands.—The spectrum due to the water of crystallisation consists of only a very broad and intense band with three maxima at 3281, 3331 and 3396 cm.$^{-1}$, which coincide approximately with a few of the bands observed with Epsomite.

Thenardite and Glauber's Salt.—The crystal of thenardite belongs to the orthorhombic bipyramidal class and the space group is V_h^{24}. The unit cell contains eight molecules of Na_2SO_4. Glauber's salt crystallises in the monoclinic class with well-developed *c* (001) and *a* (100) faces. Details regarding its structure are not known.

In Table III are given the internal frequencies of thenardite and Glauber's salt along with the corresponding frequencies of the free sulphate ion.

TABLE III

Substance	Internal oscillations cm.$^{-1}$			
Free SO_4 ion ..	983 (ν_1)	458 (ν_2)	620 (ν_3)	1105 (ν_4)
Thenardite (Na_2SO_4) ..	995	451 467	607 629 665	1087 1117 1133
Glauber's salt .. ($Na_2SO_4.10H_2O$)	992	441 463	609 627	1088 1117 1136

It is noticed that all the degenerate lines split up into the corresponding components. All the lines are broad and diffuse in the case of Glauber's salt, while they are quite sharp in thenardite. This diffuse nature of the Raman lines is prominent in all the sulphates, so far studied, which possess water of crystallisation. Embirikos (1930) has also observed that the lines become more diffuse with increasing number of molecules of water of crystallisation.

Like the other sulphates, thenardite and Glauber's salt give only a comparatively small number of lattice lines despite the fact that theoretically many more can be expected.

The five high frequency lines which appear in the spectrum of Glauber's salt, namely 3271, 3332, 3378, 3438 and 3516 are to be attributed to the water molecules.

In conclusion the author wishes to express her sincere thanks to Professor R. S. Krishnan for suggesting the problem and for his help and guidance.

Summary

The Raman spectra of single crystals of the sulphates of zinc, magnesium, magnesium-ammonium and sodium (both thenardite and Glauber's salt) have been investigated using the λ 2537 resonance radiation of mercury as exciter. The important results obtained may be summarised as follows:—

The Raman spectra of thenardite, the anhydrous sodium sulphate and of magnesium-ammonium sulphate have been recorded for the first time. In the case of the sulphates of zinc, magnesium and sodium (Glauber's salt) the recorded spectra indicate the existence of 23, 24 and 20 frequency shifts of which 16, 11 and 17 respectively are newly reported. The low frequency spectrum in each case has the following shifts:—

(*a*) Zinc: 56, 70, 104, 128, 151, 212, 252 and 373 cm.$^{-1}$;

(*b*) Magnesium: 56, 75, 97, 118, 150, 252 and 303 cm.$^{-1}$;

(*c*) Magnesium-ammonium: 54, 89, 130, 147, 198, 220 and 265 cm.$^{-1}$;

(*d*) Thenardite: 52, 76, 122 and 164 cm.$^{-1}$; and

(*e*) Glauber's salt: 53, 134, 158, 231 and 292 cm.$^{-1}$ The Raman lines of the hydrated sulphate are found to be more diffuse than the corresponding lines of the anhydrous sulphate. The results obtained have been discussed in the light of the known structures of these crystals.

REFERENCES

Bouhet and Lafont .. *Journ. Chem. Phys.*, 1949, **46**, 66.

Krishnamurthy .. *Nature*, 1930, **126**, 169.

———— .. *Ind. Journ. Phys.*, 1930, **5**, 183.

———— .. *Ibid.*, 1930, **5**, 633.

Lakshmana Rao .. *Proc. Ind. Acad. Sci.*, 1941, **14 A**, 48.

Nayar, P. G. N. .. *Ibid.*, 1938, **8**, 419.

Nisi, H. .. *Jap. J. Physics.*, 1931, **7**, 1.

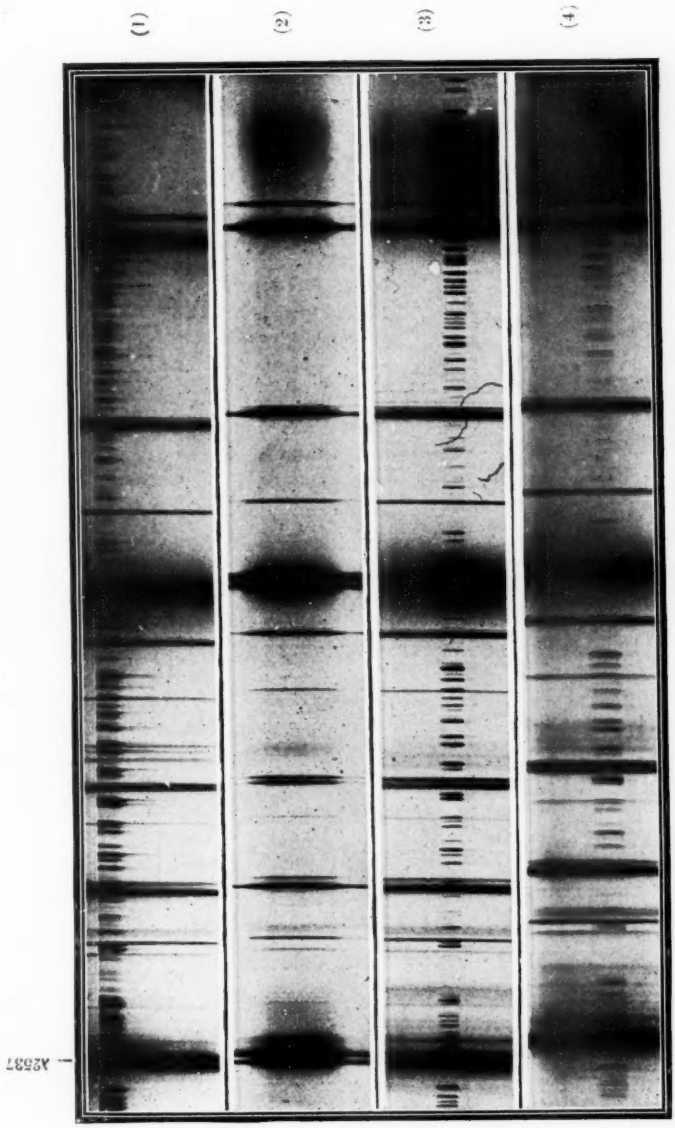

Raman Spectra of Crystalline Sulphates

(1) Na_2SO_4 (2) $Na_2SO_4\,10H_2O$ (3) $ZnSO_4\,7H_2O$ (4) $MgSO_4\,7H_2O$

RAMAN SPECTRA OF CRYSTALLINE ACETATES (SODIUM, MAGNESIUM AND BARIUM)

By V. M. Padmanabhan

(*Department of Physics, Indian Institute of Science, Bangalore* 3)

Received January 30, 1953

(Communicated by Prof. R. S. Krishnan, F.A.SC.)

Introduction

Although the Raman spectra of acetic acid, its salts and esters in the liquid state have been studied in great detail (Hibben, 1939), very little work has been done on their spectra in the crystalline state. Only sodium acetate has been recently investigated by Marignan (1948). He used the method of complementary filters and confined himself to the region of frequency shifts from 2,900 to 3,500 cm.$^{-1}$ As the crystals, though small in size, can easily be grown from aqueous solutions by the method of slow evaporation and as they are transparent to the ultraviolet, it was considered desirable to investigate their Raman spectra. The results obtained in the case of sodium, magnesium and barium acetates are reported here.

Results and Discussion

The experimental details are the same as those described by the author in the previous papers (Padmanabhan, 1948, 1950). Using λ 2536 as the exciting radiation and a medium quartz spectrograph exposures of the order of 10 hours were found to be sufficient to obtain spectra of reasonable intensity.

In Fig. 1 (on Plate XX) the Raman spectra of the three crystals are reproduced along with the mercury arc spectrum. The recorded spectra exhibit as many as 15 lines with sodium acetate, 23 with magnesium acetate and 23 with barium acetate. The frequency shifts are listed in Table I.

The broad line at about 3500 cm.$^{-1}$ due to the O–H oscillation is very weak in barium acetate, while the corresponding line in magnesium and in sodium acetate is more intense. The low frequency lines can be clearly seen in the three spectra, those of magnesium acetate being the most intense among them. Most of the lines in this region have been recorded for the first time. The lines 46, 60 and 109, 126 in sodium acetate form close doublets, of which the former is more intense than any other lattice line.

TABLE I

Sodium acetate cm.$^{-1}$	Magnesium acetate cm.$^{-1}$	Barium acetate cm.$^{-1}$
46 (L)		
	52 (L)	
60 (L)	61 (L)	60 (L)
81 (L)	79 (L)	
		91 (L)
		102 (L)
109 (L)	114 (L)	
126 (L)		130 (L)
	140 (L)	142 (L)
165 (L)	169 (L)	160 (L)
196 (L)	196 (L)	197 (L)
	218 (L)	215 (L)
	(P) 254	
	306	
	340	332
480		498
	(D) 538 (ν_5)	540 (ν_5)
	668 (ν_3)	656 (ν_3)
	920 } (ν_2)	909 } (ν_2)
910 (ν_2)	(P) 930 }	918 }
1350 (ν_2')	(D) 1350 (ν_2')	1344 (ν_2')
	1429 }	1415 }
1416 (ν_4')	(D) 1450 } (ν_4')	1434 } (ν_4')
		1458 }
2939 (ν_1')	(P) 2938 (ν_1')	2939 (ν_1')
2980	2982	2989
3030 (ν_3')	3032 (ν_3')	3019 (ν_3')
3406	3543	3470

(L) Lattice oscillations. (P) Polarised Raman line.
(D) Depolarised Raman line.

Similarly there are two doublets in the lattice spectrum of barium acetate also with frequency shifts 91, 102 and 122, 131 cm.$^{-1}$

All the three acetates crystallise in the monoclinic class. Magnesium acetate [$Mg(CH_3COO)_2 \cdot 4H_2O$] tetrahydrate belongs to the space group C^2_{2h} with two molecules in the unit cell while sodium acetate trihydrate ($CH_3COONa \cdot 3H_2O$) belongs to C^3_{2h} with 8 molecules in the unit cell (Padmanabhan, 1952). The space group of barium acetate trihydrate has not yet been determined.

The observed frequency shifts in all the three cases can be roughly classified into three groups—lattice frequencies, frequencies due to the acetate ion and water bands.

Lattice Oscillations.—The lattice frequencies are indicated in Table I by the letter L within brackets, along with the frequency shifts. From symmetry considerations it can be shown that for magnesium acetate, 12 lattice lines are theoretically allowed in Raman effect (6 translatory and 6 rotatory) of which only 8 have been recorded. Polarisation studies show that the lines 61 and 140 are symmetric while the other lines are antisymmetric. Among the low frequency lines, since those with frequency shifts 61, 169 and 196 cm.$^{-1}$ appear in all the spectra without much shift, they may be attributed to the oscillations of the acetate ion. However, complete polarisation studies for all the three crystals are necessary for a more detailed analysis of the lattice spectra.

Internal Frequencies Due to the Acetate Ion.—Following Engler (1937) and treating methyl groups as a unit, the rest of the acetate ion may be visualised as of the type . The fundamental vibrations of a group of type $A.B_2C$ are six in number (ν_1 to ν_6) of which three will give rise to polarised Raman lines. The methyl group may be considered as having a pyramidal structure with four characteristic frequencies (ν_1' to ν_4') of which two will be polarised and the other two depolarised. In Table I, the types of oscillation and polarisation of the frequencies due to the acetate ion are indicated. The Raman lines corresponding to ν_1 ($\sim$1650) and ν_4 ($\sim$1100) have not been observed showing thereby that even if present they are of negligible intensity. The state of polarisation of the lines 668 and 3032 could not be judged properly. Some of the lines such as 910 and 1416 cm.$^{-1}$ which appear single in the spectrum of sodium acetate split up into two or three lines in the spectra of magnesium and barium acetates. This might be due to the presence of more than one acetate ion in the molecule.

Water Bands.—The broad line with a frequency shift of 3406 cm.$^{-1}$ in sodium acetate is due to the O—H oscillation, while the corresponding lines in magnesium and barium acetates are those at 3543 and 3470 cm.$^{-1}$ respectively.

The author's thanks are due to Professor R. S. Krishnan for his kind interest and encouragement.

Summary

Using λ 2536 as exciter, the Raman spectra of single crystals of sodium, magnesium and barium acetates have been investigated. The spectra of

magnesium and barium acetates and the lattice spectrum of sodium acetate have been reported for the first time. The recorded spectra exhibit as many as 15 lines with sodium acetate, 23 with magnesium acetate and 23 with barium acetate. Tentative assignments have been made for some of the lines observed.

REFERENCES

Engler .. *Z. Physik. Chem.*, 1937, **35 B**, 433.

Hibben .. *The Raman Effect and its Chemical Applications.* 1939.

Marignan .. *Bull. Soc. Chem. France*, 1948, 351–2.

Padmanabhan, V. M. .. *Proc. Ind. Acad. Sci.*, 1948, **28**, 485.

.. *Curr. Sci.*, 1952, **21**, 97.

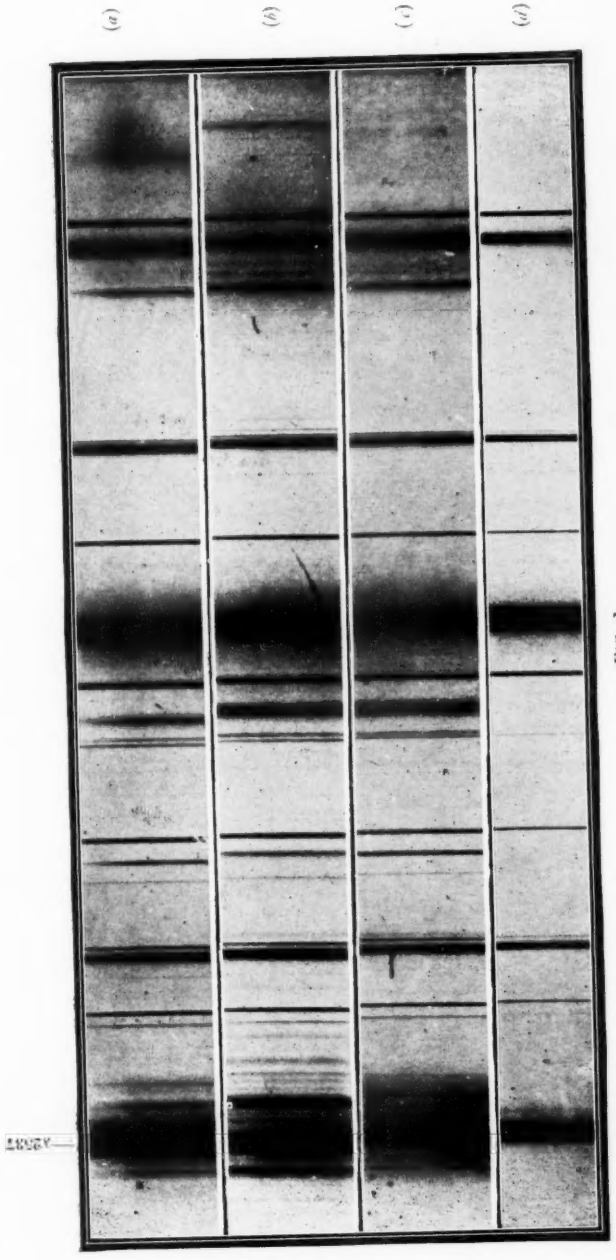

FIG. 1

Raman Spectra of Crystalline Acetates

(*a*) Sodium Acetate (*b*) Magnesium Acetate (*c*) Barium Acetate (*d*) Comparison Hg Spectrum

TEMPERATURE VARIATION OF THE RAMAN SPECTRUM OF TOPAZ

By R. Srinivasan

(*Department of Physics, Indian Institute of Science, Bangalore* 3)

Received February 24, 1953

(Communicated by Prof. R. S. Krishnan, F.A.SC.)

1. Introduction

The temperature variation of Raman spectra of solids is of great interest because of its direct bearing on the theory of the solid state. The Raman spectrum of a solid yields directly its characteristic vibrations and any theory of the solid state can be valid only if it conforms to the observed vibration spectrum of the solid. The study of the temperature variation of Raman spectrum in such substances as diamond and quartz has clearly indicated that the failure of the Gruneisen's Law of thermal expansion lies in assuming a constant value of γ for all frequencies. But such data on the temperature variation of Raman spectra are available only for relatively a few simple crystals. It was therefore considered desirable to investigate the temperature variation of the Raman spectrum of topaz in some detail.

The Raman spectrum of topaz was recorded by R. S. Krishnan (1947) at room temperature using the powerful ultraviolet technique and he reported the appearance of 32 sharp Raman lines. The Raman spectrum of topaz was photographed by T. Kopcewicz (1937) at two temperatures, namely, 20° and 500° C. using λ 4358 ÅU as the exciting radiation. He found that the low frequency lines shifted proportionately more than the high frequency lines. He could, however, claim an accuracy of 5 wave numbers only for his measurements.

2. Details of Experiment

Only colourless crystals of topaz are transparent to the λ 2537 radiation. One such piece having dimensions $6 \times 6 \times 5$ mm. was used in the present investigation. To record the spectrum at higher temperatures, the crystal was kept inside a heater provided with suitable windows. The heating current was taken from the D.C. mains through a series of adjustable resistances. The temperature was controlled by periodic adjustment of the resistance so as to keep the current flowing through the heater constant. Such adjustment was not found to be frequently necessary. The temperature

remained constant and very steady over long intervals of time—as much as 24 hours. The steady state was reached within 30 minutes after switching on the heating current. The temperature was measured by means of an iron-constantan thermocouple whose junction was kept close to the crystal. To measure the thermo E.M.F. a calibrated microammeter was used for the range from room temperature to 250° C. and a standard millivoltmeter above 250° C.

The λ 2537 radiation from a specially designed quartz mercury arc was used for exciting the Raman spectrum and a Hilger medium quartz spectrograph for recording it. With a slit width of 0·04 mm. an exposure of twenty hours was sufficient to get a fairly intense spectrogram. A comparison iron arc spectrum was superposed on each spectrogram. The measurements were made using a Hilger cross-slide micrometer reading upto 1/1000 mm. Spectrograms were taken at 30°, 110°, 150°, 200°, 250°, 300°, 350°, 400° and 450° C.

The spectrograms were microphotometered with the aid of a Moll microphotometer.

3. RESULTS

The results of the experiment are given in the following tables. Table I contains the frequency shifts in wave numbers of the prominent Raman lines of topaz at various temperatures. It should be mentioned that on certain negatives the frequency shifts of some of the lines could not be measured. They are therefore not entered in Table I.

TABLE I

Frequency Shifts of Some of the Prominent Raman Lines of Topaz at Various Temperatures

Temp. °C.	269·6 cm.$^{-1}$	458 cm.$^{-1}$	520 cm.$^{-1}$	927 cm.$^{-1}$	985 cm.$^{-1}$	3643 cm.$^{-1}$
30	269·6	457·8	521·8	926·9	985·0	3643·2
110	269·1	457·4	521·1	925·4	979·9	3636·2
150	268·3	456·1	518·5	922·2	980·0	3634·7
200	267·6	456·3	515·3	920·6	975·6	3633·6
250	266·7	455·4	511·1	918·6	973·6	3632·1
300	265·9	454·5	..	..	971·7	3631·6
350	264·8	..	508·8	916·6	969·4	3630
400	264·5	452·6	..	915·5	..	3629·2
450	263·0	451·1	..	915·1	967·5	3628·1

The intense Raman lines of topaz form close doublets and as such their widths at different temperatures could not be measured accurately. The Raman line at 458 cm.$^{-1}$ was free from this trouble. Its width at half intensity was therefore estimated from the microphotometer records and the values for different temperatures are entered in Table II.

TABLE II

Width of the 458 cm.$^{-1}$ *line at Various Temperatures*

Temp. T °K	Width (W) cm.$^{-1}$	W/ $\sqrt{T}$
303	12	0·69
423	12·6	0·61
523	13·9	0·61
623	15·5	0·62
723	16·9	0·63

From the measured frequency shifts, the values of $\chi \left(= -\frac{1}{\tilde{\nu}} \frac{d\tilde{\nu}}{dT}\right)$ for eight Raman lines have been calculated for 3 different ranges—and are entered in Table III.

TABLE III

χ for Various Raman Frequencies

$\tilde{\nu}$ value in cm.$^{-1}$ at 30° C.	$\tilde{\nu}$ value in cm.$^{-1}$ at 450° C.	$\chi = -\frac{1}{\tilde{\nu}} \frac{d\tilde{\nu}}{dT} \times 10^6$		
		30–150° C.	150–300° C.	300–450° C.
240·9	236·5	21	46	65
269·6	263·0	42	57	71
289·5	283·2	46	55	59
457·8	451·1	15	36	51
521·8	..	55	97	..
926·9	915·1	45	34	18
985·0	967·5	56	41	30
3643·2	3628·1	20	6	6

The variation of $\Delta\tilde{\nu}$ with temperature for 6 Raman lines is illustrated in Figs. 1 to 4. In Fig. 2 is also included the curve showing the variation of width with temperature for 458 cm.$^{-1}$

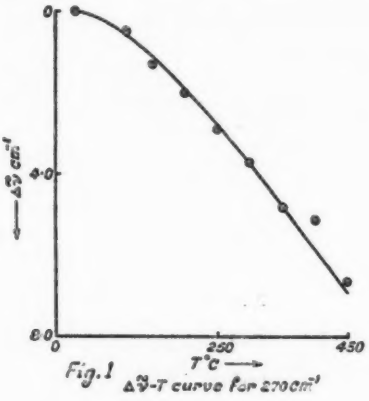

Fig. 1 $\Delta\tilde{\nu}$-T curve for 270 cm^{-1}

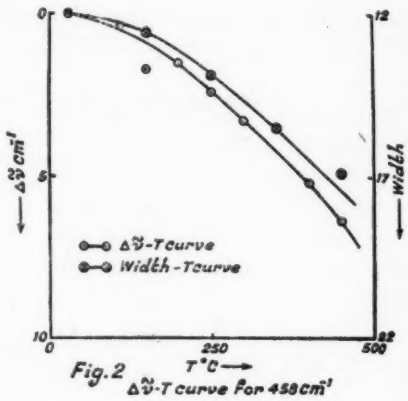

Fig. 2 $\Delta\tilde{\nu}$-T curve for 458 cm^{-1}

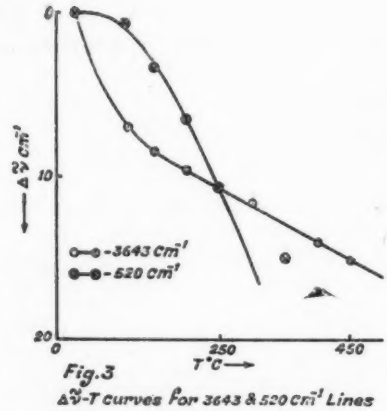

Fig. 3 $\Delta\tilde{\nu}$-T curves for 3643 & 520 cm^{-1} Lines

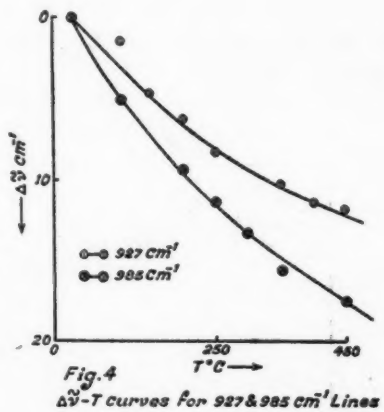

Fig. 4 $\Delta\tilde{\nu}$-T curves for 927 & 985 cm^{-1} Lines

FIGS. 1–4

The specimen of topaz used in the present investigation was rather small and in order to get the photographs in a resonable time it became necessary to use a small dispersion instrument and a reasonably wide slit. In view of this, the doublets 920–934 and 3636–3649 reported by R. S. Krishnan could be recorded by the author only as 2 lines having frequency shifts 926·9 and 3643·2 cm.$^{-1}$ respectively.

4. Discussion

From a perusal of the χ values given in Table III and the curves exhibited in Figs. 1 to 4, it is apparent that the Raman lines in topaz can be classified into two groups, namely:—

(1) those whose χ values increase with temperature and

(2) those whose χ values decrease with temperature.

Under the first category come the lines with low frequency shifts, namely, 241, 270, 290, 458 and 522 cm.$^{-1}$ The lines 927, 985 and 3643 cm.$^{-1}$ fall under the second category. It should be mentioned, that in all the crystals investigated so far by the earlier workers the values of χ progressively increase with temperature irrespective of the nature of the Raman lines.

The second important result that emerges from the present investigation is the fact that the Raman lines of topaz do not exhibit wide variations in their χ values. For example, in the range from 30°–150° C., the χ values for the different lines vary from 15×10^{-6} to about 56×10^{-6}, *i.e.*, by a factor of 4. In the case of quartz and calcite, on the other hand (Narayanaswami, 1947), χ values vary by a factor of 45 and 20 respectively. Moreover, unlike in the case of quartz and calcite, the Raman lines of topaz do not exhibit any grouping based on the absolute values of χ.

The behaviour of the 458 cm.$^{-1}$ line of topaz may be compared with that of the 466 cm.$^{-1}$ line of crystal quartz. Over the same range of temperature, the χ's for these two Raman lines have nearly the same value.

The temperature-width curve for the 458 cm.$^{-1}$ line of topaz shows a close parallelism to the $\Delta\tilde{\nu} - T$ curve (curve II). Such a correlation between the width-temperature curves and the frequency-temperature curves was suggested by Raman (1947) and experimentally verified by Narayanaswami (1947) in calcite and quartz. The width of the 458 cm.$^{-1}$ line of topaz is also found to be proportional to the square root of the absolute temperature (see Table II). It may be recalled that such a relation was reported for the Raman lines of calcite and quartz by Ornstein and Went (1935) and for diamond by R. S. Krishnan (1946).

In conclusion, the author wishes to express his gratitude to Prof. R. S. Krishnan for having suggested this problem and for his kind interest throughout the course of the investigation. He also expresses his sincere thanks to Dr. P. S. Narayanan for his unstinting help and co-operation.

Summary

The temperature variation of the frequency shifts of the intense Raman lines of topaz has been investigated over the range of temperature from 30° C.

to 450° C., using the λ 2536 ÅU radiation of the mercury arc as the exciter. From the observed variation, values of $\chi \left(= -\frac{1}{\tilde{\nu}} \frac{d\tilde{\nu}}{dT}\right)$ have been calculated for the lines 241, 270, 289, 458, 522, 927, 985 and 3643 cm.$^{-1}$ In the case of the first five lines, χ increases with temperature, while for the rest, χ decreases with temperature. Unlike the case of calcite and quartz the absolute values of χ for the different Raman lines of topaz do not show wide variations.

The temperature variation of the width of the 458 cm.$^{-1}$ line has also been measured. The width of this line is found to increase proportional to the square root of the absolute temperature.

REFERENCES

1. Kopcewicz, T. .. *Journ. de. Phys. et. le Rad.*, 1937, **8**, 6.
2. Krishnan, R. S. .. *Proc. Ind. Acad. Sci.*, 1946, **24 A**, 45.
   ——————— .. *Ibid.*, 1947, **26**, 460.
3. Narayanaswami, P. K. .. *Ibid.*, 1947, **26**, 511.
   ——————— .. *Ibid.*, 1947, **26**, 521.
4. Ornstein and Went .. *Physica*, 1935, **2**, 503.
5. Raman, C. V. .. *Proc. Ind. Acad. Sci.*, 1947, **26 A**, 339.

RAMAN SPECTRUM OF RUTILE

Polarisation Studies

By P. S. Narayanan

(*Department of Physics, Indian Institute of Science, Bangalore* 3)

Received February 24, 1953

(Communicated by Prof. R. S. Krishnan, F.A.SC.)

1. Introduction

The Raman spectrum of rutile was first studied by the author (Narayanan, 1950) and utilising the observed frequencies, a theoretical study of the vibration spectrum of rutile has been made by Dayal (1950) and more recently by Matossi (1951). Dayal assumed that all the six oxygen atoms that surround a titanium atom in rutile are bound by the same force and this has no theoretical justification except one of simplicity. Matossi making no such assumption arrived at the interesting result that two of the oxygen atoms are attached to each Ti atom far more strongly than the other four, indicating that rutile might be regarded as being built of a body-centred arrangement of TiO_2 molecules. He concluded that the spectrum must be considered as one of 'modified coupled TiO_2 molecules'. Consequently TiO_2 (rutile) was found to be 'geometrically a co-ordination compound, dynamically molecular and spectroscopically of a transition type'.

However, the numerical values of the force constants on which the conclusions mentioned above depend, require a correct assignment of the observed Raman frequencies to the several species and for this polarisation data are necessary. Such information, obtained by the author from a study of the polarisation of the three most intense lines and their relative intensities for different orientations of the crystal is given below.

2. Experimental Details and Results

The specimen of rutile used for the present study was cut and polished in the form of a rectangular parallelepiped (5 mm. $\times$ 5 mm. $\times$ 6 mm.) with two of its faces perpendicular to the optic axis and the other four parallel to it. It was noticed that the faces perpendicular to the optic axis could be polished more easily than the others. Also along the optic axis, which was determined accurately with the help of the interference figures observed with convergent polarised light, there was a very small amount of strain birefringence. The Raman spectrum excited by λ 4358 radiation of a mercury arc

was recorded with the help of a Hilger two-prism spectrograph of high light-gathering power. The scattered light from the crystal passed through a Wollaston double-image prism and the two images were focussed on the slit of the spectrograph with a quartz lens. Using a slit width of 75 μ, exposures of the order of 4 days were necessary to record even the intense lines. Also, since the crystal used was small, there was a certain amount of unavoidable continuous spectrum overlaying the Raman lines and this made it impossible to study the polarisation characteristics of the weaker lines.

The depolarisation factors of the three intense lines are listed in Table I. Since the slit width used in the earlier work was comparatively large and there is more than one line in the neighbourhood of 600 cm.$^{-1}$, the frequency shift given in Table I for Type A_{1g} is slightly different from the value given before (*loc. cit.*) which referred to the position of maximum intensity.

TABLE I

Case	Direction of optic axis	Type	Frequency shift in cm.$^{-1}$	Experimental Depolarisation			Theoretical Depolarisation		
				I.L. Electric vector along		Unpolarised light	I.L. Electric vector along		Unpolarised light
				OY	OZ		OY	OZ	
I	OZ			–	~0·1	0·1	*f*	0	0
II	OY	A_{1g}	610	–	–	–	*f*	0	0
III	OX			–	0	0	*f*	0	0
I	OZ			–	~0	0			
II	OY		236	–	–	·5			
III	OX			–	–	~1			
I	OZ			0	∞	1	0	∞	1
II	OY	E_g	444	–	–	~1	1	*f*	1
III	OX			–	∞	∞	∞	∞	∞

Incident light along OX Scattered light along OY.

The picture taken with the optic axis perpendicular to the plane of scattering and parallel to it (coinciding with the direction of illumination) show a marked difference, the line 610 cm.$^{-1}$ being of very small intensity when the optic axis is perpendicular to the plane of scattering. The spectra corresponding to case I and with polarised incident radiation (vertical and

horizontal) suggest that the line 515 cm.$^{-1}$ has a depolarisation value $\rho > 1$. Further, spectra taken with unpolarised incident radiation and the optic axis along the direction of illumination revealed the existence of a very weak line at about 820 cm.$^{-1}$ The low frequency Raman line 150 cm.$^{-1}$ was practically absent when the optic axis was perpendicular to the plane of scattering.

3. Discussion

The total intensities and depolarisation factors for different orientations corresponding to the four symmetry types of oscillations allowed in Raman effect for a tetragonal crystal like rutile may easily be written out from a knowledge of the non-vanishing components of the polarisability tensor (Placzek, 1934; Saksena, 1940). Of these only those of types A_{1g} and E_g are given in Table I along with the experimental results.

The most interesting observation of the present study is that the Raman line at 440 cm.$^{-1}$ is not the most intense one as seen in the earlier spectrograms obtained by the author (1950). When the optic axis is along the direction of incidence the line at 610 cm.$^{-1}$ is nearly twice as intense as that at 440 cm.$^{-1}$ The complete polarisation of this line in case III enables one to identify it as belonging to the type A_{1g}. The large variation in intensity of the line 610 cm.$^{-1}$ arising from the totally symmetric oscillation is in agreement with the known large birefringence of rutile. Similarly the polarisation values of the 440 cm.$^{-1}$ line makes it possible to identify it beyond doubt as arising from the degenerate mode (Type E_g).

But the polarisation values of the broad line at 236 cm.$^{-1}$ in all the cases studied do not coincide with that to be theoretically anticipated for type B_{1g} and as such no definite assignment could be made for it.

In view of these polarisation data and consequent revision of the assignment of the Raman lines, it will be of interest to recalculate the force constants, which will give information concerning the structure of rutile. For this the more general expressions given by Matossi (1951) were employed. The rutile structure is tetragonal with the basis Ti (000, $\frac{1}{2}\,\frac{1}{2}\,\frac{1}{2}$) and O ($uuo$; $\frac{1}{2}+u, \frac{1}{2}-u, \frac{1}{2}$; $\bar{u}\bar{u}o$; $\frac{1}{2}-u, \frac{1}{2}+u, \frac{1}{2}$) with $u = \cdot 31$; $a = 4{\cdot}58$ ÅU and $c = 3{\cdot}73$ ÅU. The structure may be pictured in the following manner. The titanium atoms are at the corners and the body centre of the tetragonal unit cell. To each Ti at the corners are attached two oxygen atoms at equal distances along the direction of one of the basal diagonals. To the Ti at the body centre are attached two oxygen atoms at equal distances but in the direction of the other basal diagonal. Now, the system of force constants used by Matossi may be summarised as follows: k_1 (horizontal) Ti − O (5 and 1); k_2 (oblique) Ti—O (5 and 2); k' (horizontal) O—O (4 and 2);

k'' (oblique) O — O (4 and 1); d_1, the bond bending force in the horizontal plane O—Ti— (1—5—3); d_2 similar to d_1 but in vertical plane and d_3 at O (5—4—5'), the numbers within brackets referring to the atoms marked in the paper quoted. However, it was necessary to make some assumptions before the numerical evaluations could be made and so k' and d_3 were put equal to zero. Since it was not possible to determine definitely the Raman line due to the oscillation B_{1g}, d_1 was also set equal to zero and the value of (k_2) which was evaluated using the infra-red active frequency $\omega_6 = 330$ cm.$^{-1}$ (extraordinary ray) for the type A_{2u}, will thus be the upper limit. It can be easily seen that this approximation will not affect the magnitude of k_2 much. The frequencies calculated with $k_1 = 2{\cdot}8 \times 10^5$ dynes/cm., $k_2 = {\cdot}52 \times 10^5$ dynes/cm. and $k'' = {\cdot}55 \times 10^5$ dynes/cm. are: $\omega_1 = 610$, $\omega_2 = 685$, $\omega_3 = 173$, $\omega_4 = 895$, $\omega_5 = 444$, $\omega_6 = 330$, $\omega_8 = 536$ and $\omega_9 = 200$ cm.$^{-1}$ The value of the force constant d_2 may be adjusted to account satisfactorily the position of the infra-red maxima (ordinary ray). The main result of the above interpretation, which cannot be attributed to the simplifications, is the great difference between k_1 and k_2 and this can be taken as indicating the molecular character of rutile.

While the experimentally observed lines at 150 cm.$^{-1}$ and 820 cm.$^{-1}$ may be due to the modes B_{1g} and B_{2g}, we find still a large number of lines which have to be attributed to the octaves or combinations of the fundamental frequencies or to violation of the selection rules for the fundamentals.

In conclusion, the author wishes to express his sincere thanks to Prof. R. S. Krishnan for his help and suggestions.

SUMMARY

A study of the intensity and polarisation of the Raman lines of rutile has been made for different orientations of the crystal. The polarisation data show that the Raman line 610 cm.$^{-1}$ belongs to the totally symmetric mode A_{1g} and the line 444 cm.$^{-1}$ to the degenerate mode E_g. A calculation of the numerical values of the force constants for rutile taking into account this reassignment reveals that out of the six oxygen atoms which surround any titanium atom, two are bound to it much more strongly than the others.

REFERENCES

Bisheswar Dayal .. *Proc. Ind. Acad. Sci.*, 1950, **32 A**, 304.
Matossi, F. .. *Journ. Chem. Phy.*, 1951, **19**, 1543.
Narayanan, P. S. .. *Proc. Ind. Acad. Sci.*, 1950, **32 A** 279.
Placzek .. *Handbuch der Radiologie*, 1934, Vol. VI.
Saksena, B. D. .. *Proc. Ind. Acad. Sci.*, 1940, **11 A**, 229.

RAMAN SPECTRUM OF CRYSTALLINE AMMONIUM HYDROGEN MALATE

By T. S. Krishnan

(From the Department of Physics, Indian Institute of Science, Bangalore 3)

Received February 24, 1952

(Communicated by Prof. R. S. Krishnan, F.A.SC.)

Introduction

Ammonium hydrogen malate crystallises in the orthorhombic system. It is piezoelectric and possesses strong electro-mechanical coupling constants. A study of its Raman spectrum is therefore of interest. This has been carried out and the results are presented in this paper.

The specimen of ammonium hydrogen malate used in the present investigation had well-developed faces and was about 2 cm. long. This was grown in the Bell Telephone Laboratories, U.S.A., and was presented to Prof. R. S. Krishnan by Dr. W. P. Mason. Being transparent to the ultra-violet, the λ 2536 resonance radiation of mercury was used for exciting the Raman spectrum. An exposure of 3 hours was found to be sufficient to record most of the Raman lines. During continued exposure to the ultra-violet radiation, the portion of the crystal facing the arc became frosted and got decomposed. The longest exposed negative had therefore only 15 hours of exposure.

2. Results and Discussion

An enlarged photograph of the Raman spectrum of ammonium hydrogen malate taken with the aid of a Hilger medium quartz spectrograph is reproduced in Fig. 1 on Plate XXI. The corresponding microphotometric record is also reproduced in the same figure. The recorded spectrum exhibits 26 Raman lines the positions and frequency shifts of which have been indicated in the figure. The frequency shifts are also entered in Table I along with the rough estimates of their relative intensities.

The 26 Raman lines of ammonium hydrogen malate can be divided into two groups:—(i) lattice lines with frequency shifts ranging from 65 to 190 cm.$^{-1}$ and (ii) internal frequencies with frequency shifts above 321 cm.$^{-1}$ Of the five lattice lines, the one at 100 cm.$^{-1}$ is the most intense. There is also a band extending from 65 to 120 cm.$^{-1}$ For a proper assignment of the lattice frequencies a knowledge of the crystal structure of ammonium hydrogen malate is necessary. This is not available in the literature.

TABLE I

Raman Shifts in Wavenumbers

Ammonium hydrogen malate (Author)	Malic acid (Marie Theodoresco)	Ammonium hydrogen malate (Author)	Malic acid (Marie Theodoresco)
65 (6)		959 (6)	955
100 (8)		1047 (2)	1066
123 (3)		1111 (4)	1113
149 (2)		1215 (3)	1227
190 (1)		1254 (3)	1283
321 (1*b*)	334	1325 (6)	1335
384 (1)	400	1350 (2)	1355
472 (2*b*)		1408 (6)	1403
	521		1416
	611	1464 (2*b*)	
	652	1654 (3*b*)	1621
	684		1679
727 (1)			1720
774 (2*b*)	750	2930 (10)	
	836	2970 (6)	
868 (1)	887	3377 (4*vb*)	
904 (5)		3500 (4*b*)	

The chemical formula for ammonium hydrogen malate is

$$\begin{array}{l} CH_2—COOH \\ | \\ CH\,(OH)—COO\,(NH_4) \end{array}$$

The nearest compound whose Raman spectrum has been studied is malic acid. It has the structural formula

$$\begin{array}{l} CH_2—COOH \\ | \\ CH\,(OH)—COOH \end{array}$$

The 21 frequency shifts reported by Marie Theodoresco (1942) for malic acid have also been included in Table I. As is to be expected, there is some correspondence between the frequency shifts lying in the region 310–1650 cm.$^{-1}$ of ammonium hydrogen malate and those of malic acid.

The lines with frequency shifts 611, 652 and 1720 cm.$^{-1}$ reported in the case of malic acid have not been observed in the case of ammonium hydrogen malate. This might be due to the fact that in the spectrum taken with the λ 2536 excitation, these lines, even if present, would have fallen on mercury

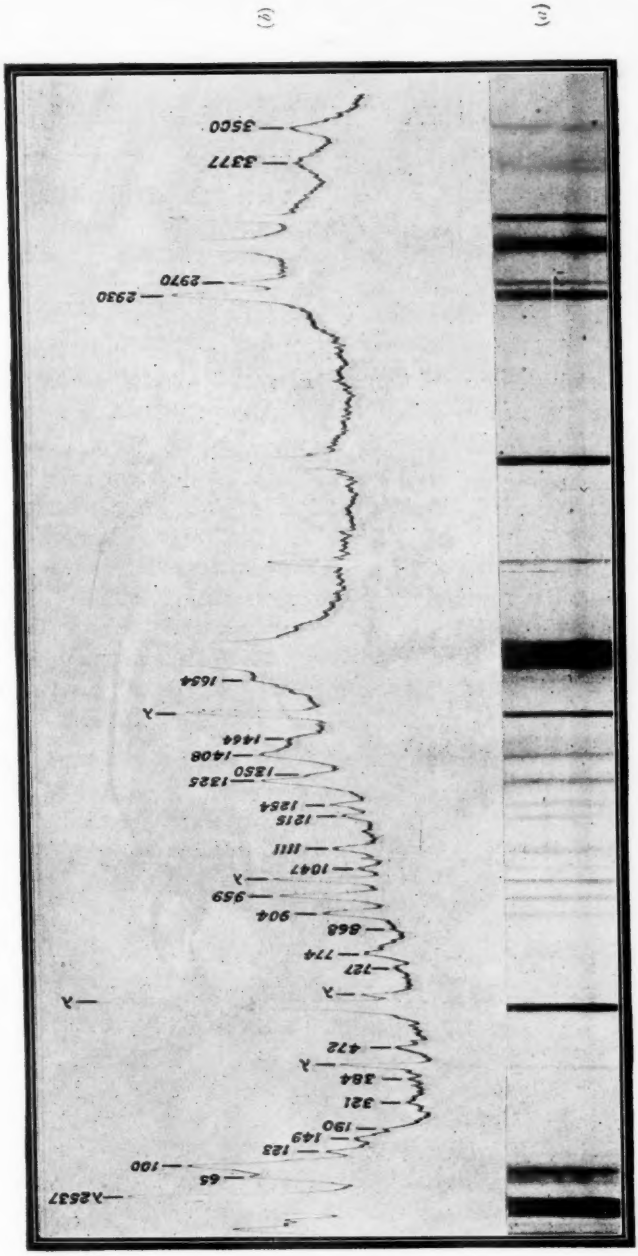

FIG. 1. (*a*) Raman Spectrum of Ammonium Hydrogen Malate taken with a Medium Quartz Spectrograph.
(*b*) Its Micrometer Record.

lines and thus remained unobserved. It is surprising to note that Marie Theodoresco has not reported the appearance of C—H and O—H frequencies in the spectrum of malic acid.

The two lines with frequency shifts 2930 and 2970 in the spectrum of ammonium hydrogen malate are evidently due to the C—H oscillations. The one with the lower frequency shift is more intense than the other. The two broad lines with mean frequency shifts 3377 and 3500 cm.$^{-1}$ are due to the O—H oscillations. The other internal frequencies can be assigned as follows:—321, 384 and 472 cm.$^{-1}$ to C—C deformation frequencies; 868, 904 and 959 to C—C frequencies; 1047, 1111, 1215, 1254, 1325 and 1350 cm.$^{-1}$ to C—OH frequencies; 1408 and 1464 cm.$^{-1}$ to C—H deformation frequencies and 1654 cm.$^{-1}$ to carboxyl group frequency.

It is surprising to note that the spectrum of ammonium hydrogen malate does not exhibit any of the Raman lines characteristic of the vibrations of the NH_4 group. A careful examination of the Raman spectrum and the microphotometric record reproduced in Fig. 1, however, reveals the existence of broad and diffuse bands in the neighbourhood of 1400 cm.$^{-1}$, 1700 cm.$^{-1}$, 3000 cm.$^{-1}$ and 3100 cm.$^{-1}$. These regions roughly correspond to those where the characteristic frequencies of the NH_4 ion ($\nu_1 = 3033$, $\nu_2 = 1685$, $\nu_3 = 3134$ and $\nu_4 = 1397$) appear. The diffuse and feeble bands appearing in the spectrum of ammonium hydrogen malate should therefore be attributed to the vibrations of the NH_4 ions in this crystal.

In conclusion the author wishes to express his gratitude to Prof. R. S. Krishnan for suggesting the problem and for the guidance and to Dr. P. S. Narayanan for the valuable help given in the course of the work. The author is also grateful to Dr. W. P. Mason for the specimen of ammonium hydrogen malate.

3. Summary

Using the λ 2536 radiation of the mercury arc as exciter, the Raman spectrum of a single crystal of ammonium hydrogen malate has been photographed. The spectrum exhibits 26 Raman lines with frequency shifts 65, 100, 123, 149, 190, 321, 384, 472, 727, 774, 868, 904, 959, 1047, 1111, 1215, 1254, 1325, 1350, 1408, 1464, 1654, 2930, 2970, 3377 and 3500 cm.$^{-1}$

Reference

Marie Theodoresco .. *Compt. Rend.*, 1942, **274**, 169-71.

LIGHT SCATTERING IN GOLD SOLS

By S. R. Sivarajan

(Department of Physics, Indian Institute of Science, Bangalore 3)

Received March 4, 1953

(Communicated by Prof. R. S. Krishnan, F.A.SC.)

1. Introduction

The optical properties of gold sols have been the subject of numerous investigations. These include studies on their colour, absorption, depolarisation of the light scattered by them and their dependence on wavelength (Steubing, 1908; Lange, 1928; Subbaramaiya, 1935; Krishnan, 1937). On the theoretical side, Mie's theory of light scattering by spherical metallic particles failed, however, to explain satisfactorily *all* the experimental observations. Later, Gans (1912) taking into account the departure from spherical shape (and assuming the particles to be small compared to the wave-length of light) was able to account better for the observed colour, absorption and depolarisation in the case of gold sols. Lange and R. S. Krishnan observed the variation of ρ_u with wavelength to be in agreement with that calculated from Gans' theory.

But no systematic work has been done so far on the intensity of scattering by gold sols and its dependence on wavelength, taking into account the influence of absorption. However, some visual observations were made by Steubing (1908). It was therefore considered worthwhile to investigate the intensity of scattering using a photomultiplier tube and the results obtained by the author from such measurements are given below.

2. Experimental Details and Results

The gold sols I, II, V and VI (Krishnan, 1937) were prepared by the methods described by Subbaramaiya (1935).

The intensity measurements were made using two RCA 931–A electron photomultiplier tubes and a 'ratio circuit' similar to that employed by Mariner and Stamm (1951). The necessary stabilisation of the rectified high voltage was achieved by the use of a constant voltage transformer on the primary side.

The light from a point source quartz mercury arc run with a large inductance in series with it was focussed by means of a lens on to a small aperture and the well-defined emergent beam was then focussed by a second

lens at the centre of the rectangular optical glass cell containing the sol. This cell was kept inside a light tight box, blackened completely on the inside and having apertures for the incident, transmitted and transversely scattered beams. The measuring photomultiplier with its condensing lens system was enclosed completely in a metal box and this could be fitted into the aperture provided for that purpose. In addition, suitable baffles were placed round the glass cell to avoid any stray light from falling on the condensing lens of the photomultiplier. Thus only the transversely scattered light from the sol was allowed to enter the sensitive region of the photomultiplier tube. A small portion of the light direct from the mercury arc was allowed to fall on the second photomultiplier tube. It served as a reference cell to eliminate errors arising from possible fluctuations of intensity of the arc and to balance out the dark currents. With no light falling on the measuring photomultiplier, the current from the reference tube alone was used to check the constancy of intensity of the incident light. It was found that within an hour of striking, the intensity of the light from the arc became constant and all measurements were made only after this steady state was reached. The details of the working of the ' ratio circuit ' used will be found in the paper quoted above.

The intensity measurements were made for all the four sols with the λ 3650, λ 4358 and λ 5461 radiations of the mercury arc, for unpolarised, vertically polarised and horizontally polarised beams.

However, in the case of absorbing sols to arrive at the true intensities from the measured values, it is necessary to make a suitable correction for absorption. This has been worked out by Putzeys and Dory (1940) for an incident beam of rectangular cross-section and for a rectangular scattering cell. They have derived the following equation.

$$i = i_0 \alpha^{l_3} \frac{\alpha^{0.5b} - \alpha^{-0.5b}}{b \ln \alpha},$$

where i and i_0 refer to the observed and the true intensities. α is the transmission coefficient, b the depth of the incident beam in the direction of scattering and l_3 the distance between the centre of the scattering volume and the inner surface of the cell in the direction of observation. The values of α used were obtained from a measurement of the absorption spectra of these sols using a Beckmann photo-electric spectrophotometer.

The scattering volume was the same in the case of all the sols and their refractive indices do not differ much from one another. As we are not concerned here with the absolute intensity of scattering, no refraction and volume corrections (Carr and Zimm, 1950) were made. Further, to enable

a comparison of the intensity of scattering with that calculated from Gans' theory the contribution due to the solvent alone was subtracted in each case from the scattering due to the solution. Suitable corrections were also made for the difference in the incident intensity at the three wavelengths and for the difference in sensitivity of the photomultiplier for these wavelengths.

The final corrected values are listed in Table I taking the intensity at λ 4358 for gold sol I (for incident unpolarised radiation) as 10. The letters U, V, H refer to the nature of the incident light.

TABLE I

Intensity of Scattering by Gold Sols

Gold Sol	λ	3650		4358		5461	
	Nature of Incident Light	Extinction Coefficient	Intensity	Extinction Coefficient	Intensity	Extinction Coefficient	Intensity
I	U	·88	18·5	·73	10	·80	15·5
	V		3·7		5		8·3
	H		·53		·13		·6
II	U	·9	36	·76	15·1	·84	35·0
	V		8·1		7·2		17·6
	H		·64		·43		4·00
V	U	·22	90	·18	57·8	·3	160
	V		18·8		27·6		88
	H		·88		·92		9·0
VI	U	·56	196	·43	113·1	·62	220
	V		39·5		54·3		107
	H		4·1		5·7		20

U = Unpolarised; V = Vertically polarised; H = Horizontally polarised.

From Table I, it will be seen that for any sol for a particular wavelength the sum of the intensities for the vertically (V) and horizontally (H) polarised light beams is not equal to that for unpolarised light (U). This arises because of the absorption and the reflection losses due to the polaroid employed for polarising the incident beam.

3. DISCUSSION

Though the method of calculating theoretically the intensity of scattering in the case of the gold sols containing small anisotropic particles has been indicated by Gans (1912), no attempt has been made yet to evaluate the intensities for the different possible states of polarisation of the incident light and compare them with experimental observations. Following Gans,

let us consider a small prolate spheroidal particle at the origin of the co-ordinate system OXYZ fixed in space. Let $\xi\eta\zeta$ be the co-ordinate system fixed in the article, ξ coinciding with the figure axis and having the direction cosines α_1, α_2, α_3 with respect to OXYZ. If now a plane polarised beam of light of unit intensity and frequency n be incident on the particle along OX, with its electric vector making an angle δ with the Y axis, the scattered intensity observed along OY can be regarded as that due to the moments f_z along the Z axis and f_x along the X axis, their values being

$$f_x = m_0^2 \frac{3}{4\pi} \mathrm{V} \left[l \cos (2\pi nt - \psi) - l' \cos (2\pi nt - \psi')\right] \times \left[\alpha_1 (\alpha_2 \cos \delta + \alpha_3 \sin \delta)\right]$$

and

$$f_z = m_0^2 \frac{3}{4\pi} \mathrm{V} \left[l \cos (2\pi nt - \psi) - l' \cos (2\pi nt - \psi')\right] \times \left[\alpha_3 (\alpha_2 \cos \delta + \alpha_3 \sin \delta)\right] + l' \cos (2\pi nt - \psi') \sin \delta$$

Here l and l' are given by [Equation (31) of the paper quoted]

$$le^{-i\phi} = \frac{m'^2 - 1}{3 + (m'^2 - 1)\frac{3}{4\pi}\mathrm{P}} \qquad l'e^{-i\phi'} = \frac{m'^2 - 1}{3 + (m'^2 - 1)\frac{3}{4\pi}\mathrm{P}'},$$

where m'^2, P and P′ have the same significance as in Gans' paper.

To obtain the transversely scattered intensity due to a large number of randomly oriented particles, we have to evaluate $\overline{f_z^2}$ and $\overline{f_x^2}$ by the usual methods. Considering first only a vertically polarised beam, it can be shown that

$$\overline{f_x^2} = m_0^4 \frac{9}{16\pi^2} \mathrm{V}^2 \left\{\frac{1}{15} \left[l^2 + l'^2 - 2ll' \cos (\psi - \psi')\right]\right\}.$$

and

$$\overline{f_z^2} = m_0^4 \frac{9}{16\pi^2} \mathrm{V}^2 \left\{\frac{1}{5} \left[l^2 + l'^2 - 2ll' \cos (\psi - \psi')\right] + l'^2 + \frac{2}{3} l' \left[l \cos (\psi - \psi') - l'\right]\right\}$$

For horizontally polarised incident light $\overline{f_x'^2}$ and $\overline{f_z'^2}$ are identical and are equal to $\overline{f_x^2}$. The intensity per unit volume (containing N particles) is given by

$$\mathrm{I} = \frac{16\pi^4 \mathrm{N}}{r^2 \lambda^4} \overline{f^2},$$

The quantity within brackets may now be evaluated using for m'^2 the values quoted by Gans (1912).

From his experiments on the dispersion of depolarisation and the absorption in gold sols Krishnan concluded that the particles in them behave as prolate spheroids with an axial ratio (B/A) equal to ·75. Using this value the quantities within brackets were evaluated. These quantities when divided by λ^4 give the intensity of scattering (except for a constant factor) and are given in columns 4, 5 and 6 of Table II. For purposes of comparison the calculated values have been given relative to λ 4200. ρ_u and ρ_v values are also included in the same Table.

TABLE II

λ	ρ_u	ρ_v	$\frac{\overline{f_x^2} + \overline{f_z^2}}{A}$	$\frac{2\overline{f_x^2}}{A}$	$\frac{\overline{f_z^2} + 3\overline{f_x^2}}{A}$
4200	·0104	·0052	·7915	·0082	·7997
4500	·0108	·0055	·6124	·0066	·619
5000	·0275	·014	·989	·0273	1·016
5250	·0557	·0286	1·584	·0882	1·673
5500	·0835	·0436	2·018	·1685	2·186
6000	·0623	·0321	1·104	·0688	1·173
6500	·0387	·0198	·483	·0188	·503

$A = (\lambda/4200)^4$

Thus we find that for an elongated rotational ellipsoid of axial ratio ·75, the ratio of intensities of scattering at λ 5500 and λ 4200, for incident unpolarised and vertically polarised beams is nearly the same and is about 2·5. This is in very good agreement with what is observed in the case of gold sol II. The relative intensities in the other cases are also of the same order of magnitude. But for a more accurate comparison it is essential to know the specific value of B/A for each sol. Also one should remember that the wavelengths at which measurements were carried out are slightly different from those for which the calculations have been made. On the other hand we notice in Table II that the ratio of the intensities of scattering for λ 5461 and λ 4358 is over 20 for a horizontally polarised incident beam. The experimental values though roughly of the same order of magnitude are not in such good agreement with the theoretical value and might be attributed to the same reasons as those mentioned above. However, the

interesting fact which emerges from this study is the close relation between the intensity of scattering at different wavelengths and the corresponding absorption. This is evident from Table I where we find that for λ 3650 and λ 5461 which correspond to regions of greater absorption than λ 4358, the intensities of scattering are also larger. Further, the intensity of scattering increases in the order, gold sol I, II, V and VI. This is in agreement with the observation of R. S. Krishnan (1937) that the particle size increases in the same order.

In conclusion the author wishes to express his sincere thanks to Prof. R. S. Krishnan for suggesting the problem and for his help and encouragement.

4. Summary

The wavelength dependence of the intensity of light scattering by four different gold sols has been investigated experimentally for incident unpolarised light and for incident light polarised with vibrations vertical and horizontal. Photomultiplier tubes have been used for intensity measurements. Suitable corrections have been made for absorption, etc. The intensity of scattering for a gold sol containing very small prolate spheroidal particles of axial ratio B/A = ·75 has been calculated from Gans' theory and compared with the experimental observations. The relation between the intensity of scattering for the different wavelengths and the corresponding absorption has been pointed out.

References

1. Carr and Zimm .. *J. Chem. Phys.*, 1950, **18**, 1616.
2. Gans, R. .. *Ann. der Physik*, 1912, **37**, 883.
3. Krishnan, R. S. .. *Proc. Ind. Acad. Sci.*, 1937, **5 A**, 94.
4. Lange, B. .. *Zeits. f. Phys. Chemie.*, 1928, **132**, 27.
5. Mariner and Stamm .. *Rev. Sci. Inst.*, 1951, **22**, 61.
6. Mie, G. .. *Ann. der Physik.*, 1908, **25**, 377.
7. Putzeys and Dory .. *Ann. de la Societe Scientifique de Bruxelles series* 1, March 1940.
8. Staubing, H. .. *Ann. der Physik*, 1908, **26**, 329.
9. Subbaramaiya, D. S. .. *Proc. Ind. Acad. Sci.*, 1935, **2 A**, 358.

THE CHARACTERISTIC VIBRATIONS OF CRYSTAL LATTICES—PART I

By K. S. Viswanathan

(From the Raman Research Institute, Bangalore)

Received December 23, 1952

(Communicated by Sir C. V. Raman, F.R.S., N.L.)

A. Introduction

The importance of the knowledge of the different modes of atomic vibrations of a crystal, which constitutes the core of any theory on the thermal and optical behaviour of solids, needs hardly to be stressed. The first great step towards a proper theory on the thermal energy of solids was undertaken by Einstein who evaluated the specific heat of crystals on the assumption that the different atoms of the crystals are independent oscillators, each contributing the same amount to its thermal energy. The later theory of Debye rests on the assumption that the proper vibrations of the atoms of the crystal can be identified with the different modes of vibrations of an elastic body and as such seeks to replace their thermal energy with the energy content of elastic bodies. While the Debye theory clearly ignores the lattice structure of crystals and the atomic constitution of matter, these were taken into account in the theory of Born-Karman[1] which was proposed almost simultaneously (1913). The Born lattice dynamics sought to enumerate the different normal modes of vibrations of a crystal composed of N atoms and postulated the existence of a total number of (3N—3) frequencies, forming a continuous spectrum spread over a wide range of frequencies. On this basis, each degree of freedom of the system corresponds to a wave whose wavelength is determined by the cyclic boundary conditions. An attempt to apply the Born-Karman theory to some simple cases of cubic crystals was made by Blackman[2] who reported the presence of several maxima in the frequency spectrum; but still no qualitative description on the nature of the frequency spectrum of a general crystal is available in the literature. On the other hand, the application of the theory to any physical problem involving quantitative calculations is severely complicated so that the attempts to make progress in this direction have not been successful, even with several simplifying assumptions regarding the nature of the inter-atomic forces.

An entirely different approach to the problem, considering the movements of the individual atoms as distinct from a wave that progresses through it, was made by Sir C. V. Raman (1943).[3,4] This theoretical procedure predicts, for a crystal with p atoms in each of its unit cells, the presence of a discrete set of $(24p-3)$ monochromatic frequencies, which are observable as sharply defined lines either in the first-order or the second-order Raman spectrum. In addition, the high frequency spectrum of these normal vibrations representing the internal oscillations of its unit cells, should be supplemented by an elastic spectrum, continuous in nature and which is a consequence of the translatory movements of its lattice cells.

Assuming the existence of waves that travel through the same type of atoms in the lattice arrangement of the crystal and with no special restrictive assumptions either on the nature of the interacting forces or on the structure of the lattice cells, it is shown in this paper that the group velocity of these waves vanishes for $(24p-3)$ frequencies, which are characteristic of the crystal structure. In Part II of this paper, it is proved that the state of disturbance in the crystal arising out of an initial disturbance confined to a small region of it tends asymptotically to a superposition of these $(24p-3)$ characteristic vibrations. These results clearly show that even a picture of an infinity of waves through the crystal and consequently of frequencies associated with them leads, naturally to the conclusion that only a discrete set of $(24p-3)$ normal vibrations, as conceived by Sir C. V. Raman, are physically significant; the effect of the elastic waves which (at ordinary temperatures) contribute in much lesser a measure to the vibrational energy of the crystal can be accounted for by an elastic spectrum of the Debye type, but with a greatly reduced proportion of the degrees of freedom associated with it.

1. The Equations of Motion

We consider a crystal consisting of p atoms in each of its unit cells and denote the displacements of any atom parallel to the three mutually orthogonal co-ordinate axes x^i by q_{irs} $(i = 1, 2, 3)$. Throughout this paper, we use the letters r and ρ exclusively to represent the index number of a particular atom among the p atoms in any cell, while σ and s will be used to indicate the cell number of the crystal.

The general equations of motion for the atoms of the lattice and the relationship between the force constants occurring in the most general form of the potential energy expression, were given by Raman and Born. For the sake of completeness, these results are quoted here. If m_r denotes the

mass of the rth atom in any cell, the expressions for the kinetic and potential energies are given by

$$2T = \sum_{irs} m_r \dot{q}_{irs}^2 \tag{1}$$

$$2V = \sum_{irs} \sum_{j\rho\sigma} k_{irs}^{j\rho\sigma} q_{irs} q_{j\rho\sigma}$$

If $\mathbf{d}_1$, $\mathbf{d}_2$, $\mathbf{d}_3$ be the three primitive translational vectors of the crystal lattice, then the position of any cell of the crystal is specified by the vector $\mathbf{s} = (s_1, s_2, s_3)$ or $\mathbf{s} = s_1\mathbf{d}_1 + s_2\mathbf{d}_2 + s_3\mathbf{d}_3$. Two cells σ_i and σ_j will hereafter be called *conjugate* with respect to the cell $\mathbf{s}$ if

$$\sigma_i - \mathbf{s} = \mathbf{s} - \sigma_j \tag{2}$$

The *group* property implied in the translational symmetry of the crystal yields now the following relations between the force constants involved in the expression (1).

$$(a)\quad k_{irs}^{j\rho\sigma} = k_{j\rho\sigma}^{irs}$$

$$(b)\quad k_{irs}^{irs} = k_{irs'}^{irs'}$$

$$(c)\quad k_{irs}^{j\rho\sigma} = k_{irs'}^{j\rho\sigma'} \tag{3}$$

where (s, s') and (σ, σ') denote two pairs of cells given by $\mathbf{s} - \mathbf{s}' = \sigma - \sigma'$.

Since the interatomic forces are quite short-ranged, the force constants diminish rapidly with distance and we restrict the interaction of any atom in the cell $\mathbf{s}$ to all the atoms in the $2N + 1 = \prod_{r=1,2,3} (2l_r+1)$ surrounding cells given by $\sigma = \mathbf{s} + \mathbf{k}$; $\mathbf{k} = (k_1, k_2, k_3)$ where k_1, k_2, k_3 assume all integral values in the intervals $\pm l_1$; $\pm l_2$; and $\pm l_3$ respectively.

The equations of motion of the particles in the rth cell can now be written as

$$-m_r \ddot{q}_{irs} = \sum_{j,\rho,\sigma} k_{irs}^{j\rho\sigma} q_{j\rho\sigma} \tag{4}$$

$$\begin{pmatrix} i = 1, 2, 3 \\ r = 1, 2 \ldots . p \end{pmatrix}$$

We shall assume wave solutions for the above equations of the form

$$q_{irs} = A_r^i \, e^{i(\omega t + a.s)} \tag{5}$$

where $\mathbf{a}$, considered to be a vector of the reciprocal lattice, denotes the wave vector. If $\mathbf{b}_1$, $\mathbf{b}_2$, $\mathbf{b}_3$ denote the three fundamental vectors of the reciprocal lattice, then we can write

$$\mathbf{a} = \theta_1\mathbf{b}_1 + \theta_2\mathbf{b}_2 + \theta_3\mathbf{b}_3 \text{ so that we have}$$

$$\mathbf{a}\cdot\mathbf{s} = \sum_{i=1}^{3} s_i\theta_i \text{ since } \mathbf{b}_i \cdot \mathbf{d}_j = \delta_{ij}. \tag{6}$$

Substituting (5) in (4) we get the following $3p$ equations linear in the A's

$$A_r^{\,i}\,(k_{lrs}^{ir} + \sum_{\sigma} k_{lrs}^{ir\sigma}\, e^{ia.(\sigma-s)} - m_r\omega^2) + \sum_{\rho,\ j}{}' \ A_\rho^{\,j}\,(k_{lrs}^{j\rho s} + \sum_{\sigma} k_{lrs}^{j\rho\sigma}\, e^{ia.(\sigma-s)}) = 0 \qquad (7)$$

the accent indicating that the term $\rho = r;\ j = i$ is omitted in the summation of the second term and the summation for σ covers the 2N surrounding cells of s.

We shall now arrange the $3p$ terms in each of the above $3p$ equations into p groups in *lexical* order with respect to the letter ρ, the three terms in each group involving the quantities $A_\rho^{\,i}\ (i = 1, 2, 3)$ themselves being arranged in increasing order with respect to the index i. Then if,

$$\left.\begin{aligned} s' &= 3\,(r-1) + i \\ t' &= 3\,(\rho - 1) + j \end{aligned}\right\}\ i, j = 1, 2, 3$$

and $a_{s't'} = k_{lrs}^{j\rho s} + \sum_{\sigma} k_{lrs}^{j\rho\sigma}\, e^{ia.(\sigma-s)}$, we get on eliminating the A's from (7) the following equation, due to Born.

$$|\,A - M\omega^2\,| = 0, \qquad (8)$$

where A denotes the matrix $(a_{s't'})$ and M, the diagonal matrix defined by $m_{s's'} = m_{r'}$.

2. The Group Velocity of the Waves

We can now easily see that the matrix (A) is hermitian. For, if σ_1 and σ_3 denote any two cells conjugate to the cell s, then from (3) we get

$$k_{lrs}^{j\rho\sigma_1} \equiv k_{lr\sigma_2}^{j\rho s} = k_{jps}^{ir\sigma_2} \text{ and so}$$

$$k_{lrs}^{j\rho\sigma_1}\, e^{ia.(\sigma_1-s)} = k_{jps}^{ir\sigma_2}\, e^{ia.(s-\sigma_2)}$$

$$\therefore\quad a_{s't'} = k_{lrs}^{j\rho s} + \sum_{\sigma} k_{lrs}^{j\rho\sigma}\, e^{ia.(\sigma-s)}$$

$$= k_{jps}^{ir} + \sum_{\sigma} k_{jps}^{ir\sigma}\, e^{ia.(s-\sigma)} = \bar{a}_{t's'} \qquad (9)$$

for the 2N cells over which the summation for σ extends, can be split up into N pairs of conjugate cells.

Letting $z = \omega^2$, we rewrite (8) as

$$s_0 z^{3p} + s_1 z^{3p-1} + \cdot + s_t z^{3p-t} + \ldots + s_{3p-1} z + s_{3p} = 0 \qquad (10)$$

If $m_{s'} = m_r \begin{pmatrix} s' = 3(r-1)+i \\ i = 1, 2, 3 \end{pmatrix}$, then the coefficients $s_0 \ldots . s_{3p}$ are given by the following scheme.

$$s_0 = (-1)^{3p} (m_1 m_2 \ldots . m_p)^3.$$

$$s_1 = (-1)^{3p-1} (m_1 m_2 \ldots . m_p)^3 \sum_{i,r} \frac{a_{s's'}}{m_r}.$$

$$s_t = (-1)^{3p-t} \sum m_{s_1'} m_{s_2'} \ldots . m_{s_k'} \mathrm{B} \qquad (11\,a)$$

where B is a principal minor of order t, which is the complementary minor of the determinant formed from the elements of the rows $s_1', s_2', \ldots . s_k'$ $(k = 3p - t)$ of the determinant A and the summation extends over the $({}^{3p}C_t)$ principal minors of order t of $|A|$. In virtue of the hermitian property of (A), the principal minors of (A) are themselves hermitian and their determinants are therefore real. In particular, we have $s_{3p} = |A|$, the determinant of the matrix (A). While the reality of the roots of (9) follows immediately from the hermitian form of A, they should in addition be positive because of the positive nature of the potential energy expression.

If a denotes the absolute magnitude of the wave vector **a** so that $\mathbf{a} = e\mathbf{a}$, **e** being a directional unit vector, then the group velocity of the waves is given by $\frac{d\omega}{da}$. Equation (10) is of degree $3p$ in z and if its roots are denoted by $z_k = \omega_k^2$ $(k = 1, 2 \ldots . 3p)$, we get on differentiating (10) with respect to a,

$$2\omega_k \frac{d\omega_k}{da} \left(\sum_{t=0}^{3p-1} (3p - t)\, s_t\, z_k^{3p-t-1} \right) = - \left(\sum_{t=1}^{3p} z_k^{3p-t} \frac{ds_t}{da} \right) \qquad (11)$$

Denoting the cofactor of $a_{s't'}$ in $|A|$ by $A_{s't'}$ we have now

$$\frac{ds_{3p}}{da} = \sum_{s',t'} \frac{da_{s't'}}{da} A_{s't'}$$

$$= \sum_{s'=1}^{3p} \frac{da_{s's'}}{da} A_{s's'} + \sum_{\substack{s',t' \\ s'<t'}} \left\{ \frac{da_{s't'}}{da} A_{s't'} + \frac{da_{t's'}}{da} A_{t's'} \right\}$$

$$= \sum_{s'=1}^{3p} \frac{da_{s's'}}{da} A_{s's'} + 2 \sum_{s'<t'} \mathrm{R} \left(\frac{da_{s't'}}{da} A_{s't'} \right) \qquad (12)$$

since $A_{s't'}$ and $A_{t's'}$ are also complex conjugates.

Now $$\frac{da_{s's'}}{da} = -2 \sum_{\sigma_i} k_{krs}^{i\sigma_i} \mathbf{e} \cdot (\boldsymbol{\sigma}_i - \mathbf{s}) \sin \mathbf{a} \cdot (\boldsymbol{\sigma}_i - \mathbf{s})$$

the summation here being over a set of N non-conjugate cells.

If $\sigma_i = \mathbf{s} + \mathbf{k}_i$ where $\mathbf{k}_i = (k_i^1, k_i^2, k_i^3)$, then $\mathbf{a}\cdot(\sigma_i - \mathbf{s}) = \sum_{j=1}^{3} k_i^j \theta_j$ and $\sin \mathbf{a}\cdot(\sigma_i - \mathbf{s})$ will be equal to zero whenever θ_1, θ_2 and θ_3 each assumes any one of the values 0 or π. Hence $\frac{da_{s's'}}{da}$ vanishes for the set of points $(0, 0, 0)$; $(0, \pi, 0)$; $(0, 0, \pi)$; $(\pi, 0, 0)$; $(0, \pi, \pi)$; $(\pi, 0, \pi)$; $(\pi, \pi, 0)$ and (π, π, π) in the θ-space. (13)

If $\frac{da_{s't'}}{da} = x + iy$ and $A_{s't'} = x' + iy'$, then $R\left(\frac{da_{s't'}}{da} A_{s't'}\right) = (xx' - yy')$.

Now, each term in the expression for y' contains at least one factor of the type $\sum_{\sigma} k_{irs}^{j\rho\sigma} \sin \mathbf{a}\cdot(\sigma - \mathbf{s})$ and $A_{s't'}$ is real if each one of the quantities θ_1, θ_2 and θ_3 takes the values 0 or π. Further,

$$x = -\sum_{\sigma} k_{irs}^{j\rho\sigma}\, \mathbf{e}\cdot(\sigma - \mathbf{s}) \sin \mathbf{a}\cdot(\sigma - \mathbf{s}).$$

Hence $R\left(\frac{da_{s't'}}{da} A_{s't'}\right)$ and consequently $\frac{ds_{3p}}{da}$ which is a function of the θ's vanishes at the set of eight points given in (13).

Since the principal minors of order t of A are themselves hermitian, a similar argument applies to each determinant $|\,B\,|$ in (11 *a*) and we get

$$\frac{ds_t}{da} = 0 \quad (t = 1, 2 \ldots . 3p) \tag{14}$$

if $\theta_1 = 0$ or π; $\theta_2 = 0$ or π; $\theta_3 = 0$ or π.

It follows therefore from (11) that the group velocity of the waves associated with each of the eight points of (13) or with the $24p$ frequencies corresponding to them should be equal to zero.

The force constants k's are not all entirely independent. For a small translation of the entire crystal specified by $\mathbf{u} = (u_1, u_2, u_3)$, we get from (4) that $\sum_{j,\rho,\sigma} u_j k_{irs}^{j\rho\sigma} = 0$ ($\sigma = 1$, to $2N + 1$).

Since this relation is true for any arbitrary vector $\mathbf{u}$, we get

$$\sum_{\rho,\sigma} k_{irs}^{1\rho\sigma} = \sum_{\rho,\sigma} k_{irs}^{2\rho\sigma} = \sum_{\rho,\sigma} k_{irs}^{3\rho\sigma} = 0. \tag{15}$$

We shall now consider in greater detail the behaviour of $\frac{d\omega}{da}$ at the point $\theta_1 = \theta_2 = \theta_3 = 0$. By adding the elements of the columns $3s + i$ ($i = 1, 2, 3$; $s = 1, 2 \ldots . p$) respectively to the corresponding elements of the first, second and third columns, we can easily see with the aid of the relations (15) that ω^6 is a factor of $|\,A - M\omega^2\,|$.

$\therefore$ Three of the frequencies corresponding to zero values of θ_1, θ_2 and θ_3 are zero and also the expression $\frac{d\omega}{da} = \mathrm{U}(a)$ tends to a definite value $(-s_{3p}''^{(0)}/2s_{3p-1}^{(0)})^{\frac{1}{2}}$ for these three frequency branches. Hence subtracting these three modes which correspond to a translation of the entire crystal, one can see that the group velocity of the waves associated with each of the $(24p-3)$ characteristic frequencies is equal to zero.

3. The Effect of an Initial Disturbance

We consider here the nature of the propagation of an initial disturbance confined to a small region into the entire crystal and the state of movements of the atoms about their equilibrium positions at a later instant. Any such disturbance will set out a train of progressive waves in the medium and physically it is easy to see that wave clusters having zero group velocity alone could have any significant influence over the vibrations of the atoms near the source of disturbance at a subsequent instant. In this section, it is shown that there is such a tendency on the part of the disturbance agitating the atoms to resolve itself gradually into a set of harmonic vibrations, with exactly the same frequencies as of these wave clusters and that the contributions to the vibrational energy of the atoms due to all other frequencies are insignificant, being second-order quantities. Next, the dependence of the amplitudes of vibrations of the atoms on the factor $t^{-3/2}$ is interesting and suggests a correlation with thermal conductivity.

We shall suppose that initially all the atoms in the cell with index zero (0, 0, 0) of the lattice are displaced by small amounts and that the velocities of all the atoms are zero. In other words, the initial state of movements of the atoms is described by

$$q_{irs}(0) = \frac{1}{8\pi^3 c}\int_{\Delta} u_r^i \, e^{ia.s} \, d\mathrm{V} = u_r^i \, \delta_{s0} \tag{16}$$

and $$\dot{q}_{irs}(0) = 0, \tag{17}$$

where $d\mathrm{V} = da_1 da_2 da_3 = c\,d\theta_1 d\theta_2 d\theta_3$, (a_1, a_2, a_3) being the components of the wave vector in any three orthogonal directions in the reciprocal lattice and c is the determinant of the transformation $a_i = \sum_j c_{ij}\,\theta_j$ $(i, j = 1, 2, 3)$; Δ denotes the volume enclosed by the parallelopiped whose corners are given by $\pi(\pm \mathbf{b}_1 \pm \mathbf{b}_2 \pm \mathbf{b}_3)$.

At any subsequent instant, the displacements of the atoms from their equilibrium positions can be obtained by the superposition of the waves of the type (5) and we have

$$q_{irs}(t) = \frac{1}{16\pi^3 c}\sum_{k=1}^{3p}{}' \int_{\Delta} \mathrm{A}^i_{r,k}\,(e^{i\omega_k t} + e^{-i\omega_k t})\, e^{ia.s}\, d\mathrm{V} \tag{18}$$

where $A^i_{r,k}$ denotes the amplitude A^i_r of the rth particle in any cell in the direction x^i corresponding to the frequency branch ω_k of (10) and we should further have

$$\sum_{k=1}^{3p} A^i_{r,k} = u^i_r \tag{19}$$

to be in conformity with the initial conditions (16, 17).

A discussion of the variation of the above integral with time is not in general possible, as it requires a knowledge of the force constants and the actual expressions for the frequency branches; however the analogy of a linear lattice shows that no particle can acquire a sensible amplitude until the fastest group corresponding to the elastic waves reaches that lattice point. We obtain here an asymptotic approximation of (18), which describes the nature of the movements of the atoms a long time after the initial disturbance.

We shall denote the eight saddle points (13) at which $\frac{d\omega}{da} = 0$ by $\mathbf{a}^\alpha = (a_1^\alpha, a_2^\alpha, a_3^\alpha)$ $(\alpha = 1, 2 \ldots 8)$ and the corresponding value of ω_k by v_k^α $(k = 1, 2 \ldots 3p)$. For $\mathbf{a}^1 = (0, 0, 0)$, three of the frequencies of (10) are zero and these frequencies may be denoted by $v_1^1 = v_2^1 = v_3^1 = 0$. Further, let $\Delta_k = |b_{rs}|$ where $|b_{rs}|$ is the determinant of order three whose elements are given by $b_{rs} = b_{sr} = \frac{\partial^2 \omega_k}{\partial a_r \partial a_s}$ and let the values of Δ_k and $A^i_{r,k}$ which are functions of $\mathbf{a}$ at the eight saddle points be denoted by Δ_k^α and $A^{i,\alpha}_{r,k}$. Then from the result proved in the Appendix, we get the following expression for the asymptotic value of $q_{irs}(t)$.

$$q_{irs}(t) = \frac{1}{c\,(2\pi t)^{3/2}} \sum_{k=4}^{3p} \frac{A^{i,1}_{r,k}}{|\Delta_k^1|^{\frac{1}{2}}} \cos\left(v_k^1 t + k^1 \frac{\pi}{4}\right)$$

$$+ \frac{1}{c\,(2\pi t)^{3/2}} \sum_{\alpha=2}^{8} \sum_{k=1}^{3p} \frac{A^{i,\alpha}_{r,k}}{|\Delta_k^\alpha|^{1/2}} \cos\left(v_k^\alpha t + \mathbf{a}^\alpha \cdot \mathbf{s} + k^r \frac{\pi}{4}\right)$$

$$(i = 1, 2, 3;\ r = 1, 2 \ldots p) \tag{20}$$

here k^α is the signature of the matrix of the determinant Δ_k^α.

An equation analogous to (20) can be derived by an exactly similar procedure if initially a group of atoms in any cell have small velocities, but no displacements. When this is done, the general expressions for the vibrations of the atoms about their mean positions under any initial condition regarding their velocities and displacements are easily obtained by the principle of superposition. In any case, *the state of movements of the atoms tends asymptotically to a superposition of the* (24 p–3) *characteristic vibrations of the crystal, with amplitudes that vary inversely as* $t^{3/2}$.

These vibrations were first predicted and described by Sir C. V. Raman. The $(3p-3)$ modes contained in the first summation can be pictured as the oscillations with respect to each other of the p interpenetrating Bravais lattices of atom of which the crystal is built up, while since $\mathbf{a}^{\alpha} \cdot \mathbf{s}$ is an integral multiple of π, the remaining $21p$ modes represent the oscillations of the alternate layers of equivalent atoms against each other. The number of the distinct characteristic frequencies might be considerably reduced for crystals exhibiting a high degree of symmetry. It is worthy of note that the $21p$ modes have the same status as the remaining $(3p-3)$ modes as far as the dynamical behaviour of the system is concerned, though it is the latter that are active in the first order Raman effect; their importance arises in the second order Raman effect in crystals, where they exhibit themselves as combinations and overtones of the fundamental frequencies.

I am very much indebted to Professor Sir C. V. Raman, N.L., for his encouragement and suggestions, during the course of this work.

SUMMARY

It has been shown that the structure of a crystal as a three-dimensional repetitive pattern of lattice cells of atoms leads automatically to the result that the group velocity of the waves associated with the $(24p-3)$ characteristic frequencies should be equal to zero, and hence that oscillations having these frequencies are in the nature of stationary normal modes of vibration of the crystal lattice. It has further been proved that any arbitrary initial disturbance asymptotically settles into a superposition of these $(24p-3)$ characteristic vibrations which were first predicted by Raman, and that their amplitudes of vibration vary inversely as $t^{3/2}$ and further, that the energies associated with other frequencies of vibration are of negligible magnitude.

APPENDIX

Consider the integral $\mathrm{I} = \int_{\mathrm{D}} f(x) \exp. i [\omega(x)\, t - k \cdot x]\, d\mathrm{V}$, (1)

where $x=(x_1, x_2, x_3)$ and $k=(k_1, k_2, k_3)$ and $d\mathrm{V} = dx_1\, dx_2\, dx_3$. We shall assume that $f(x)$ is integrable in D and that the region of integration contains only one stationary point of $\omega(x)$ at $x = x_0 = (x_{10}, x_{20}, x_{30})$. When t is large enough as to make exp. $i\omega(x)\, t$ a very rapidly fluctuating function compared to $f(x)$ exp. $ik.x$, an approximation to the above integral can be effected by the application of the principle of stationary phases due to Kelvin. A fairly good estimate of (1) can be obtained if $\mathrm{M}t = 0(|k|^2)$, where M is a constant of the dimensions of distance, for in this case $\omega(x)\, t$ is a second order quantity compared to $k.x$. The principle of Kelvin states that the maximum contribution to an integral containing a very rapidly fluctuating

function arises only from the regions in the neighbourhood of points at which the function is stationary. A rigorous justification of this principle for integrals involving one variable was given by Watson[5]; a formal extension of it to integrals of the type (18) involving three variables is given below.

If we write $(x_i - x_{i0}) = \xi_i\,(i = 1, 2, 3)$, for small values of ξ_1, ξ_2, ξ_3, we have by Taylor's theorem

$$\omega(x) = \omega(x_0) + \tfrac{1}{2} \sum_{r,s} a_{rs}\,\xi_r\,\xi_s \tag{2}$$

where $a_{rs} = a_{sr} = \left(\dfrac{\partial^2 \omega}{\partial x_r\,\partial x_s}\right)_{x=x_0}$

Hence an approximation for (1) would be $I \sim f(x_0)\, e^{i[\omega(x_0)t - k\cdot x_0]}$

$$\int_{D_1} e^{\frac{it}{2} \sum_{r,s} a_{rs}\,\xi_r\,\xi_s}\, d\xi_1\, d\xi_2\, d\xi_3 \tag{3}$$

D_1 being any small region completely enclosing the point x_0.

If we transform the variables ξ_1, ξ_2, ξ_3 to a new set of variables η_1, η_2, η_3 so that the new co-ordinate axes coincide with the directions of the principal diameters of the quadric $\sum_{r,s} a_{rs}\,\xi_r\,\xi_s = 1$ in the ξ space, then

$$\sum_{r,s} a_{rs}\,\xi_r\,\xi_s = \lambda_1\,\eta_1^2 + \lambda_2\,\eta_2^2 + \lambda_3\eta_3^2 -, \tag{4}$$

$\lambda_1, \lambda_2, \lambda_3$ being the eigenvalues of the matrix $(a_{rs}) = A$. Since (a_{rs}) is symmetric, the roots of $|A - \lambda I| = 0$ are real. Also, we have $d\xi_1\, d\xi_2\, d\xi_3 = d\eta_1\, d\eta_2\, d\eta_3$. Hence (3) becomes

$$I \sim f(x_0)\, e^{i[\omega(x_0)\, t - k\cdot x_0]} \int_{D_2} e^{\frac{it}{2}(\lambda_1\eta_1^2 + \lambda_2\eta_2^2 + \lambda_3\eta_3^2)}\, d\eta_1\, d\eta_2\, d\eta_3 \tag{5}$$

D_2 being the region corresponding to D_1 in the η space.

If therefore $\lambda_1, \lambda_2, \lambda_3$ are all positive (say) then by writing $\sqrt{\lambda_r\, t}\,\eta_r = y_r$ $(r = 1, 2, 3)$, we can take the limits for y_1, y_2, y_3 to be $-\infty$ to $+\infty$ as t is large. Hence (5) becomes

$$I \sim \frac{f(x_0)\, e^{i\,[\omega(x_0)\, t - k.x_0]}}{|\Delta|^{1/2}\, t^{3/2}} \prod_r \int_{-\infty}^{+\infty} e^{-y_r^2/2i}\, dy_r \tag{6}$$

$(r = 1, 2, 3)$, Lt $t \to \infty$

$$= \left(\frac{2\pi}{t}\right)^{3/2} \frac{f(x_0)}{|\Delta|^{1/2}}\, e^{i\,[\omega(x_0)\, t - k.x_0 + 3\pi/4]}$$

for from (4), $\lambda_1\,\lambda_2\,\lambda_3 = \Delta$, the determinant of the matrix A.

In general we have

$$I = \left(\frac{2\pi}{t}\right)^{3/2} \frac{f(x_0)}{|\Delta|^{1/2}} \exp i\,[\omega(x_0)\,t - k.x_0 + s\pi/4] \text{ Lt } t \to \infty \tag{7}$$

where s is the *signature of the matrix* (A), *i.e.*, the difference between the number of positive eigenvalues to the number of negative eigenvalues of the matrix A.

Similarly the value of the integral

$I' = \int_D f(x) \exp i\,(-\omega(x)\,t + k.x)\,dV$, is given by

$$I' = \left(\frac{2\pi}{t}\right)^{3/2} \frac{f(x_0)}{|\Delta|^{1/2}} \exp i\,[-\omega(x_0)\,t + k\cdot x_0 - s\pi/4) \tag{8}$$

When the region of integration contains several stationary points, it can be split up into subregions in each of which the function has only one stationary point and the final result simply consists of the sums of terms like (7).

REFERENCES

1. Born, Max .. *Atom theories Das Festen Zustandes Teubner, Leipzig*, 1923.
2. Blackman, M. .. *Proc. Roy. Soc.*, 1935, **148 A**, 390.
3. Raman, C. V. .. *Proc. Ind. Acad. Sci.*, 1943, **18 A**, 237.
4. ———— .. *Ibid.*, 1947, **26**, 339.
5. Watson, G. N. .. *Proc. Camb. Phil. Soc.*, 1918, **19**, 49.

THE CHARACTERISTIC VIBRATIONS OF CRYSTAL LATTICES—PART II

By K. S. Viswanathan

(From the Raman Research Institute, Bangalore)

Received March 9, 1953

(Communicated by Sir C. V. Raman, N.L.)

1. Introductory Remarks

The transference of a particular state from one part of a medium to another, without any bodily movement of the medium itself, is well known as *wave motion* in a material substance. For a discrete structure, such as a crystal, the disturbance arising from a wave progressing through the medium is defined only at the set of lattice points which are the mean positions of the atoms of the crystal. Wave propagation in crystal lattices should further be consistent with the constraints imposed by the dynamical equations of motion of the system and this in general makes the waves dispersive. By assuming waves through atoms of the same type in the crystal architecture, it was shown in a preceding paper that there are $(24\,p - 3)$ frequencies for the system which have the remarkable property of making the group velocity of the waves associated with them, equal to zero. These frequencies, in their turn, correspond to eight wave vectors in the reciprocal lattice.

To assign the direction of propagation of these eight types of wave fronts, we first note that an equation of the form $\eta = r \cos(\omega t - \mathbf{a}.\mathbf{s})$ denotes a wave front progressing in the direction of the vector $\mathbf{a}$ and that at any instant, the displacement is a constant for all points on the plane $\mathbf{a}.\mathbf{s} = \text{constant}$. The vector $(0, 0, \pi)$ now indicates the direction $\mathbf{b}_3$ of the reciprocal lattice and thus at any instant the displacements arising out of a plane wave of this wave-vector should be the same for all the atoms in a plane defined by the $\mathbf{d}_1$, $\mathbf{d}_2$ axes of the crystal. This vector, in effect, denotes modes in which alternate such layers of the crystal vibrate with opposite phases at any instant and with the same amplitudes. As the displacements of a wave in a crystal are defined only at its lattice points, the concept of a wave motion here ceases to have meaning except in a formal sense and the $3p$ modes associated with this vector are strictly stationary modes of vibrations; and a similar argument applies to each of the $(24\,p - 3)$ modes mentioned above. Again, three of the frequency branches ω_k $(k = 1, 2, 3)$ of the secular equation

(I, 8) tend to zero with $\mathbf{a}$ and as $\underset{a\to 0}{\mathrm{Lt}} \frac{\omega_k}{a} = \frac{d\omega_k}{da}$, we get the interesting result that the group and wave velocities of the elastic waves are identical.

It was further shown in Part I that any arbitrary initial disturbance inside the crystal tends asymptotically to a superposition of these characteristic vibrations. The object of the present paper is to discuss the reduction of the distinct number of terms of the asymptotic expression in the case of degeneracy in these modes and to consider some interesting corollaries resulting from it.

2. DEGENERACY

We adopt throughout the notation of Part I, except with slight modifications. Writing $\mathbf{q}_{rs} = (q_{1rs}, q_{2rs}, q_{3rs})$; $\mathbf{A}_r = (\mathbf{A}_r^1, \mathbf{A}_r^2, \mathbf{A}_r^3)$ and $\mathbf{A}_r(\mathbf{a}^\alpha) = \mathbf{A}_r(\alpha)$, the asymptotic expression (I, 20) for the displacements of the atoms from their equilibrium positions becomes

$$\mathbf{q}_{rs} = \frac{1}{c\,(2\pi t)^{3/2}} \sum_{k=1}^{3p} \frac{\mathbf{A}_{r,k}^{(1)}}{|\Delta_k^1|^{\frac{1}{2}}} \cos\left(v_k^1 t + k^1 \pi/4\right) + \frac{1}{c\,(2\pi t)^{3/2}} \sum_{\alpha=2}^{8} \sum_{k=1}^{3p} \frac{\mathbf{A}_{r,k}^{(\alpha)}}{|\Delta_k^\alpha|^{\frac{1}{2}}} \cos\left(v_k^\alpha t + \mathbf{a}^\alpha \cdot \mathbf{s} + k^\alpha \pi/4\right) \quad (1)$$

For crystals possessing symmetry, degeneracies may arise and the number of distinct terms contained in (1) could be considerably reduced. It has been shown by E. V. Chelam[1] that if under a symmetry operation of the crystal two vectors $\mathbf{a}^\alpha$ and $\mathbf{a}^{\alpha'}$ go over into each other, the set of $3p$ frequencies associated with each of them are the same for both the vectors. The set of all vectors which are transforms of each other under the symmetry group of the crystal constitutes an *equivalent* set. The $3p$ frequencies associated with all the vectors in an equivalent set are the same and differ only in their order of arrangement. The vector $\mathbf{a}^1 = (0, 0, 0)$ representing the unit element of the translational group forms always a set by itself. A further degeneracy among the $3p$ frequencies associated with any of the eight vectors $(\mathbf{a}^\alpha)$ is also possible depending on the crystal symmetry. We now prove an interesting result that if,

$$v_k^\alpha = v_s^{\alpha'}, \text{ then } \Delta_k^\alpha = \Delta_s^{\alpha'}. \quad (2)$$

Differentiating the equation (I, 10)

$$\sum_{t=0}^{3p} s_t z^{3p-t} = 0 \quad (3)$$

twice with respect to a and making use of the results $\frac{ds_t}{da} = 0; \frac{d\omega}{da} = 0$ at the eight points $\mathbf{a} = \mathbf{a}^\alpha$ $\left(\frac{d\omega_k}{da} \neq 0 \text{ at } \mathbf{a} = 0 \text{ for } k = 1, 2, 3\right)$, we get

$$2\omega(\alpha)\frac{d^2\omega}{da^2}(\alpha) = -\frac{\sum_{t=1}^{3p}\frac{d^2s_t}{da^2}(\alpha)\, z^{3p-t}(\alpha)}{\sum_{t=0}^{3p-1} s_t(\alpha)(3p-t)\, z^{3p-t-1}(\alpha)}. \tag{4}$$

Here functions of the vector $\mathbf{a}^\alpha$ are denoted simply by its suffix α in the argument, for example $s_t(\mathbf{a}^\alpha) = s_t(\alpha)$. It is obvious from (4) that if $\omega_k(\alpha) = \omega_s(\alpha)$, then $\frac{d^2\omega_k}{da^2}(\alpha) = \frac{d^2\omega_s}{da^2}(\alpha)$, the numerators and denominators in both the functions being equal to each other. For the case $\omega_k(\alpha) = \omega_s(\alpha')$, if we could prove that $\frac{d^2s_t}{da^2}(\alpha) = \frac{d^2s_t}{da^2}(\alpha')$, then from (4) it would follow that $\frac{d^2\omega_k}{da^2}(\alpha) = \frac{d^2\omega_s}{da^2}(\alpha')$.

To show this result, we note that the coefficients s_t $(t = 1, 2 \ldots . 3p)$ are symmetric functions of the roots of (3) and hence are *invariants* for all the vectors of an equivalent set. Thus, if $\mathbf{a}^\alpha$ and $\mathbf{a}^{\alpha'}$ are two vectors belonging to an equivalent set, then

$$s_t(\alpha) = s_t(\alpha') \qquad (t = 1, 2 \ldots . 3p) \tag{5}$$

Now the coefficients $s_1, s_2 \cdots s_{3p}$ of the various powers of z in (3) can be considered to be the components of a vector $\mathbf{s}$ in a $3p$-dimensional space N. This process sets a homomorphism between the vectors of the reciprocal space R and the corresponding vectors $\mathbf{s} = (s_1, s_2 \cdots s_{3p})$ in N; all equivalent vectors in R map the same vector in N. Starting from a vector $\mathbf{s}(\rho)$ in N, another one whose components are the derivatives $\frac{ds_i}{da}$ *at the point* $\mathbf{a} = \mathbf{a}^\rho$ of s_i could be obtained by means of the operator D, *i.e.*, $\mathbf{Ds}(\rho) = \frac{d\mathbf{s}}{da}(\rho)$. To a linear transformation $t: \mathbf{a} \to \mathbf{a}' = t\mathbf{a}$ in R corresponds in N the transformation $\mathbf{T}: \mathbf{Ts}(\mathbf{a}) = \mathbf{s}(\mathbf{a}')$. All linear correspondences in R which transform into themselves the vectors of an equivalent set, go over into the identity matrix I in R, in view of the relations (5). If $\mathbf{a}^\alpha$ and $\mathbf{a}^{\alpha'}$ are two vectors of an equivalent set in R such that $\mathbf{a}^{\alpha'} = t'\mathbf{a}^\alpha$, this correspondence in N is given by $\mathbf{s}(\alpha') = \mathbf{Is}(\alpha) = \mathbf{s}(\alpha)$. (6)

As the identity matrix commutes with all matrices in N, we have now

$$\mathbf{D}^2\mathbf{s}(\alpha') = \mathbf{D}^2\mathbf{Is}(\alpha) = \mathbf{ID}^2\mathbf{s}(\alpha) = \mathbf{D}^2\mathbf{s}(\alpha)$$

so that we get

$$\frac{d^2\mathbf{s}}{da^2}(\alpha') = \frac{d^2\mathbf{s}}{da^2}(\alpha).$$

Thus, if $\omega_k(\alpha) = \omega_s(\alpha')$, we get from (4)

$$\frac{d^2\omega_k}{da^2}(\alpha) = \frac{d^2\omega_s}{da^2}(\alpha'). \tag{7}$$

In a similar way we could show that

$$\frac{\partial^2\omega_k}{\partial a_i \partial a_j}(\alpha) = \frac{\partial^2\omega_s}{\partial a_i \partial a_j}(\alpha') \tag{7 a}$$

and from this, result (2) follows.

Let now the distinct frequencies in (1) be denoted by $c_1, c_2 \ldots c_\rho$. Then if $\nu_k^\alpha = \nu_s^{\alpha'} = c_r$, we can write $\Delta_k^\alpha = \Delta_s^{\alpha'} = \Delta_r$ and $k^\alpha = k_r$. The equation (1) now reduces to the form

$$\mathbf{q}_{rs}(t) = \frac{1}{c\,(2\pi t)^{3/2}} \sum_{r=1}^{\rho} \frac{\cos(c_r t + k_r \pi/4)}{|\Delta_r|^{\frac{1}{2}}} \left(\sum_{\alpha,k} \mathbf{A}_{r,k} \cos \mathbf{a}^\alpha \cdot \mathbf{s}\right) \tag{8}$$

the summation inside the brackets being over all values of α and k such that $\nu_k^\alpha = c_r$.

3. Effect of a Translation

We shall suppose that initially all the cells of the crystal bounded by the parallelopiped (D) whose edges are $l_1\mathbf{d}_1$, $l_2\mathbf{d}_2$, $l_3\mathbf{d}_3$ undergo a small translation specified by the vector $\mathbf{u} = (u_1, u_2, u_3)$. Then the initial conditions are described by

$$\mathbf{q}_{rs}(0) = \frac{\mathbf{u}}{8\pi^3 c} \int_\Delta \sum_\sigma e^{i\alpha\cdot(s-\sigma)}\, dV \tag{9}$$

the summation extending over all the cells contained in D and $\dot{\mathbf{q}}_{rs}(0) = 0$.

At a later instant, the displacements of the atoms about their equilibrium positions are given by

$$\mathbf{q}_{rs}(t) = \frac{1}{16\pi^3 c} \sum_{k=1}^{3\rho} \int_\Delta \mathbf{A}_{r,k} (e^{i\omega_k t} + e^{-i\omega_k t}) \left(\sum_\sigma e^{i\alpha\cdot(s-\sigma)}\right) dV \tag{10}$$

where we have from the initial conditions (9) the following relation

$$\sum_{k=1}^{3\rho} \mathbf{A}_{r,k} = \mathbf{u}. \tag{11}$$

If we write $\mathbf{A}_{r,k}\,(\sum_{\sigma} e^{-ia\cdot\sigma}) = \mathbf{B}_{r,k}$, then the asymptotic value of (10) is given by

$$\mathbf{q}_{rs}(t) = \frac{1}{c\,(2\pi t)^{3/2}} \sum_{k=4}^{3p} \frac{\mathbf{B}_{r,k}^{(1)}}{|\Delta_k^1|^{\frac{1}{2}}} \cos(v_k^1 t + k^1\pi/4)$$

$$+ \frac{1}{c\,(2\pi t)^{3/2}} \sum_{a=2}^{8} \sum_{k=1}^{3p} \frac{\mathbf{B}_{r,k}^{(a)}}{|\Delta_k^a|^{\frac{1}{2}}} \cos(v_k^a t + \mathbf{a}^a\cdot\mathbf{s} + k^a\pi/4) \quad (12)$$

Now

$$e^{-ia\cdot\sigma} = \sum_{\sigma} e^{-i(\sigma_1\theta_1+\sigma_2\theta_2+\sigma_3\theta_3)}$$

$$= \prod_{r=1}^{3} \frac{(1 - e^{-il_r\theta_r})}{(1 - e^{-i\theta_r})}$$

so that

$$\mathbf{B}_{r,k}^{(a)} = \mathbf{A}_{r,k}^{(a)} \prod_{r=1}^{3} \frac{(1 - e^{-il_r\theta_r})}{(1 - e^{-i\theta_r})}, \quad (13)$$

where the θ's have any one of the values 0 or π.

If l_1, l_2, l_3 are all even *or* if the region that undergoes a translation contains an integral number of supercells of the lattice, then

$$\mathbf{B}_{r,k}^{(a)} = 0 \text{ from (13)} \qquad (\text{for } a = 2,\ 3\cdots 8),$$

so that the asymptotic state of movements of the atoms consists only of the $(3p - 3)$ modes of vibrations in which equivalent atoms in successive cells vibrate with the same phases and amplitudes. If two of these numbers are even and the other odd (say, l_1 and l_2 are even and l_3 is odd), then $\mathbf{B}_{r,k}^{(a)} = 0$ for the set of points $(0, \pi, \pi)$; $(\pi, 0, 0)$; $(\pi, 0, \pi)$; $(\pi, \pi, 0)$ and (π, π, π). At the point $(0, 0, \pi)$, $\mathbf{B}_{r,k}^{(a)} = l_1 l_2\,\mathbf{A}_{r,k}^{(a)} \neq 0$. Thus in this case, in addition to the $(3p - 3)$ modes, the state of vibrations of the atoms of the crystal consists of $3p$ other modes in which equivalent atoms in consecutive cells along the direction of the axis d_3 vibrate with opposite phases. Similarly, when the region undergoing the translation contains an even number of cells along only one of the axes of the crystal, it can be seen that the amplitudes of $12p$ vibrations are equal to zero and when l_1, l_2, l_3 are all odd, all the $(24p - 3)$ modes will be active.

It should be mentioned that the above statements are true only to a first order of approximation, as we have in deriving (1) neglected infinitesimals of order higher than $t^{-3/2}$. We note that a translation of an unit cell of the crystal results in exciting all the $(24p - 3)$ vibrations. The same translation applied to an adjacent cell along one of the crystal axes causes displacements in which the amplitudes of the vibrations of the planes intersecting this axis

against each other, occur with opposite signs to the corresponding vibrations excited by its neighbour. The physical explanation of the above results now follows from the fact that in any bodily movement of two adjacent cells, such vibrations annul each other leaving only $(12p - 3)$ vibrations intact. By the same reasoning, we can show that an initial disturbance consisting of translations by the same amount, but in opposite directions of two supercells excites none of these vibrations and the displacements of any atom arising out of such a disturbance tends asymptotically to zero. Applied to an actual crystal, say the diamond[2] in which degeneracies are present, these results show that a translation of one of its supercells excites only the 1332 vibration, while in a disturbance arising out of a translation of an unit consisting of an even number of cells along only one of its axes, all the eight distinct modes of oscillation of the crystal will be active.

The author's grateful thanks are due to Professor Sir C. V. Raman for suggesting the problem and for his guidance during the course of this work.

SUMMARY

It is shown that the wave and group velocities of the elastic waves are identical. An initial disturbance consisting of a translation of a supercell excites asymptotically the $(3p - 3)$ characteristic vibrations only, the amplitudes of the remaining $21p$ modes being zero to a first order of approximation. A translation of a single unit cell results in exciting all the $(24p - 3)$ modes of vibrations of the crystal. The question of reduction of the asymptotic expression for the displacements of the atoms about their mean positions to its simplest form, when degeneracies are present in these vibrations, is also considered.

REFERENCES

1. Chelam, E. V. .. *Proc. Ind. Acad. Sci.*, 1943, **18A**, 283.
2. ———— .. *Ibid.*, 1943, **18**, 257.
3. Viswanathan, K. S. .. *Ibid.*, 1953, **37**, 424.

THE INFRA-RED ABSORPTION SPECTRA OF SODIUM NITRATE AND CALCITE

By A. K. Ramdas

(From the Raman Research Institute, Bangalore)

Received February 17, 1953

(Communicated by Sir C. V. Raman)

1. Introduction

The infra-red absorption and reflexion spectra of sodium nitrate have been studied in the region of short wavelengths ($\lambda < 20\,\mu$) by Schæfer and his co-workers,[1] while Liebisch and Rubens[2] studied the reflexion spectrum in the long-wave range between $20\,\mu$ to $300\,\mu$. Calcite has been the subject of numerous investigations. Special mention may be made of Schæfer and his collaborators[3] who investigated absorption and reflexion spectra in the range $1\,\mu$ to $20\,\mu$ and Liebisch and Rubens[2] who examined the reflexion spectrum in the range $20\,\mu$ to $300\,\mu$. In view of the greatly improved instruments available at the present time in the field of infra-red spectroscopy, it appeared important to reinvestigate these crystals in order to get a more complete and detailed picture of their infra-red absorption spectra. The author has studied the absorption spectra of calcite and of sodium nitrate in the range $1\,\mu$ to $22\,\mu$ with a Beckman infra-red spectrophotometer provided with potassium bromide optics.

Sodium nitrate and calcite have similar crystal structures and hence should show similar infra-red behaviour. As Bhagavantam and Venkatarayudu[4] have emphasized, the infra-red and Raman spectra of crystals must be interpreted in accordance with the number of normal modes, their selection rules and symmetry properties appropriate to the unit cell of the crystal. In this paper it is proposed to present the experimental results obtained by the author and discuss the infra-red data in the light of the appropriate selection rules and the Raman effect data.

2. Experimental Results

The crystals were studied with the cleavage sections perpendicular to the infra-red radiation; the % transmission was read off directly with the spectrophotometer at $0{\cdot}05\,\mu$ intervals and at still closer intervals near absorption maxima.

Sodium Nitrate.—Figs. 1 and 2 show the % cut-off with wavelength of sodium nitrate specimens (thickness: Sp. I: 2·34 mm., Sp. III: 1 mm.). The following features are noticed in Figs. 1 and 2.

I. Many well-defined and sharp absorption maxima are seen in range 2 μ to 3·5 μ, *viz.*, at 2·3 μ, 2·42 μ, 2·65 μ, 2·85 μ, 3·2 μ. These have come out better with Sp. I than with Sp. III because Sp. I is thicker and hence brings out these weak absorption bands better.

II. Sharp and intense absorption maxima in the range 3·5 μ to 6·5 μ, *viz.*, at 3·6 μ, 4·1 μ, 4·75 μ, 5·6 μ, 5·8 μ, 6·3 μ. These bands have come out better with Sp. III than with Sp. I. The well resolved absorption maxima at 5·6 μ, 5·8 μ and 6·3 μ seen in Fig. 2 merge into an intense and broad absorption band extending from 5·6 μ to 9 μ as can be seen in Fig. 1.

III. Absorption maxima, very intense and broad compared to the bands mentioned in I and II, are seen in the range 6·5 μ to 14 μ. In Fig. 2

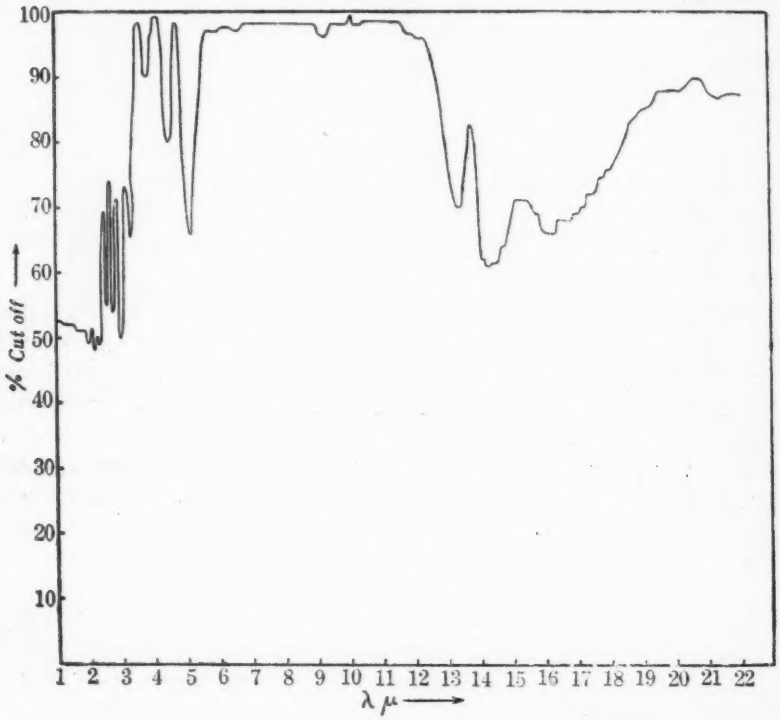

FIG. 1. Infra-red absorption spectrum of sodium nitrate (Specimen I).

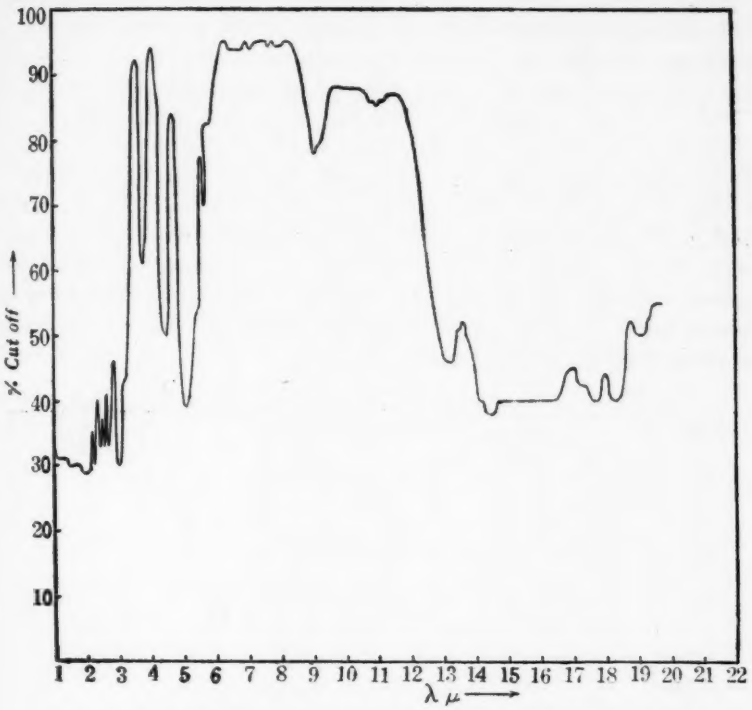

Fig. 2. Infra-red absorption spectrum of sodium nitrate (Specimen III).

we notice the following absorption bands: (1) between 6·7 and 8·0 μ, very strong; (2) at 8·3 μ, a strong companion to the 6·7 μ–8 μ band ; (3) from 9·8 μ to 10·6 μ, medium; (4) a medium strong and fairly sharp absorption maximum at 11·8 μ; (5) a very weak but very sharp and well-defined absorption maximum at 13·8 μ.

In Fig. 1, we notice an extremely broad absorption band running from 6 μ to 9 μ and from 9·5 μ to 11·6 μ and an inflexion at about 11·8 μ. These have been resolved into bands described above, by using the thinner specimen III. The 13·8 μ band, however, has come out sharper and stands out better in Fig. 1.

IV. In the range 14 μ to 22 μ, we notice in Fig. 1, a rather broad band medium in intensity, from 15·0 μ to 15·3 μ and considerable absorption between 19 μ to 22 μ. In Fig. 2, there are indications of these being resolved into constituent bands.

Calcite.—Fig. 3, giving the % cut-off with wave-length of a cleavage section of calcite (Specimen II: 0·33 mm.) shows a great similarity with Figs. 1 and 2. We see (1) weak but well-defined bands at 2·3 μ, 2·5 μ, 2·8 μ; (2) an inflexion at 3·1 μ; (3) exceedingly sharp and intense band at 3·47 μ; (4) a comparatively weaker absorption maximum at 4·8 μ; (5) indication of a band at 5·75 μ; (6) an intense absorption maximum at 6·3 μ clearly separated from an equally intense broad absorption band extending from 6·7 μ to 7·8 μ and in the slope of this band, an inflexion at 8·45 μ; (7) a series of bands at 9·3 μ (very weak), 9·9 μ (medium), 10·6 μ (weak), 11·3 μ (weak), 11·7 μ (inflexion), 12·8 μ (weak), and 14·1 μ (very intense and sharp); (8) beyond 17 μ, there is a very broad absorption band, extending upto the limit of observation; there are some indications of absorption maxima in this region.

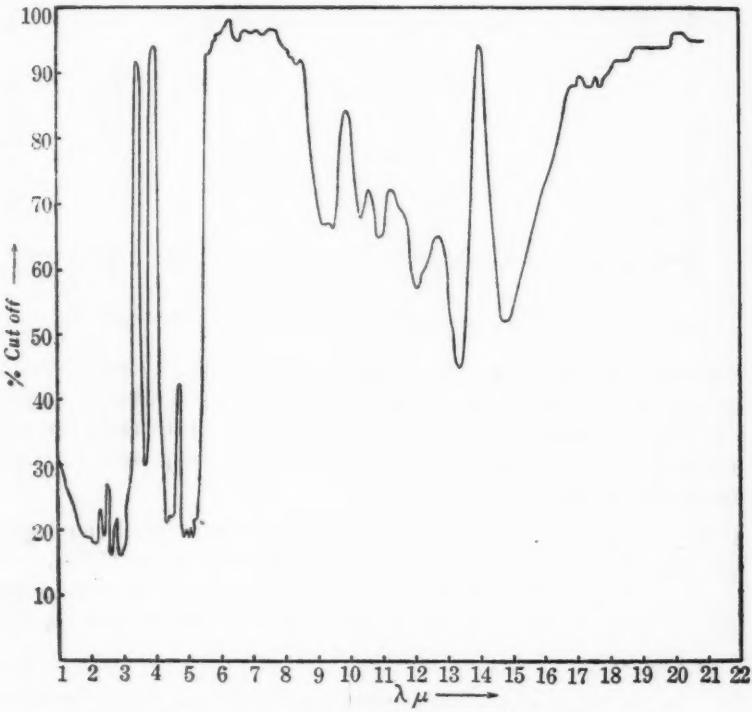

FIG. 3. Infra-red absorption spectrum of calcite (Specimen II).

Special attention may be drawn here to the remarkable sharpness of the harmonics both in calcite and sodium nitrate.

3. Discussion of the Results

Sodium nitrate and calcite have the same crystal structure, their space group being D_{3d}^6 with two molecules per unit cell. Bhagavantam and Venkatarayudu[4] have shown that for these cases the number of modes of vibrations and the selection rules with respect to their infra-red and Raman activity are as given in Table I.

Table I

Class	Total No.	Internal	External R.	External T.	Translations	R.	I.R.
A_1	1	1	0	0	0	a*	ia*
A_2	3	1	1	1	0	ia	ia
B_1	4	1	1	1	1	ia	a
B_2	2	1	0	1	0	ia	ia
E_1	6	2	1	2	1	ia	a
E_2	4	2	1	1	0	a	ia

* *a* = Active; *ia* = Inactive

Thus we see that there are three internal frequencies active in infra-red and three active in Raman effect, the two sets being mutually exclusive as a result of the presence of a centre of symmetry. In addition there are two internal and three external frequencies which are inactive in both infra-red and Raman effect. The free carbonate and nitrate ion belong to the point group D_{3h} which has one frequency active in Raman effect only, one active in infra-red only and two active in both. The transformation from free ion to the crystal can be pictured as follows:

Free ion		Crystal	
(A_1) ω_1 (Raman active)	$\rightarrow$ (A_1) ν_1 (Raman active),	(A_2) ν_1' (inactive in both)	
(B_1) ω_2 (Infra-red active)	$\rightarrow$ (B_2) ν_4' (inactive in both),	(B_1) ν_4 (I. red active)	
(E) ω_3 (active in both)	$\rightarrow$ (E_1) ν_2 (Raman active),	(E_2) ν_5 (,,)	
(E) ω_4 (,,)	$\rightarrow$ (E_1) ν_3 (,,),	(E_2) ν_6 (,,)	

The extent of this splitting will naturally depend on the strength of the coupling between the two carbonate (or nitrate) ions. As regards the lattice oscillations, we notice that there are two Raman active external vibrations and five infra-red active.

The depolarisation studies of Raman lines with directional excitation with polarised and unpolarised light, and the polarisation of the infra-red absorption bands, enable one to find out and classify the different fundamental oscillations. In Table II we give the Raman active and infra-red active frequencies of sodium nitrate.

TABLE II. *Sodium nitrate*

Raman active*	Infra-red active
ν_1 (A_1) : 1068 cm.$^{-1}$	ν_4 (B_1) : 845 cm.$^{-1}$
ν_2 (E_2) : 720 ,,	ν_5 (E_1) : 725 ,,
ν_3 (E_2) : 1385 ,,	ν_6 (E_1) : 1385 ,,
L_6 (E_2) : 98 ,,	L_1 (B_1) : 71 ,,
L_7 (E_2) : 185 ,,	L_2 (B_1) : 217 ,,
	L_3 (E_1) : 71 ,,
	L_4 (E_1) : 133 ,,
	L_5 (E_1) : 217 ,,

Note.—The Raman active frequencies are those actually observed, while infra-red frequencies are derived from the reststrahlen data for the remote frequencies and from the present studies for the nearer ones.

Similarly we give the frequencies for calcite in Table III.

TABLE III. *Calcite*

Raman active†	Infra-red active
ν_1 (A_1) : 1086 cm.$^{-1}$	ν_4 (B_1) : 885 cm.$^{-1}$
ν_2 (E_2) : 712 ,,	ν_5 (E_1) : 706 ,,
ν_3 (E_2) : 1434 ,,	ν_6 (E_1) : 1484 ,,
L_6 (E_2) : 156 ,,	L_1 (B_1) : 106 ,,
L_7 (E_2) : 284 ,,	L_2 (B_1) : 357 ,,
	L_3 (E_1) : 106 ,,
	L_4 (E_1) : 182 ,,
	L_5 (E_1) : 330 ,,

* T. M. K. Nedungadi[5]; † Bhagavantam[6]

Note.—See remarks made under Table II.

Schæfer and his co-workers[3] gave a detailed analysis of their infra-red absorption and reflexion data for calcite. Their assignments were based on the assumption of a free carbonate ion. However, as we have seen above, the normal modes of the free ion (carbonate and nitrate) split and increase in number, in the crystalline state; this as well as the selection rules governing them are found to be verified experimentally. Hence, in this paper, the assignments are made according to selection rules appropriate to the crystal.

Besides these internal frequencies, there are low frequency lattice frequencies characteristic of the crystal structure. Though these frequencies lie beyond the range studied to be observed as fundamentals, we may expect harmonics of the lattice frequencies, and combinations and differences between internal frequencies and lattice frequencies, when permitted by the selection rules.

In giving the assignments to the observed absorption bands, the following principles are to be borne in mind. A difference band is observed only if the corresponding summation also occurs. Though the combination between high frequency internal vibrations are likely to occur, the possibility of difference bands between them can be ruled out. The polarisation character of the vibration must be considered while giving the assignments to the different absorption bands.

In the light of these facts, the interpretation of the absorption data has been given in Tables IV and V. In the short wavelengths ($\lambda < 6\,\mu$), Schæfer and his collaborators have further resolved some of the absorption bands using rock-salt and quartz optics. Using a very thick specimen (2 cm. thick $\perp$ to optic axis), and quartz optics, Plyler[7] was able to record some absorption bands for calcite in the range $1\,\mu$ to $3\,\mu$. The data of these workers as well as those obtained in this work, are used in the following tables. Following the above considerations, it has been possible to give proper assignments to almost all the observed absorption bands and from Tables IV and V, we see that the assignments are unique in most cases. It is interesting to note that many of the absorption bands can be only explained as combinations (or differences) between internal and external vibrations and some as harmonics of external vibrations alone.

In conclusion, the author wishes to express his thanks to Prof. Sir C. V. Raman, F.R.S., N.L., for his keen interest and guidance and to the Investigator-in-charge, C.S.I.R. Radiation Scheme, Poona, for his permission to use the infra-red spectrophotometer.

TABLE IV

Sodium Nitrate

Observed		Assignment		Calculated
λμ	cm.$^{-1}$	Combination	Type	cm.$^{-1}$
2·3	4348	$\nu_3+\nu_4+\nu_5+\nu_6$	$B_1+B_2+3E_1$	4340
2·42	4132	$3\nu_6$, $2\nu_5+\nu_6$	$B_1+B_2+E_1$, $B_1+B_2+2E_1$	4155
2·45	4082	——		——
2·61	3831	$\nu_1+\nu_3+\nu_6$	$B_1+B_2+E_1$	3838
2·65	3774	——		——
2·85	3509	$2\nu_3+\nu_5$	$B_1+B_2+2E_1$	3495
2·885	3466	——		——
3·2	3125	——		——
3·325	3008	——		——
3·56	2809	$\nu_3+\nu_6$	$B_1+B_2+E_1$	2770
3·65	2740			
4·10	2439	$\nu_1+\nu_5$	E_1	2453
4·75	2105	$\nu_2+\nu_6$	$B_1+B_2+E_1$	2105
		$\nu_3+\nu_5$	,,	2110
4·79	2088	——		——
5·28	1894	——		——
5·6	1786	$\nu_1+\nu_3$	E_1	1793
5·8	1724	——		——
6·35	1575	$\nu_2+\nu_4$	E_1	1565
		ν_6+L_7	$B_1+B_2+E_1$	1570
6·7	1493	ν_6+L_6	$B_1+B_2+E_1$	1483
		ν_5+L_3	,,	1456
		$\underline{\nu_6}$	E_1	1385
		ν_3-L_3	$B_1+B_2+E_1$	1314
8·0	1250	ν_6-L_6	$B_1+B_2+E_1$	1287
8·3	1205	ν_1+L_4	E_1	1201
		ν_6-L_7	$B_1+B_2+E_1$	1200
9·8	1020	ν_4+L_7	E_1	1030
10·6	943	ν_1-L_4	E_1	935
11·83	845	$\underline{\nu_4}$	B_1	845
13·8	725	$\underline{\nu_5}$	E_1	725
15·0	667	ν_4-L_7	E_1	660
15·3	654			
18	556	Harmonics of lattice frequencies		
?	?			

TABLE V

Calcite

Observed			Assignment		Calculated
λμ	cm.$^{-1}$	Polarisation	Combination	Type	cm.$^{-1}$
1·76	5682	O			
1·9	5263	,,	$\nu_3+\nu_4+2\nu_6$	$B_1+B_2+2E_1$	5287
2·0	5000	,,	$3\nu_3+\nu_6$	$B_1+B_2+3E_1$	5008
2·2	4545	,,	$\nu_3+\nu_4+\nu_5+\nu_6$	$B_1+B_2+3E_1$	4509
2·3	4348	,,	$2\nu_3+\nu_6$	$B_1+B_2+2E_1$	4352
2·33	4292	,,	$2\nu_1+\nu_3+\nu_5$	$B_1+B_2+E_1$	4312
2·5	4000	,,	$\nu_1+\nu_3+\nu_6$	$B_1+B_2+E_1$	4004
2·533	3948	,,			
2·74	3650	,,	$2\nu_1+\nu_6$	E_1	3656
2·786	3589	,,	$2\nu_3+\nu_5$	$B_1+B_2+2E_1$	3574
3·04	3289	,,	$\nu_1+\nu_2+\nu_6$	$B_1+B_2+E_1$	3282
3·1	3226	,,	$\nu_1+\nu_3+\nu_5$	$B_1+B_2+E_1$	3226
3·25	3077	E	$2\nu_1+\nu_4$	B_1	3057
3·33	3003	O			
3·47	2882	,,	$\nu_3+\nu_6$	$B_1+B_2+E_1$	2918
3·71	2695	E	$3\nu_4$	B_1	2655
3·87	2584	O	$\nu_1+\nu_6$	E_1	2570
4·16	2404	E			
4·5	2222	O	$\nu_2+\nu_6$	$B_1+B_2+E_1$	2196
4·64	2155	O+E	$\nu_3+\nu_5$	$B_1+B_2+E_1$	2140
5·15	1942	O			
5·1	1961	E	$\nu_1+\nu_4$	B_1	1971
5·545	1803	O	$\nu_1+\nu_5$	E_1	1792
			ν_3+L_2	E_1	1791
5·75	1739	E	ν_6+L_7	$B_1+B_2+E_1$	1768
6·3	1587	,,	$\nu_4+\nu_2$	E_1	1597
6·7	1493	C			
↓	↓		$\underline{\underline{\nu_6}}$	E_1	1484
7·8	1282		$\nu_2+\nu_6$	$B_1+B_2+E_1$	1418
8·45	1183	O	ν_1+L_3	E_1	1192
8·76	1142	E	ν_4+L_7	E_1	1169
9·3	1075	O	ν_3-L_2	E_1	1077
9·9	1010	O	ν_5+L_7	$B_1+B_2+E_1$	990
			ν_1-L_3	E_1	980
			$3L_5$	$B_1+B_2+E_1$	990
10·6	943	C	L_2+2L_7	B_1+E_1	925
11·3	885	E	$\underline{\underline{\nu_4}}$	B_1	885
12·8	781	C	$2L_5+L_3$	$B_1+B_2+2E_1$	766
14·1	709	O	$L_6+L_7+L_5$	$B_1+B_2+3E_1$	770
			$\underline{\underline{\nu_5}}$	E_1	706
17·0	588	C	Harmonics of lattice frequencies		
↓					
?					

O = ordinary; E = extraordinary; C = cleavage

SUMMARY

The infra-red absorption spectra of sodium nitrate and calcite crystals have been studied in the range 1 μ to 22 μ with a Beckman infra-red spectrophotometer, using three different thicknesses of a cleavage section in each case. The thinner plates exhibit the structure of the more intense absorption bands while the thicker ones show their harmonics as well as the weaker bands very clearly. The remarkable sharpness of the harmonics is a noteworthy feature. Much new detail has been observed with sodium nitrate in the region of wavelength greater than 8 μ. A strong absorption in the region beyond 17 μ has been found in both crystals. This is ascribable to harmonics of lattice oscillations. The entire body of data is satisfactorily explained in terms of the normal modes of vibration jointly of the two units ($NaNO_3$ or $CaCO_3$) contained in the unit cell of the crystal lattice.

REFERENCES

1. Schæfer and Schubert .. *Ann. de. Phys.*, 1918, **55**, 577.
   —— and Bormuth .. *Zeit. f. Physik*, 1930, **62**, 508.
2. Liebisch and Rubens .. *Sitz. Preuss. Akad. Wiss*, 1919, 198.
3. Schæfer and Matossi .. *Das Ultrarote Spektrum*, 1930.
4. Bhagavantam and Venkatarayudu .. *Proc. Ind. Acad. Sci.*, 1939, **9A**, 224.
5. Nedungadi .. *Ibid.*, 1939, **10A**, 197.
6. Bhagavantam .. *Ibid.*, 1940, **11A**, 62.
7. Plyler .. *Phy. Rev.*, 1929, **33**, 948.

THE INFRA-RED ABSORPTION SPECTRA OF SODIUM CHLORATE AND POTASSIUM CHLORATE CRYSTALS

By A. K. Ramdas

(From the Raman Research Institute, Bangalore)

Received March 11, 1953

(Communicated by Sir C. V. Raman)

1. Introduction

The infra-red reflexion spectrum of sodium chlorate was examined by Schæfer and Schubert[1] in short wavelengths ($\lambda\mu < 20$) and observed maxima at $10{\cdot}04\,\mu$ and $16{\cdot}04\,\mu$, while Laski[2] who investigated the spectrum in the range $20\,\mu$ to $120\,\mu$ by the reststrahlen method noticed maxima at $25{\cdot}0\,\mu$, $60{\cdot}0\,\mu$ and $83{\cdot}0\,\mu$. The present author has studied the infra-red transmission spectrum of sodium chlorate crystals in the range $1\,\mu$ to $22\,\mu$ using a Beckman infra-red spectrometer (Model IR 2). The author has also studied the transmission spectrum of a thick specimen of potassium chlorate crystal, and observed a few more absorption bands than reported in the previous papers.[3] It is proposed to present these experimental observations in this paper and discuss them in the light of the Raman effect data for these two crystals.

Two crystals of sodium chlorate were studied (sp. I = 2·1 mm., and sp. II = 1 mm. thick). The potassium chlorate crystal was studied as previously in the 001 plane (sp V = 1 mm. thick). The Fig. 1 gives the percentage cut-off *vs.* wavelength for sodium chlorate (sp. II) and Fig. 2 for potassium chlorate.

The following absorption maxima are noticed in Fig. 1 (sodium chlorate:

(1) Weak absorption maxima at $2{\cdot}6\,\mu$, $3{\cdot}5\,\mu$, $4{\cdot}0\,\mu$, $4{\cdot}1\,\mu$ and $4{\cdot}3\,\mu$. Of these the $3{\cdot}5\,\mu$ absorption maximum is the strongest.

(2) A very intense absorption band extending from $5{\cdot}1\,\mu$ to $5{\cdot}4\,\mu$.

(3) Two well-defined absorption bands at $6{\cdot}3\,\mu$ and $6{\cdot}95\,\mu$, of medium intensity.

(4) Very strong and very broad maxima between $9\,\mu$ to $13{\cdot}4\,\mu$; from $15\,\mu$ to $17{\cdot}8\,\mu$; and from $19{\cdot}9\,\mu$ to $20{\cdot}7\,\mu$.

In Fig. 2, (potassium chlorate) in addition to the absorption maxima reported in the previous papers, *viz.*, 5·3 μ (sharply defined and strong); 6·3 μ and 6·9 μ (well-defined and medium); 10 μ to 10·8 μ (very strong with a flat top); 13·5 μ (medium); 16·2 μ (strong and sharply defined); 17·25 μ, 18 μ, and 18·75 μ (inflexions in the slope of the 16·2 μ band); and 20·3 μ (strong, sharply defined, with indications of structure)—we notice the following additional bands: (1) 2·85 μ (very weak); (2) 3·5 μ (well defined); (3) 4·1 μ (very weak); (4) 4·3 μ (very weak); (5) the 20·3 μ band definitely shows a structure and maxima at 20·1 μ and 20·4 μ can be easily recognised.

2. Discussion of the Results

(i) *Sodium chlorate.*—Sodium chlorate belongs to the space group T^4, and contains four molecules per unit cell. The vibrations of this crystal class are classified as: A (totally symmetric); E (symmetric with respect to the three two-fold axes and doubly degenerate with respect to the four

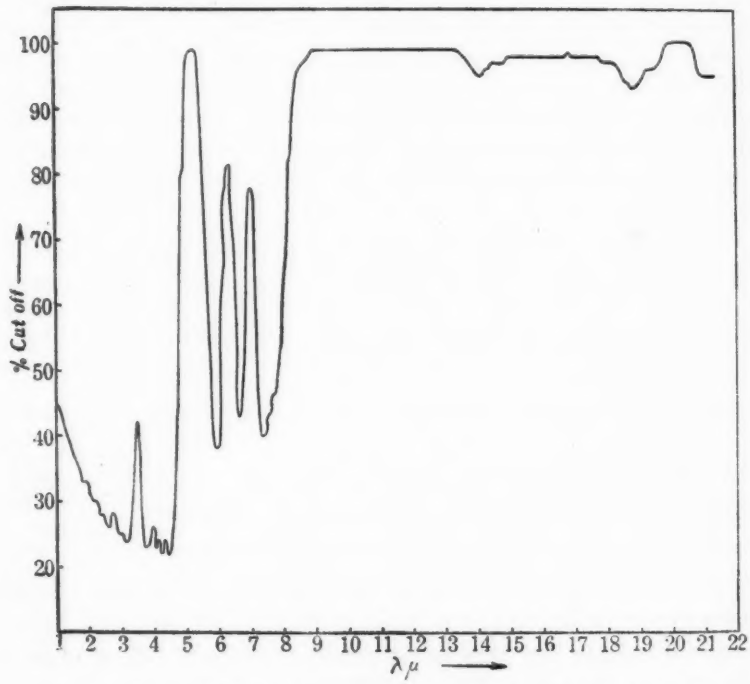

Fig. 1. Infra-red absorption spectrum of sodium chlorate (Specimen II)

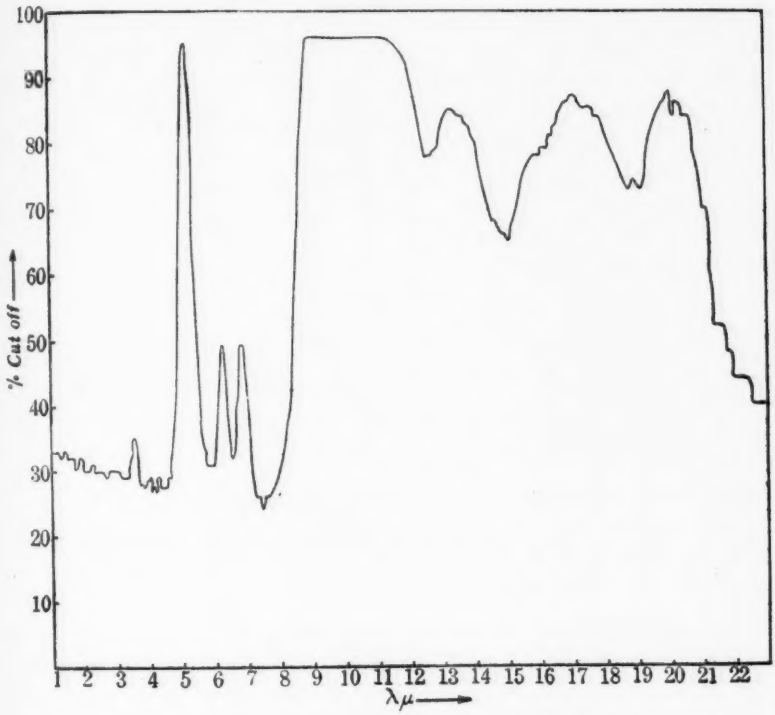

FIG. 2. Infra-red absorption spectrum of potassium chlorate (Specimen V)

three-fold axes); and F (triply degenerate with respect to the three two-fold axes). Further, selection rules permit all these vibrations to appear as fundamentals in the Raman effect but *only* those belonging to the F-class to appear in the infra-red.

The Raman spectrum of single crystal of sodium chlorate has been very thoroughly studied (Couture, L. and Mathieu, J. P.[4]; Chandrasekharan[5]) and with the exception of two, all the Raman lines observed have been classified according to their polarisation characteristics. In Table I we give all the Raman lines observed, with their symmetry types.

Corresponding to each of the F-type oscillation in the high frequency region (*i.e.*, the internal frequencies) there are broad absorption bands, *viz.*, from $9{\cdot}0\,\mu$ to $13{\cdot}4\,\mu$ corresponding to $10{\cdot}72\,\mu$ (933 cm.$^{-1}$), $10{\cdot}33\,\mu$ (968 cm.$^{-1}$), $10{\cdot}16$ (984 cm.$^{-1}$); from $15\,\mu$ to $17{\cdot}8\,\mu$ corresponding to $16{\cdot}0\,\mu$ (625 cm.$^{-1}$); and from $19{\cdot}9\,\mu$ to $20{\cdot}7\,\mu$ corresponding to $20{\cdot}53\,\mu$ (487 cm.$^{-1}$). It is possible

TABLE I

Vibration	cm.$^{-1}$	Type	Vibration	cm.$^{-1}$	Type
ν_1'	933	*F*	L_1	66·5	E
ν_1''	936	A	L_2	92·5	*F*?
ν_2'	963	E	L_3	122·5	*F*
ν_2''	968	*F*	L_4	130·0	E
ν_2'''	984	*F*	L_5	179·0	E
ν_3'	617	A			
ν_3''	625	*F*			
ν_4'	480	E			
ν_4''	487	*F*			
ν_2''''	1026	?			

to give a reasonable interpretation of the higher harmonics in terms of the observed Raman lines following the selection rules which permit: F^2; $F \times F$; $E \times F$; $A \times F$; F^3; $A^2 \times F$; $A \times F \times F$; $A \times F^2$; $A \times E \times F$; $F \times F \times F$; $F \times F^2$; etc.

As regards the low frequency oscillations, they naturally lie beyond the range investigated. Laski, however, has observed reflexion maxima at 60 μ (167 cm.$^{-1}$) and 83 μ (120·5 cm.$^{-1}$). The latter can be attributed to the F-type lattice oscillation L_3 (122·5 cm.$^{-1}$). There is no F-type Raman line corresponding to 167 cm.$^{-1}$ Combination and difference bands of the type $\nu \pm L$, *i.e.*, between internal and lattice oscillations can however occur in the range under investigation when allowed by the selection rules. This no doubt contributes to the notable breadth of the fundamental absorption bands. An examination of the infra-red absorption bands using crystals much thinner than those used in the present investigation is necessary.

In Table II we give the assignments of the observed absorption maxima.

(ii) *Potassium chlorate.*—Potassium chlorate belongs to the space group C_{2h}^2, and contains two molecules per unit cell. Due to the coupling between these two molecules and due to the removal of degeneracy of vibrations of chlorate ion in the free state, the internal vibrations of the chlorate ion in the crystal increase in number as shown in a previous paper (see Table III), *i.e.*, there are six Raman active internal vibrations and six infra-red active, the two sets being mutually exclusive because of the presence of a centre of symmetry. This difference and splitting was ignored in the previous papers

TABLE II

Observed λμ	Observed cm.$^{-1}$	Assignment	Calculated cm.$^{-1}$
2·6	3846	$3\nu_2'' + \nu_1''$	3840
3·5	2857	$\nu_1' + \nu_2' + \nu_2''$	2864,
		$\nu_1' + \nu_1'' + \nu_2'''$	2853
4·0	2500	$2\nu_1' + \nu_3''$	2491
4·1	2439	$\nu_2'' + \nu_2''' + \nu_4''$	2439
4·3	2326		
5·1	1961	$2\nu_2'''$	1968
↓	↓	$\nu_2'' + \nu_2'''$	1952
5·4	1852	$\nu_2' + \nu_2'''$	1947
		$2\nu_2''$	1936
		$\nu_2' + \nu_2''$	1931
		$\nu_1'' + \nu_2'''$	1920
		$\nu_2''' + \nu_1'$	1917
		$\nu_1'' + \nu_2''$	1904
		$\nu_1' + \nu_2''$	1901
		$\nu_2' + \nu_1'$	1896
		$\nu_1'' + \nu_1'$	1869
		$2\nu_1'$	1866
6·3	1587	$\nu_2'' + \nu_3'$	1585
6·95	1440	$\nu_2'' + \nu_4'$	1448
9·0	1111	ν_2'''	984
↓	↓	ν_2''	968
13·4	746	ν_1'	933
15·0	667		
↓	↓	ν_2''	625
17·8	562		
19·9	502·5		
↓	↓	ν_4''	487
20·7	483		

TABLE III

Free ion	Crystal	
Raman and Infra-red active	Raman active	Infra-red active
ν_1 (A_1)	ν_1 (A_1)	ω_1 (B_2)
ν_3 (A_1)	ν_3 (A_1)	ω_3 (B_2)
ν_2 (E)	ν_2 (A_1), ν_2' (A_2)	ω_2 (B_2), ω_2' (B_1)
ν_4 (E)	ν_4 (A_1), ν_4' (A_2)	ω_4 (B_2), ω_4' (B_1)

in giving the assignments of the observed absorption bands. But actually it is possible to recognise the difference in the corresponding infra-red active

and Raman active fundamentals. In Table IV we give the Raman active vibrations observed by Shantakumari[6] and infra-red active fundamentals observed in the present work.

TABLE IV

Raman effect	Infra-red
ν_1 $(A_1) = 930$ cm.$^{-1}$	ω_1 $(B_2) = 910$cm.$^{-1}$
ν_3 $(A_1) = 620$,,	ω_3 $(B_2) = 617$,,
ν_2 (A_1), ν_2' $(A_2) = 975$,,	ω_2 (B_2), ω_2' $(B_1) = 960$,,
ν_4 (A_1), ν_4' $(A_2) = 486$,,	ω_4 (B_2), ω_4' $(B_1) = 493$,,

The frequencies ω_1 and ω_3 (ω_2') are chosen so as to represent the data best. The crystal structure of potassium chlorate is almost uniaxial (pseudo-hexagonal) and hence the splitting due to removal of degeneracy may not be significant. However, in the present work the $20{\cdot}3\,\mu$ (493 cm.$^{-1}$) band does show recognisable structure with maxima at $20{\cdot}1\,\mu$ (497·5 cm.$^{-1}$) and $20{\cdot}4\,\mu$ (490 cm.$^{-1}$) and similarly Venkateswaran[7] working with crystal powder did notice Raman lines at 478 cm.$^{-1}$ and 493 cm.$^{-1}$. This point requires further investigation.

The selection rules permit the following combinations to appear in infra-red: $A_1 \times B_1$; $A_1 \times B_2$; $A_2 \times B_1$; $A_2 \times B_2$; $A_1^2 \times B_1$; $A_1^2 \times B_2$; $A_2^2 \times B_1$; $A_2^2 \times B_2$; B_1^3; B_2^3; $A_1 \times B_1^3$; $A_1 \times B_2^3$; $A_2 \times B_1^3$; $A_2 \times B_2^3$; $A_1^3 \times B_1$; $A_1^3 \times B_2$; $A_2^3 \times B_1$; $A_2^3 \times B_2$, etc. In Table V we give the assignments of the observed absorption maxima on this basis.

From Table V it is seen that most of the bands are very satisfactorily explained on the basis indicated above.

The bands 9, 11, 12 and 13 are interpreted as combinations between internal and external vibrations. The combinations allowed to appear in infra-red are $\omega \pm$ Raman active L, and $\nu \pm$ infra-red active L. The observed Raman lines are L_1 (54 cm.$^{-1}$), L_2 (82 cm.$^{-1}$), L_3 (98 cm.$^{-1}$), L_4 (127 cm.$^{-1}$) and L_5 (145 cm.$^{-1}$). With this data only the absorption maximum at $13{\cdot}5\,\mu$ (741 cm.$^{-1}$) can be explained. Since the data regarding the lattice oscillations, especially the infra-red active, are incomplete no interpretation can be given at present to the remaining bands at $17{\cdot}25\,\mu$, $18{\cdot}0\,\mu$ and $18{\cdot}75\,\mu$.

My best thanks are due to Prof. Sir C. V. Raman, F.R.S., N.L., for his guidance and encouragement and to the Investigator-in-charge, C.S.I.R. Radiation Scheme, Poona, for his kind permission to use the infra-red spectrophotometer.

TABLE V

Observed			Assignment	Calculated
No.	λμ	cm.$^{-1}$		cm.$^{-1}$
1	2·85	3509	$3\omega_2 + \nu_3$	3500
2	3·5	2857	$\omega_1 + 2\nu_2$	2860
3	4·1	2439	$\omega_4 + 2\nu_2$	2443
4	4·3	2326	$\omega_1 + \nu_1 + \nu_4$	2326
5	5·3	1887	$\omega_2 + \nu_1$	1890
6	6·3	1587	$\omega_2 + \nu_3$	1580
7	6·9	1449	$\omega_2 + \nu_4$	1446
8	10–10·8	1000–926	$\omega_4 + \nu_4$, ω_2, ω_1	979, 960, 910
9	13·5	741	$\omega_3 + L_4$	744
10	16·2	617	ω_3	617
11	17·25	581·5	$\nu_4 + L$	—
12	18·0	556·0	$\nu_4 + L$	—
13	18·75	533·0	$\nu_4 + L$	—
14	20·3	493	ω_4	49

3. SUMMARY

The infra-red absorption spectrum in the range 1 μ to 22 μ of sodium chlorate crystals shows besides intense regions of absorption maxima between 9 μ and 13·4 μ, 15 μ and 18·7 μ, 19·9 μ and 20·7 μ, numerous absorption bands, *viz.*, at 3·5, 4·0, 4·1, and 4·3 μ; from 5·1 to 5·4 μ; and at 6·3 and 6·95 μ. All these are satisfactorily interpreted in terms of the Raman lines, following selection rules appropriate to the space group T^4 to which sodium chlorate belongs. By using a fairly thick crystal of potassium chlorate, some additional bands not previously noticed are observed, *viz.*, at 2·85, 3·5, 4·1 and 4·3 μ. By recognising the difference between the infra-red active fundamentals and Raman active fundamentals in the crystal of potassium chlorate, it is possible to give a satisfactory explanation of all the absorption maxima.

REFERENCES

1. Schæfer and Schubert .. *Z. für Physik.*, 1921, **7**, 309.
2. Laski .. *Z. für Krist.*, 1927, **65**, 607.
3. Ramdas .. *Proc. Ind. Acad. Sci.*, 1952, **36 A**, 55.
4. Couture and Mathieu .. *Ann. de. Phy.*, 1948, **12**, 521.
5. Chandrasekharan .. *Proc. Ind. Acad. Sci.*, 1950, **32 A**, 374.
6. Shantakumari .. *Ibid.*, 1950, **32 A**, 177.
7. Venkateswaran .. *Ibid.*, 1938, **7 A**, 144.

A REDETERMINATION OF THE ROTATORY DISPERSION OF SODIUM CHLORATE

By S. Chandrasekhar

(From the Raman Research Institute, Bangalore)

Received February 18, 1953

(Communicated by Sir C. V. Raman, F.R.S., N.L.)

1. Introduction

Sodium chlorate is the best known example of a crystal belonging to the cubic system exhibiting optical activity. As an aqueous solution of it does not display such activity, it is clear that the optical rotatory power is a consequence of the crystal structure which belongs to the space group T^4–$P2_13$. Precise data regarding the rotatory power and its variation with wave-length are obviously needed as a starting point for any theoretical discussion of the optical behaviour of the crystal in relation to its structure. Determinations have been made in the visible region of the spectrum by Sohncke (1878), Voigt (1908), Perucca (1919) and also by Ramaseshan (1948). Measurements extending far into to the ultra-violet were first made by Guye (1889) and later by Rose (1909), both of whom have obtained values of the rotation from 7200 A.U. to 2500 A.U. Though it is known that sodium chlorate transmits light upto nearly 2200 A.U., it appears that no one has since pursued the measurements farther into the ultra-violet. The data obtained by Guye and Rose, which are the most extensive, have been presented in Table I. From the data it can be seen that in the visible region Biot's Law is approximately valid, but as we proceed into the ultra-violet, the rotatory power increases at a much *slower* rate than is required by Biot's Law.

Though these experimental studies are on record, there appears to have been only one attempt to represent the data by means of a rotatory dispersion formula (Int. Crit. Tables, 1930). The formula is

$$\rho = \frac{1{\cdot}078}{\lambda^2 - 0{\cdot}0062}. \qquad (1)$$

But this formula is valid only from 7188 A.U. to 3184 A.U., and fails farther in the ultra-violet. This is to be expected since any one-term Drude equation varies faster with decrease of wave-length than expected from Biot's Law.

The present work was taken up with a view to redetermine the rotatory dispersion of sodium chlorate accurately and to extend the measurements

farther into the spectrum on either side. It has been possible to go up to 8756 A.U. in the infra-red and upto 2378 A.U. in the ultra-violet. Some significant results have emerged from these readings, which we shall describe later. A rotatory dispersion formula has been suggested which fits the data accurately over the whole range of wave-lengths. The relative merits of this formula and a formula of the Drude type have also been discussed.

Throughout, the rotatory power (ρ) is expressed in degrees per millimetre and λ in microns.

TABLE I

Rotatory Dispersion of Sodium Chlorate—Earlier Determinations

λ	ρ (Guye)	λ	ρ (Rose)
·2504	14·96	·2573	14·73
·2777	13·90	·2748	14·07
·2827	13·43		
·2992	12·42	·3256	10·67
·3234	10·79	·3404	9·80
·3337	10·08	·3467	9·44
·3564	8·861	·3611	8·69
·3735	8·100	·4308	6·01
·4071	6·754	·4862	4·67
·4283	6·055	·5270	3·94
·4553	5·331	·5893	3·13
·5310	3·881	·6563	2·50
·6507	2·559	·6867	2·27
·7177	2·068	·7188	2·07

2. EXPERIMENTAL DETAILS

Depending on the particular region of the spectrum which was being studied, four different experimental methods had to be employed. Before describing these in detail, we shall present the values of the rotatory power obtained by the various methods separately in Table II. The accuracy of the determinations by different methods have been checked against each other by arranging that they overlap, and as will be seen from Table II they agree satisfactorily.

We shall now describe the experimental procedure.

(A) A large crystal of sodium chlorate (about $5\frac{1}{2}\times5\times4\frac{1}{2}$ cm.) grown in the Bell Telephone Laboratories* was used for these measurements. For

* The crystal was kindly loaned by Dr. R. S. Krishnan, to whom the author's thanks are due.

TABLE II

Rotatory Dispersion of Sodium Chlorate—Present Determination

λ	ρ				Most probable value of ρ
	A	B	C	D	
·23783				14·27	14·27
·23994				14·6	14·6
·24469			15·03		15·03
·246406			15·11	15·12	15·11
·24827		15·205	15·19		15·21
·2536		15·275	15·264		15·28
·25763		15·23		15·255	15·23
·2652		14·92			14·92
·26989		14·67			14·67
·27528		14·31			14·31
·28035		13·96			13·96
·28936		13·31			13·31
·29254		13·095			13·095
·29673		12·74			12·74
·30215		12·38			12·38
·31256		11·67			11·67
·33415		10·19			10·19
·36525	8·537	8·534			8·537
·37042		8·288			8·288
·39064		7·438			7·438
·40466	6·886				6·886
·40778	6·787				6·787
·43583	5·884				5·884
·49164	4·571	4·572			4·571
·54607	3·671				3·671
·57696	3·275				3·275
·57907	3·249				3·249
·5893	3·136				3·136
·62344	2·764				2·764
·69075	2·225				2·225
·7082	2·119				2·119
·77292	1·756				1·756
·8180	1·545				1·545
·8756	1·345				1·345

the visible and infra-red region of the spectrum, the polarimeter was of the simplest type consisting of two nicols. A high pressure mercury discharge lamp (Philips) served as a convenient multichromatic source of light from 9000 A.U. to 3650 A.U. By a suitable set of lenses parallel light was made to pass through the polarimeter and focus on the widened slit of a spectrograph. By taking photographs of the spectrum with different settings of

the analyser, the positions of extinction could be approximately determined for the different wave-lengths. To determine these readings more accurately, the photographs were repeated for much closer settings of the analyser on either side of extinction position for each wave-length. The time of exposure for these successive photographs was made exactly the same, varying from 30 seconds to 15 minutes depending on the brightness of the spectral line. By finding out the exposures of equal intensity on either side of the minimum, or in effect, by making use of the principle of the half-shade, the angle of extinction could be determined to within about 0·2° to 0·5°. By repeating these measurements with and without the crystal, the total rotation was estimated for the various wave-lengths. The thickness of the crystal was ascertained by means of a micrometer caliper measuring to an accuracy of 0·001 inch. A Hilger medium glass spectrograph was used for the visible spectrum. For the infra-red, a constant deviation instrument and special infra-red plates were employed. The photographs obtained in such a manner have not been reproduced here, but they exactly resemble the plates shown later. It can be seen that these plates look very much like the imprints of spectra obtained by Cotton and Descamps (see Lowry, 1935) with their polarimeter for measuring rotatory dispersion in the ultra-violet.

By replacing the entire glass optics in the above arrangement by corresponding quartz components, the measurements could just be extended upto 3650 A.U.

(B) Beyond 3650 A.U. in the ultra-violet, the absorption of light by the nicols became too great. Two natural crystals of calcite were used instead. When light is incident normally on one of the two parallel faces of calcite, the ordinary ray passes through undeviated, while the extraordinary ray, which is deflected, can be cut off by means of a suitable slit. One such crystal was mounted coaxially on a divided circle and served as the analyser while the other was fixed and was used as the polariser. A quartz mercury discharge lamp (Hanovia) was an excellent ultra-violet source of light. Though the aperture of this polarimeter was comparatively small, very satisfactory photographs were obtained as can be seen from Figs. 1, 2 and 3 in Plate XXII. The exposures in this region varied between 10 minutes and half an hour. In fact, calcite crystals have been used as polarisers by most of the pioneers working in this field (see Lowry, *loc. cit.*). In this manner, the rotation could be determined upto 2482 A.U., beyond which the absorption of light by the two calcite crystals began to creep in, so that even with exposures of 2 hours, the lines were too weak to be recorded.

(C) One of the calcite crystals was replaced by a reflection polariser as was used by Servant (1939) for the measurement of the rotatory dispersion of quartz in the Schumann region. A cleavage surface of a lithium fluoride crystal reflecting at Brewster's angle was found to give almost perfect polarisation. Transmission pictures revealed that the intensity of the light passing through the large specimen of sodium chlorate, which was being used for all the above measurements, was considerably cut off beyond 2446 A.U. It was therefore possible to measure the rotation only upto that wave-length by giving long exposures of half to one hour.

(D) But with thinner specimens of sodium chlorate the transmission extended easily upto 2300 A.U., without any notable diminution of intensity. To increase the transmitted light, the faces of the crystal were well polished by rubbing on a breathed-on glass surface. The readings were taken upto 2378 A.U., with a crystal of thickness 7·62 mm. by giving exposures of one hour.

The accuracy of the methods described above is quite high. For instance, the total rotation for 2536 A.U., for a thickness of 42·65 mm. is about 651·5° and this can be measured to within about 0·5°. If the thickness of the crystal is ascertained to an accuracy of 0·1%, the error in estimating the rotatory power is only about 0·2%. In this manner, the error of measurement for wave-lengths lying between 5893 A.U. and 2447 A.U. has been placed at 0·2 to 0·3%. As the total rotation is comparatively smaller farther in the ultra-violet (where the thin specimen of sodium chlorate was used) and in the infra-red region, the error is slightly greater, being a little over 1%. In the first three methods described above, the measurements were made at the room temperature, which was 25° C. approximately. But, when the readings were being taken with the thinner specimen (method D), the weather became rather humid and a heater had to be kept in the vicinity to prevent the crystal from getting damaged. Hence, the temperature rose to approximately 30° C.

3. DISCUSSION OF RESULTS

A comparison of Tables I and II shows that the general trend of the values obtained in the present determination agrees approximately with those of the earlier workers. In the visible region the agreement is extremely good. To illustrate this, the rotatory power as obtained by the various authors for a common wave-length is given in Table III.

In the ultra-violet, the present measurements give values slightly higher (about 1 to 2%) than those obtained by Guye and Rose. This might possibly

TABLE III

Name of Author	λ	ρ
Voigt	·590	3·170
Rose	·5893	3·13
Perucca	·5893	3·12
Ramaseshan	·5893	3·14
The present Author ..	·5893	3·136

be due to the difference in the temperature at which these measurements were made. Guye's values are given at 13° C. while the present data are at 25° C.

The small extension of the measurement into the ultra-violet has proved to be very fruitful. From the earlier measurements given in Table I, it will be seen that as we proceed into the ultra-violet the rate of increase of the rotatory power with decrease of wave-length becomes progressively smaller. This is also seen in the present determination but, in addition, it has been found that beyond 2536 A.U., there is an actual diminution in the magnitude of the rotation, the decrease becoming more pronounced as we move farther into the ultra-violet. This observation, which was first made with the large crystal of sodium chlorate, has been confirmed with the smaller specimen also. It appears that this anomalous behaviour of the rotatory dispersion of sodium chlorate has been noticed for the first time.

The photographs reproduced in Plate XXII were all obtained with the calcite polarising prisms (method B). In Fig. 1, the angle between each successive settings of the analyser is 8°. Though some lines have been over-exposed, the plate clearly shows the extinction positions for the different wave-lengths. As the specimen used was very large (42·65 mm.) four clear extinction bands are seen, the total rotation for the successive bands differing by 180°. Fig. 2 shows a similar photograph with much closer settings of the analyser (2°). Fig. 3 is an enlarged reproduction of the spectra obtained in the region of 2500 A.U. A line has been drawn through the minima of intensity for the different wave-lengths. It can be seen that extinction band changes its course beyond 2536 A.U., thus clearly demonstrating the diminution of the rotatory power in the ultra-violet. This observation has been verified with the smaller specimen also.

4. A ROTATORY DISPERSION FORMULA

As has already been pointed out, it is not possible to fit the data with a one-term formula of the Drude type. An attempt has therefore been made to represent the data by means of a two-term formula of the same type. The following formula gives an approximate fit:—

$$\rho = \frac{1\cdot293}{\lambda^2 - (0\cdot1)^2} - \frac{0\cdot1724}{\lambda^2 - (0\cdot21)^2}. \tag{2}$$

This formula makes use of a characteristic wave-length at 1000 A.U., and another at 2100 A.U., almost at the limit of continuous absorption of light in sodium chlorate. The calculated and experimental values for a few wave-lengths are given in Table IV.

TABLE IV

Rotatory Dispersion using Formula (2)

λ	ρ (expt.)	ρ (calc.)
·2464	15·1	15·1
·2536	15·3	15·3
·2925	13·1	13·0
·3652	8·54	8·55
·5791	3·25	3·38

Though a fairly good fit has been obtained, the formula is questionable from the theoretical standpoint. For, it does not fulfil Kuhn's summation rule which states that the sum of the numerators determining the contributions of the different absorption frequencies to the rotatory power should vanish,

i.e., if $\rho = \sum_r \frac{Q_r}{\lambda^2 - \lambda_r^2}$, then $\sum_r \frac{Q_r}{\lambda_r^2} = 0.$

When this criterion is applied to (2), it is found that it is not even approximately satisfied, the strength of the positive term being nearly thirty times as great as that of the negative term. Hence it appears that a formula of the Drude type is not appropriate for the case of sodium chlorate. Instead,

TABLE V

Rotatory Dispersion using Formula (3)

λ	ρ (expt.)	Contribution of positive term	Contribution of negative terms	ρ (calc.)
·23783	14·27	29·831	15·697	14·13
·23994	14·6	29·134	14·637	14·5
·24469	15·03	27·673	12·629	15·04
·246406	15·11	27·165	12·011	15·15
·24827	15·21	26·637	11·393	15·24
·2536	15·28	25·208	9·884	15·32
·25763	15·23	24·211	8·947	15·26
·2652	14·92	22·495	7·536	14·96
·26989	14·67	21·529	6·835	14·69
·27528	14·31	20·493	6·153	14·34
·28035	13·96	19·59	5·61	13·98
·28936	13·31	18·533	4·818	13·32
·29254	13·10	17·659	4·582	13·08
·29673	12·74	17·06	4·30	12·76
·30215	12·38	16·338	3·974	12·36
·31256	11·67	15·075	3·455	11·62
·33415	10·19	12·897	2·682	10·22
·36525	8·537	10·524	1·986	8·538
·37042	8·288	10·195	1·901	8·294
·39064	7·438	9·052	1·619	7·433
·40466	6·886	8·371	1·464	6·907
·40778	6·787	8·231	1·433	6·798
·43583	5·884	7·115	1·199	5·916
·49164	4·571	5·487	0·895	4·592
·54607	3·671	4·389	0·711	3·678
·57696	3·275	3·909	0·636	3·273
·57907	3·249	3·880	0·632	3·248
·5893	3·136	3·740	0·610	3·130
·62344	2·764	3·324	0·548	2·776
·69075	2·225	2·687	0·457	2·230
·7082	2·119	2·552	0·439	2·113
·77292	1·756	2·131	0·382	1·749
·8180	1·545	1·896	0·351	1·545
·8756	1·345	1·650	0·320	1·330

the following formula has been suggested, which fits the newer measurements quite accurately over the entire range of wave-lengths:

$$\rho = \frac{1{\cdot}2387\,\lambda^2}{[\lambda^2 - (0{\cdot}09)^2]^2} - \frac{0{\cdot}1374\,\lambda^2}{[\lambda^2 - (0{\cdot}185)^2]^2} - 0{\cdot}123, \qquad (3)$$

In this formula, the ultra-violet absorption wave-lengths are 900 A.U., and 1850 A.U. The third term represents the small contribution of the infra-red. As the exact behaviour of optically active crystals in the infra-red is not known, this contribution has been included in the form of a very small constant. The above formula is not open to the same objection as that raised against (2), for each term in (3), neglecting the infra-red, separately fulfils the summation condition, as has been shown in an earlier paper by the present author (1952). The calculated values are given in comparison with the experimental data in Table V. Though the weight of the negative term in formula (3) appears very small it can be seen from the table that contribution is very large in the ultra-violet, becoming almost equal in magnitude to that of the positive term.

It can be seen from the above table that the agreement is quite satisfactory, the deviation being generally within the limits of experimental error.

It can easily be shown that the characteristic wave-lengths occurring in rotatory dispersion formula (3) can also be used to represent the ordinary dispersion of sodium chlorate quite well. Accordingly, a formula of the Sellmeyer-Drude type involving these two wave-lengths has been fitted up. The formula is:—

$$n^2 - 1 = \frac{1{\cdot}1825\,\lambda^2}{\lambda^2 - (0{\cdot}09)^2} + \frac{0{\cdot}07992\,\lambda^2}{\lambda^2 - (0{\cdot}185)^2} - 0{\cdot}00864\,\lambda^2. \qquad (4)$$

The third term represents a small infra-red contribution. The calculated values are given with the available experimental data. The values from

TABLE VI

The Dispersion of Sodium Chlorate

λ	n (expt.)	n (calc.)
·231	1·616	1·618
·2573	1·585	1·585
·2748	1·572	1·572
·3256	1·549	1·549
·3404	1·544	1·544
·3467	1·542	1·542
·3611	1·539	1·539
·4862	1·522	1·522
·5173	1·519	1·519
·5893	1·515	1·515
·6563	1·513	1·513
·6867	1·512	1·512
·7188	1·511	1·511

FIG. 1

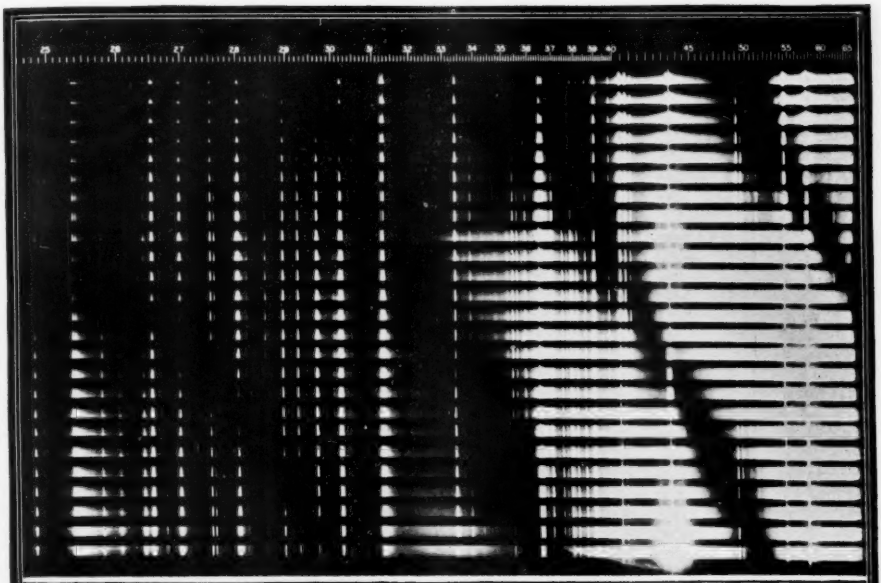

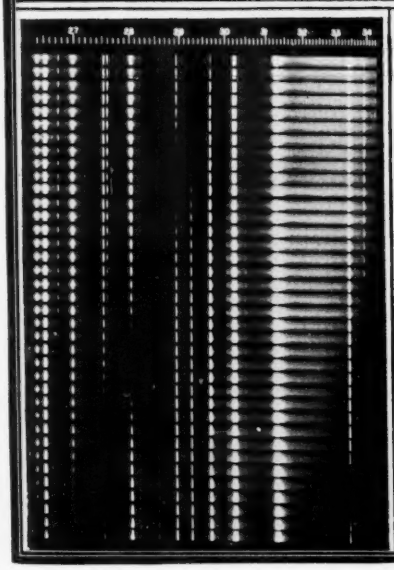

FIG. 2

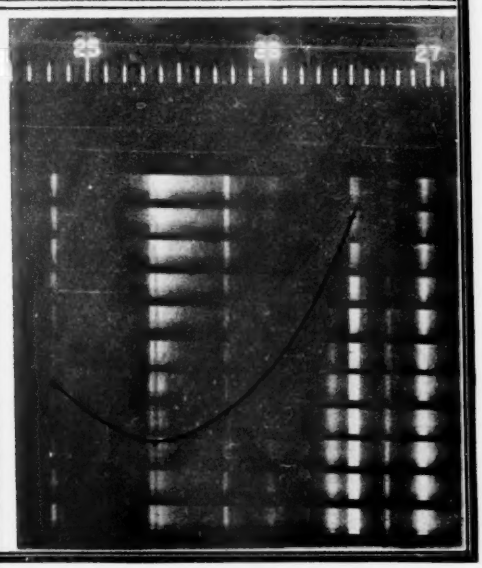

FIG. 3

7188 A.U., to 2573 A.U., are from the data due to Rose (*loc. cit.*), while the value at 2310 A.U., is from Borel's determination (Landolt-Bornstein, 1923).

It can be seen that the calculated and experimental values agree very well. This indicates that the wave-lengths of 900 A.U. and 1850 A.U., appearing in formula (4), approximately represent the absorption wave-lengths of sodium chlorate.

In conclusion, I record here my thanks to Prof. Sir C. V. Raman for the encouragement and the suggestions he gave me during this work. My thanks are also due to Dr. S. Ramaseshan for the discussions I had with him.

5. Summary

The rotatory dispersion of sodium chlorate has been redetermined and its wave-lengths range extended from 8756 A.U. to 2378 A.U. The rate of increase of the rotatory power with diminishing wave-length falls off in the ultra-violet. Beyond 2536 A.U. there is actually a diminution in the magnitude of the rotation, the value at 2378 A.U. being nearly 6% less than that at 2536 A.U. A rotatory dispersion formula of the Drude type containing a negative term gives a tolerable fit with the data, but such a formula is inappropriate since it violates the summation rule for optical rotatory power. The formula now proposed is

$$\rho = \frac{1{\cdot}2387\,\lambda^2}{[\lambda^2 - (0{\cdot}09)^2]^2} - \frac{0{\cdot}1374\,\lambda^2}{[\lambda^2 - (0{\cdot}185)^2]^2} - 0{\cdot}123.$$

It fits the data accurately over the whole range of wave-lengths, and is not open to the same objection. The negative term becomes comparable in magnitude to the positive term in the ultra-violet region. The characteristic wave-lengths appearing in the formula also fit the ordinary dispersion curve.

References

1. Chandrasekhar, S. .. *Proc. Ind. Acad. Sci.*, 1952, **36 A**, 118.
2. Guye, C. E. .. *C. R.*, 1889, **108**, 349.
3. *Int. Crit. Tables*, 1930.
4. *Landolt-Bornstein Tables*, 1923.
5. Lowry, T. M. .. *Optical Rotatory Power*, Longmans, Green & Co., 1935.
6. Perucca, E. .. *Nuov. Cim.*, 1919, **18**, 112.
7. Ramaseshan, S. .. *Proc. Ind. Acad. Sc.*, 1948, **28 A**, 360.
8. Rose, H. .. *Diss. Gott.*, 1909.
9. Servant, R. .. *Ann. de. Physique*, 1939, **12**, 397.
10. Sohncke, L. .. *Wied Ann.*, 1878, **3**, 529.
11. Voigt, W. .. *Phys. Zs.*, 1908, **9**, 588.

THEORETICAL INTERPRETATION OF THE OPTICAL ACTIVITY OF QUARTZ

By S. Chandrasekhar

(*From the Raman Research Institute, Bangalore*)

Received March 11, 1953

(Communicated by Sir C. V. Raman)

1. Introduction

α-Quartz belongs to the trigonal enantiomorphous hemihedral class of symmetry, the space-group being represented by D_3^4 (or the enantiomorphous D_3^6). The structure accordingly has a threefold screw axis. The unit cell consists of three SiO_2 triplets spaced at equal intervals along the vertical axis, each turned through 120° with respect to its predecessor. It can scarcely be doubted that this screw structure is responsible for the optical rotatory power of quartz. Theories which seek to correlate the optical activity with the ultimate structure of the substance exhibiting it have been put forward by various authors in the past (*vide* the reviews by Condon, 1937; Kauzmann *et al.*, 1940). Applications of these theories to evaluate the results in particular crystals have been comparatively few. For the case of quartz, there have been three attempts to calculate the rotatory power theoretically. The first is by Hylleraas (1927), who has applied Born's general theory of coupled oscillators (1915). Hylleraas has deduced from the known data for the double refraction and the rotatory power, the values of two lattice constants, which agree well with the X-ray data. The second attempt is by de Mallemann (1930) who has estimated the rotatory power in terms of the refractivities of the atoms constituting the crystal. More recently, Ramachandran (1951) has made detailed calculations of the first order terms of the polarisability theory and obtains good values for the rotatory power for the propagation of light both along and at right angles to the optic axis. Though all these authors get a fairly good agreement with the observed values, none of them has derived an explicit law of rotatory dispersion for quartz, which is certainly a characteristic and noteworthy feature of the phenomenon.

The rotatory power of quartz has been the subject of extensive experimental study. Accurate data is available over a wide range of wavelengths. Numerous attempts have been made to represent these data by means of rotatory dispersion formulæ (*vide* Servant 1939, 1941). Most of these formulæ,

which generally involve a large number of terms, fail in the remote ultraviolet and besides, they are open to objection from the theoretical standpoint. For, as has been pointed out in an earlier paper (author, 1952 *b*), the negative terms appearing in these formulæ have been assigned arbitrary strengths and do not conform to the summation rule of Kuhn (1927). It has also been shown by the present author (1952 *a*) that the entire data from the visible to the extreme ultraviolet is accurately represented by the formula

$$\rho = \frac{k\lambda^2}{(\lambda^2 - \lambda_0^2)^2}, \tag{1}$$

where $k = 7{\cdot}186$ and $\lambda_0 = 0{\cdot}0926283\,\mu$. The rotatory dispersion at right angles to the optic axis has been measured by Bruhat and Weil (1936), who have summarised their results as follows. The ratio of the rotatory powers normal to and along the optic axis of quartz is independent of the wavelength between the range 5780 A.U. to 2540 A.U., the ratio being $-0{\cdot}54$, to within an accuracy of 0·5 per cent. It is obvious, therefore, that the rotatory dispersion formula normal to the optic axis would also be of the same type as (1) with the value of λ_0 unaltered, the constant k being reduced in the ratio of $-0{\cdot}54$.

In the present paper, a theoretical interpretation of the optical activity of quartz, based on coupled oscillators, has been put forward, in which the approach to the problem is quite different from the three previous attempts to evaluate the rotatory power of this crystal. Briefly, the basis of the theory is as follows. While the screw structure of quartz is responsible for its optical activity, one may remark that it would not by itself suffice. For, if we assume that each SiO_2 unit constituting such a structure is an optically independent entity, it can readily be shown that the rotatory power would vanish. It is necessary therefore, to consider the SiO_2 groups as forming a connected system, if the observed optical behaviour of the crystal is to be understood. The basic idea of this paper is that the screw-like structure of the crystal influences the spectroscopic behaviour of the constituent units and it is this which ultimately gives rise to its rotatory power. It is shown, from simple considerations of symmetry, that the characteristic frequency of the individual units is split into two components which differ from each other, as a result of the coupling between the neighbouring entities in the crystal. It is further shown that this splitting affords a ready explanation of the rotatory power of quartz both along and normal to the optic axis. The principal merit of this treatment is that it leads directly to an expression for the rotatory power of the same form as (1), which, as has already been pointed out, agrees very well with the actual observed data for quartz.

2. THE QUARTZ MODEL

Let us construct a simple model based on the screw structure of quartz. We shall replace each SiO_2 triplet by a linear resonator located at its centre of gravity and lying approximately along the line joining the oxygens. Let the natural frequency of vibration of the charged particle in each resonator when uncoupled be ω_0. Let us assume that there is a feeble coupling between the neighbouring resonators. Since the successive resonators are exactly identical, there would be a resonance interaction and the frequencies would be affected. Thus, the question that comes up for consideration is that of finding how the presence of a threefold axis in the structure influences the modes and frequencies of vibration of these constituent units. We shall proceed to examine this point. The characteristic feature of this model is that by a translation of c/3 and a rotation of 120° about the c-axis, the entire system is brought into coincidence with itself. We may, therefore, assume that such an operation, which is a purely geometrical procedure, would not alter the physical state and accordingly the modes and frequencies of vibration of the system. This indicates that the effect of the symmetry operation on a normal co-ordinate would be either to leave it unchanged or transform it into its negative. Fixing our attention on any particular normal mode, we notice that for this to be the case, the particles in the successive resonators should vibrate with equal amplitude and in directions differing by 120° as measured about the optic axis, and their phases should satisfy one or other of the following conditions; (*a*) the phases identical in the successive resonators or (*b*) the phases opposite in the successive resonators.* It is evident that the frequency of vibration would be different in the two cases, the magnitude of the difference being dependent on the strength of the interaction between the neighbours. In other words, the natural frequency ω_0 of the individual units is split into two frequencies, ω_1 and ω_2, as a result of the coupling between the successive resonators. This *simplified* picture is, of course, a purely *classical* one. We shall now see how the optical activity of quartz could be accounted for, on the basis of these remarks.

3. THE THEORY

It can easily be seen in the simplified model presented above, that the dynamic or vibrational pattern of the entire crystal (including both modes of vibration) can be completely reproduced by a unit consisting of a pair of adjacent resonators. Let us call this unit the compound resonator. We

* It will be noticed that a similar result has been arrived at with regard to the atomic vibrations in the successive cells of a crystal lattice by Sir C. V. Raman in his treatment of crystal dynamics (1943).

shall base our calculations on such a compound resonator and then extend them to the whole crystal, remembering of course, that the successive compound resonators are situated about a threefold screw axis.

Let the charge and mass of the particle in each resonator be q and M respectively. Let us, for convenience, put $q = fe$ and $M = fm$, where e and m are respectively the charge and mass of the electron, and f is the oscillator strength according to the usual definition. Let us choose a rectangular set of axes, the Z axis being parallel to the optic axis.

Propagation along the Optic Axis.—When plane polarised light is incident along the optic axis of quartz, it is split into two circular vibrations of opposite senses, which travel with different velocities in the medium. Since these two vibrations are coherent, they combine at every point to form a plane polarised vibration which is rotated with respect to the plane of polarisation of the incident light, the rotation increasing directly as the thickness traversed. If n_l and n_r be the refractive indices for left-handed and right-handed circular light, then the rotation per unit length is given by

$$\rho = \frac{\pi}{\lambda}(n_l - n_r). \tag{2}$$

We shall now proceed to calculate n_l and n_r.

Let right-circularly polarised light represented by

$$\left.\begin{aligned} x &= \mathrm{E}_0 \cos \omega t \\ y &= -\mathrm{E}_0 \sin \omega t \end{aligned}\right\} \tag{3}$$

be incident along OZ. The force exerted by the light wave on the charged particle of any resonator whose direction cosines are α, β, γ, is

$$\mathrm{F}_1 = fe\mathrm{E}_0 [\alpha \cos \omega t - \beta \sin \omega t]. \tag{4}$$

The force on the particle on the successive resonator which is rotated through $\theta (= 120°)$ about the Z axis would be

$$\begin{aligned} \mathrm{F}_2 = {} & (\alpha \cos \theta - \beta \sin \theta) fe\mathrm{E}_0 \cos (\omega t - \phi) \\ & - (\alpha \sin \theta + \beta \cos \theta) fe\mathrm{E}_0 \sin (\omega t - \phi) \end{aligned} \tag{5}$$

where $\phi = \dfrac{2\pi \bar{n} d}{\lambda}$, $\bar{n}$ being the mean refractive index and d is the distance between the two resonators as measured along the optic axis. Since ϕ is small, we may put $\cos \phi = 1$ and $\sin \phi = \phi$ in (5) and we get

$$\begin{aligned} \mathrm{F}_2 = fe\mathrm{E}_0 [& \{\alpha (\cos \theta + \phi \sin \theta) - \beta (\sin \theta - \phi \cos \theta)\} \cos \omega t \\ & + \{\alpha (\phi \cos \theta - \sin \theta) - \beta (\cos \theta + \phi \sin \theta)\} \sin \omega t]. \end{aligned} \tag{6}$$

Let us confine our attention to the compound unit formed by these two adjacent resonators. We have just seen that the compound resonator has two normal modes of vibration, one in which the two particles vibrate with equal amplitude and in the same phase and the other in which the two particles vibrate with equal amplitude but opposite in phase. Hence the force exerted on these particles expressed in the two normal co-ordinates are respectively

$$R_{\xi_1} = \frac{1}{\sqrt{2}}(F_1 + F_2) \tag{7}$$

$$R_{\xi} = \frac{1}{\sqrt{2}}(F_1 - F_2). \tag{8}$$

Substituting for F_1 and F_2, we get

$$R_{\xi_1} = \frac{feE_0}{\sqrt{2}}[\{\alpha\ (1 + \cos\theta + \phi\sin\theta) - \beta(\sin\theta - \phi\cos\theta)\}\cos\omega t + \{\alpha(\phi\cos\theta - \sin\theta) - \beta(1 + \cos\theta + \phi\sin\theta)\}\sin\omega t] \tag{9}$$

$$= (a_{\xi_1}{}^{\gamma})\, feE_0\cos(\omega t + \sigma) \tag{10}$$

where

$$(a_{\xi_1}{}^{\gamma})^2 = (\alpha^2 + \beta^2)\ (1 + \cos\theta + \phi\sin\theta),$$

neglecting higher powers of ϕ. Therefore, the equation of motion of the particles would be of the form

$$\ddot{\xi}_1 + \omega_1{}^2\,\xi_1 = (a_{\xi_1}{}^{\gamma})\frac{feE_0}{M}\cos(\omega t + \sigma) \tag{11}$$

$$\therefore \qquad \xi_1 = (a_{\xi_1}{}^{\gamma})\frac{feE_0\cos(\omega t + \sigma)}{M(\omega_1{}^2 - \omega^2)}. \tag{12}$$

Hence, the dipole moment induced

$$= \{(a_{\xi_1}{}^{\gamma})\, fe\}^2\,\frac{E_0}{M(\omega_1{}^2 - \omega^2)}$$

$$= (a_{\xi_1}{}^{\gamma})^2\, f\,\frac{e^2}{m}\,\frac{E_0}{(\omega_1{}^2 - \omega^2)} \tag{13}$$

putting $M = fm$. The dipole moment could be expressed as two components at right angles to each other, say m_{ξ} and $m_{\dot{\xi}}$,

where

$$m_{\xi} = \alpha^2(1 + \cos\theta + \phi\sin\theta)\, f\frac{e^2}{m}\,\frac{E_0}{(\omega_1{}^2 - \omega^2)}$$

and

$$m_k = \beta^2 (1 + \cos\theta + \phi \sin\theta)\, f \frac{e^2}{m} \frac{E_0}{(\omega_1^2 - \omega^2)}.$$

These results are for a single compound resonator. Since the successive compound resonators are situated about a threefold axis of symmetry, it can easily be shown that the mean polarisability per unit volume for right circular vibration

$$= \frac{N' (m_g + m_k)}{2E_0},$$

where N′ is the number of compound resonators per unit volume and is equal to N/2, where N is the number of resonators per unit volume.

$$\therefore \quad (n_r^2 - 1)_{\xi_1} = 4\pi N' \frac{(m_g + m_k)}{2E_0}$$

$$= \pi N (a_{\xi_1}^{r})^2 \frac{e^2}{m} \frac{f}{(\omega_1^2 - \omega^2)}, \tag{16}$$

In a similar manner we get for the other mode of vibration

$$(n_r^2 - 1)_{\xi_2} = \pi N (a_{\xi_2}^{r})^2 \frac{e^2}{m} \frac{f}{(\omega_2^2 - \omega^2)}, \tag{17}$$

where

$$(a_{\xi_2}^{r})^2 = (\alpha^2 + \beta^2)\ (1 - \cos\theta - \phi \sin\theta).$$

Let us write

$$(n_r^2 - 1) = (n_r^2 - 1)_{\xi_1} + (n_r^2 - 1)_{\xi_2}. \tag{18}$$

For left-circular light given by

$$\left.\begin{aligned} x &= E_0 \cos\omega t \\ y &= E_0 \sin\omega t \end{aligned}\right\} \tag{19}$$

we have similarly,

$$(n_l^2 - 1)_{\xi_1} = \pi N (a_{\xi_1}^{l})^2 \frac{e^2}{m} \frac{f}{(\omega_1^2 - \omega^2)} \tag{20}$$

and

$$(n_l^2 - 1)_{\xi_2} = \pi N (a_{\xi_2}^{l})^2 \frac{e^2}{m} \frac{f}{(\omega_2^2 - \omega^2)}, \tag{21}$$

where

$$(a_{\xi_1}^{l})^2 = (\alpha^2 + \beta^2)\ (1 + \cos\theta - \phi \sin\theta)$$

$$(a_{\xi_2}^{l})^2 = (\alpha^2 + \beta^2)\ (1 - \cos\theta + \phi \sin\theta)$$

and

$$(n_l^2 - 1) = (n_l^2 - 1)_{\xi_1} + (n_l^2 - 1)_{\xi_2} \tag{22}$$

$$\therefore \quad (n_l^2 - n_r^2) = \pi N \frac{e^2}{m} f \left[\frac{(a_{\xi_1}^{\ l})^2 - (a_{\xi_1}^{\ r})^2}{\omega_1^2 - \omega^2} + \frac{(a_{\xi_2}^{\ l})^2 - (a_{\xi_2}^{\ r})^2}{\omega_2^2 - \omega^2}\right] \tag{23}$$

where

$$(a_{\xi_1}^{\ l})^2 - (a_{\xi_1}^{\ r})^2 = -2(\alpha^2 + \beta^2)\phi \sin\theta$$

$$(a_{\xi_2}^{\ l})^2 - (a_{\xi_2}^{\ r})^2 = 2(\alpha^2 + \beta^2)\phi \sin\theta.$$

It will be noticed that the numerators of the two terms of (23) are equal in magnitude but opposite in sign, and this is in conformity with the summation rule of Kuhn's which states that the sum of the numerators determining the contributions of the different absorption frequencies to the rotatory power should vanish. Putting $(n_l + n_r) = 2\bar{n}$ in (23), we get

$$2\bar{n}(n_l - n_r) = 2\pi N \frac{e^2}{m} f (\alpha^2 + \beta^2)\phi \sin\theta \left[\frac{1}{\omega_2^2 - \omega^2} - \frac{1}{\omega_1^2 - \omega^2}\right]. \tag{26}$$

Let

$$\left.\begin{aligned} \omega_1^2 &= \omega_0^2 + 2\pi^2\epsilon \\ \omega_2^2 &= \omega_0^2 - 2\pi^2\epsilon \end{aligned}\right\}. \tag{27}$$

We shall assume that the resonators are feebly coupled, so that ϵ is a small quantity. Substituting $\phi = 2\pi\bar{n}d/\lambda$ and expressing in ν's $(= \omega/2\pi)$, we find that

$$(n_l - n_r) = \frac{Ne^2 d \sin\theta}{m\lambda}\left(\frac{\alpha^2 + \beta^2}{2}\right)\frac{f\epsilon}{(\nu_0^2 - \nu^2)^2} \tag{29}$$

neglecting $\epsilon^2/4$ in the denominator.

Hence, the rotation per unit length

$$\rho = \frac{\pi}{\lambda}(n_l - n_r) = \frac{\pi Ne^2 d \sin\theta}{m\lambda^2}\left(\frac{\alpha^2 + \beta^2}{2}\right)\frac{f\epsilon}{(\nu_0^2 - \nu^2)^2} \tag{30}$$

$$= \frac{A_0\lambda^2}{(\lambda^2 - \lambda_0^2)^2}, \tag{31}$$

where

$$A_0 = \frac{\pi Ne^2 d \sin\theta\, \lambda_0^4}{mc^4}\left(\frac{\alpha^2 + \beta^2}{2}\right) f\epsilon.$$

If, more generally, we assign several resonators having different frequencies of vibration to each SiO_2 unit, then, assuming that the resonance interaction

between identical resonators in the successive units predominates, it can easily be shown that

$$\rho = \sum_k \frac{A_k \lambda^2}{(\lambda^2 - \lambda_k^2)^2} \tag{32}$$

The ordinary refractive index along the optic axis is given by the relation

$$\begin{aligned}(n_\omega^2 - 1) &= \tfrac{1}{2}\left[(n_l^2 - 1) + (n_r^2 - 1)\right] \\ &= \pi N \frac{e^2}{m} (\alpha^2 + \beta^2) f \left[\frac{1 + \cos\theta}{(\omega_1^2 - \omega^2)} + \frac{1 - \cos\theta}{(\omega_2^2 - \omega^2)}\right] \\ &= 4\pi N \frac{e^2}{m} \frac{f\left(\frac{\alpha^2 + \beta^2}{2}\right)}{(\omega_0^2 - \omega^2)}\end{aligned} \tag{33}$$

approximately, assuming that $\omega_1 \approx \omega_2$. Thus, we notice that if the coupling between the neighbours is feeble, the splitting of the frequency manifests itself only in a second order effect like optical activity and not in a grosser effect like refraction.

Propagation Normal to the Optic Axis.—The theory of propagation of light in an optically active birefringent medium for directions inclined to the optic axis has been dealt with by various workers (*vide* Pockels, 1906). Along such directions, two similar elliptically polarised waves with opposite senses of rotation and lying crossed to each other (*i.e.*, the major axis of one falling on the minor axis of the other) travel unchanged. The axes of the ellipses coincide with the principal planes. If ρ is the rotatory power along any direction and δ the phase difference due to birefringence alone (if $\rho = 0$), then the actual phase difference per unit length between the two elliptic waves is given by

$$\Delta = [\delta^2 + (2\rho)^2]^{\frac{1}{2}} \tag{34}$$

and the ratio of the axes

$$\chi = \left(\frac{2\rho}{\delta}\right). \tag{35}$$

Proceeding in the same manner as before, approximate expressions for the refractive indices of the two ellipses may be derived. We shall base our arguments on the same compound resonator which was considered previously.

Let a right-rotating ellipse given by

$$\left.\begin{aligned} x &= \mathrm{E}_0 \cos \omega t \\ z &= -\left(\frac{2\rho}{\delta}\right) \mathrm{E}_0 \sin \omega t \end{aligned}\right\} \tag{36}$$

be incident along the Y axis.

$$\therefore\ \mathrm{F}_1 = fe\mathrm{E}_0 \left[\alpha \cos \omega t - \left(\frac{2\rho}{\delta}\right) \gamma \sin \omega t\right] \tag{37}$$

and

$$\mathrm{F}_2 = fe\mathrm{E}_0 \left[(\alpha \cos \theta - \beta \sin \theta) \cos (\omega t - \psi_y) - \left(\frac{2\rho}{\delta}\right) \gamma \sin (\omega t - \psi_y)\right] \tag{38}$$

where $\psi_y = \dfrac{2\pi \bar{n} p_y}{\lambda}$, where $\bar{n}$ is the mean refractive index and p_y the distance between the resonators as measured along the Y axis.

$$\therefore\ \mathrm{R}_{\xi_1} = \frac{fe\mathrm{E}_0}{\sqrt{2}} \left[\left\{\alpha (1 + \cos \theta) - \beta \sin\theta + \psi_y \gamma \left(\frac{2\rho}{\delta}\right)\right\} \cos \omega t + \left\{\psi_y \alpha \cos \theta - \psi_y \beta \sin \theta - 2\gamma \left(\frac{2\rho}{\delta}\right)\right\} \sin \omega t\right]. \tag{39}$$

Therefore the moment induced m_y

$$= \tfrac{1}{2} \left[\alpha^2 (1 + \cos \theta)^2 + \beta^2 \sin^2 \theta - 2\alpha\beta \sin \theta (1 + \cos \theta) + 2\psi_y \left(\frac{2\rho}{\delta}\right) \alpha\gamma (1 - \cos\theta) + 2\psi_y \left(\frac{2\rho}{\delta}\right) \beta\gamma \sin\theta\right] f \frac{e^2}{m} \frac{\mathrm{E}_0}{(\omega_1^2 - \omega^2)} \tag{40}$$

neglecting higher powers of ψ_y and $\left(\frac{2\rho}{\delta}\right)$. If, on the other hand, we consider a similar ellipse given by

$$\left.\begin{aligned} y &= \mathrm{E}_0 \cos \omega t \\ z &= -\left(\frac{2\rho}{\delta}\right) \mathrm{E}_0 \sin \omega t \end{aligned}\right\} \tag{41}$$

propagated along the X direction, the moment

$$m_x = \tfrac{1}{2} \left[\alpha^2 \sin^2 \theta + \beta^2 (1 + \cos \theta)^2 + 2\alpha \beta \sin \theta (1 + \cos \theta) - 2\psi_x \left(\frac{2\rho}{\delta}\right) \alpha\gamma \sin\theta + 2\psi_x \left(\frac{2\rho}{\delta}\right) \beta\gamma (1 - \cos\theta)\right] f \frac{e^2}{m} \frac{\mathrm{E}_0}{\omega_1^2 - \omega^2} \tag{42}$$

where $\psi_x = \dfrac{2\pi\bar{n}p_x}{\lambda}$, where p_x is the distance between the resonators as measured along the X axis. Without any loss of generality, we may choose the axes suitably so that $\psi_x = \psi_y = \psi$. Since the successive compound resonators are situated about a threefold axis of symmetry, the mean polarisability per unit volume is

$$\frac{N'(m_x + m_y)}{2E_0} = \frac{N(m_x + m_y)}{4E_0},$$

where N and N′ have the same significance as before.

$$\therefore \quad (n_r^2 - 1)_{\xi_1} = 4\pi N' \frac{(m_x + m_y)}{2E_0} \tag{43}$$

$$= \pi N (a_{\xi_1}')^2 \frac{e^2}{m} \frac{f}{(\omega_1^2 - \omega^2)}, \tag{44}$$

where

$$(a_{\xi_1}')^2 = \left[(\alpha^2 + \beta^2)(1 + \cos\theta) + \psi\left(\frac{2\rho}{\delta}\right)\Gamma\right],$$

where

$$\Gamma = \alpha\gamma(1 - \cos\theta - \sin\theta) + \beta\gamma(1 - \cos\theta + \sin\theta)$$

In a similar manner,

$$(n_r^2 - 1)_{\xi_2} = \pi N (a_{\xi_2}')^2 \frac{e^2}{m} \frac{f}{(\omega_2^2 - \omega^2)}, \tag{45}$$

where

$$(a_{\xi_2}')^2 = \left[(\alpha^2 + \beta^2)(1 - \cos\theta) - \psi\left(\frac{2\rho}{\delta}\right)\Gamma\right].$$

For the crossed left-rotating ellipse given by

$$\left.\begin{aligned} x \text{ (or } y) &= \left(\frac{2\rho}{\delta}\right) E_0 \cos\omega t \\ z &= E_0 \sin\omega t \end{aligned}\right\} \tag{46}$$

we have

$$(n_l^2 - 1)_{\xi_1} = \pi N (a_{\xi_1}')^2 \frac{e^2}{m} \frac{f}{(\omega_1^2 - \omega^2)} \tag{47}$$

and

$$(n_l^2 - 1)_{\xi_2} = \pi N (a_{\xi_2}')^2 \frac{e^2}{m} \frac{f}{(\omega_2^2 - \omega^2)}, \tag{48}$$

where

$$(a_{\xi_2}')^2 = \left[4\gamma^2 - \psi\left(\frac{2\rho}{\delta}\right)\Gamma\right]$$

and

$$(a_{\xi_1}{}')^2 = \left[\psi\left(\frac{2\rho}{\delta}\right)\Gamma\right]$$

$$\therefore \quad (n_l{}^2 - n_r{}^2) = (n_l{}^2 - n_r{}^2)_{\xi_1} + (n_l{}^2 - n_r{}^2)_{\xi_2} \tag{49}$$

$$= \pi N \frac{e^2}{m} f\left[\frac{(a_{\xi_1}{}')^2 - (a_{\xi_1}{}'')^2}{\omega_1{}^2 - \omega^2} + \frac{(a_{\xi_2}{}')^2 - (a_{\xi_2}{}'')^2}{\omega_2{}^2 - \omega^2}\right], \tag{50}$$

where

$$(a_{\xi_1}{}')^2 - (a_{\xi_1}{}'')^2 = \left[4\gamma^2 - (\alpha^2 + \beta^2)\,(1 + \cos\theta) - 2\psi\left(\frac{2\rho}{\delta}\right)\Gamma\right]$$

and

$$(a_{\xi_2}{}')^2 - (a_{\xi_2}{}'')^2 = \left[-(\alpha^2 + \beta^2)\,(1 - \cos\theta) + 2\psi\left(\frac{2\rho}{\delta}\right)\Gamma\right].$$

Now,

$$\frac{2\pi}{\lambda}(n_l{}^2 - n_r{}^2) = 2\bar{n}\,\Delta = 2\bar{n}\,[\delta^2 + (2\rho)^2]^{\frac{1}{2}} \qquad \text{from (34)}$$

$$= 2\bar{n}\left[\delta + \frac{2\rho^2}{\delta}\right] \quad \text{approximately.} \tag{51}$$

From (50), $\frac{2\pi}{\lambda}(n_l{}^2 - n_r{}^2)$ may be written as two parts, say P and Q, where

$$\mathrm{P} = \frac{2\pi}{\lambda}\pi N \frac{e^2}{m} f\left[\frac{4\gamma^2 - (\alpha^2 + \beta^2)\,(1 + \cos\theta)}{\omega_1{}^2 - \omega^2} - \frac{(\alpha^2 + \beta^2)\,(1 - \cos\theta)}{\omega_2{}^2 - \omega^2}\right] \tag{52}$$

and

$$\mathrm{Q} = \frac{2\pi}{\lambda} \cdot \pi N \frac{e^2}{m} f\left[2\psi\left(\frac{2\rho}{\delta}\right)\Gamma\right]\left[\frac{1}{(\omega_2{}^2 - \omega^2)} - \frac{1}{(\omega_1{}^2 - \omega^2)}\right]. \tag{53}$$

P could be approximately written as

$$\frac{2\pi}{\lambda}\pi N \frac{e^2}{m} f\left[\frac{4\gamma^2 - 2\,(\alpha^2 + \beta^2)}{\omega_0{}^2 - \omega^2}\right] \tag{54}$$

assuming that $\omega_1 \approx \omega_2$.

Now, in the above model, it can easily be seen that the expression for the extraordinary refractive index is

$$n_e{}^2 - 1 = 4\pi N \frac{e^2}{m} \frac{f\gamma^2}{(\omega_0{}^2 - \omega^2)} \tag{55}$$

while that for the ordinary index is (33).

Hence

$$\mathrm{P} = \frac{2\pi}{\lambda}(n_e{}^2 - n_\omega{}^2) = 2\bar{n}\,\delta. \tag{56}$$

Thus from (51) and (56), we find that we may equate

$$Q = 2\bar{n}\left(\frac{2\rho^2}{\delta}\right). \tag{57}$$

Comparing the values of Q from (53) and (57) and substituing for ψ, we get,

$$\rho = \frac{4\pi^3 Ne^2 p\, \Gamma f}{m\lambda^2}\left[\frac{1}{\omega_2^2 - \omega^2} - \frac{1}{\omega_1^2 - \omega^2}\right]. \tag{58}$$

Here again we notice that Kuhn's summation rule is fulfilled. Substituting $(\omega_1^2 - \omega_2^2) = 4\pi^2\epsilon$, and expressing in terms of ν's, we get

$$\rho = \frac{\pi Ne^2\, p\, \Gamma f\epsilon}{m\lambda^2(\nu_0^2 - \nu^2)^2} = \frac{B_0\lambda^2}{(\lambda^2 - \lambda_0^2)^2}, \tag{59}$$

where

$$B_0 = \frac{\pi Ne^2 p\lambda_0^4 \Gamma f\epsilon}{mc^4}.$$

We thus arrive at the interesting result that the rotatory dispersion formulæ normal to and along the optic axis are identical in form. This is in conformity with the observations of Bruhat and Weil.

4. Evaluation of the Magnitude of the Splitting of the Characteristic Frequency

It will be noticed that, throughout, in the derivation of the formulæ for the rotatory power, the assumption has been made that the resonators are feebly coupled, so that ϵ is taken to be a small quantity. It would, therefore, be of great interest to make an actual estimation of the extent of the splitting of the characteristic frequency of each resonator. In fact, from the known data for the refraction and the rotation, such an estimation is possible.

It has been shown in an earlier paper by the present author, that the ordinary dispersion of quartz along the optic axis can be fitted up fairly well by a one-term formula of the Sellemeyer-Drude type involving the characteristic wavelength appearing in (1). The formula is

$$n_\omega^2 - 1 = \frac{1{\cdot}35\lambda^2}{\lambda^2 - (0{\cdot}0926283)^2}. \tag{60}$$

Now, in the model which we have just considered, the expressions for the rotatory power and the refraction are respectively:

$$\rho = \frac{\pi Ne^2 d \sin\theta\, \lambda_0^4\, F\epsilon}{mc^4}\,\frac{\lambda^2}{(\lambda^2 - \lambda_0^2)^2} \tag{31 a}$$

where $F = \frac{1}{2}(\alpha^2 + \beta^2) f$, ρ is expressed in radians per cm. and λ in cm.,

$$\text{and } n_\omega^2 - 1 = \frac{Ne^2 \lambda_0^2 F}{m\pi c^2} \frac{\lambda^2}{(\lambda^2 - \lambda_0^2)}. \tag{33 a}$$

It should be pointed out here that the constant occurring in the numerator of formula (60) is independent of the units in which λ is expressed. On the other hand, that appearing in the rotatory dispersion formula (1) is only valid when λ is expressed in microns.

If we assume that the characteristic wavelength λ_0 of each resonator has the same value as that used in (1), then from (60) and (33 *a*) we obtain the relation

$$\frac{Ne^2 \lambda_0^2 F}{m\pi c^2} = 1{\cdot}35. \tag{61}$$

For α-quartz, the average volume occupied by a single SiO_2 triplet has been calculated to be $37{\cdot}4 \times 10^{-24}$ c.c. (Sosman, 1927).

$$\therefore N = 2{\cdot}68 \times 10^{22} \text{ resonators per c.c.}$$

We also have $e = 4{\cdot}8 \times 10^{-10}$ e.s.u.

$$\frac{e}{m} = 5{\cdot}3 \times 10^{17} \text{ e.s.u.}$$

$$\lambda_0 = 0{\cdot}926283 \times 10^{-5}$$

$$c = 3 \times 10^{10} \text{ cm./sec.}$$

and hence from (61), we find that

$$F = 6{\cdot}5 \tag{62}$$

From the X-ray data, the parameter c of the unit cell of α-quartz is found to be 5·393 A.U. Therefore,

$$d = c/3 = 1.8 \times 10^{-8} \text{ cm.}$$

Also,

$$\sin\theta = \sin 120^\circ = \sqrt{3}/2$$

$$\lambda_0^4 = 0{\cdot}736 \times 10^{-20}$$

$$\frac{\lambda^2}{(\lambda^2 - \lambda_0^2)^2} = 3{\cdot}027 \times 10^8, \text{ for } \lambda = 5893 \times 10^{-8} \text{ cm.}$$

For $\lambda = 5893 \times 10^{-8}$ cm. $\rho = 217°$ per cm. $= 217/57{\cdot}3$ radians per cm. Hence, from (31 *a*),

$$\epsilon = 6{\cdot}36 \times 10^{29}$$

$$= \nu_1^2 - \nu_2^2 = 2\nu_0\,\delta\nu_0$$

$$= \frac{2c^2}{\lambda_0^3}\,\delta\lambda_0 \text{ (numerically)}$$

$$\therefore\ \delta\lambda_0 = 28 \text{ A.U.}$$

We thus see that the characteristic wavelength λ_0 of each resonator is split into a close doublet, λ_1 and λ_2, which differ by 28 A.U. as a result of the coupling between the neighbouring resonators. It is gratifying to find that the assumption that the coupling constant is small is supported by the above calculation.

5. The Ratio $\rho_\perp/\rho_{||}$

We shall now proceed to evaluate the birefringence and the ratio of the rotatory powers normal to and along the optic axis. The expressions for the two refractive indices are given by (33) and (55) respectively, while

$$\frac{\rho_\perp}{\rho_{||}} = \frac{B_0}{A_0} = \frac{p\,[\alpha\gamma\,(1 - \cos\theta - \sin\theta) + \beta\gamma\,(1 - \cos\theta + \sin\theta)]}{d\cdot\tfrac{1}{2}\,(\alpha^2 + \beta^2)\sin\theta}. \tag{62}$$

The value of the various constants occurring in these formulæ may be obtained from the X-ray data for quartz.

Assuming that the resonators be exactly along the line joining the oxygens in each SiO_2 triplet, it is readily shown that they are inclined at an angle of about 64° 46′ to the vertical Z-axis. Fig. 1 (*b*) shows the projection of a compound resonator formed by the two SiO_2 units A and B, on the X-Y plane. The axes of X and Y have been chosen to be equally inclined to AB, since in such a case, ψ_x and ψ_y occurring in (40) and (42) would be equal. As has already been pointed out, the successive compound resonators are situated about a threefold axis of symmetry and hence it is enough if we just consider the unit AB for our calculations. The direction cosines of the resonator A are found to be $\alpha = -0{\cdot}8738$, $\beta = 0{\cdot}2342$ and $\gamma = 0{\cdot}4263$. When these values are substituted in the expressions for the refractive indices, it is found that the birefringence is not exactly accounted for. Hence the values have been altered to $-0{\cdot}8$, $0{\cdot}1523$ and $0{\cdot}5812$ respectively, in which case the calculated birefringence agrees exactly with the experimental value.

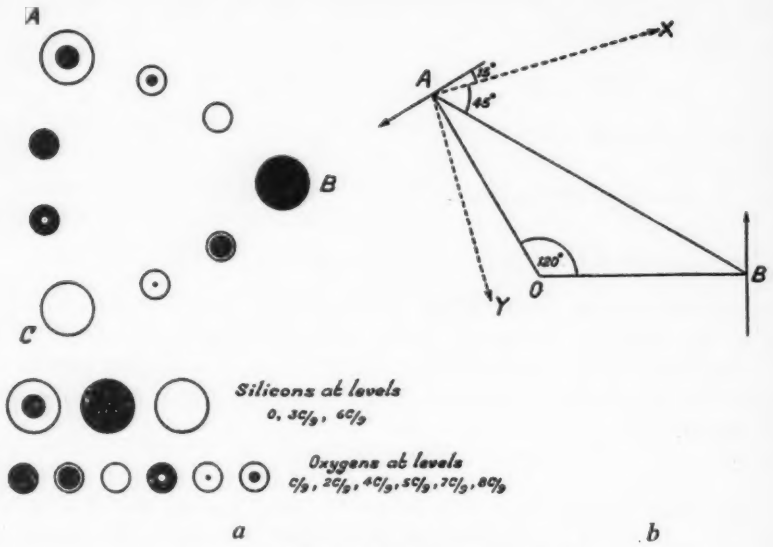

FIG. 1. Projection of unit cell on basal plane

From the X-ray data, it is readily shown that p ($= AB/\sqrt{2}$) and d are 2·8 A.U. and 1·8 A.U. respectively. We then obtain the result

$$\frac{\rho_\perp}{\rho_{||}} = -0{\cdot}5,$$

which differs but slightly from the observations of Bruhat and Weil.

6. DISCUSSION OF RESULTS

We have seen how, by means of an elementary model, the rotatory dispersion of quartz, both along and transverse to the optic axis, can be explained in a simple manner. The model also accounts for the refractive dispersion of quartz quite satisfactorily. For, quartz is a unique substance in which the dispersion of $\rho_{||}$, $\rho_\perp$*, n_ω and n_ϵ are all represented fairly well by means of a single absorption wavelength at about 926 A.U. (Chandrasekhar, 1952 *a*; Ramdas, 1952). Thus, the approximation involved in replacing each SiO_2 triplet by a single resonator is to a large extent justified.

* In an earlier paper, the present author (1952 *b*) had fitted a formula for $\rho_\perp$. This formula is incorrect as it is based on the preliminary observations of Bruhat and Grivet, the later and more accurate measurements of Bruhat and Weil having been inadvertently overlooked. The data of the latter authors establish clearly the fact that λ_0 is the same for $\rho_\perp$ and $\rho_{||}$.

These are also certain general features about optical activity which emerge from this theory. First of all, we notice from (31) that ρ is proportional to $\sin\theta$. Hence, it follows that the sense of the rotation depends on the sign of θ. This leads to the result that the two enantiomorphous forms have opposite rotation. The refractive index, on the other hand, is independent of θ, and therefore, is the same for right and left-rotating quartz. Secondly we find that ρ is proportional to ϵ, the coupling constant. Thus, if the coupling vanishes, the rotation would be zero. This is in conformity with the well-known result of the coupled oscillator theory, that only coupled electrons contribute to the rotatory power. Thirdly, the rotation is proportional to the phase of the incident light wave. If the wavelength of the incident radiation is made very large compared to the interatomic dimensions, then the rotatory power would vanish. This also follows indirectly from the rotatory dispersion formula itself. In refraction, however, the phase does not come into consideration.

In view of the remarkable agreement of the formula (1) with the observed data for quartz, it appears that the idea that its optical activity arises as a result of the splitting of the characteristic frequency in the crystal structure is certainly justified. This is further supported by the fact that the magnitude of the splitting, as estimated from the known data for refraction and rotation, is very small, which is actually the assumption underlying the theory. In fact, such a model may be used, more generally, to give a simple explanation of the optical activity of crystals which are not active in the state of solution.

In conclusion, I record my sincere thanks to Prof. Sir C. V. Raman for the discussions I had with him during the course of this work.

7. Summary

As a result of the interaction between the successive entities constituting the crystal, the spectroscopic behaviour of the individual units would be altered and it is found that this affords a ready explanation of the optical activity of quartz. Replacing each SiO_2 unit by a linear resonator of natural frequency ω_0, it is shown from simple considerations of symmetry, that ω_0 is split into two frequencies ω_1 and ω_2. By a classical discussion, it is demonstrated that this splitting gives rise to optical activity both along and transverse to the optic axis. The expression for the rotatory power is found to be of the form

$$\rho = k\lambda^2/(\lambda^2 - \lambda_0^2)^2$$

which fits remarkably well with the observed data for quartz. From the known values of refraction and rotation, the magnitude of the splitting has

been estimated to be 28 A.U., which supports the assumption underlying the theory that the resonators are feebly coupled. By assuming that the resonators lie approximately, though not exactly, along the line joining the oxygens in each SiO_2 triplet, it has been possible to quantitatively account for the birefringence and the negative rotation transverse to the optic axis.

REFERENCES

Born .. *Phys. Z.*, 1915, **16**, 251.

Bruhat and Weil .. *Journ. de Phys. et le Red.*, 1936, **7**, 12.

Chandrasekhar .. *Proc. Ind. Acad. Sci.* (*a*), 1952, **35A**, 103.

——— .. *Ibid.*, (*b*), 1952, **36A**, 118.

Condon .. *Rev. Mod. Phys.*, 1937, **9**, 432.

de Mallemann .. *Trans. Far. Soc.*, 1930, **26**, 281.

Hylleraas .. *Zeits. f. Phys.*, 1927, **44**, 871.

Kauzmann, Walter and Eyring .. *Chem. Revs.*, 1940, **26**, 339.

Kuhn .. *Z. f. Physik. Chemie*, 1929, **4B**, 14.

Pockels .. *Lehrbuch der Kristalloptik*, 1906.

Ramachandran .. *Proc. Ind. Acad. Sci.*, 1951, **33A**, 217.

Raman .. *Ibid.*, 1943, **18A**, 237.

Ramdas .. *Ibid.*, 1952, **35A**, 89.

Servant .. *Annales de Phys.*, 1939, **12**, 397.

——— .. *Comp. Rend.*, 1941, **212**, 1140.

Sosman .. "The Properties of Silica," *Amer. Chem. Soc.*, 1927.

ILLUSTRATIONS OF RAMAN SPECTRA WITH DESCRIPTIVE NOTES

REPRESENTATIVE Raman spectra are reproduced in the accompanying plates and these have been selected out of numerous investigations made during the past twenty years by workers at the Indian Institute of Science. The plates illustrate the various aspects of study in gases, liquids and solids. The last few plates represent the scattering of light by crystals taken with the mercury resonance radiation λ 2536 as the exciter. Second order Raman spectra of crystals have been recorded using this technique.

DESCRIPTIVE NOTES ON PLATES

Plate XXIII (S. Bhagavantam, from Andhra University, Waltair), Raman spectrum of deuterium. A double-image prism was interposed in the path of the scattered beam to show the state of polarisation of the various lines. The lines marked as V.R. are the vibrational Raman lines excited respectively by λ 3654, 4046 and 4358 radiations of the mercury arc and the others are rotational lines. A comparison of the vertical and horizontal components would reveal that the rotational lines are almost completely depolarised whereas the vibrational lines show perfect polarisation.

Plate XXIV, Fig. 1 (R. Ananthakrishnan), Raman spectrum of D_2O taken with a Hilger two-prism spectrograph showing three imperfectly resolved bands with frequency shifts 2365, 2515 and 2662 cm.$^{-1}$ In addition to the above the photograph shows three sharp bands with a frequency shift of 1235 cm.$^{-1}$, a feeble companion about 1110 cm.$^{-1}$ and a strong low frequency band $\Delta \nu = 175$ cm.$^{-1}$ Fig. 2, Raman spectrum of ordinary water for comparison. Note the remarkable similarity exhibited by them.

Plate XXV, Figs. 1, 2 and 3 (R. Ananthakrishnan), Raman spectrum of toluene, phenol and chlorobenzene under high dispersion and high resolving power. The photographs bring out fainter lines and finer details.

Plate XXVI (R. Ananthakrishnan), Fine structure of Raman lines. Note that the Raman line (802 cm.$^{-1}$) of cyclohexane shows no satellite lines. The other compounds show satellite lines.

Plate XXVII, Fig. 1 (R. Ananthakrishnan), Raman spectrum of carbon tetrachloride under high dispersion showing a faint line of frequency shift 434 cm.$^{-1}$ marked in the photograph, close to the line 459 cm.$^{-1}$ due to the

total symmetric oscillation. Note also the faint line corresponding to a shift of 145 cm.$^{-1}$

Plate XXVIII, Fig. 1, Raman spectrum of silicon tetrachloride taken with a Hilger two-prism spectrograph showing a line of frequency shift 440·5 cm.$^{-1}$ close to the line of 423 cm.$^{-1}$ shift due to the total symmetric oscillation. Fig. 2, the principal Raman line 459 cm.$^{-1}$ of carbon tetrachloride showing the unresolved isotope structure, the wing to its right and the octave line at 434 cm.$^{-1}$ to its left.

Plate XXIX, Figs. 1, 2 and 3 (C. S. Venkateswaran), show the low frequency Raman lines and the influence of temperature on the same for coumarin, phenol and naphthalene respectively. Note at the liquid state the whole structure becomes a broad diffuse band and the temperature has little influence as long as the substance is in the solid state. In coumarin and naphthalene the wings extend up to only 70 or 80 wave numbers. In phenol the extension of the wing is much greater.

Plate XXX, Figs. 4, 5, 6 and 7 (C. S. Venkateswaran), illustrate the low frequency bands differing in sharpness and character depending on the compound.

Plate XXXI, Figs. 1 and 2 (R. Ananthakrishnan), are Raman spectra of cyclopropane and ethylene oxide respectively in liquid and vapour state. The lower spectrograms in Figs. 1 and 2 show the state of polarisation of the vibrational Raman lines. Note that the spectrum of ethylene oxide shows great similarity to that of cyclopropane.

Plate XXXII, Figs. 1 and 2 (R. Ananthakrishnan), show the Raman spectrum of propylene and iso-butane. The bottom photographs in Figs. 1 and 2 show the state of polarisation of the Raman lines. The spectrum of propylene shows sharp and well polarised lines while the iso-butane lines are diffuse and show a high degree of depolarisation.

Plate XXXIII, Figs. 1, 2 and 3 (P. S. Srinivasan), are the Raman spectra of isoprene (C_5H_8), dipentene ($C_{10}H_{16}$) and ocimene ($C_{10}H_{16}$) respectively.

Plate XXXIV, Figs. 1, 2 and 3 (C. S. Venkateswaran), Raman spectrum of formic acid (liquid), sodium formate (aq. solution) and lead formate crystals respectively. The presence of 2834 and 2732 cm.$^{-1}$ gives experimental evidence of the existence of CH groups in formic acid.

Plate XXXV (C. S. Venkateswaran), Raman spectrum of selenious acid crystal, molten state and aqueous solution of different concentration. The crystal shows well-defined lines and the molten acid exhibits broad bands. The character of the bands does not alter very much with temperature.

Plate XXXVI (P. G. N. Nayar), Raman spectrum of inorganic hydrates, study of the structure of water bands.

Plate XXXVII (T. M. K. Nedungadi), Effect of orientation on the Raman spectrum of sodium nitrate. Figs. 1, 2 and 3 contain 9 pictures taken without analysing the scattered light. Figs. 4, 5 and 6 (containing 12 pictures) have been taken with incident light polarised. The diagrams given by the side of the spectrograms show the directions of the incident and scattered rays, as also the disposition of the NO_3 group relative to them. The directions of the optical vibrations in the incident light (I.L.) are indicated as also those in the scattered radiations (S.L.). Vibrations along OX and OY are represented by arrows parallel to these axes, whereas the circle with a central dot indicates that the vibrations are along OZ. Note the 1065 line changes in intensity to a remarkable extent with orientation, *i.e.*, when the plane of the NO_3^- ion coincides with the plane containing the incident and scattered rays. Compare Figs. 1 (*a*), 2 (*a*) and 3 (*a*), Figs. 1 (*b*) and 2 (*b*). The 1065 line is fairly strong while in 3 (*b*) it is extremely faint. Also note the interesting behaviour of the two low frequency lines which appear in Fig. 2 (*c*) while the 1065 line due to the internal oscillation is absent and *vice versa* in Fig. 2 (*b*). This reciprocal behaviour is shown by every one of the 12 spectrograms of Plate XXXVIII (Figs. 4, 5 and 6) obtained with the incident light polarised and the scattered light analysed. Figs. 7 (*a*) and 7 (*b*) of Plate XXXVIII show the spectrograms for two cases of longitudinal scattering of unpolarised light by the crystal. Note that the low frequency lines in Fig. 7 (*a*) disappear in the light scattered along the optic axis whereas in the perpendicular direction [Fig. 7 (*b*)] they appear strongly.

Plate XXXIX (T. M. K. Nedungadi). Fig. 1, Raman spectrum of quartz (enlarged); Figs. 2 (*a*) and 2 (*b*) are the spectra of light scattered backwards with the illumination respectively along and perpendicular to the optic axis, the incident light being unpolarised. In the light scattered along the optic axis the line 263 and the doublet at 800 disappear, whereas for the perpendicular direction they appear clearly.

Intense spectrograms taken at a series of temperatures—192, 25, 100, 200, 300, 410 and 530° C. are reproduced in Fig. 3. Note the lines 127, 207 and 465 are equally sharp at the liquid-air temperature. At room temperature the line 207 is diffuse. With rise of temperature all the lines broaden but the rate at which the 207 line broadens is much faster and at 530° C. it is completely washed out while the other two lines are present though broader. The broadening of 207 is unsymmetrical as the outer edge of the band is always approximately limited by the original position of the line. The shift

of the line 127 is much more pronounced than broadening. The particular mode of oscillation giving rise to the line 207 is involved in the α, β transformation of quartz.

Plate XL (V. Chandrasekharan). Fig. 1 (*b*) shows clearly the bands in a perfectly clear and transparent sphere of quartz traversed by an intense beam of λ 2537 radiation. The complete spectrum (see Fig. 1 *c*) shows clearly the variation in the band width for different mercury arc lines. A major portion of their intensity recorded is due to the Tyndall scattering by the few inclusions present in the crystal.

Fig. 1 (*a*) is a high enlargement of the portion between λ 2537 and the triplet λ 2654. It shows clearly the bands of the Brillouin Components of λ 2537 and two symmetric Raman lines 207 and 466 cm.$^{-1}$ excited by it while the strong line 128 cm.$^{-1}$ and the weaker 800 (doublet) and 1159 cm.$^{-1}$ lines belonging to the degenerate class E, sub-groups E_1, E_2 and E_3 respectively show no trace of banding.

Fig. 2 (P. S. Narayanan). Fig. 2 (*a*), Raman spectrum of ammonium dihydrogen phosphate taken with λ 2537 line of the mercury arc. Fig. 2 (*c*), effect of orientation on the Raman spectrum Fig. 2 (*a*) picture with the scattered light taken along the tetragonal axis. Fig. 2 (*b*) is the mercury arc spectrum. The Raman spectrum consists of 20 lines of which 4 are lattice lines, 8 are due to the internal oscillations of PO_4 group, and 8 due to NH_4 groups. The continuous distribution of intensity in the lattice spectrum indicates the possibility of the existence of hindered rotation of the NH_4 and PO_4 groups.

Plate XLI, Figs. 1 (*a*) and (*b*), are spectrograms of naphthalene crystal and (*c*) methyl methacrylate glass. Figs. 2 (*a*), and (*b*), benzophenone liquid and (*c*) benzophenone crystal. These figures illustrate the close similarity of the spectroscopic behaviour of liquids, amorphous solids and crystals in the region of higher frequencies. In all these cases the larger frequency shifts are seen as sharp lines.

Plate XLII, Figs. 1 and 2. This series of six spectrograms illustrate the sharpness of the spectral shifts given by crystals and the increase in their number with increasing complexity of crystal structure. Fluorite gives only one frequency shift while alumina gives 7, beryllium silicate 25, topaz 32, rochelle-salt 49 and cane sugar 63 distinct frequency shifts. The mercury lines have been marked off with the symbol λ in the spectrograms.

Plate XLIII (R. S. Krishnan). Figs. 1 (*a*) and (*b*) Raman spectrum of gypsum, while (*c*) and (*d*) barytes with two different exposures in each

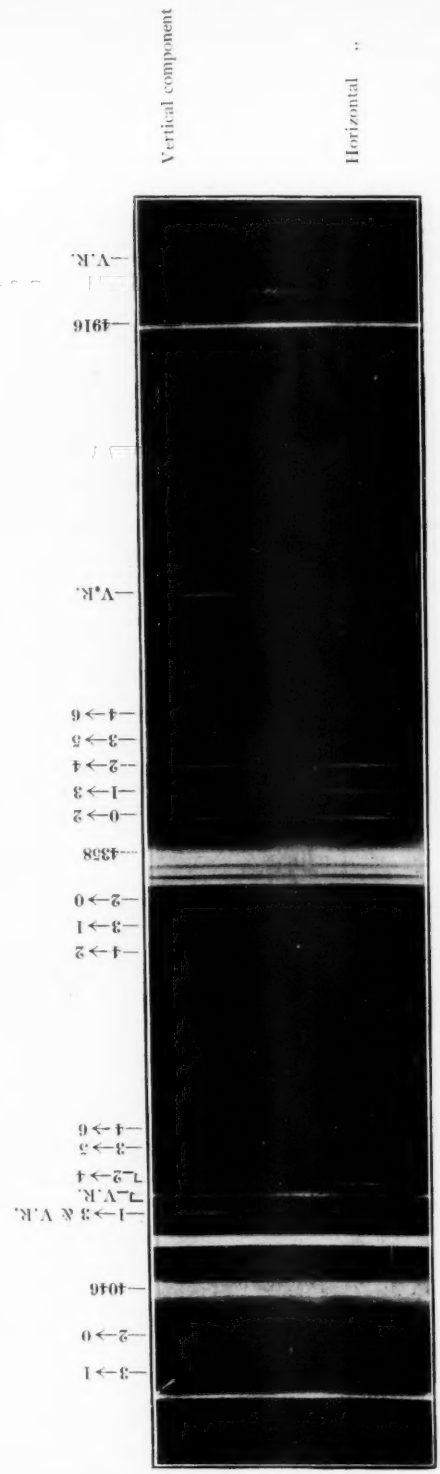

Raman Spectrum of Deuterium taken with a double image prism in the path of the scattered beam to show the state of polarisation of the various lines.

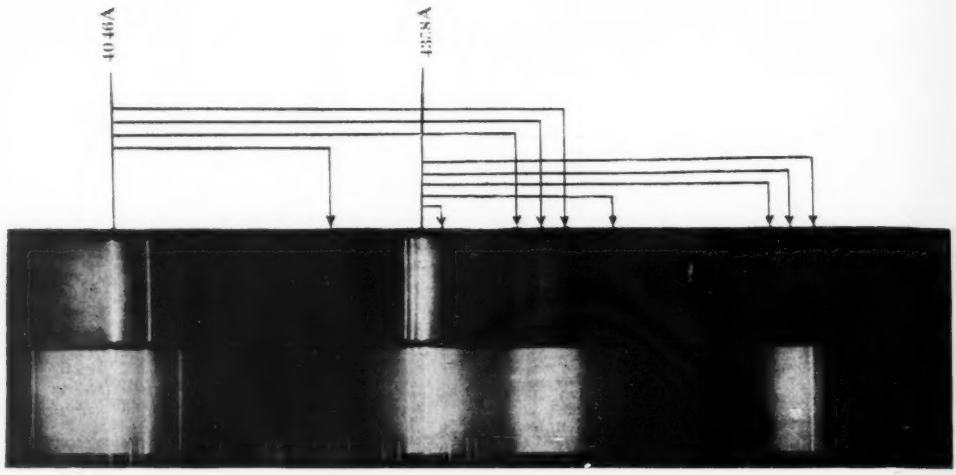

FIG. 1. Raman Spectrum of D_2O.

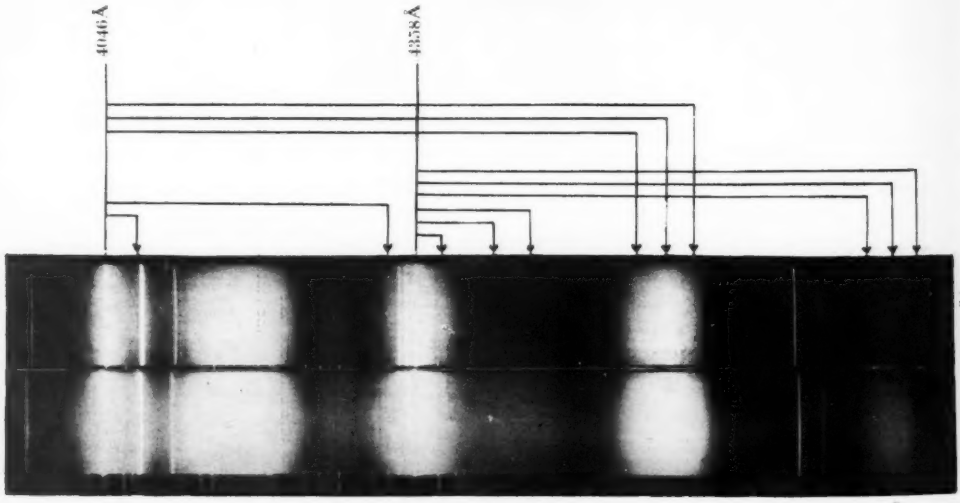

FIG. 2. Raman Spectrum of H_2O.

Raman Spectra
(1) Toluene, (2) Phenol, (3) Chlorobenzene

Fine Structure of Raman Lines.

FIG. 1. Raman Spectrum of CCl_4
(Littrow Spectrograph)

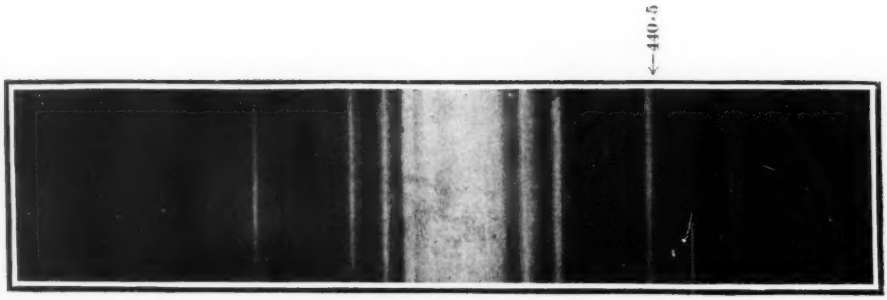

FIG. 1. Raman Spectrum of $SiCl_4$
(Two-prism Spectrograph)

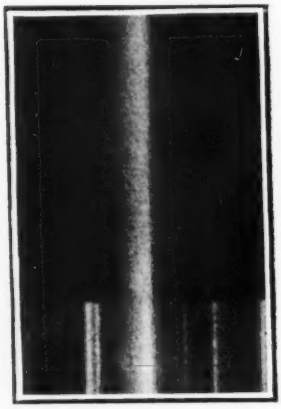

FIG. 2. 459 cm.$^{-1}$ line of CCl_4 showing unresolved isotope structure, the wing to its right and the octave line at 434 cm.$^{-1}$ to its left.

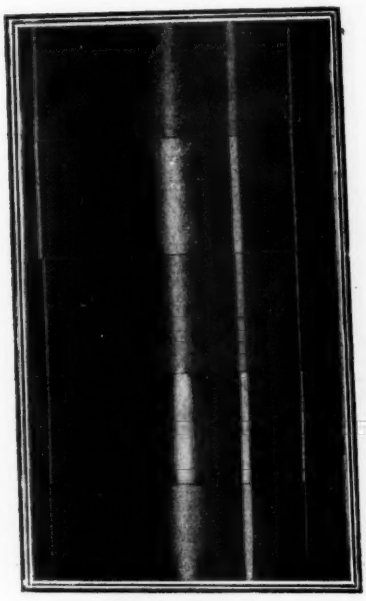

FIG. 1. Coumarin

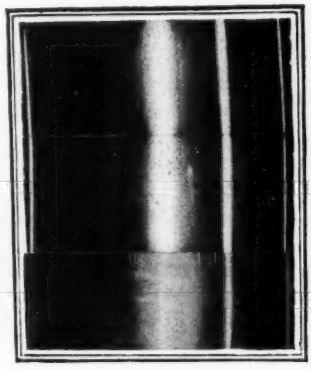

FIG. 2. Phenol

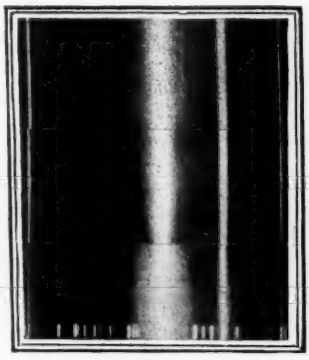

FIG. 3. Naphthalene

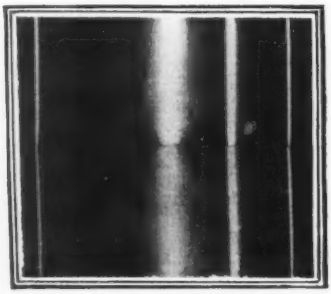

FIG. 4. Catechol

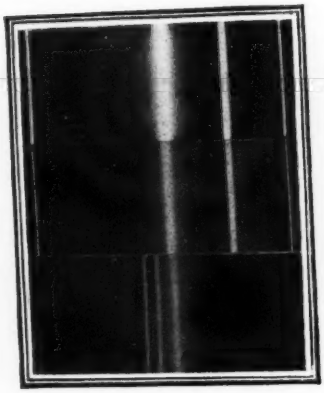

FIG. 6

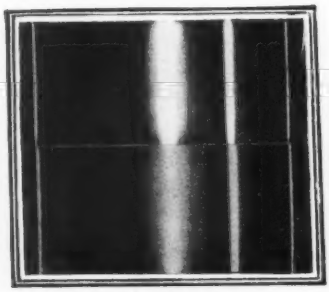

FIG. 5. Dichlorobenzene

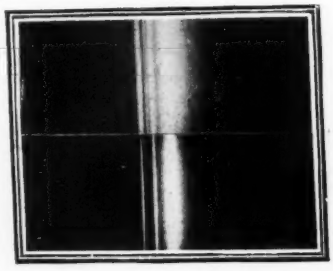

FIG. 7. Benzophenone

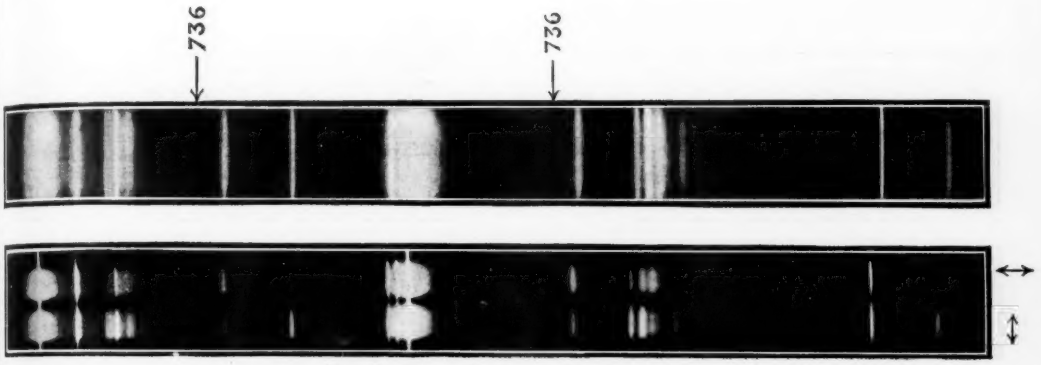

FIG. 1. Raman Spectrum of Cyclo-propane

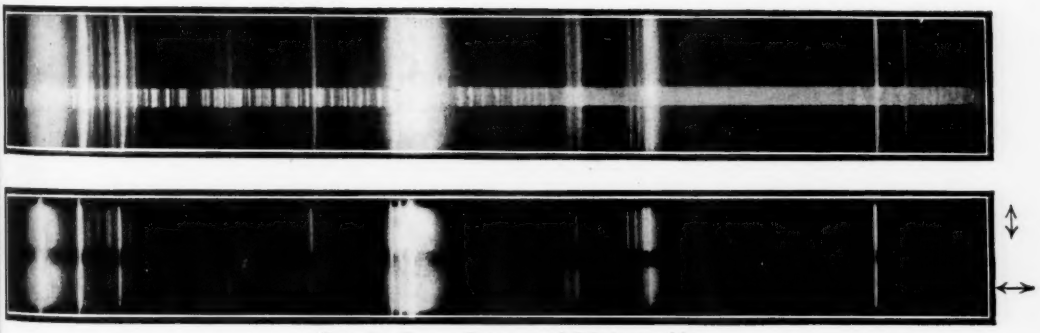

FIG. 2. Raman Spectrum of Ethylene oxide

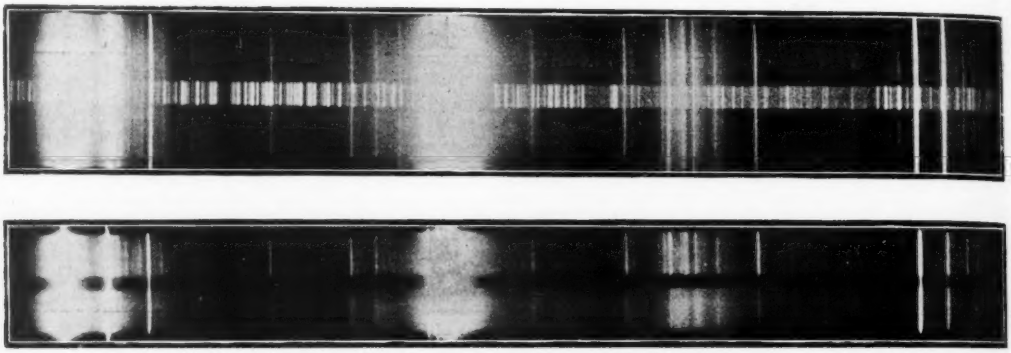

FIG. 1. Raman Spectrum of Propylene

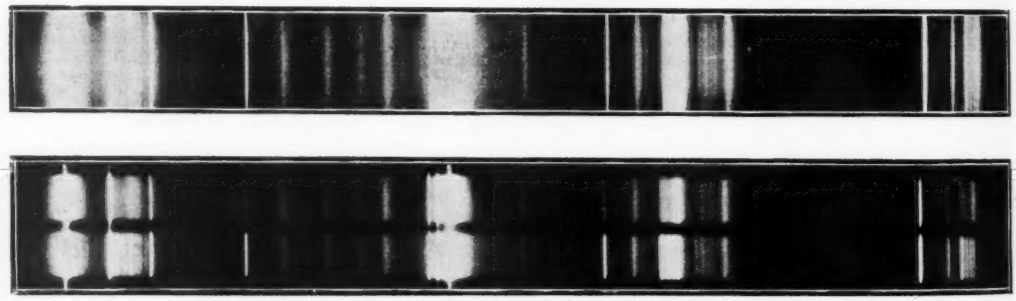

FIG. 2. Raman Spectrum of Iso-Butane

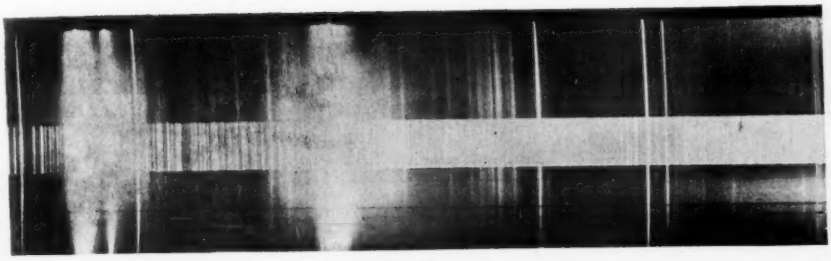

FIG. 1. Isoprene.

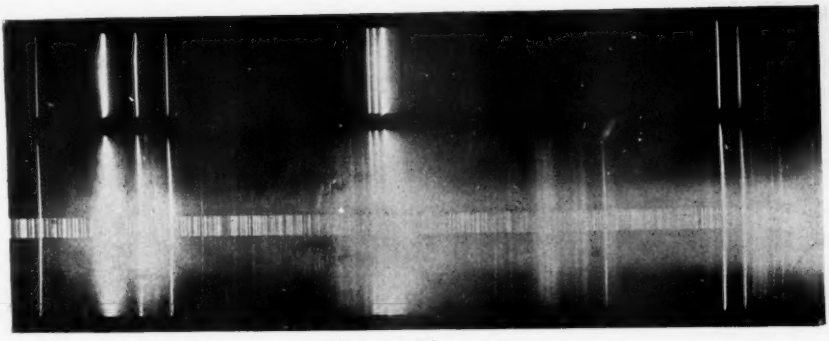

FIG. 2. Dipentene.

FIG. 3. Ocimene.

RAMAN SPECTRA

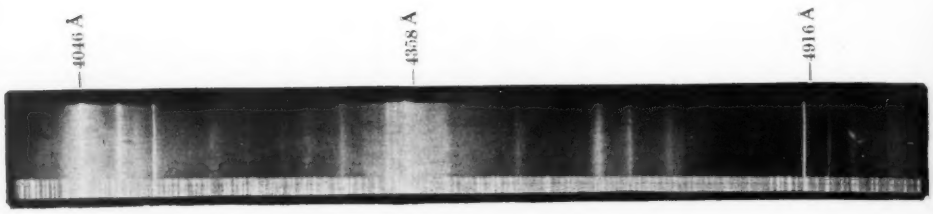

FIG. 1. Formic acid (liquid).

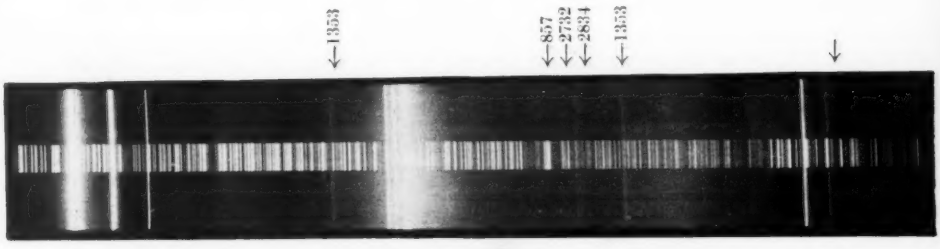

FIG. 2. Sodium formate (aq. soln.).

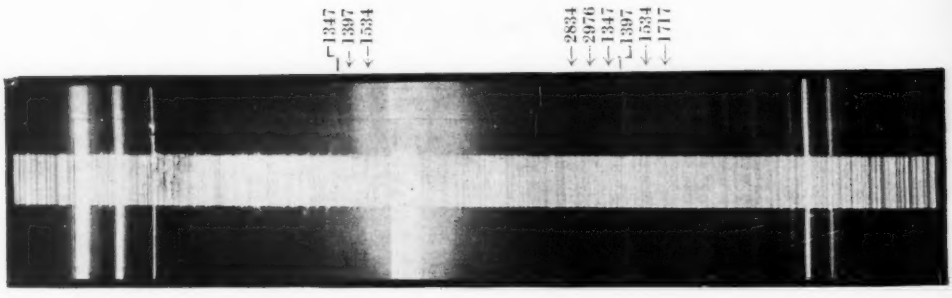

FIG. 3. Lead formate (crystals).

Raman Spectra

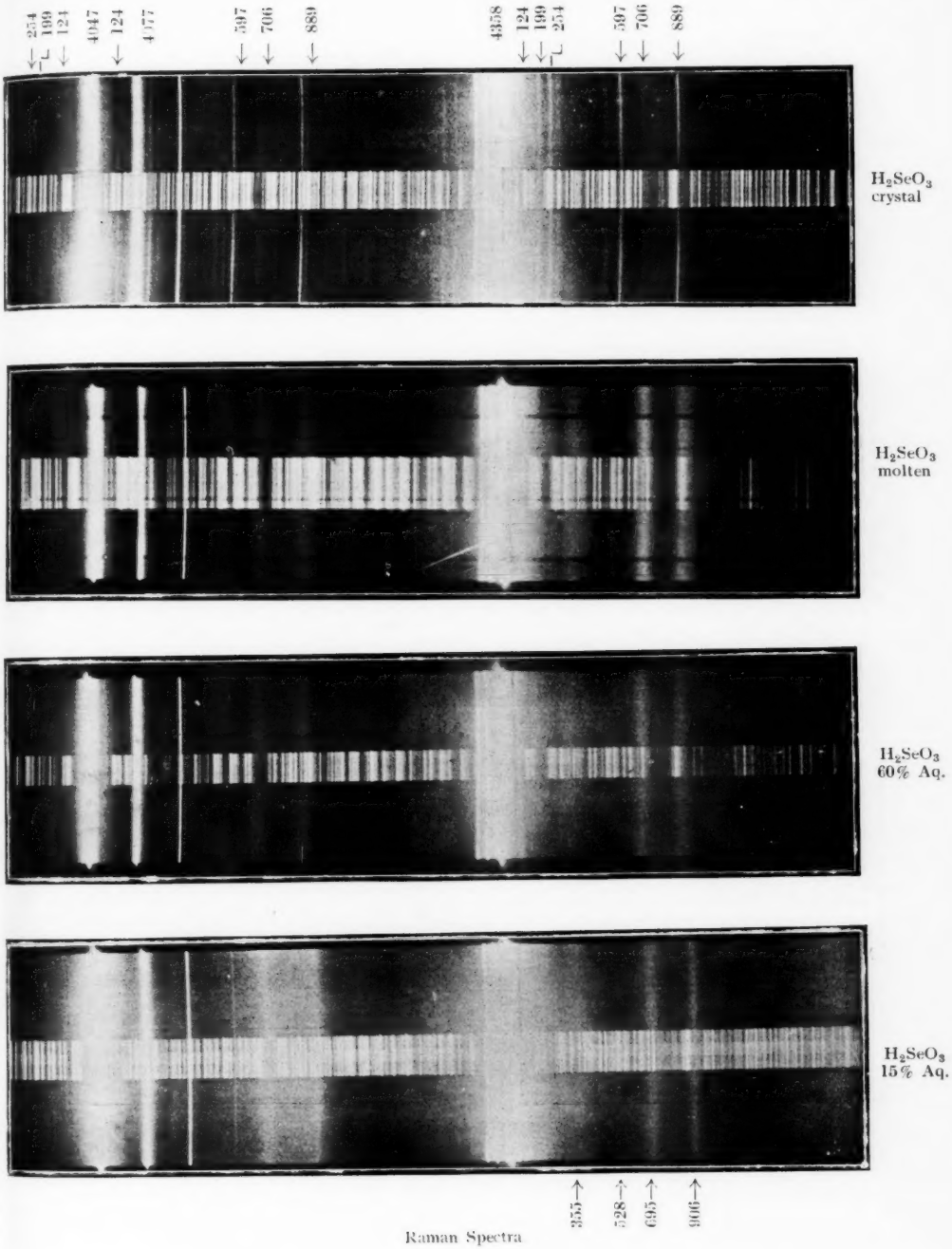

Raman Spectra

STRUCTURE OF WATER BANDS IN CRYSTALS

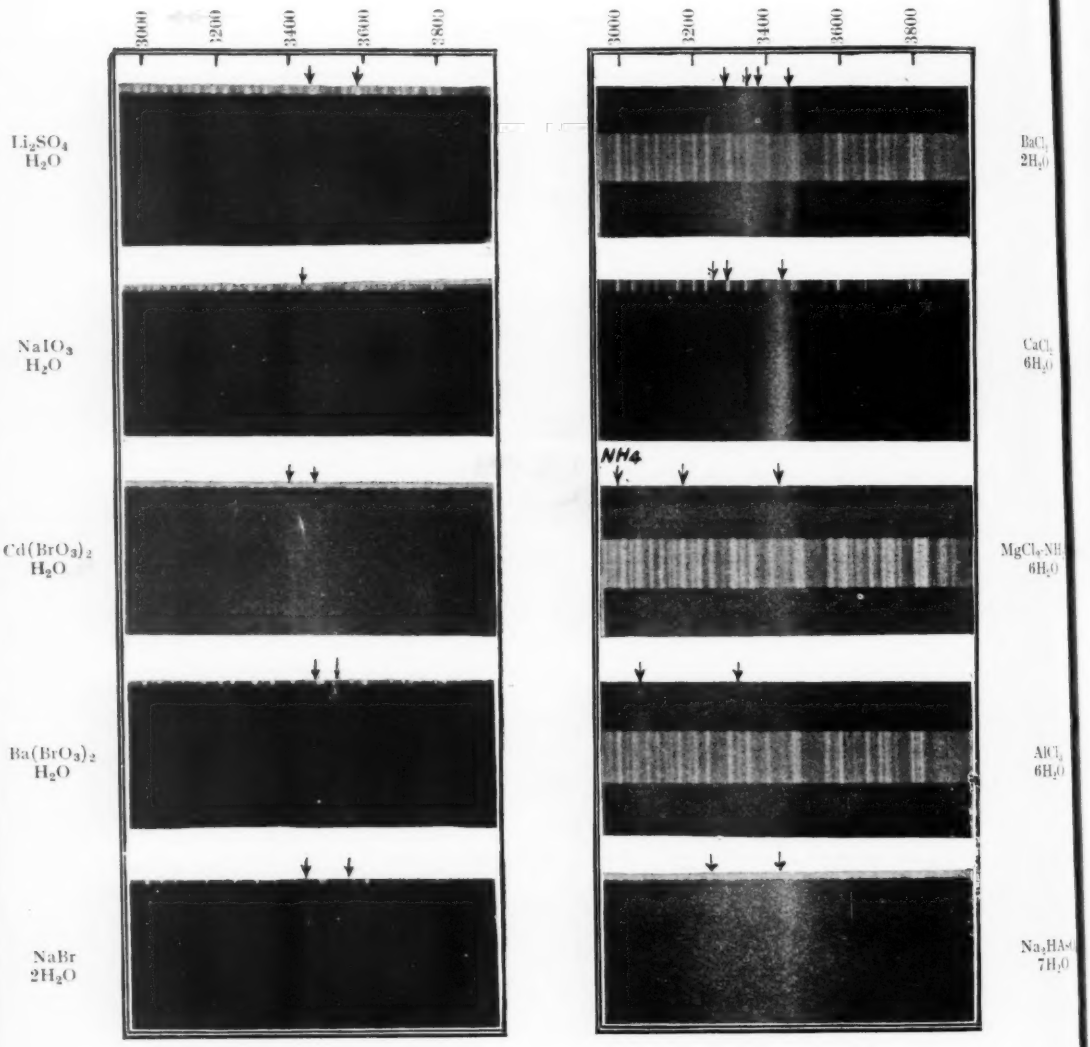

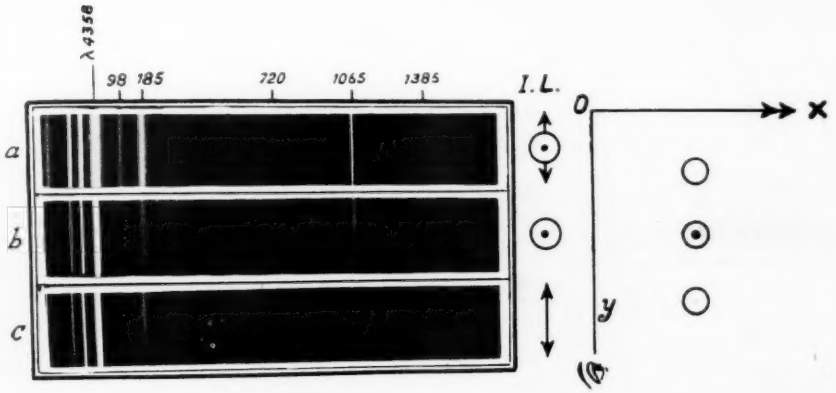

Fig. 1

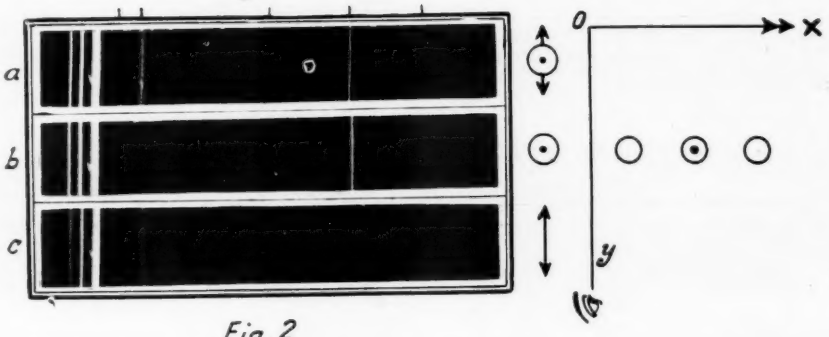

Fig. 2

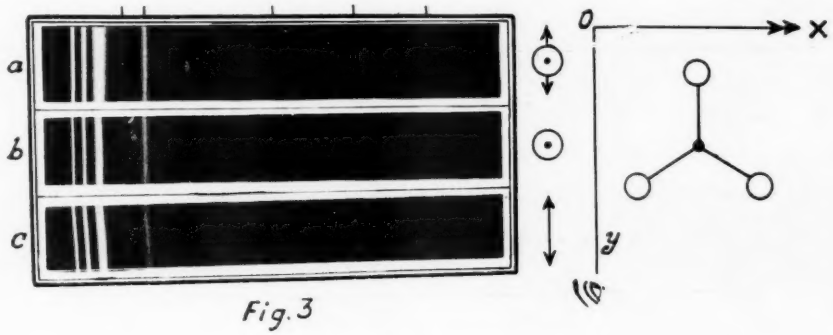

Fig. 3

Raman Spectrum of Sodium Nitrate

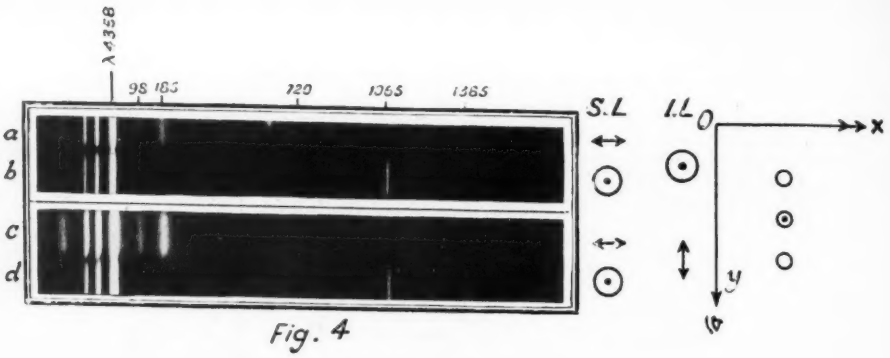

Fig. 4

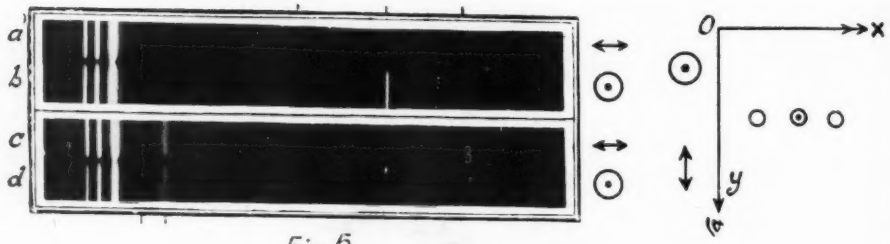

Fig. 5

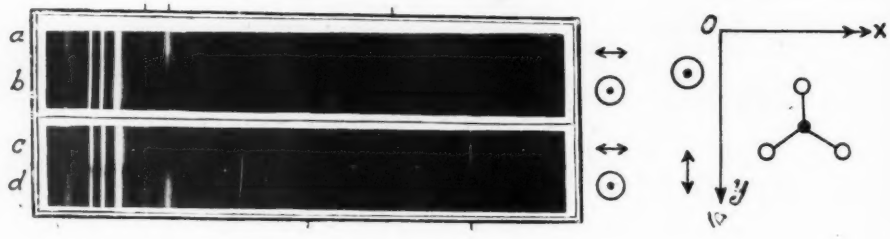

Fig 6

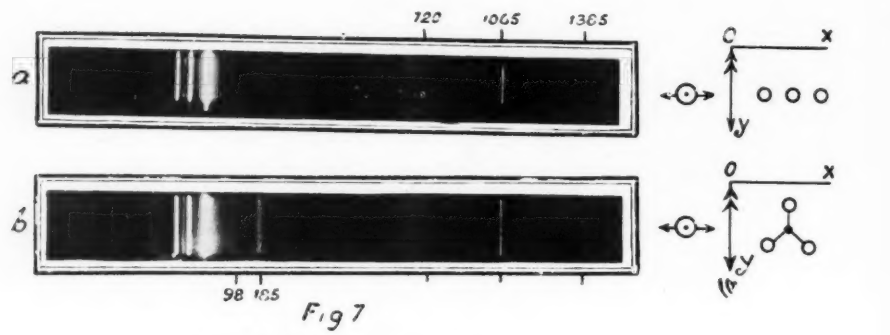

Fig 7

Raman Spectrum of Sodium Nitrate

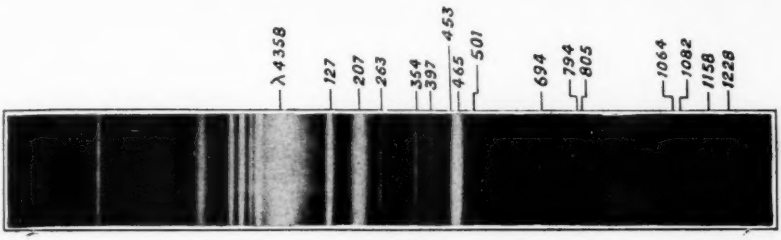

Fig.1

Fig. 2

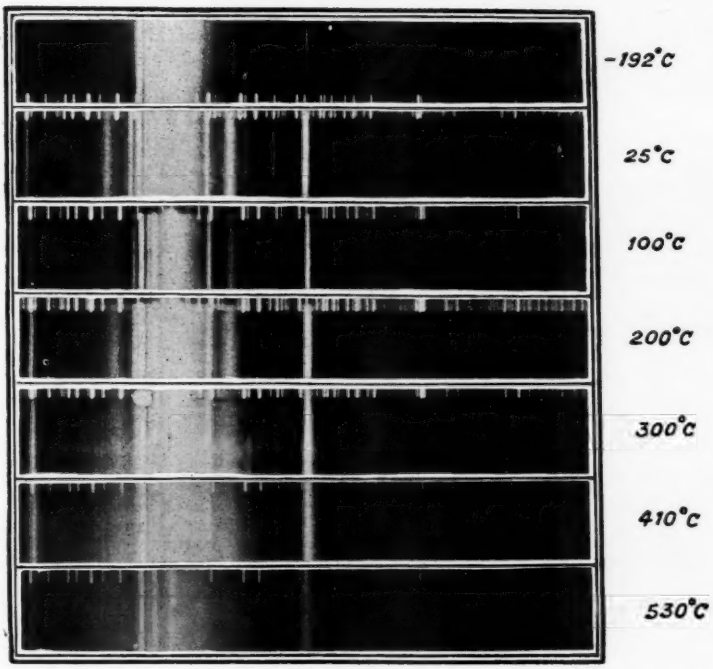

Fig.3

Raman Spectrum of Quartz

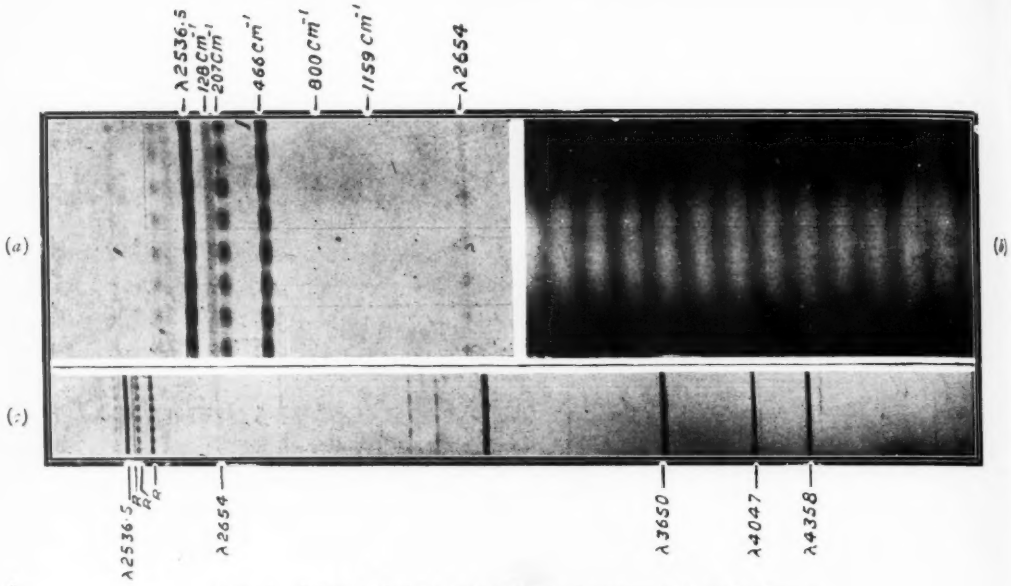

FIG. 1 Effect of Optical Activity on the Scattering of Light by Quartz

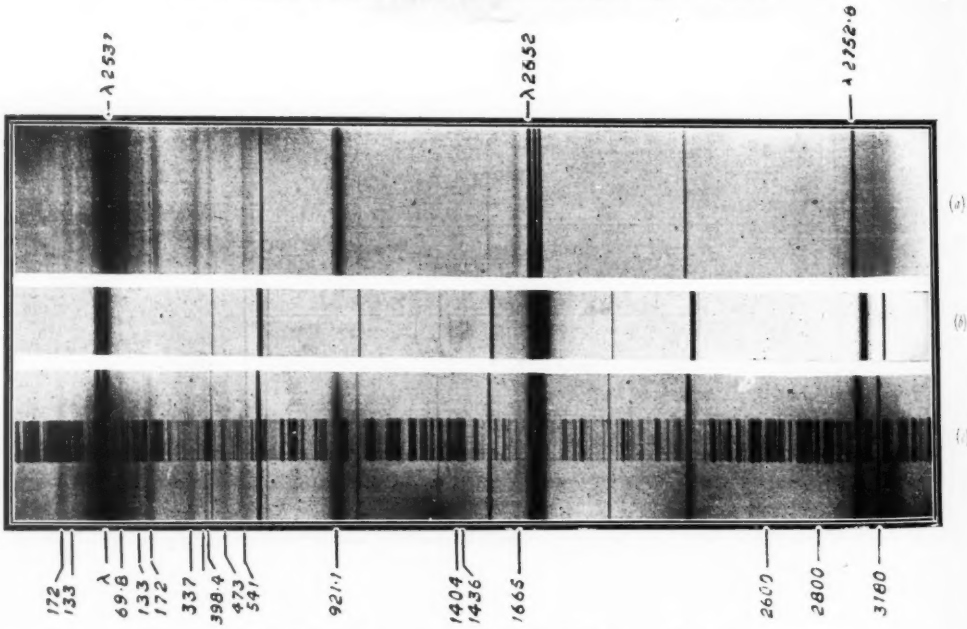

FIG. 2 Raman Spectrum of Ammonium Dihydrogen Phosphate

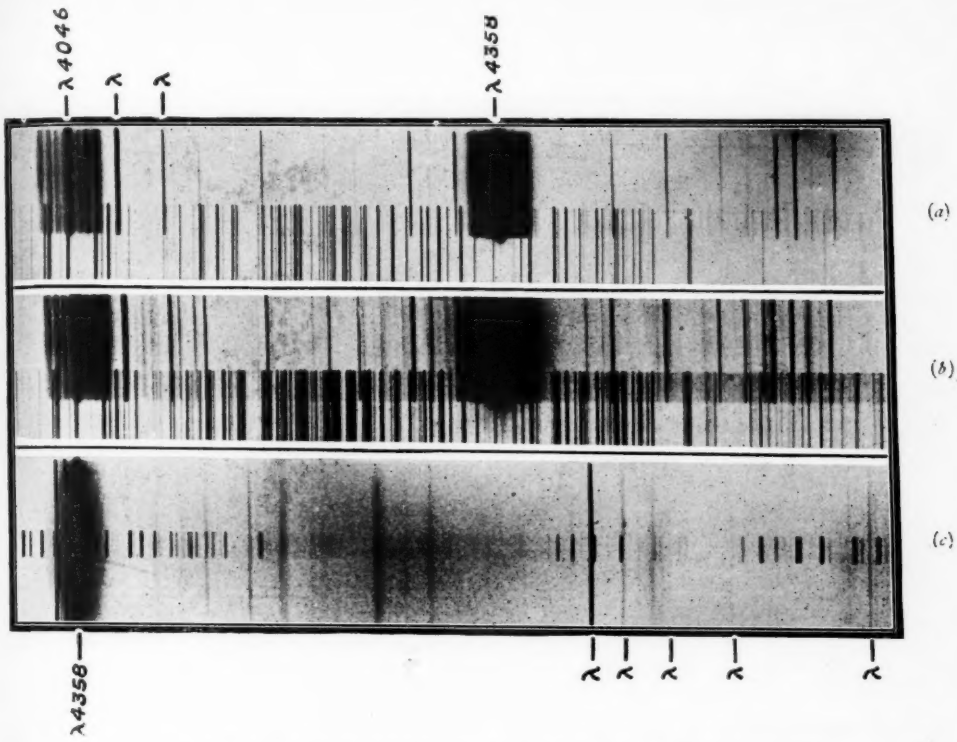

FIG. 1. (*a*) and (*b*) Naphthalene Crystals. (*c*) Methyl Methacrylate Glass

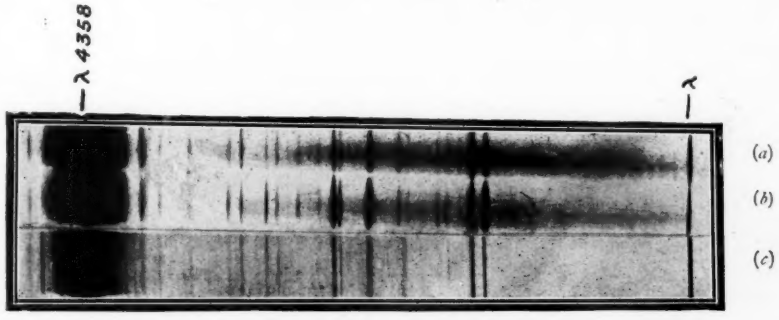

FIG. 2. (*a*) and (*b*) Benzophenone Liquid. (*c*) Benzophenone Crystal

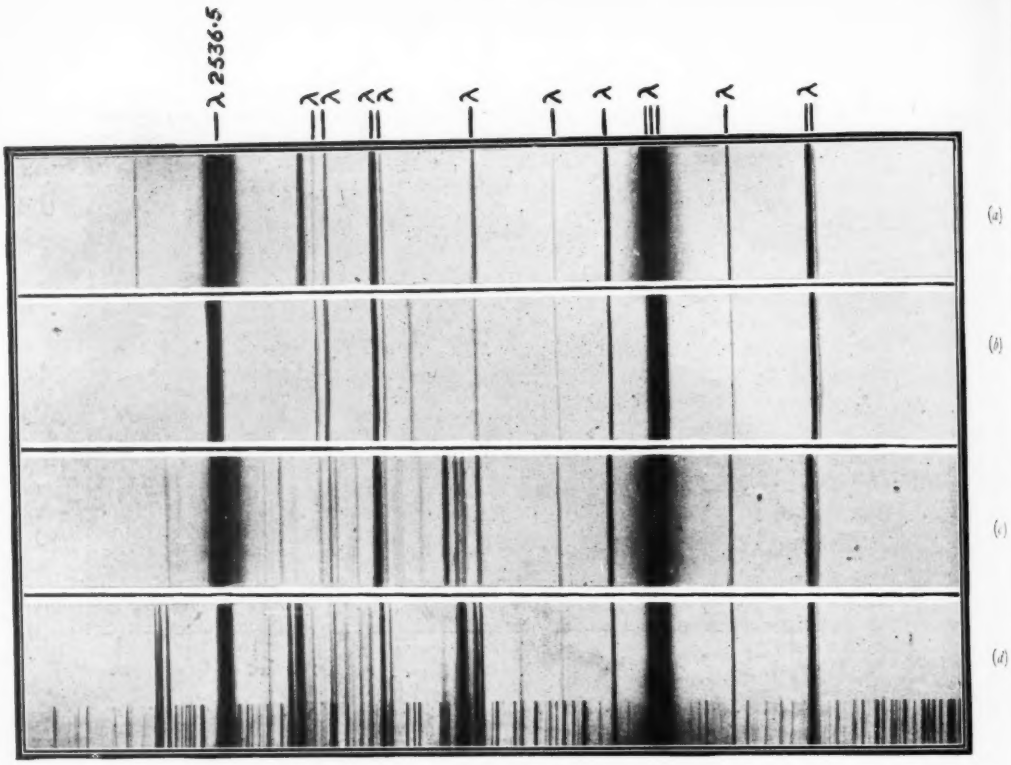

FIG. 1. (*a*) Fluorite. (*b*) Alumina. (*c*) Beryllium Silicate. (*d*) Topaz.

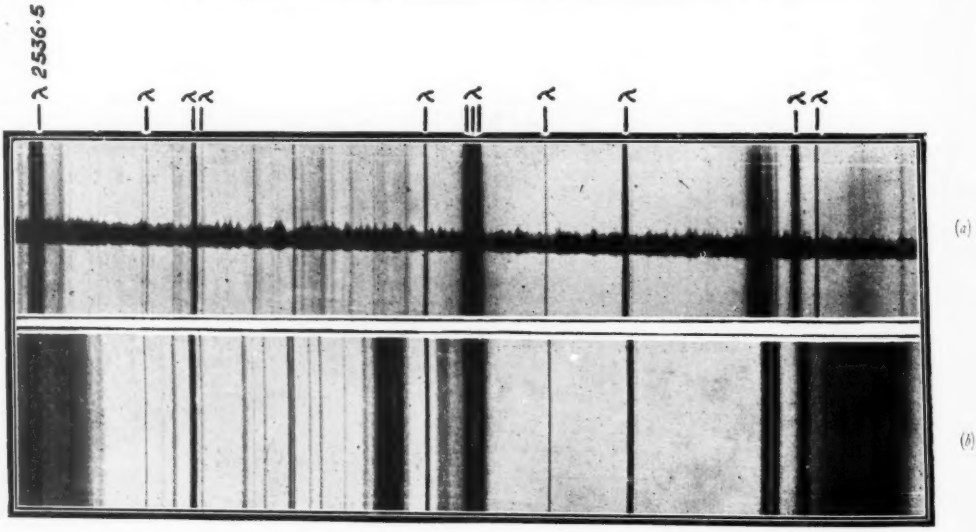

FIG. 2. (*a*) Cane-Sugar. (*b*) Rochelle Salt.

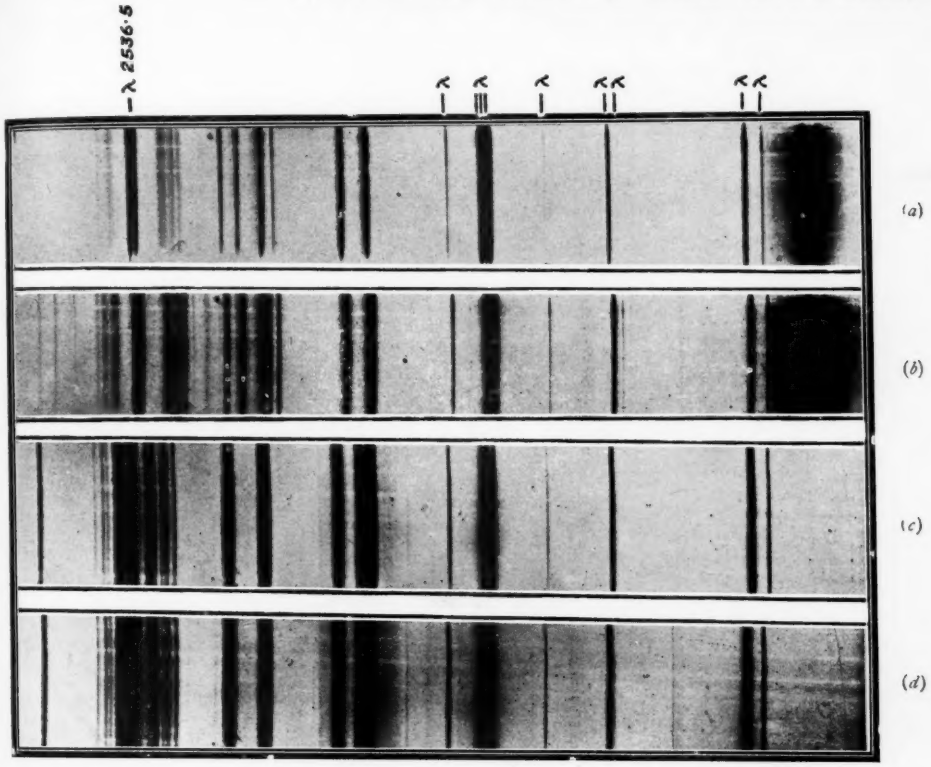

FIG. 1. (*a*) and (*b*) Gypsum, (*c*) and (*d*) Barytes, with two different exposures in each case

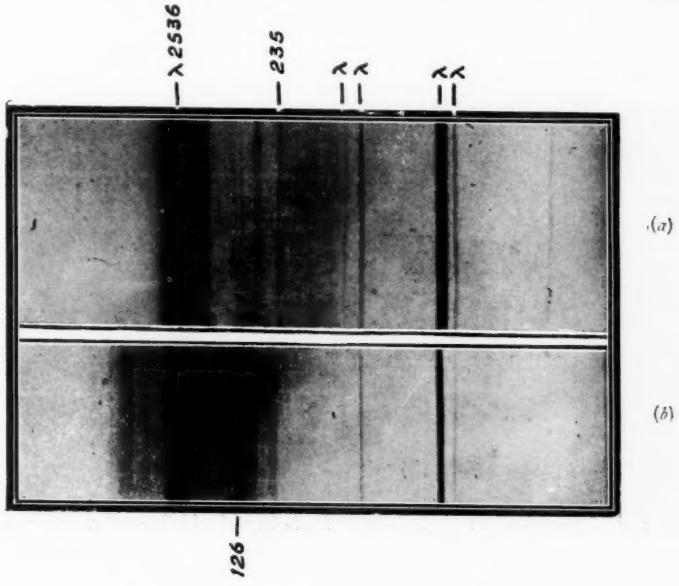

FIG. 2. (*a*) Rock-salt; (*b*) Potassium Bromide

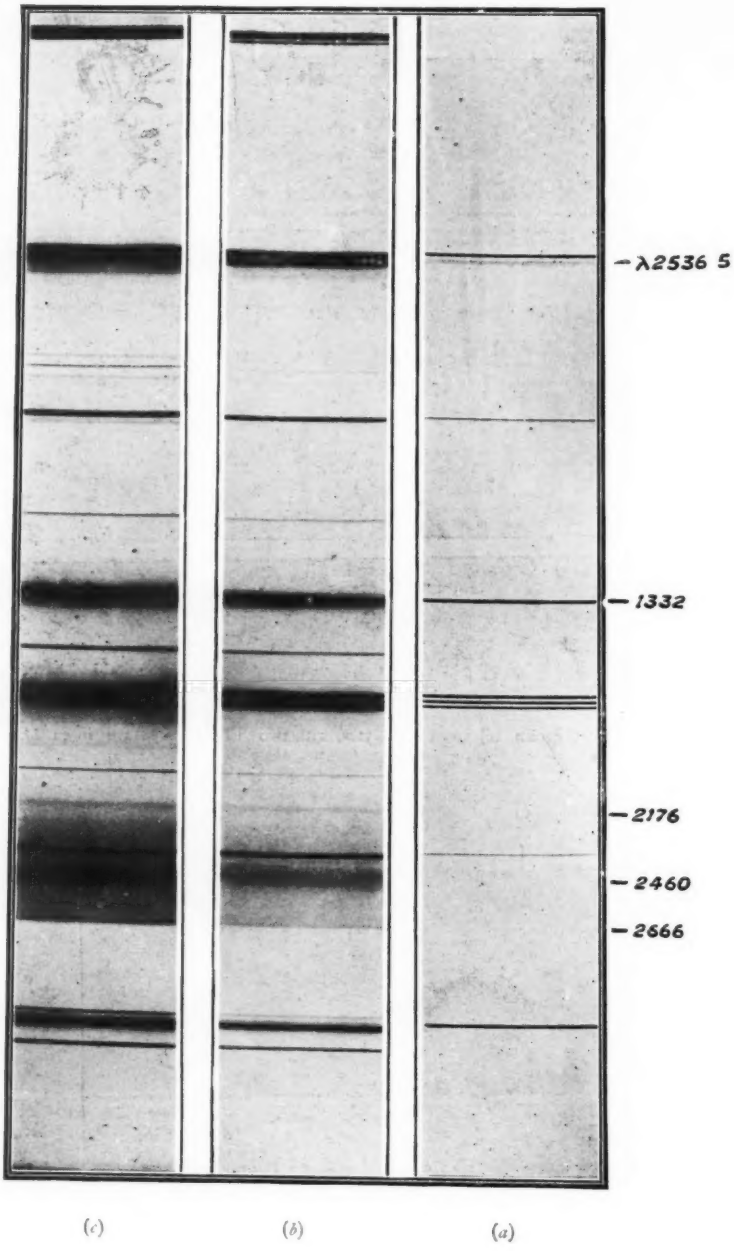

FIG. 1. Diamond (Medium Spectrograph) (*a*), (*b*), (*c*) with increasing exposures

case. Figs. 1 (*c*) and (*d*) illustrate strongly exposed spectra of barytes. Its second order spectrum is clearly seen in both figures but better in the more heavily exposed spectrogram. Fig. 2 (*a*), Raman spectrum of rock-salt, (*b*) Raman spectrum of potassium bromide. Note the sharply defined line with a frequency shift of 235 seen in the second order spectrum of rock-salt and the intense line with a frequency shift of 126 cm.$^{-1}$ in that of potassium bromide.

Plate XLIV (R. S. Krishnan) [(Figs. 1 (*a*), (*b*) and (*c*)]. These illustrate the case of diamond. Note the development of the second order spectrum in the region of frequency shifts between 2666 and 2176 with increasing exposures.

A. JAYARAMAN.

300–53 Printed at The Bangalore Press, Bangalore City, by C. Vasudeva Rao, Superintendent (I/c.)
and Published by The Indian Academy of Sciences, Bangalore